Universität Rostock

Traditio et Innovatio

Synthesis of Polycyclic Heteroaromatic Hydrocarbons by C-H Activation Reactions: Application of Cycloisomerization and Pd-catalyzed Cross-Coupling Reactions

Cumulative Dissertation

to acquire the academic degree

Doctor rerum naturalium (Dr. rer. nat.)

of the Faculty of Mathematics and Natural Sciences

at the University of Rostock

submitted by Aleksandra Khomutetckaia, born on 2nd January 1997 in Kirghizstan

Rostock, 2024

https://doi.org/10.18453/rosdok_id00004866

The present work was accomplished at the Department of Chemistry of the University of Rostock, at the chair for Organic Chemistry in the work group of Prof. Dr. Dr. h.c. mult. Peter Langer during the period from October 2020 to March 2024.

Reviewer:

Prof. Dr. Dr. h.c. mult. Peter Langer, Universität Rostock, Institut für Chemie

Prof. Dr. Thomas J. J. Müller, Heinrich-Heine-Universität Düsseldorf, Institut für Organische Chemie und Makromolekulare Chemie

Date the dissertation was submitted: 11.03.2024

Date of thesis defence: 11.06.2024

Statement of Authorship

Ich versichere hiermit an Eides statt, dass ich die vorliegende Arbeit selbstständig angefertigt und ohne fremde Hilfe verfasst habe. Dazu habe ich keine außer den von mir angegebenen Hilfsmitteln und Quellen verwendet und die den benutzten Werken inhaltlich und wörtlich entnommenen Stellen habe ich als solche kenntlich gemacht.

I hereby affirm that I have written the present work by myself without outside assistance. No resources were utilised other than those stated. All references as well as verbatim extracts were quoted, and all sources of information were specifically acknowledged.

Rostock, 11th March 2024

Aleksandra Khomutetckaia

Acknowledgements

I want to thank **Prof. Dr. Dr. h.c. mult. Peter Langer** for giving me the opportunity to work on this challenging and fascinating topic, for believing in me and for the scientific freedom he provided. I am equally grateful to **Dr. Peter Ehlers** for his constant support, for his open door in case of problems or questions, for training me in the laboratory and supporting in the measurements of the physical properties of the synthesized substances, as well as for many useful discussions and advice in various situations.

I would like to thank **Dr. Alexander Villinger** for his work on single crystal structures, **Dr. Dirk Michalik** and **Heike Borgwaldt** for the measurement of numerous NMR spectra. In addition, I would like to thank the technical staff **Maximilian Quasdorf** and **Alexander Klotzek** for providing working materials, **Dr. Martin Hein** for giving me the opportunity to do basic internships with students, and **Dr. Holger Feist** for conducting workshops on safe laboratory work.

Special thanks to **Niels Hildebrandt**, who worked diligently and conscientiously under my supervision and thus made an important contribution to the results of my research work.

I wish to thank **my colleagues Prof. Dr. Dr. h.c. mult. Peter Langer's group** as well as my colleagues from **Prof. Dr. Peter H. Huy's** and **Prof. Dr. Malte Brasholz's** working groups for their friendly and respectful cooperation, constructive discussions and suggestions within and outside the daily PhD routine as well as for their support in various questions. Furthermore, I would like to thank my colleagues in the analytical department of the institute as well as the Leibniz Institute for Catalysis for the fast processing and measurement of my numerous samples.

I am grateful to the **Landesgraduiertenförderung** giving me a scholarship for my Ph.D. studies.

Finally, I would like to thank **my parents**, **my sister** and **my friends**, who have always supported and encouraged me and my love for chemistry.

Summary

This dissertation focusses on the development of new synthetic routes to polycyclic aromatic hydrocarbons containing five-, six-, and seven-membered heterocyclic rings and the characterisation of these novel compounds. The synthetic investigations were directed to the application of C-H activation reaction. In particular, Pd-catalyzed C-H activations as well as acid mediated cycloisomerization reaction of 2-alkynyl biaryl derivatives were employed as key ring-closing synthesis steps. Hence, several heteroatom doped polycyclic aromatic compounds have been obtained, including benzoimidazoquinolines, diindenopyrene and dibenzopyrene derivatives. The optical and electrochemical properties of selected compounds have been studied in detail and the results have been verified by density functional theory and time-dependent density functional theory computations.

Zusammenfassung

Diese Dissertation befasst sich mit der Entwicklung neuer Synthesewege zu polycyclischen aromatischen Kohlenwasserstoffen mit fünf-, sechs- und siebengliedrigen heterocyclischen Ringen und der Charakterisierung dieser neuen Verbindungen. Die Anwendung der C-H-Aktivierungsreaktion stand im Mittelpunkt der synthetischen Untersuchungen. Als Schlüsselelement in den ringschließenden Syntheseschritten wurden insbesondere Pd-katalysierte C-H-Aktivierungen sowie säurevermittelte Cycloisomerisierungsreaktionen von 2-Alkinylbiarylderivaten eingesetzt. Auf diese Weise wurden heteroatomdotierte polycyclische aromatische Kohlenwasserstoffe, darunter Benzoimidazochinoline, Diindenopyren- und Dibenzopyrenderivate erhalten. Die optischen und elektrochemischen Eigenschaften ausgewählter Verbindungen wurden eingehend untersucht und durch Ergebnisse aus Dichtefunktionaltheorierechnungen verifiziert.

Table of Contents

Table of Contents 6

List of Abbreviations 7

Introduction 8

Overview and Aim of the Research 27

References 28

Contribution in Research Paper 34

I Synthesis and Properties of Benzo[*h*]imidazo[1,2-*a*]quinolines and 1,2*a*-Diazadibenzo[*cd*,*f*]azulenes. 38

II Serendipitous discovery of Pd-catalyzed intramolecular cyclization of ortho-bromo(hetero)aryl-substituted (hetero)aryl-1,2-diketones: Applications in the synthesis of carba- and heterocyclic benzoin derivatives 39

III Synthesis and Properties of Diindeno[1,2,3-*cd*:1′,2′,3′-*mn*]pyrene and Two of Its Aza-Analogs 40

IV Synthesis and Properties of Azadibenzo[*a*,*e*]pyrenes 41

Appendix 42

Applications in the synthesis of benzo[4',5']thieno[2',3':3,4]-naphthobenzofurans 42

Synthesis and Properties of 1*H*-Pyrrolo[3',2':3,4]fluoreno-[9,1-*gh*]quinolines and 7*H*-Pyrrolo[2',3',4':4,10]anthra[1,9-*fg*]-quinolines 45

Resume 52

List of Abbreviations

BTBT	benzothienobenzothiophene
DSSC	dye-sensitized solar cell
equiv.	equivalent(s)
HOMO	highest occupied molecular orbital
LUMO	lowest unoccupied molecular orbital
NTCDA	1,4,5,8-Naphthalenetetracarboxydianhydride
OFETs	organic field-effect transistor
OLEDs	organic light-emitting diodes
OPVs	organic photovoltaic cells
OSC	organic semiconductor
PAHs	polycyclic aromatic hydrocarbons
PHAs	polycyclic heteroaromatic compounds
*p*TsOH	*para*-toluenesulfonic acid
RTP	room-temperature phosphorescent
S_EAr	electrophilic aromatic substitution
TADF	thermally activated delayed fluorescence
TFA	trifluoroacetic acid
TfOH	triflic acid
UV/Vis	Ultraviolet–visible

Introduction

Polycyclic aromatic hydrocarbons are organic compounds which are composed of carbon and hydrogen atoms. Chemically, PAHs consist of two or more benzene rings linked by linear, cluster, or angular arrangements. The simplest is naphthalene, which has two aromatic rings, while compounds with three fused rings are anthracene and phenanthrene (Figure 1).

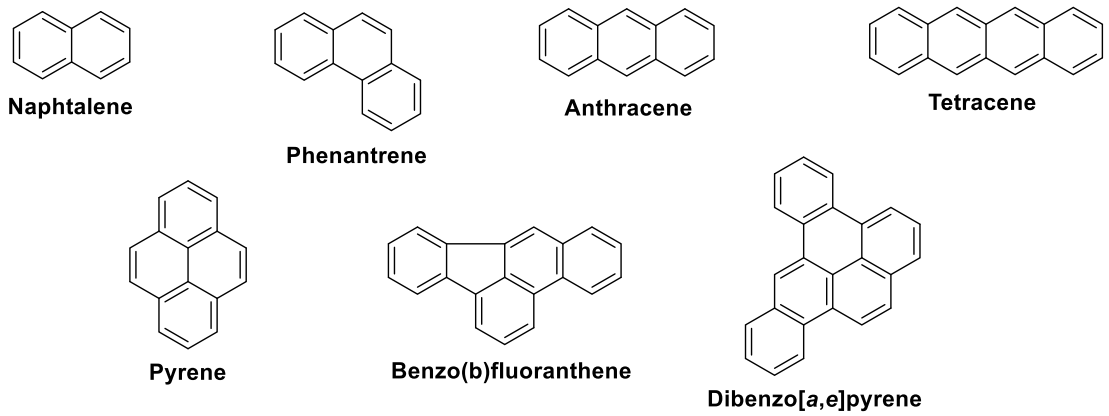

Figure 1. Examples of PAHs.

PAHs may be produced by burning organic materials such as coal and wood, and are also found in tobacco smoke. These PAHs have been found in the environment and have been linked to toxic, mutagenic and carcinogenic effects.[1–4] Despite their negative properties, PAHs are promising materials for organic electronics due to their unique structural, optical and electrochemical properties.

For example, certain PAHs are chiral and may provide improved performance and functionality for chiral transistors. Some PAHs can exist as biradicaloids, having two unpaired electrons that can form a conjugated π-system. This allows for charge transfer and modulation of their electronic properties. They can also absorb light over a wide range of wavelengths from ultraviolet to near infrared, and some can generate carriers by photoexcitation or thermally induced charge separation. Additionally, some PAHs can form heterostructures with other materials, such as graphene or metal oxides, to enhance light absorption and charge collection.[5,6] These properties make PAHs suitable materials for creating organic field-effect transistors (OFETs) with high electrical conductivity and the ability to control current, and

allow them to serve as active components in organic light-emitting diodes (OLEDs), organic photovoltaic cells (OPVs) or fluorescent dyes (Figure 2).[7–11]

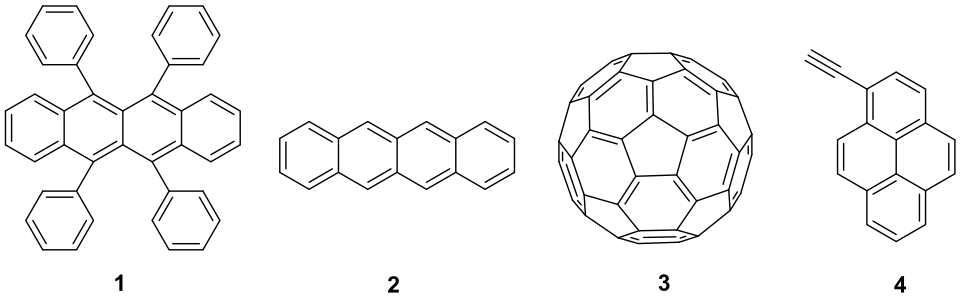

Figure 2. Examples of PAHs with semiconducting properties. **1**: rubrene is a molecular organic semiconductor, used in OLEDs and OFETs; **2**: tetracene is a molecular organic semiconductor, used in OLEDs and OFETs; **3**: C_{60} is used in OPVs; **4**: 1-ethynyl pyrene is violet-fluorescent dye.

One of the most prominent examples of this has been pyrene. Pyrene consists of four fused benzene rings with extensive π-electron delocalization. Pyrene is characterized by its unprotected π-system upon functionalization, moderately long fluorescence lifetime with blue emission, and long-lived excited singlet state associated with excimer formation. In addition to its photophysical properties, it has high chemical stability and carrier mobility. And various synthetic approaches to the synthesis and modification of pyrene have been developed in order to study its electrooptical properties. The incorporation of nitrogen into the heterocyclic framework enhances light absorption, improves charge transfer, and allows rearrangement of energy levels. Therefore, pyrene systems are remarkable candidates for organic semiconductor materials.[12–14]

Changes in the properties of polycyclic compounds can be achieved by introducing heteroatoms such as N, S and O into the aromatic scaffold of PAHs (Figure 3).[15] This can be through the placement of heteroatoms both at the periphery of the molecule and within the polycyclic system. In addition, the number of rings and the geometric arrangement of the heteroatoms can also have an effect on the properties. Of particular importance is the sp^2-hybrid framework of the heterocyclic PAH, which actively participates in molecular organization by creating a close interaction between π-electronic clouds, dipole moments, and heteroatomic

contacts. This control of the organization provides an excellent framework for self-assembling materials.[16–20]

Nitrogen can successfully replace carbon in aromatization reactions to form functional polycyclic aromatic hydrocarbons. Prominent examples of nitrogen-containing heterocyclic structures are the aza-pyrene and ullazine scaffolds. Their stability and unique optical and electronic properties have attracted much attention. The high electronegativity of the nitrogen reduces the LUMO energy of the polycyclic aromatic compounds, which facilitates the injection of electrons and increases the stability of the anionic charge carriers. In addition, new functionalities such as hydrogen bonding, protonation, metal complexation, and improved solubility are provided by the presence of an unpartitioned electron pair from nitrogen atoms within the molecular scaffold.[21–23]

Sulfur-based organic semiconductors have properties that make their heterocyclic derivatives attractive building blocks for the development of a new generation of luminescent materials. Sulfur has two unpaired electron pairs and an empty d-orbital in its $3s^2 3p^4$ outer electronic configuration. Sulfur easily forms sulfoxide or sulfone with electron-deficient properties favoring electron injection and transport during the oxidation process. Thus, substances based on thienoacene and [1]benzothieno[3,2-*b*][1]benzothiophene (BTBT) frameworks represent an important family of π-conjugated molecules and an example of well-functioning OSC molecules within them.

Oxygen-containing heterocyclic compounds are used in lithium-ion battery applications. For example, 1,4,5,8-Naphthalenetetracarboxydianhydride (NTCDA) is a conjugated compound used in the preparation of organic materials for electronic, luminescent, fuel cell, and photoconductive devices due to its thermal stability and strong electronic acceptor properties. The thermal stability of NTCDA is a key advantage, allowing heat treatment to nearly 450°C without physical or chemical decomposition.[24–26]

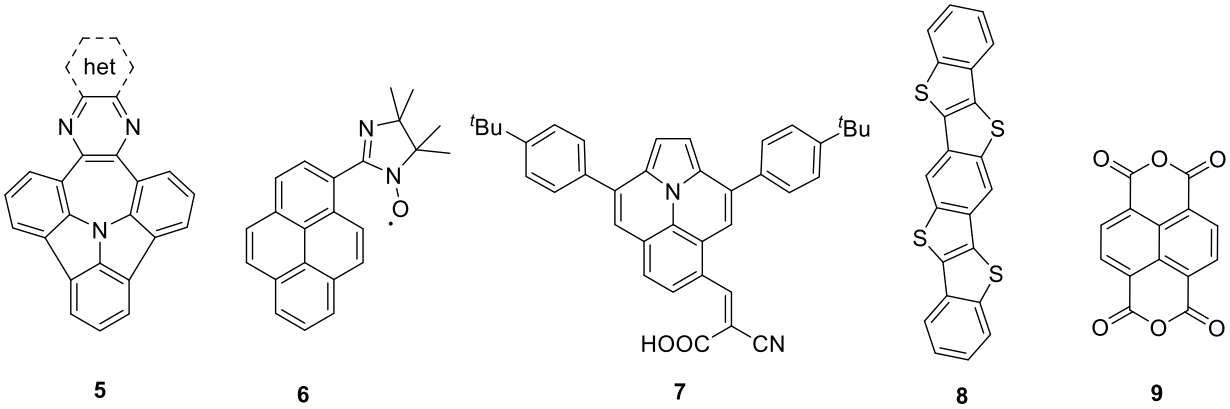

5 6 7 8 9

Figure 3. Examples of polycyclic heteroaromatic semiconductors. 5: TADF/RTP OLED emitters; 6: 1-imino nitroxide pyrene is used for high performance OFETs; 7: ullazine-based organic dyes for dye-sensitized solar cells (DSSCs); 8: organic semiconductor based on BTBT; 9: NTCDA is used in lithium-ion battery applications.

Doping of PAHs by heteroatoms allows to alter the properties of the respective polycyclic compound. For example, PAHs can exhibit biological activity, making them important in drug development. Their integration into medicinal chemistry allows the creation of compounds with improved bioactivity, pharmacokinetic properties and specific interactions with biological targets. PHAs may serve as a central scaffold in the development of anti-viral, anti-cancer, antibiotic, and central nervous system therapeutics (Figure 4).[27–29] For example, Vialinin B exhibits high inhibitory activity against the production of tumor necrosis factor TNF-α. TNF-α is a potent multifunctional cytokine involved in various biological processes and plays a key role in the pathogenesis of inflammatory diseases such as rheumatoid arthritis. Therefore, Vialinin B is a promising candidate for developing novel antiallergic agents.[30,31] Another example is Raloxifene, which is a selective estrogen receptor modulator, a mixed estrogen receptor agonist and antagonist in various tissues. Compounds with nitrogen-containing polycyclic aromatic hydrocarbons, such as 5-arylated imidazopyridines, show inhibitory effects on several human cancer cell lines, including those in the colon (HCT-116, SW-620), lung (A549), pancreas (MIAPACA), liver and other tissues.

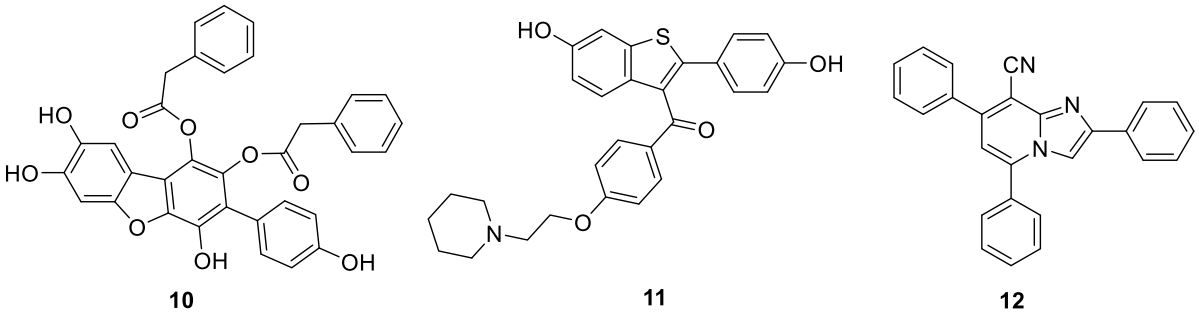

Figure 4. Examples of biological active PAHs. **10**: vialinin B is antiallergic agent; **11**: raloxifene is used against osteoporosis in postmenopausal women; **12**: 2,5,7-triphenylimidazo[1,2-*a*]pyridine-8-carbonitrile activity against various cancer cell lines.

Nowadays, chemical synthesis plays a central role in the advancement of many scientific disciplines, ranging from materials science to pharmaceutical industry. It offers versatile approaches for the discovery and creation of innovative molecules with diverse applications, such as in materials science and drug development. An emerging technology called C-H activation facilitates the rapid assembly and later modification of functional molecules to achieve desired chemical and physical properties.[32–34] C-H bond activation is a method of direct carbon-carbon bond formation through the activation of a carbon-hydrogen bond (Scheme 1).

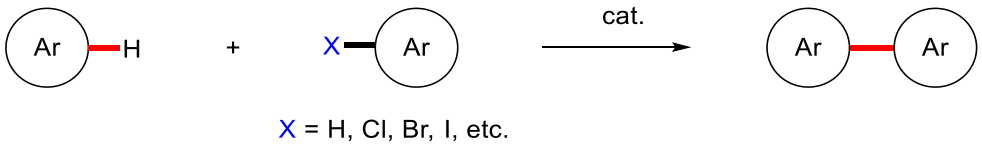

Scheme 1. C-H activation general reaction.

C-H bond cleavage can be achieved by a variety of methods. Given the dissociation energy of the bonds, relatively low strength bonds can be easily achieved through a variety of reactions, such as the electrophilic aromatic substitution (S_EAr).[35] S_EAr is one of the most important synthetic organic reactions. It has become a common method for functionalizing aromatic compounds since its discovery in the 1870s by Charles Friedel and James Crafts. Its wide use in chemical industry provides millions of tons of aromatic products every year for

manufacturing chemical raw materials, household and consumer products, and medicines. For example, sulfadiazine, an antimicrobial used in the treatment of urinary tract infections and burns is produced through nitration and chlorosulfonation reactions. Important polymers, such as the thermosetting phenol-formaldehyde resins, are also produced by means of S_EAr reactions.

At the end of the 19th century, the first examples of transition metal-induced activation of the C-H bond were described (Scheme 2). This was demonstrated by Volhardt in the reaction between thiophene and mercuric chloride to form chloromercurythiophene, and by Dimroth who described the synthesis of arylmercury acetates from $Hg(OAc)_2$ and various aromatic hydrocarbons.[36]

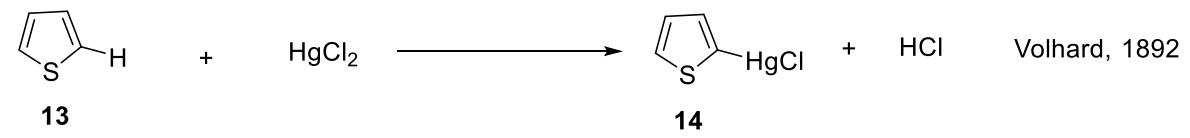

13 **14**

Scheme 2. Pioneering example of electrophilic C-H metalations.

A large number of electrophilic species are formed by the action of Lewis acid catalysts. In this activation reaction, a new C(aryl)-M bond is formed without changing the oxidation state of the metal, based on the electronic interaction between the π-electron cloud of the substrate and the electrophilic metal center (Scheme 3). This significantly increases the acidity of the C(aryl)-H bond, which is easily lost during rearomatization.[37]

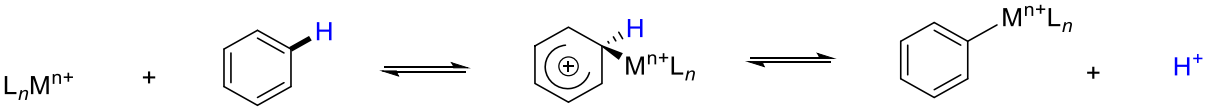

Scheme 3. Mechanism of the S_EAr reaction by a metal complex.[38]

Metals such as Aluminum, Boron, Cadmium, Cobalt, Copper, Iron, Lithium, Magnesium, Molybdenum, Nickel, Platinum, Silicon, Silver, Tin, and Ytterbium are widely used as Lewis

acid reagents. Therefore, various elements can be used as Lewis acid reagents, and each has its own advantages for diverse applications. For example, in the synthesis of quinolone derivatives (Scheme 4), which have various functions including anticancer and antiplatelet activity, $AlCl_3$ is used as a catalyst in the S_EAr reaction.[39]

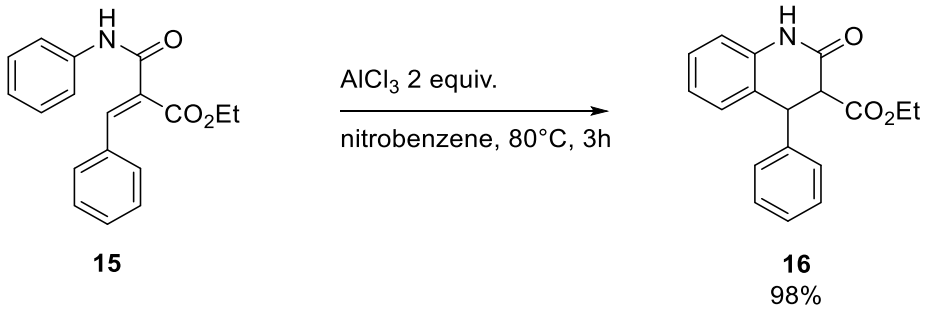

15 **16** 98%

Scheme 4. C-H activation by Lewis acid-mediated cyclization.

In contrast to the activation of electrophiles by Lewis acids, also Brønsted acids are capable for such reactions and have been employed in several applications. They allow activation of carbonyl, imine, alkene, alkyne, alkyne, and hydroxy groups to form oxonium salts, iminium salts, carbocations, and vinyl carbocations, which facilitates subsequent nucleophilic addition. Using Brønsted acid-based catalysts, cationic electrophiles can be formed by direct protonation of the functional group.

For example, an efficient method was developed to prepare arylbenzofuranones via C-H activation/lactonization under the action of Brønsted acid TfOH (Scheme 5).[40] Arylbenzofuranone are prominent structural units found in natural products and pharmaceutically relevant compounds with high biological activity and therapeutic value. This metal-free protocol provides an easy-to-use, rapid, one-pot method for high yields of various α-arylbenzofuranones with a wide range of substrates.

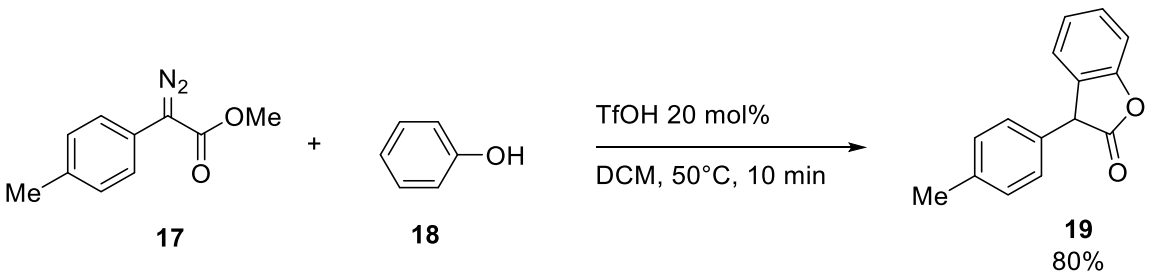

Scheme 5. TfOH-catalyzed cascade C-H activation/lactonization of phenols with α-aryl-α-diazoesters.

Simultaneously to the development of reagents and application of S_EAr reactions, strategies to implement catalytic functionalization of aromatic compounds was investigated to avoid or reduce the employment of stoichiometric amounts of, mostly toxic, metal salts or -waste, respectively. For example, in 1965, Chatt reported the introduction of a ruthenium(0) complex into the C-H bond of naphthalene (Scheme 6).

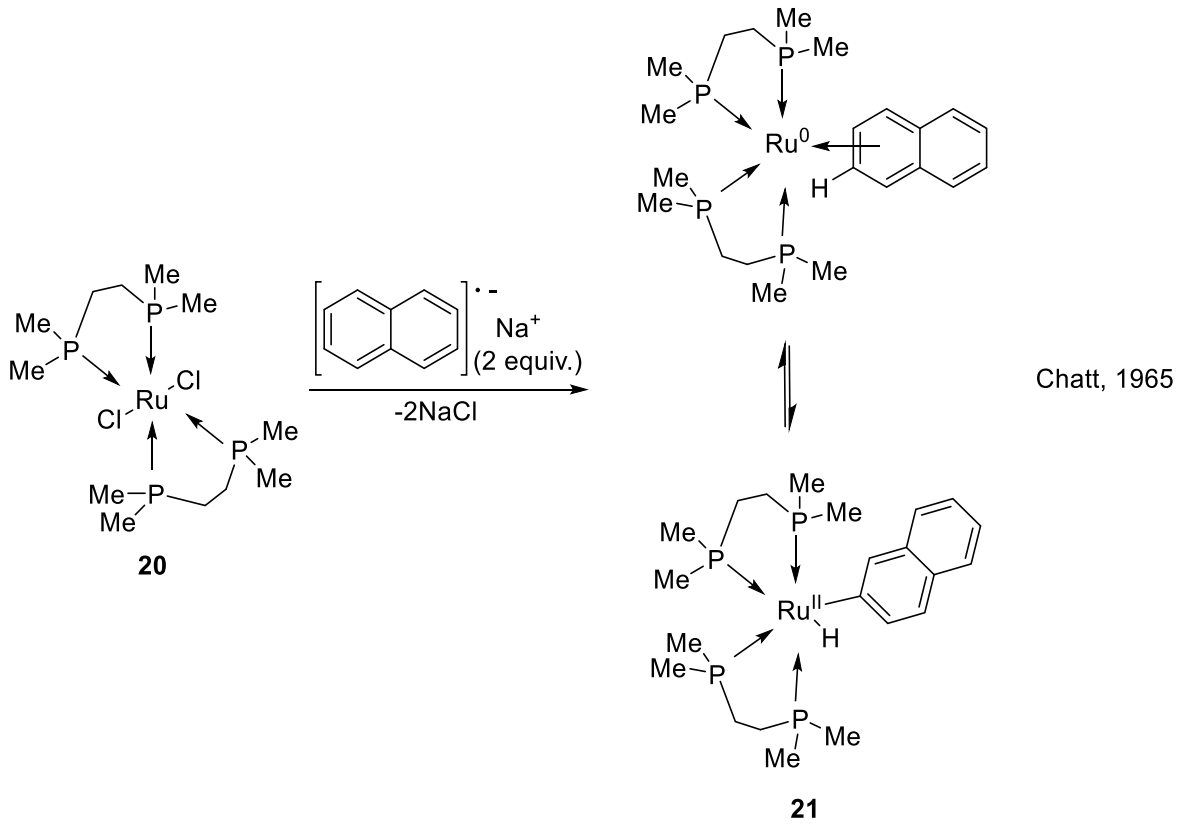

Scheme 6. Chatt's pioneer C-H activation on naphthalene.

In the last decades, a large number of C-H activation methods have been developed that convert C-H bond into functional groups for subsequent chemical modifications.[41–43] These efforts have greatly improved the understanding of cleaving and functionalizing inert C-H bonds and highlight the potential of C-H activation for developing and improving chemical synthesis.

The C-H bond activation process is generally understood to involve a transition metal. Typically, the metal complex is coordinated to a polar group and incorporated into the proximal C-H bond to form an organometallic complex. It then undergoes cross-coupling or substitution reactions to form a C-C or C-X bond (X = heteroatom). One important reaction step is the insertion of metal complex into the carbon hydrogen bond (Scheme 7).[44,45]

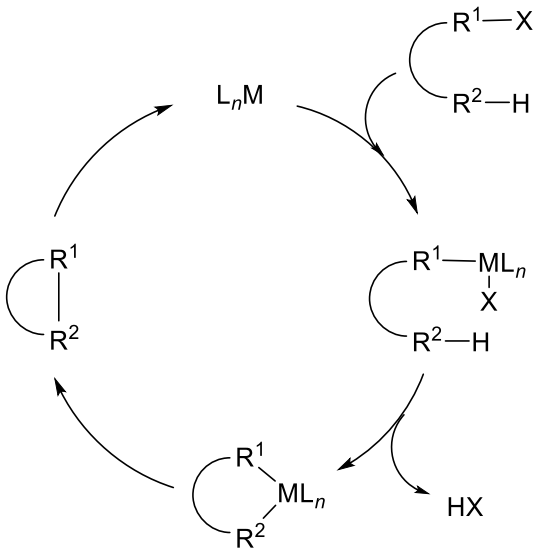

Scheme 7. Typical mechanism of C-H activation at L_nM species.

Late transition metals, Pd, Rh, Ru, Ir, Ni and Cu have emerged as the most versatile catalyst systems for C-H bond activation. They have successfully demonstrated efficiency in many applications in organic synthesis and have overcome difficulties previously related to thermodynamic and kinetic aspects.

For example, the Pd-catalyzed activation of the C-H bond can be used in the synthesis of aromatic polycyclic compounds.[46–50] These compounds can be used as small-molecule OFETs for the development of electronic devices. Compared to silicon, organic semiconductors offer access to cheaper and lighter devices with ease of fabrication and tunable molecular and material properties, including HOMO / LUMO energy levels and charge carrier mobility. It includes the ability to generate circularly polarized luminescence in OLEDs and to regulate carrier mobility, which makes OSCs a potentially promising material for optoelectronic applications in the future. A prominent example is the synthesis of helicenes (Scheme 8). Unlike more traditional OSCs such as pentacene, they have the advantage of a helical geometry, which confers unique properties.

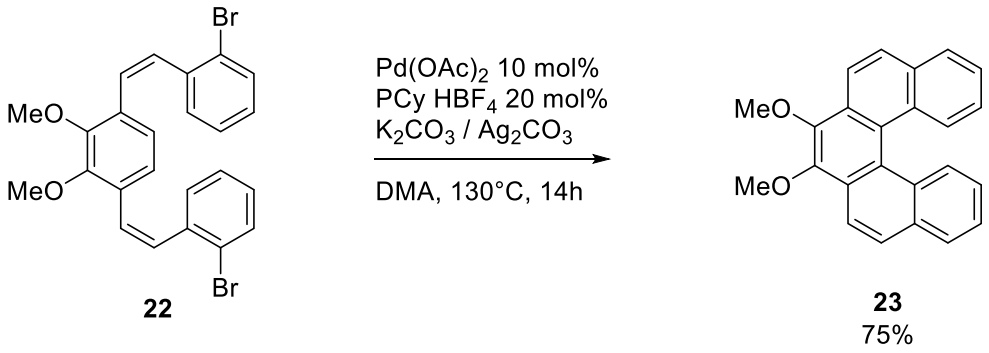

Scheme 8. C-H arylation by Pd and Ru catalysts.

Moreover, base metal catalysts like Fe, Mn, and Co have been extensively studied in homogeneous and heterogenous catalysis, such as C-H activation reactions.[51–56] Due to their outstanding properties such as lack or reduced toxicity, environmental friendliness, relative abundance in the earth's crust and low cost, researchers have focused on the application of these catalysts in organic synthesis. Despite early successes in this area, research groups in organometallic chemistry have only recently begun to focus on the mechanistic aspects of these base metals. This is due to the difficulties in working with base metal organometallic compounds, which result from their different reactivity compared to their heavy metal counterparts. Thus, the usual experimental procedures for mechanistic studies are greatly complicated by the formation of paramagnetic intermediates caused by single electron transfer processes, and the higher nucleophilicity of the reactive forms. Iron catalysts, for instance, which are known to be readily available, inexpensive and non-toxic, have received much

attention. New methodologies have emerged to demonstrate the important role of this transition metal in modern organic synthesis. For example, aryl-substituted benzo[*h*]quinolines are synthesized using the iron-based homogeneous catalyst by C-C bond formation (Scheme 9).[57]

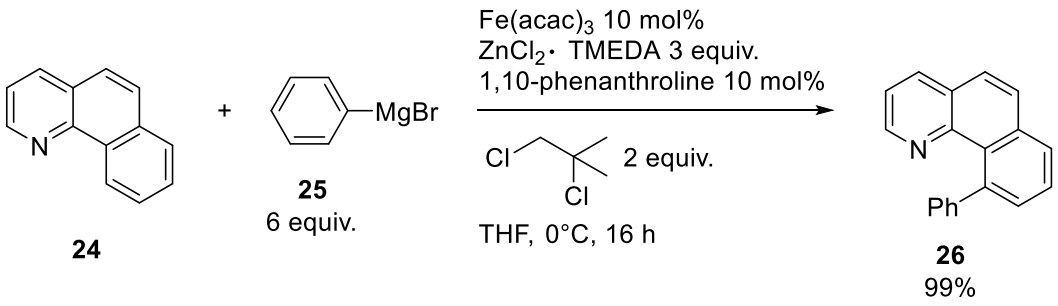

Scheme 9. Iron-catalyzed arylation of heterocycles via directed C–H Bond Activation.

Although many approaches exist for their synthesis and for the construction of aryl-heteroaryl C(sp^2)-C(sp^2) bonds, the most general and efficient method for the synthesis of PHAs is the use of Pd-catalyzed cross-coupling and C-H bond activation reactions.[58–62] PHAs play a key role in forming a variety of biologically active compounds and materials with optical and electrochemical properties in materials science. Most of the reactions carried out with Pd catalysts have a high tolerance for functional groups.[63] Despite its high cost, palladium is attractive for applications in the commercial production of high value chemicals because of its superior selectivity, sensitivity and versatility over other transition metals. Furthermore, the steric and electronic properties of various palladium-ligand complexes have been studied in detail, allowing this chemistry to be used with high confidence in novel reactions.[64,65]

Various compounds, such as boronic acids, organozinc, organotin, organosilicon compounds and Grignard reagents, are involved in cross-coupling reactions. In spite of several improvements and several industrial applications, cross-coupling reactions still require the prior activation of both reagents (heteroaryl halides and heteroaryl metal derivatives). This involves a number of steps that lead to the generation of waste, solvents, and additional purification steps. In the last few years, Pd-catalyzed direct arylation of heteroaryl C-H bonds by means of aryl halides has become an attractive alternative. These reactions replace the preactivated organometallic compound, with a simple arene, reducing the amount of metal waste in the process.

Mechanistically, the interaction of the σ C-H bond orbital with the vacant metal d-orbital of Pd leads to a synergistic electron transfer between the metal- and C-H bond orbitals.[66,67] This may be accompanied by reverse donation from the filled Pd d-orbital to the σ* C-H antibonding orbital. The electronic and steric factors of the ligands and the acidity of the corresponding bonds have an effect on the C-H bond activation process. These reactions may follow different mechanisms depending on auxiliaries, organic substrate, reaction conditions and Pd oxidation state.

Generally, Pd-catalyzed C-H activation can be divided into several different catalytic cycles depending on the change of the oxidation state of the palladium catalyst, for example, Pd(0)/Pd(II) and Pd(II)/Pd(IV).[61,68]

Pd(0)/Pd(II) catalytic cycle is initiated by the oxidative addition of an aryl halide to Pd(0) for continuation of the Pd(0)/Pd(II) catalytic cycles (Scheme 10). The Pd(0)/Pd(II) catalytic cycle starts with oxidative addition of Pd(0) catalyst to organohalides (or pseudohalides), followed by C-H bond activation via concerted metalation-deprotonation (CMD) mechanism to form Pd(II) intermediate. The final step is the reductive elimination to recover the products and to regenerate the Pd(0) catalyst.[69]

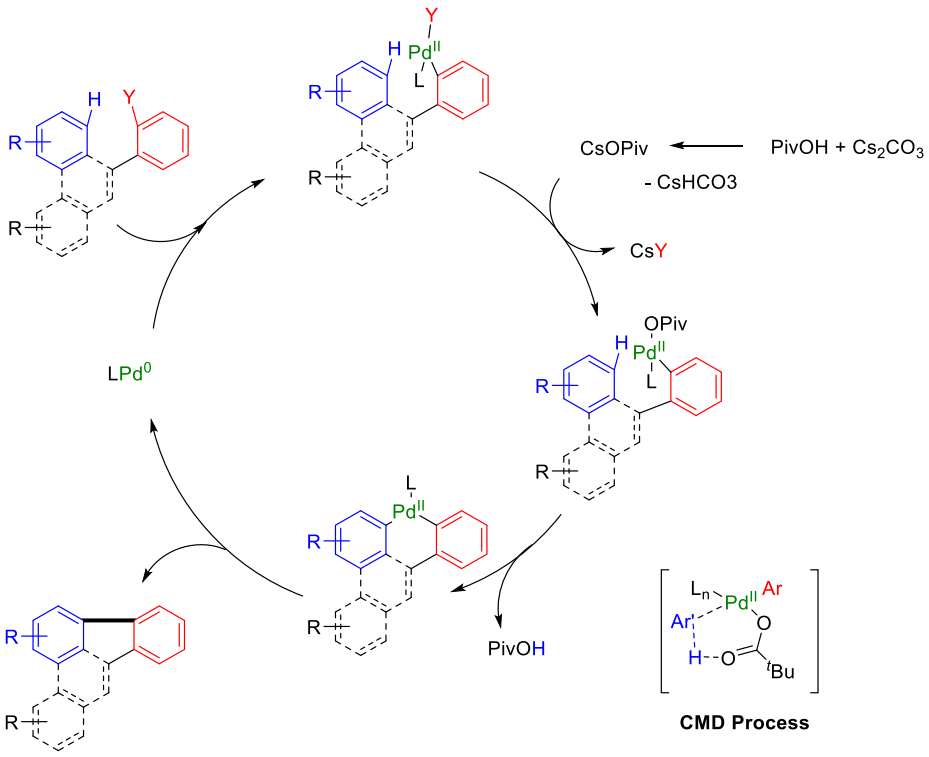

Scheme 10. Mechanism of intermolecular C-H bond activation by Pd(0)/Pd(II) catalytic mechanism.

The next type of reaction is initiated by Pd(II) catalyzed insertion of C-H into sp^3 hybridized atoms requiring mostly a directing group in the substrate and an external oxidant (Scheme 11). The first step of the reaction mechanism involves activation of the C-H substrate to form a cyclopalladium intermediate. The second step is the oxidation of Pd(II) to Pd(IV). Finally, reductive elimination completes the catalytic cycle. The active Pd(II) catalyst is regenerated by either removing an intramolecular C-C bond from the metal center.[70]

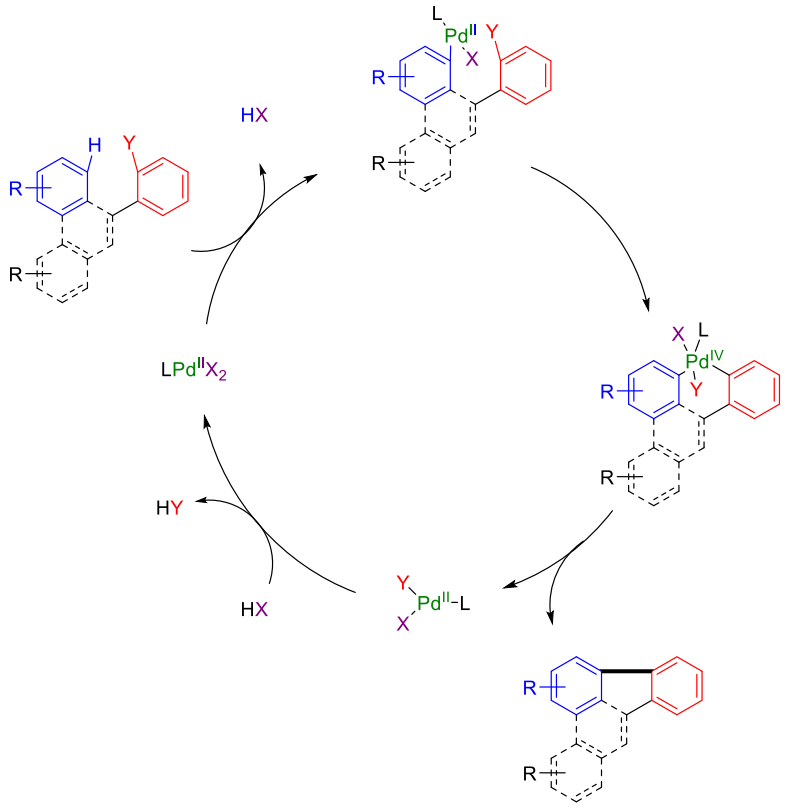

Scheme 11. Mechanism intermolecular C-H activation of Pd(II)/Pd(IV).

Due to its versatility, Pd(0)/Pd(II) catalysis has been widely used in the development of catalytic reactions. For example, in the presence of $Pd(OAc)_2$ or $PdCl_2(PhCN)_2$ catalysts, the synthesis of dibenz[*a*,*h*]anthracene and picene has been reported (Scheme 12). Dibenz[*a*,*h*]anthracene is commonly found in polluted smoke and oils and is stable and highly genotoxic. Picene is found in the tar residue from the distillation of peat tar and oil. It is of particular interest due to its constitution consisting of a combination of linear and angularly fused rings. Such polycyclic structures have been successfully used to construct J-aggregated emitting macrocycles and rigid molecular receptors.[71,72] They can be used as building blocks

for coronoidal hydrocarbons and serve as the basis for the formation of zigzag edges of topologically specific carbon nanoribbons.[73–76] These π-expanded aromatic molecules exhibit accessible redox chemistry and non-covalent interactions with a narrow energy gap between the boundary orbitals. In particular, they exhibit ultraviolet and visible near-infrared absorption and emission. Consequently, they are promising materials for various optoelectronic-, sensing- or energy conversion applications.

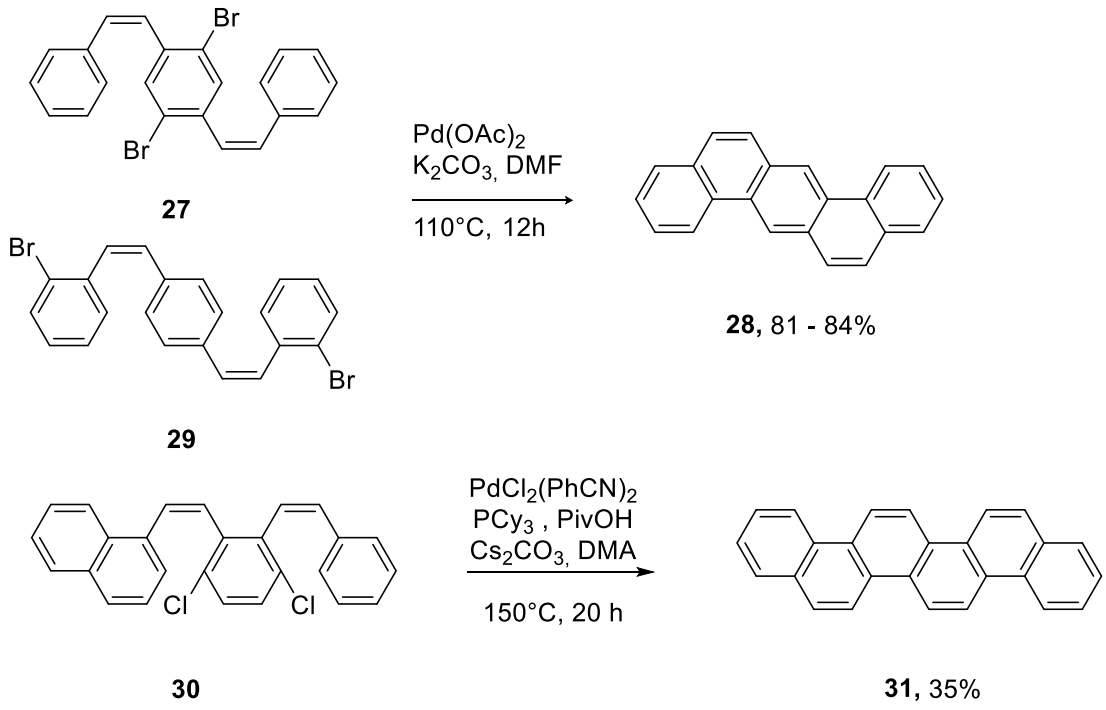

Scheme 12. Synthesis of dibenz[*a,h*]anthracene **28** and picene **31** by Pd-catalyzed intramolecular double C-H activation.

In contrast to Pd(0)/Pd(II), the redox chemistry of Pd(IV) has been less studied. However, the existence of this oxidation state has been speculated early, and evidence has been obtained subsequently. Despite the many advantages of this transformation, the use of Pd(II)/Pd(IV) catalysts has one notable limitation, namely the formation of multiple bonds, some of which may be undesirable in synthetic applications. However, this field has great potential because of the unique selectivity in some transformations.[77,78]

The dimerization process of 2-arylpyridines is the first report of C-H bond activation using Pd(IV) (Scheme 13).[79] In this system, $Pd(OAc)_2$ catalyzes the room temperature oxidative C-

H/C-H coupling of various substituted 2-arylpyridines using Oxone as the oxidant. An example of such a procedure involves conversion of two equivalents of **32**. Several additional experiments, including reactivity studies of possible intermediates, confirmed the mechanism (Scheme 13). This mechanism shows an initial activation of C-H to Pd(II), followed by oxidation of the resulting intermediate **A** by Oxone, resulting in the formation of Pd(IV) intermediate **B**. **B** then undergoes a secondary activation of the C-H bond, which then undergoes reductive elimination to form a C-C bond. The catalytic cycle is completed with the formation of product **33**.

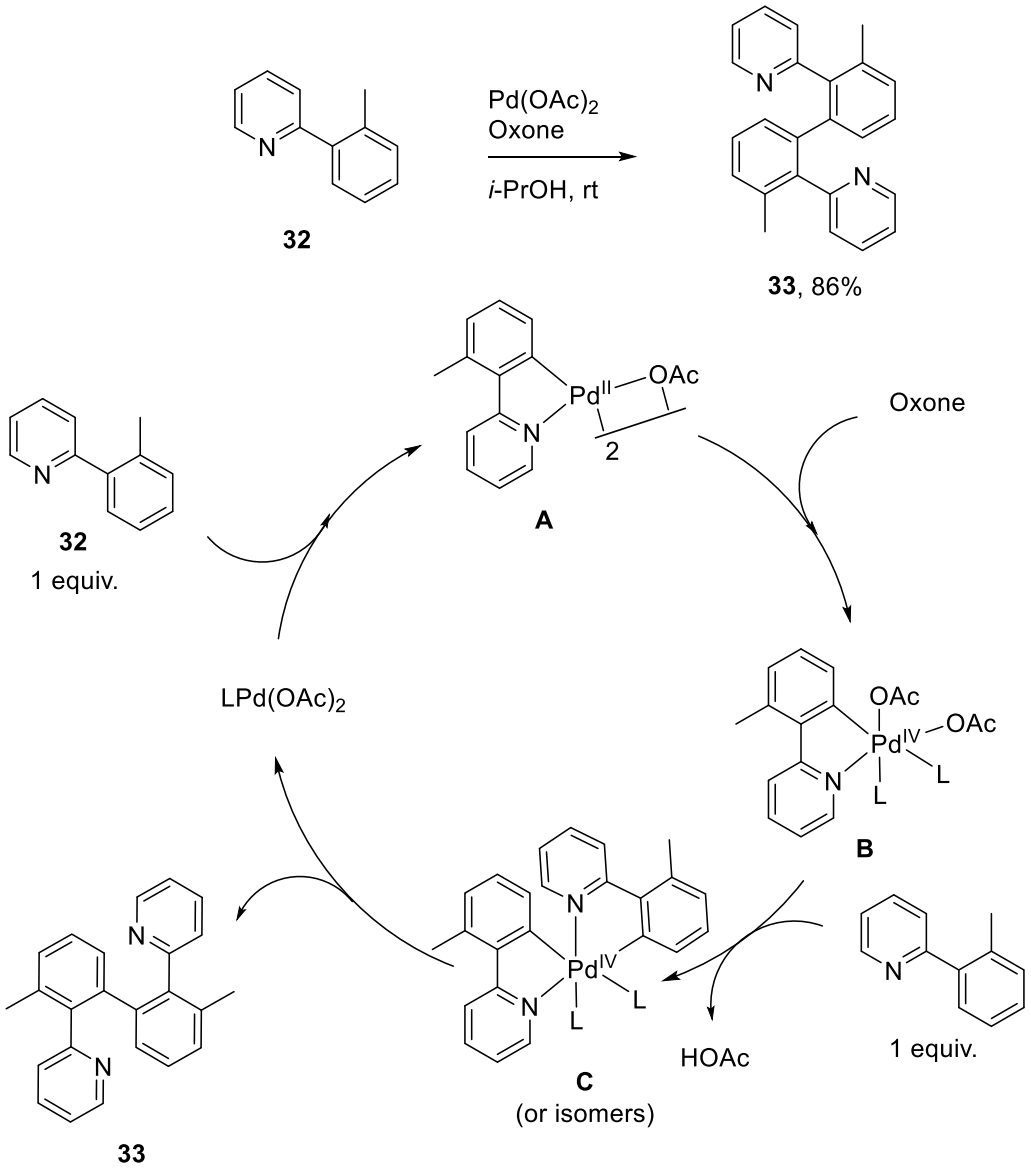

Scheme 13. Oxidative coupling of 2-arylpyridine derivatives via proposed C–H activation at Pd(IV).

Simultaneously to the employment of transition metal catalyzed CH-activation methodologies, the development of improved synthetic protocols for S_EAr reaction have evolved in recent years. In the focus of these achievements are the design of more sophisticated reaction conditions which avoid the use of stoichiometric amounts of toxic Lewis acids or the formation of toxic waste, respectively. One promising approach are cycloisomerization reactions which are formally atom-economic. When employed with less toxic catalysts this type of reaction could overcome the aforementioned drawbacks of S_EAr reactions.

Cycloisomerization is the transformation of non-cyclic starting materials into cyclic compounds. These reactions often involve the formation of carbon-carbon or carbon-heteroatom bonds and are effective in promoting the formation of complex cyclic structures. These cyclic arrangements, a type of C-H bond activation, can be diverse and provide unique opportunities for the synthesis of diverse molecules.

The most important advantage of cycloisomerization reactions is their atom economy. There is no loss of atoms in these transformations because every atom in the starting material is present in the final product. As a result, cycloisomerization is an efficient method of synthesis, maximizing the use of starting materials and minimizing waste.[80,81]

One versatile method to construct polycyclic aromatic compounds and fused five-, six-, and seven-membered ring systems are intramolecular cycloisomerizations of 2-alkynyl-biarylderivatives by Lewis and Brønsted acids, giving rise to diverse and complex cyclic compounds, such as phenanthrenes by 6-endo-dig- cyclization.[82] In the presence of terminal substituents, the formation of dibenzofulvenes, fluorenes and benzofurans by 5-exo-dig-cyclization and dibenzocycloheptene by 7-endo-dig-cyclization is also possible.[83–85] The transformations are characterized by remarkable functional group tolerance and the use of mild reaction conditions.

Phenanthrene and its derivatives have biological activity and are used in medicine to produce antiviral, antitumor, anti-inflammatory and antioxidant drugs.[86] In addition to medical applications, they also have a wide range of uses in various fields, including photoconductive, photochemical, electroluminescent and fluorescent materials.[87]

Over the past decade, the development of more sophisticated cycloisomerization protocols has seen continuous development.[88–93] For example, research in Lewis and/or Brønsted acids is aimed at developing more versatile, more selective and more reactive catalysts. Each line of

research synergistically supports and influences the others. However, the full potential of catalysts based on Lewis and Brønsted acids on this reaction has not yet been fully realized.

Lewis acid catalysts such as aluminium, boron, silicon, tin, etc., as well as d-block metal salts (titanium, zirconium, iron, copper, zinc, platinum, etc.) form adducts with electron-rich triple bonds.[37] The alkynophilic character of certain Lewis acids lead to activation of the unsaturated substrate promoting the formation of a η^2-complex with the alkyne which in the following reacts with the adjacent aromatic ring, forming a novel C-C bond and releasing the Lewis acid catalyst (Scheme 14).[94]

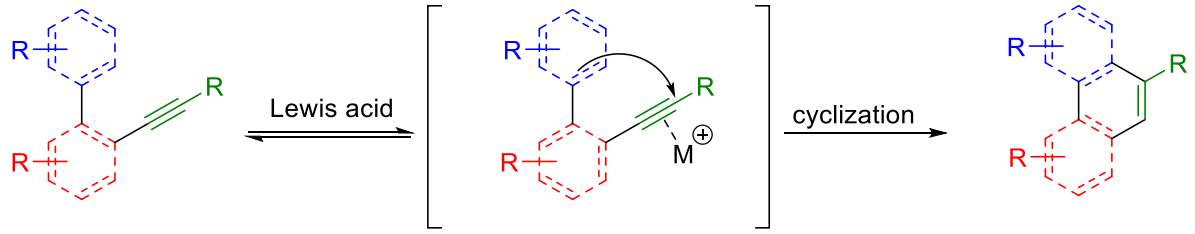

Scheme 14. Mechanism of the Lewis acid catalysed cycloisomerization reaction.[95]

Late transition metals such as gold, copper, platinum or mercury are especially known for their affinity to π-electrons and hence, are used for various reactions using triple bond containing substrates.[96,97] However, their practical use may be limited by their high cost, limited availability and/or toxicity. In addition, Lewis acids are often sensitive to air and moisture (e.g., $AlCl_3$). They may also be present as contaminants in products which is problematic in their later application as pharmaceuticals or within electronic devices. As a result, there has been interest in new metal-free catalytic methods using, for instance, Brønsted acids.

Protonation of the carbon-carbon triple bond leads to activation of the π-system and electron density redistribution with formation of a new carbo-carbon bond. Subsequent deprotonation releases the catalyst of this intramolecular cycloisomerization.[89] Alternatively, protonation of the triple bond may lead to formation of an alkenyl-carbocation which undergoes electrophilic aromatic substitution (Scheme 15).

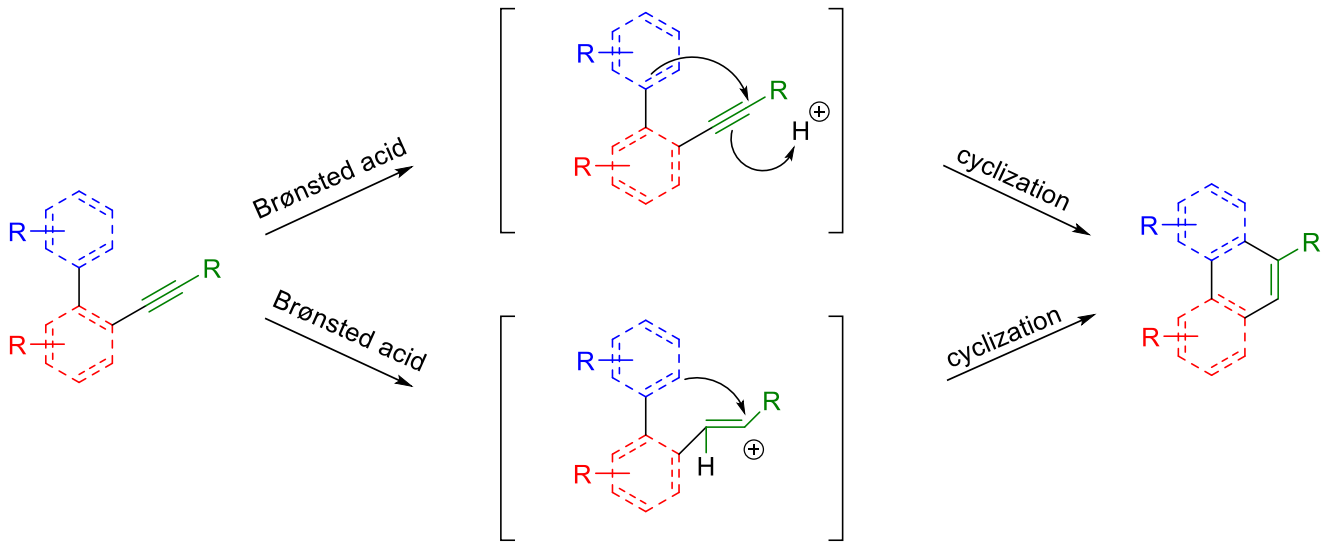

Scheme 15. Mechanism of the Bronsted acid cycloisomerization reaction.

As an example, phenanthrene can be obtained by employment of various reaction conditions using common Lewis acids such as $AlCl_3$, $InCl_3$, $PtCl_2$ as well as very rare ones such as $Nd(OTf)_3$ (Scheme 16).[83,94,95,98,99] In addition, phenanthrenes can also be obtained by metal-free synthesis with Brønsted acids, for example with TfOH. A selective, electrophilic attack of the β-carbon by the proton leads, analogously to the reaction with Lewis acids, to the formation of an alkenyl cation, which in turn is intercepted by the adjacent aromatic ring with concomitant deprotonation to give phenanthrene.[83]

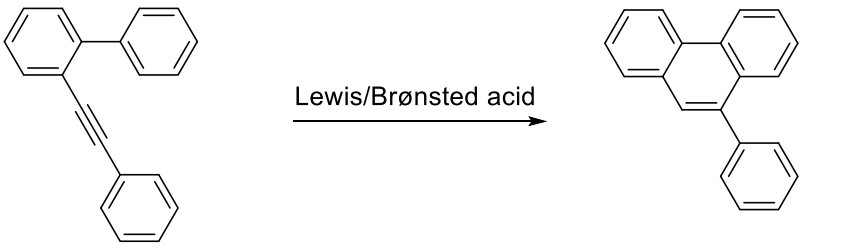

34

35

52% ($AlCl_3$)
57% ($Nd(OTf)_3$)
66% (TfOH)

Scheme 16. Synthesis of phenanthrenes by Lewis and Brønsted acids.

Cycloisomerization by Lewis- and Brønsted acids can also occur in heteroaromatic structures, for example in the synthesis of benzo[*h*]quinolines (Scheme 17). Benzo[*h*]quinolines as well as phenanthrenes are of great importance in the pharmaceutical industry and as ligands in transition metal catalysis or materials science.[100–105]

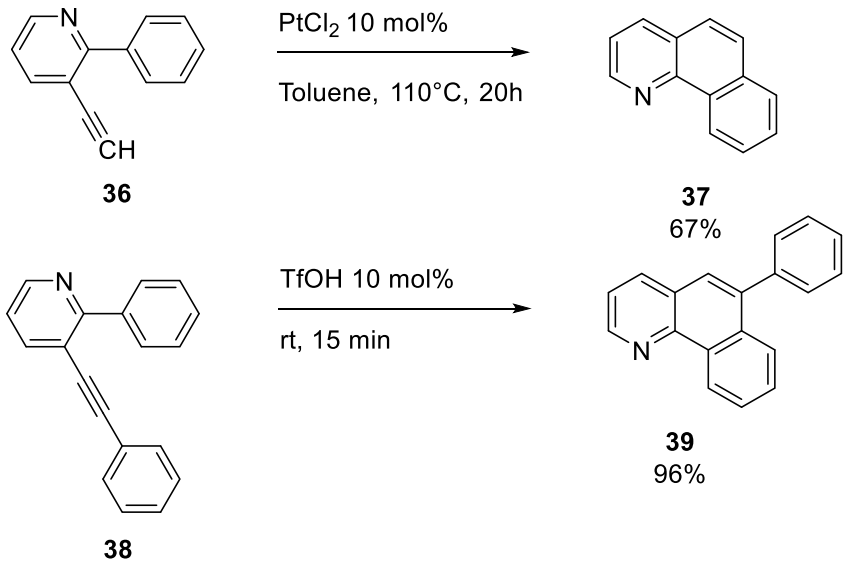

Scheme 17. Synthesis of benzo[*h*]quinolines by Lewis and Brønsted acids.[106]

Another example for the synthesis of heteroatom-doped polycyclic aromatic hydrocarbons are Ullazines. The Ullazine chromophore is a 16-π-electron heterocycle, isoelectric to pyrene and has been employed in dye-sensitized solar cells and charge transfer materials for organic field effect transistors.[15,107–109] Hence, the development of novel synthetic methods e.g. by cycloisomerization has experienced strong development in recent years (Scheme 18). Grätzel et. al. reported the synthesis of Ullazine by cycloisomerization using $InCl_3$ as Lewis acid. Later the groups of Langer synthesized respective aza-analogue using *p*TsOH as Brønsted acid.[110–113]

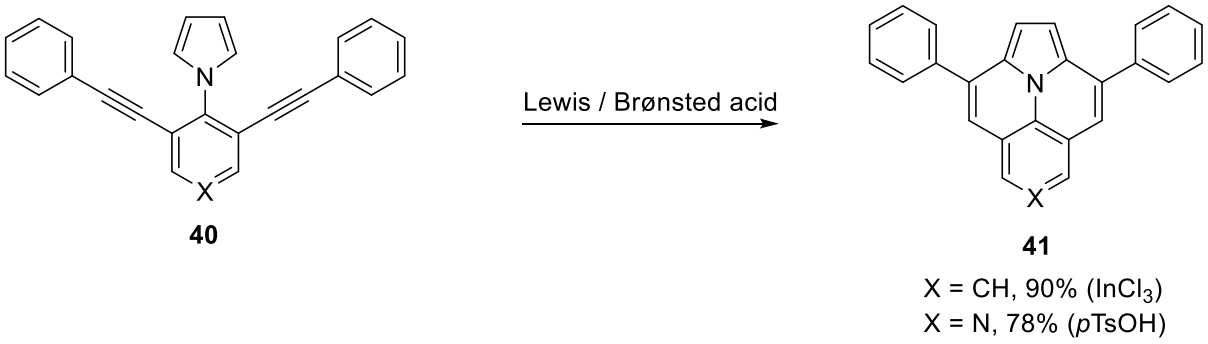

Scheme 18. Synthesis of ullazines and aza-ullazines by Lewis and Brønsted acids.

In conclusion, several approaches to the synthesis of novel CH-activation reactions have been developed for the synthesis of (heterocyclic) PAHs in recent years. One of the most employed and versatile methods are Palladium catalyzed CH activation which have been used for a huge number of known and unknown PAHs with interesting properties for application in the pharmaceutical sector or as compartments of electronic devices. Besides Palladium catalysis, the development of alternative synthetic strategies for PAH construction is a subject of ongoing research. One of these alternative approaches is the execution of cycloisomerization from 2-alkynyl-biaryl derivatives leading cyclized products formally with 100% atom economy. This methodology represents a new technique to the synthesis of novel PAHs which are structurally hard accessible by other methods and hence, several new (heterocyclic)-PAH could be synthesized and characterized using cycloisomerization.

Overview and Aim of the Research

The main objective of this study is to combine two synthetic strategies to obtain novel heterocyclic polyaromatic hydrocarbons and to study their optical and electrochemical characteristics. The main focus of these studies is the development of methodologies which are based CH-activation reaction. In this context, cycloisomerization and Palladium catalyzed CH-activation reaction were employed as key reaction steps to execute the envisioned ring-closing reactions.

As part of this research, five projects have been carried out, the completion of which has resulted in the preparation and publication of four scientific papers and one submitted paper.

New synthetic routes for the preparation of polycyclic heteroaromatic hydrocarbons were studied in Brønsted and Lewis acid mediated cycloisomerization reactions as well as in Pd-catalyzed C-H activation reactions. More than 80 unknown compounds were obtained in good to very good yields. All planned syntheses were successful except for some limitations.

All obtained products have been characterized by typical analytical methods, including NMR, IR, MS and single crystal structure analysis. Selected compounds were additionally studied towards their optical and electrochemical properties. In this regard, UV/Vis absorption and emission measurements, including solvatochromism and acidochromism were performed. Electrochemical characteristics were obtained by cyclic voltammetry and differential pulse voltammetry and density functional theory calculations were carried out for some derivatives.

In particular, in this research study, benzo[*h*]imidazo[1,2-*a*]quinolines and 1,2*a*-diazadibenzo[*cd*,*f*]azulenes were prepared by cycloisomerization under the presence of Brønsted acids.

In the synthesis of, Pd-catalyzed C-H bond activation was employed for the synthesis of diindenopyrene and its aza-analogues. This approach was further adopted to the synthesis of benzo[4,10]anthra[9,1-*gh*]isoquinolines, 1*H*-pyrrolo[3',2': 3,4]fluoreno[9,1-*gh*]quinolines and 7*H*-pyrrolo[2',3',4':4,10]anthra[1,9-*fg*]quinolines.

References

[1] S. Albanese, B. Fontaine, W. Chen, A. Lima, C. Cannatelli, A. Piccolo, S. Qi, M. Wang, B. De Vivo, *Environ. Geochem. Health* **2015**, *37*, 1–20.

[2] A. Grčić, L. Ilijin, D. Matić, A. Filipović, M. Mrdaković, D. Todorović, V. Perić-Mataruga, *Environ. Pollut.* **2021**, *288*.

[3] B. Bukowska, K. Mokra, J. Michałowicz, *Int. J. Mol. Sci.* **2022**, *23*.

[4] G. Liu, J. Niu, W. Guo, X. An, L. Zhao, *Chemosphere* **2016**, *163*, 461–470.

[5] Q. Li, Y. Zhang, Z. Xie, Y. Zhen, W. Hu, H. Dong, *J. Mater. Chem. C* **2022**, *10*, 2411–2430.

[6] L. Ripani, E. Bombonato, F. Paolucci, M. Marcaccio, *Curr. Opin. Electrochem.* **2022**, *35*.

[7] J. Wagner, P. Zimmermann Crocomo, M. Andrzej Kochman, A. Kubas, P. Data, M. Lindner, **2022**, *61*, e202202210.

[8] A. Hepp, H. Heil, W. Weise, M. Ahles, R. Schmechel, H. von Seggern, *Phys. Rev. Lett.* **2003**, *91*.

[9] R. M. Christie, *Handbook of Textile and Industrial Dyeing*, **2011**.

[10] Y. Wang, H. Wang, Y. Liu, C. A. Di, Y. Sun, W. Wu, G. Yu, D. Zhang, D. Zhu, *J. Am. Chem. Soc.* **2006**, *128*, 13058–13059.

[11] D. M. Nanditha, M. Dissanayake, A. A. D. T. Adikaari, R. J. Curry, R. A. Hatton, S. R. P. Silva, *Appl. Phys. Lett.* **2007**, *90*.

[12] T. M. Figueira-Duarte, K. Müllen, *Chem. Rev.* **2011**, *111*, 7260–7314.

[13] F. P. Kinik, A. Ortega-Guerrero, D. Ongari, C. P. Ireland, B. Smit, *Chem. Soc. Rev.* **2021**, *50*, 3143–3177.

[14] J. Wagner, D. Kumar, M. A. Kochman, T. Gryber, M. Grzelak, A. Kubas, P. Data, M. Lindner, *ACS Appl. Mater. Interfaces* **2023**, *15*, 37728–37740.

[15] C. Cebrián, *J. Mater. Chem. C* **2018**, *6*, 11943–11950.

[16] Q. Xiao, T. Sakurai, T. Fukino, K. Akaike, Y. Honsho, A. Saeki, S. Seki, K. Kato, M. Takata, T. Aida, *J. Am. Chem. Soc.* **2013**, *135*, 18268–18271.

[17] M. Kivala, W. Pisula, S. Wang, A. Mavrinskiy, J. P. Gisselbrecht, X. Feng, K. Müllen, *Chem. Eur. J.* **2013**, *19*, 8117–8128.

[18] B. He, A. B. Pun, L. M. Klivansky, A. M. McGough, Y. Ye, J. Zhu, J. Guo, S. J. Teat, Y. Liu, *Chem. Mater.* **2014**, *26*, 3920–3927.

[19] M. A. Squillaci, G. Markiewicz, A. Walczak, A. Ciesielski, A. R. Stefankiewicz, P. Samorì, *Chem. Commun.* **2017**, *53*, 9713–9716.

[20] S. Ito, Y. Tokimaru, K. Nozaki, *Angew. Chem.* **2015**, *127*, 7364–7368.

[21] Q. Tang, Z. Liang, J. Liu, J. Xu, Q. Miao, *Chem. Commun.* **2010**, *46*, 2977–2979.

[22] Z. Liang, Q. Tang, J. Xu, Q. Miao, *Adv. Mater.* **2011**, *23*, 1535–1539.

[23] H. T. Black, D. F. Perepichka, *Angew. Chem. Int. Ed.* **2014**, *53*, 2138–2142.

[24] Y. Xu, J. Chen, Z. Xiao, C. Ou, W. Lv, L. Tao, S. Zhong, *Nanoscale* **2019**, *11*, 15881–15891.

[25] A. Hamd Hssain, B. Gündüz, A. Majid, N. Bulut, *Chem. Phys. Lett.* **2021**, *780*.

[26] L. Tao, J. Zhao, J. Chen, C. Ou, W. Lv, S. Zhong, *Nanoscale Adv.* **2021**, *3*, 3199–3215.

[27] A. Gupta, S. Sasan, A. Kour, N. Nelofar, D. Manikrao Mondhe, K. K. Kapoor, *Synth. Commun.* **2019**, *49*, 1813–1822.

[28] J. Liu, D. Zuo, T. Jing, M. Guo, L. Xing, W. Zhang, J. Zhao, J. Shen, P. Gong, D. Zhang, X. Zhai, *Bioorg. Med. Chem.* **2017**, *25*, 4088–4099.

[29] Q. H. Teng, X. J. Peng, Z. Y. Mo, Y. L. Xu, H. T. Tang, H. S. Wang, H. Bin Sun, Y. M. Pan, *Green Chem.* **2018**, *20*, 2007–2012.

[30] C. Xie, H. Koshino, Y. Esumi, J. ichi Onose, K. Yoshikawa, N. Abe, *Bioorg. Med. Chem. Lett.* **2006**, *16*, 5424–5426.

[31] Y. Q. Ye, H. Koshino, J. I. Onose, K. Yoshikawa, N. Abe, S. Takahashi, *Org. Lett.* **2009**, *11*, 5074–5077.

[32] K. C. Nicolaou, *Proc. R. So.* **2014**, *470*.

[33] D. P. Khambhati, T. L. Nelson, *Sustainable Strategies in Organic Electronics*, Elsevier, **2022**, 209–227.

[34] K. R. Campos, P. J. Coleman, J. C. Alvarez, S. D. Dreher, R. M. Garbaccio, N. K. Terrett, R. D. Tillyer, M. D. Truppo, E. R. Parmee, *Science* **2019**, *363*.

[35] B. Galabov, D. Nalbantova, P. V. R. Schleyer, H. F. Schaefer, *Acc Chem Res* **2016**, *49*, 1191–1199.

[36] F. Roudesly, J. Oble, G. Poli, *J Mol Catal A Chem* **2017**, *426*, 275–296.

[37] Hisashi. Yamamoto, *Lewis Acids in Organic Synthesis*, Wiley-VCH, **2000**.

[38] D. Gallego, E. A. Baquero, *Open Chem.* **2018**, *16*, 1001–1058.

[39] S. H. Yang, S. Jo, D. Shin, *Synlett* **2017**, *28*, 1614–1619.

[40] S. Hu, Z. Lu, M. Liu, H. Xu, J. Wu, F. Chen, *J. Org. Chem.* **2020**, *85*, 14916–14925.

[41] T. Dalton, T. Faber, F. Glorius, *ACS Cent. Sci.* **2021**, *7*, 245–261.

[42] T. Rogge, N. Kaplaneris, N. Chatani, J. Kim, S. Chang, B. Punji, L. L. Schafer, D. G. Musaev, J. Wencel-Delord, C. A. Roberts, R. Sarpong, Z. E. Wilson, M. A. Brimble, M. J. Johansson, L. Ackermann, *Nat. Rev. Methods Primers* **2021**, *1*.

[43] R. H. Crabtree, A. Lei, *Chem. Rev.* **2017**, *117*, 8481–8482.

[44] Z. Lin, *Coord. Chem. Rev.* **2007**, *251*, 2280–2291.

[45] Y. Boutadla, D. L. Davies, S. A. Macgregor, A. I. Poblador-Bahamonde, *Dalton Trans.* **2009**, 5832–5840.

[46] B. Nie, W. Wu, Y. Zhang, H. Jiang, J. Zhang, *Org. Chem. Front.* **2020**, *7*, 3067–3099.

[47] S. T. J. Ryan, M. J. Fuchter, *Helicenes* **2022**, 473–503.

[48] Y. Shen, C. F. Chen, *Chem. Rev.* **2012**, *112*, 1463–1535.

[49] T. Chao, Z. H. Su, K. W. Yen, M. J. Wu, J. H. Chu, *J. Org. Chem.* **2020**, *85*, 5559–5569.

[50] A. Swain, P. Ravat, *Org. Chem. Front.* **2023**, *10*, 3714–3725.

[51] L. Ilies, *Bull. Chem. Soc. Jpn.* **2021**, *94*, 404–417.

[52] N. Yoshikai, A. Matsumoto, J. Norinder, E. Nakamura, *Angew. Chem. Int. Ed.* **2009**, *48*, 2925–2928.

[53] L. Shi, X. Zhong, H. She, Z. Lei, F. Li, *Chem. Commun.* **2015**, *51*, 7136–7139.

[54] K. P. Bryliakov, E. P. Talsi, *Coord. Chem. Rev.* **2014**, *276*, 73–96.

[55] P. K. Dutta, M. K. Ravva, S. Sen, *J. Org. Chem.* **2019**, *84*, 1176–1184.

[56] K. Sakata, M. Eda, Y. Kitaoka, T. Yoshino, S. Matsunaga, *J. Org. Chem.* **2017**, *82*, 7379–7387.

[57] J. Norinder, A. Matsumoto, N. Yoshikai, E. Nakamura, *J. Am. Chem. Soc.* **2008**, *130*, 5858–5859.

[58] C. S. Horbaczewskyj, I. J. S. Fairlamb, *Org. Process Res. Dev.* **2022**, *26*, 2240–2269.

[59] P. Devendar, R. Y. Qu, W. M. Kang, B. He, G. F. Yang, *J. Agric. Food Chem.* **2018**, *66*, 8914–8934.

[60] N. Hussain, A. Hussain, *RSC Adv.* **2021**, *11*, 34369–34391.

[61] J. He, M. Wasa, K. S. L. Chan, Q. Shao, J. Q. Yu, *Chem. Rev.* **2017**, *117*, 8754–8786.

[62] X. Chen, K. M. Engle, D. H. Wang, Y. Jin-Quan, *Angew. Chem. Int. Ed.* **2009**, *48*, 5094–5115.

[63] R. Jana, T. P. Pathak, M. S. Sigman, *Chem. Rev.* **2011**, *111*, 1417–1492.

[64] A. Biffis, P. Centomo, A. Del Zotto, M. Zecca, *Chem. Rev.* **2018**, *118*, 2249–2295.

[65] B. P. Fors, D. A. Watson, M. R. Biscoe, S. L. Buchwald, *J. Am. Chem. Soc.* **2008**, *130*, 13552–13554.

[66] B. A. Vastine, M. B. Hall, *Coord. Chem. Rev.* **2009**, *253*, 1202–1218.

[67] D. H. Ess, W. A. Goddard, R. A. Periana, *Organometallics* **2010**, *29*, 6459–6472.

[68] L. M. Xu, B. J. Li, Z. Yang, Z. J. Shi, *Chem. Soc. Rev.* **2010**, *39*, 712–733.

[69] D. Kim, G. Choi, W. Kim, D. Kim, Y. K. Kang, S. H. Hong, *Chem. Sci.* **2021**, *12*, 363–373.

[70] J. J. Topczewski, M. S. Sanford, *Chem. Sci.* **2015**, *6*, 70–76.

[71] J. M. W. Chan, J. R. Tischler, S. E. Kooi, V. Bulović, T. M. Swager, *J. Am. Chem. Soc.* **2009**, *131*, 5659–5666.

[72] S. C. Zimmerman, Z. Zeng, W. Wu, D. E. Reichert, *J. Am. Chem. Soc.* **1991**, *113*, 18.

[73] I. Gutman, S. J. Cyvin, *Introduction to the Theory of Benzenoid Hydrocarbons*, Springer Berlin, Heidelberg, **2012**.

[74] P. Ruffieux, S. Wang, B. Yang, C. Sanchez-Sanchez, J. Liu, T. Dienel, L. Talirz, P. Shinde, C. A. Pignedoli, D. Passerone, T. Dumslaff, X. Feng, K. Müllen, R. Fasel, *Nature* **2016**, *531*, 489–492.

[75] B. Yang, Y. Gu, G. M. Paternò, J. Teyssandier, A. Maghsoumi, A. J. Barker, K. S. Mali, F. Scotognella, S. De Feyter, M. Tommasini, X. Feng, A. Narita, K. Müllen, *Chem. Eur. J.* **2023**, *29*.

[76] Y. Y. Wu, Y. L. Wu, C. L. Lin, H. C. Chen, Y. Y. Chuang, C. H. Chen, C. M. Chou, *Org. Lett.* **2023**, *25*, 7763–7768.

[77] J. J. Topczewski, M. S. Sanford, *Chem. Sci.* **2015**, *6*, 70–76.

[78] C. Santiago, N. Sotomayor, E. Lete, *Molecules* **2020**, *25*.

[79] K. L. Hull, E. L. Lanni, M. S. Sanford, *J. Am. Chem. Soc.* **2006**, *128*, 14047–14049.

[80] L. Deiana, E. Badali, A. A. Rafi, C. W. Tai, J. E. Bäckvall, A. Córdova, *ACS Catal.* **2023**, *13*, 10418–10424.

[81] J. L. M. Matos, S. A. Green, Y. Chun, V. Q. Dang, R. G. Dushin, P. Richardson, J. S. Chen, D. W. Piotrowski, B. M. Paegel, R. A. Shenvi, *Angew. Chem. Int. Ed.* **2020**, *59*, 12998-13003.

[82] J. Gicquiaud, A. Hacıhasanoğlu, P. Hermange, J. M. Sotiropoulos, P. Y. Toullec, *Adv. Synth. Catal.* **2019**, *361*, 2025–2030.

[83] J. Zhang, S. Li, Y. Qiao, C. Peng, X. N. Wang, J. Chang, *Chem. Commun.* **2018**, *54*, 12455–12458.

[84] K. Alam, S. W. Hong, K. H. Oh, J. K. Park, *Angew. Chem.* **2017**, *129*, 13572–13576.

[85] K. Sprenger, C. Golz, M. Alcarazo, *Eur. J. Org. Chem.* **2020**, *2020*, 6245–6254.

[86] S. Song, X. Li, J. Guo, C. Hao, Y. Feng, B. Guo, T. Liu, Q. Zhang, Z. Zhang, R. Li, J. Wang, B. Lin, F. Li, D. Zhao, M. Cheng, *Org. Biomol. Chem.* **2015**, *13*, 3803–3818.

[87] A. M. Machado, M. Munaro, T. D. Martins, L. Y. A. Dávila, R. Giro, M. J. Caldas, T. D. Z. Atvars, L. C. Akcelrud, *Macromolecules* **2006**, *39*, 3398–3407.

[88] W. Yang, A. Lucotti, M. Tommasini, W. A. Chalifoux, *J. Am. Chem. Soc.* **2016**, *138*, 9137–9144.

[89] M. F. Baig, S. P. Shaik, N. H. Krishna, N. K. Chouhan, A. Alarifi, A. Kamal, *Eur. J. Org. Chem.* **2017**, *2017*, 4026–4034.

[90] Y. B. Chen, P. C. Qian, L. W. Ye, *Chem. Soc. Rev.* **2020**, *49*, 8897–8909.

[91] J. Gicquiaud, B. Abadie, K. Dhara, M. Berlande, P. Hermange, J. M. Sotiropoulos, P. Y. Toullec, *Chem. Eur. J.* **2020**, *26*, 16266–16271.

[92] X. Ju, X. Hu, H. Shi, S. Ma, F. He, X. Wang, X. Xie, X. She, *Org. Chem. Front.* **2021**, *8*, 4839–4844.

[93] J. R. Ludwig, R. B. Watson, D. J. Nasrallah, J. B. Gianino, P. M. Zimmerman, R. A. Wiscons, C. S. Schindler, *Science* **2018**, *361*, 1363-1369.

[94] A. Fürstner, V. Mamane, *J. Org. Chem.* **2002**, *67*, 6264–6267.

[95] A. Fürstner, V. Mamane, *Chem. Commun.* **2003**, *3*, 2112–2113.

[96] H. Lu, T. Y. Yu, P. F. Xu, H. Wei, *Chem. Rev.* **2021**, *121*, 365–411.

[97] T. Wu, W. Tang, *Chem. Eur. J.* **2021**, *27*, 3944–3956.

[98] D. Xu, R. Jin, W. Liu, F. Ba, Y. Li, A. Ding, H. Guo, *Tetrahedron Lett.* **2016**, *57*, 3235–3238.

[99] Y. Li, Y. Wang, D. Xu, R. Jin, G. Gu, H. Guo, *Synlett* **2017**, *28*, 2159–2162.

[100] H. R. P. Naik, H. S. B. Naik, T. R. R. Naik, D. S. Lamani, T. Aravinda, *Phosphorus, Sulfur Silicon Relat. Elem.* **2010**, *185*, 355–360.

[101] H. R. P. Naik, H. S. B. Naik, T. R. R. Naik, H. R. Naika, K. Gouthamchandra, R. Mahmood, B. M. K. Ahamed, *Eur. J. Med. Chem.* **2009**, *44*, 981–989.

[102] H. Paritala, S. M. Firestine, *Bioorg. Med. Chem. Lett.* **2009**, *19*, 1584–1587.

[103] P. Stoessel, D. Joosten, N. Koenen, *Polycyclic compounds*, **2016**, US 2016/0204358.

[104] T. Tokuda, D. Tanaka, *Compound, Light-Emitting Element Containing the Same, Display Device, and Lighting Device*, **2023**, US 11,605,780 B2.

[105] D.-M. Kang, M.-S. Kang, C.-J. Shin, N.-H. Lee, H.-K. Jung, M.-Y. Chae, *Compound for an Organic Optoelectronic Device, Organic Light Emitting Diode Including the Same, and Display Including the Organic Light Emitting Diode*, **2012**, US 2012/0280613.

[106] A. N. Shestakov, A. S. Pankova, M. A. Kuznetsov, *Chem. Heterocycl. Compd.* **2017**, *53*, 1103–1113.

[107] D. Miao, C. Aumaitre, J. F. Morin, *J. Mater. Chem. Mater.* **2019**, *7*, 3015–3024.

[108] S. Mathew, N. A. Astani, B. F. E. Curchod, J. H. Delcamp, M. Marszalek, J. Frey, U. Rothlisberger, M. K. Nazeeruddin, M. Grätzel, *J. Mater. Chem. A* **2016**, *4*, 2332–2339.

[109] W. Wang, F. Hanindita, Y. Hamamoto, Y. Li, S. Ito, *Nat. Commun.* **2022**, *13*.

[110] S. Boldt, S. Parpart, A. Villinger, P. Ehlers, P. Langer, *Angew. Chem.* **2017**, *129*, 4646–4649.

[111] J. H. Delcamp, A. Yella, T. W. Holcombe, M. K. Nazeeruddin, M. Grätzel, *Angew. Chem. Int. Ed.* **2013**, *52*, 376–380.

[112] N. A. Drigo, S. Paek, A. J. Huckaba, P. A. Schouwink, N. Tabet, M. K. Nazeeruddin, *Chem. Eur. J.* **2017**, *23*, 17209–17212.

[113] C. Li, Y. Liu, Z. Sun, J. Zhang, M. Liu, C. Zhang, Q. Zhang, H. Wang, X. Liu, *Org. Lett.* **2018**, *20*, 2806–2810.

Contribution in Research Paper

Original research articles describing the research presented in this thesis are presented in the following paragraphs. My advisors, Professor Peter Langer and Dr. Peter Ehlers, played an important role in this process: they directed and coordinated the research, discussed scientific aspects and results, provided the necessary infrastructure, and revised the manuscripts.

My contribution to preparing the article is as follows:

Manuscript I Publication status: published; *J. Org. Chem.* **2023**, *88 (13)*, 7929–7939.

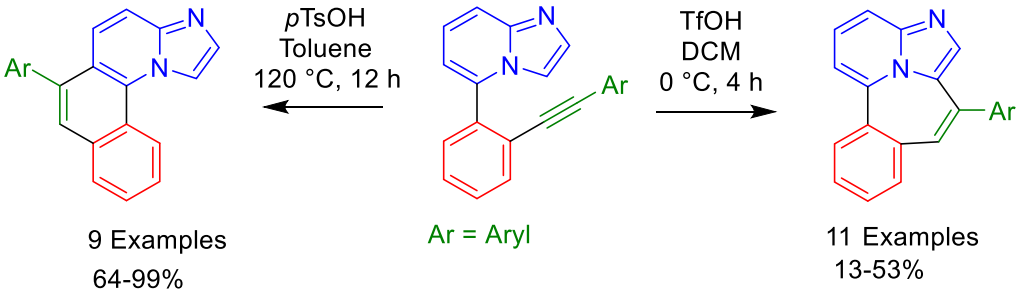

I have planned and carried out the experimental work described in the manuscript. The measurement, analysis and characterization of the optical and electrochemical properties as well as the theoretical aspects including the calculation of the quantum mechanical theory of some of the synthesized substances were performed by me under the supervision of Dr. Peter Ehlers. Dr. Alexander Villinger contributed by performing and evaluating single crystal X-ray diffraction experiments. I wrote the manuscript and the supporting information. All authors contributed to revising the paper before publication.

Own contribution: about 80%.

Manuscript II Publication status: published; *Tetrahedron.* **2023***, 135,* 133335.

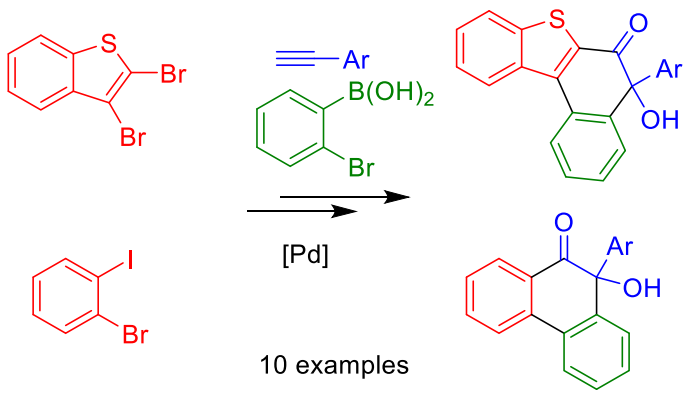

I carried out part of the main synthetic work described in the manuscript in co-operation with my colleague Dr. Erich Ammon. Dr. Alexander Villinger contributed by performing and evaluating single crystal X-ray diffraction experiments. Prof. Dr. Dr. h.c. mult. Peter Langer and Erich Ammon wrote the manuscript and the supporting information. All authors contributed to the revision of the manuscript before publication.

Own contribution: about 25%.

Manuscript III Publication status: published; *Eur. J. Org. Chem.* **2023**, e202301101.

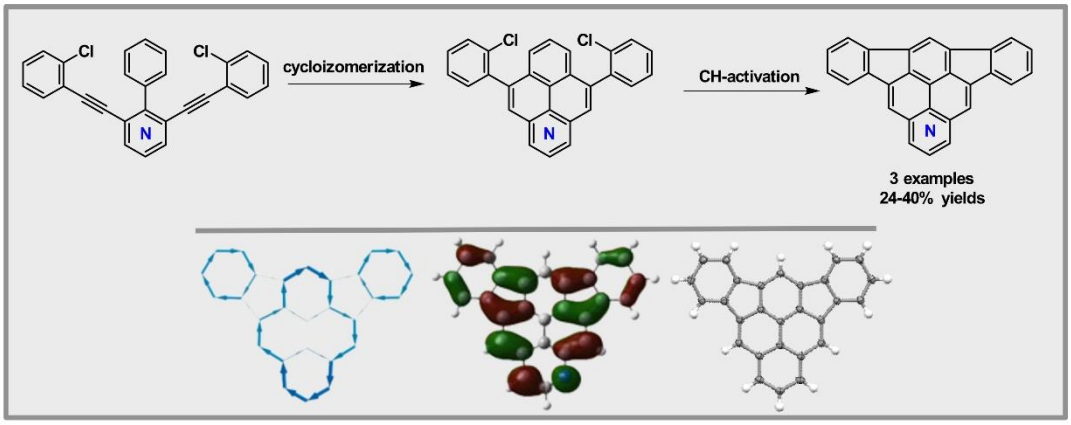

I carried out the basic synthetic work described in the manuscript. Under my supervision, Niels Hildebrandt contributed by some experimentation on the synthesis of diindenopyrene under my supervision. I was responsible for measuring, analyzing and characterizing optical and electrochemical properties and for theoretical aspects, including the calculation of density functional theory and time-dependent density functional theory, under the supervision of Dr. Peter Ehlers. Dr. Alexander Villinger contributed by performing and evaluating single crystal X-ray diffraction experiments. I wrote part of the manuscript and the supporting information. Prof. Dr. Dr. h.c. mult. Peter Langer and Dr. Peter Ehlers wrote the other part of the manuscript. All authors contributed to the revision of the manuscript before publication.

Own contribution: about 65%.

Manuscript IV Publication status: accepted; *Eur. J. Org. Chem.* **2024**, e202301299.

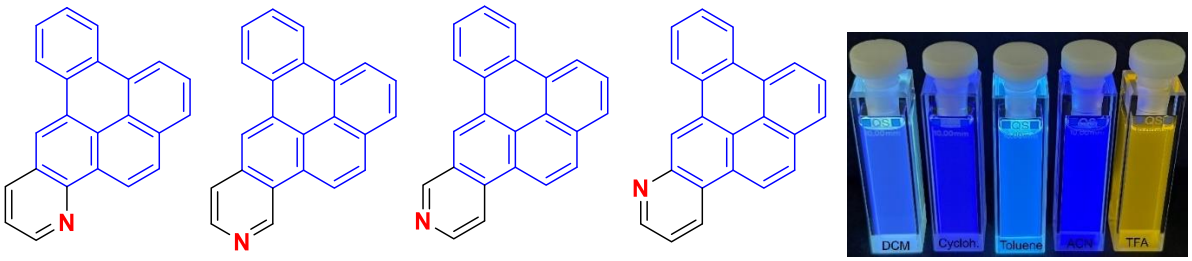

Solvatochromism

I have planned and carried out the experiments described in the manuscript. Under the supervision of Dr. Peter Ehlers, I have measured, analyzed and characterized the optical and electrochemical properties, and completed density functional and time-dependent density functional calculations. Dr. Alexander Villinger contributed by performing and evaluating single crystal X-ray diffraction experiments. I wrote the manuscript and the supporting information. All authors contributed to the revision of the manuscript before publication.

Own contribution: about 80%.

I Synthesis and Properties of Benzo[*h*]imidazo[1,2-*a*]quinolines and 1,2*a*-Diazadibenzo[*cd*,*f*]azulenes.

Aleksandra Khomutetckaia, Peter Ehlers, Alexander Villinger, and Peter Langer

J. Org. Chem. **2023**, *88 (13)*, 7929–7939.

DOI: 10.1021/acs.joc.2c02738

JOC The Journal of Organic Chemistry

pubs.acs.org/joc Article

Synthesis and Properties of Benzo[h]imidazo[1,2-a]quinolines and 1,2a-Diazadibenzo[cd,f]azulenes

Aleksandra Khomutetckaia, Peter Ehlers, Alexander Villinger, and Peter Langer*

Cite This: J. Org. Chem. 2023, 88, 7929−7939 Read Online

ACCESS | Metrics & More | Article Recommendations | Supporting Information

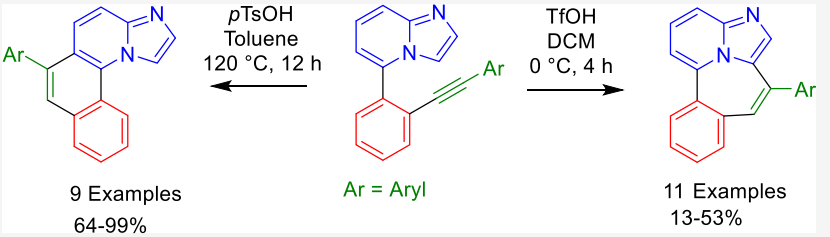

ABSTRACT: Benzo[h]imidazo[1,2-a]quinolines and 1,2a-diazadibenzo[cd,f]azulenes were prepared from a common intermediate by regioselective cycloisomerization reactions. The selectivity was controlled by the choice of Brønsted acid and solvent. The optical and electrochemical properties of the products were studied by UV/vis, fluorescence, and cyclovoltammetric measurements. The experimental results were complemented by density functional theory calculations.

INTRODUCTION

Functionalized imidazopyridines have gained significant interest in organic chemistry and, in particular, in medicinal chemistry. These compounds are of relevance in terms of their potential biological activity and physicochemical properties. 5-Arylated imidazopyridines have been identified as potential candidates for drug development. Early publications have shown that a series of 5-aryl-imidazopyridines exhibit inhibitory activity against several human cancer cell lines, such as colon, lung, pancreas, liver, and others. For example, compound **A** (Scheme 1) with phenyl substituents at positions 2, 5, and 7 shows activity against various cancer cell lines, such as A549 (lung), HCT-116 (colon), SW-620 (colon), and MIAPACA (pancreas).[1] The change of the phenyl substituent at position 5 to indole and the introduction of *N*-methylcyclohexanamine at position 2 results in cytotoxicity against five selected cancer cell lines HT-29 (colon), H460 (lung), A549 (lung), MKN-45 (stomach), and SMMC-7721 (liver) of compound **B**.[2] Activity against Hep-G2 (liver), T-24 (bladder), and SK-OV-3 (ovaries) cell lines has also been found in benzo-fused compound **C**, which contains aryl substituents at positions 5 and 7.[3]

Along with their biological activity, the optical and electrochemical properties of imidazopyridines are of particular interest. In recent years, scientific interest has been amplified because of the potential incorporation of imidazopyridines in various electronic applications of modern daily life, such as organic field effect transistors, organic light-emitting diodes, organic photovoltaic cells, organic lasers, and many more.[4,5] For instance, chiral azahelicenes containing naphtho-fused imidazopyridines show circularly polarized luminescence (CPL) with a wide range of potential applications for data storage and processing, 3D displays, or CPL lasers.[6] Moreover, imidazopyridines functionalized with a diketopyrrolopyrrol subunit in position 5 were employed as BODIPY dye analogues.[7]

Based on the work of us and others[8] on the synthesis of polycyclic heteroaromatic compounds and inspired by the impressive properties of the abovementioned 5-arylated imidazopyridines, we envisioned the development of a new strategy for the synthesis of polycyclic imidazopyridines based on the combination of Pd-catalyzed cross-coupling with acid-mediated cycloisomerization reactions. In particular, the application of simple Brønsted-acid-mediated cycloisomerization reactions first introduced by the Swager group has been recognized as a valuable tool for the construction of polycyclic compounds, especially for economical and ecological reasons.[9]

As a common synthetic intermediate, we identified 5-(2-alkynylphenyl)imidazopyridines **A,** which were planned to be prepared by the application of Suzuki−Miyaura and Sonogashira cross-coupling reactions (Scheme 2). An acid-mediated cycloisomerization of **A** would then lead to benzo[h]imidazo[1,2-a]quinolines **B** and/or to regioisomeric 1,2a-diazadibenzo-[cd,f]azulenes **C**. Herein, we report the results of studies related to the divergent synthesis of products **B** and **C**.[10] In addition, the optical and electronic properties of both series of products were studied by experimental and theoretical methods. In addition,

Received: November 14, 2022
Published: June 21, 2023

Scheme 1. Biologically Active 5-Arylimidazopyridines

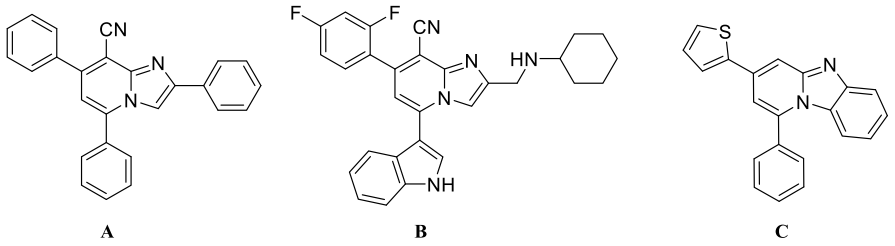

Scheme 2. Synthesis of Benzo[h]imidazo[1,2-a]quinolines B and 1,2a-Diazadibenzo[cd,f]azulenes C by Cycloisomerization of Common Intermediate A

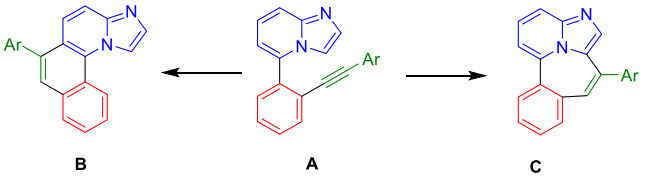

products **B** and **C** constitute, to the best of our knowledge, hitherto unknown heterocyclic core structures.

RESULTS AND DISCUSSION

Our first plan to prepare 5-(2-alkynylphenyl)imidazopyridines **5**, key intermediates of our project, relied on the reaction of 5-bromoimidazo[1,2-a]pyridine (**1**) with (2-bromophenyl)-boronic acid (**2**) to give coupling product **3**. The latter had then to be transformed to compounds **5** by Sonogashira reactions (Scheme 3). Imidazo[1,2-*a*]pyridine **1** was prepared in a 81% yield by cyclization of 6-amino-2-bromopyridine with bromoacetaldehyde dimethyl acetal (*n*BuOH, reflux, 14 h). The Suzuki−Miyaura reaction of **1** with **2** uneventfully afforded the desired coupling product **3**. However, the Sonogashira reaction of **3** with arylalkynes **4** proved to be unsuccessful and gave inseparable mixtures of the desired product and the starting material.

To solve this problem, we changed the order of the Suzuki−Miyaura and Sonogashira reactions. The Sonogashira reaction of commercially available 2-bromo-1-iodobenzene (**6**) with alkynes **4a−k** afforded 2-alkynyl-1-bromobenzenes **7a−k**. Metal−halide exchange using *n*BuLi, addition of trimethyl borate, and subsequent hydrolysis gave (2-alkynylphenyl)-boronic acids **8a−k**. The syntheses were carried out mostly in analogy to procedures reported for related transformations.[6,7,9−14] A detailed description of the experiments and the characterization data can be found in the Supporting Information. The structures of two derivatives of **7** and **8** were independently confirmed by crystal structure analyses (see the Supporting Information).

The Suzuki−Miyaura reaction of **8a−k** with **1** afforded the desired 5-(2-alkynylphenyl)imidazopyridines **5a−k** (Table 1). The reactions leading to products containing alkyl, methoxy, fluoro, and CF_3 groups proceeded in good yields. In case of the dimethylamino and chloro groups, the yields were slightly lower because of purification issues and competing side reactions, respectively. The structure of **5b** was independently confirmed by the crystal structure analysis (Figure 1). The two aryl groups of the diarylacetylene moiety are in plane, while the heterocyclic scaffold and the aryl group are twisted out of plane due to steric reasons.

The acid-mediated cycloisomerization of **8a−k** was studied next, with special emphasis on the regioselectivity. The conditions of the reactions were optimized for the transformation of **8a** to six-membered ring **9a** and seven-membered ring **10a** (Scheme 4, Table 2). Based on our previous work in the field, we considered different Brønsted acids during the optimization.[15−17] It became soon apparent that the regioselectivity depends on the choice of acid and solvent. The use of *p*-

Scheme 3. Synthesis of 5-(2-(Alkynyl)phenyl)imidazo[1,2-a]pyridines 5a−k; Conditions: (i) 6 (1.0 equiv), 4a−k (1.0 equiv), CuI (8 mol %), $Pd(PPh_3)_4$ (4 mol %), NEt_3, 20 °C, 4 h; (ii) 7a−k (1.0 equiv) *n*BuLi (1.0 equiv), $B(OMe)_3$ (2.0 equiv), THF, −78 °C, 45 min to 20 °C, 17 h; and (iii) 1 (1.0 equiv), $Pd(PPh_3)_4$ (3 mol %), 8a−k (1.5 equiv), K_2CO_3 (2.4 equiv), *n*-butanol/H_2O, 110 °C, 24 h

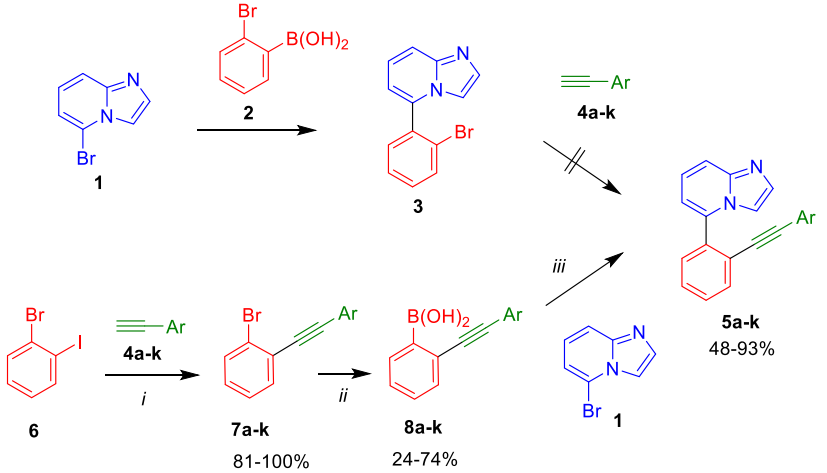

https://doi.org/10.1021/acs.joc.2c02738
J. Org. Chem. 2023, 88, 7929−7939

Table 1. Synthesis of 5-(2-(Alkynyl)phenyl)imidazo[1,2-a]pyridines 5a–k[a]

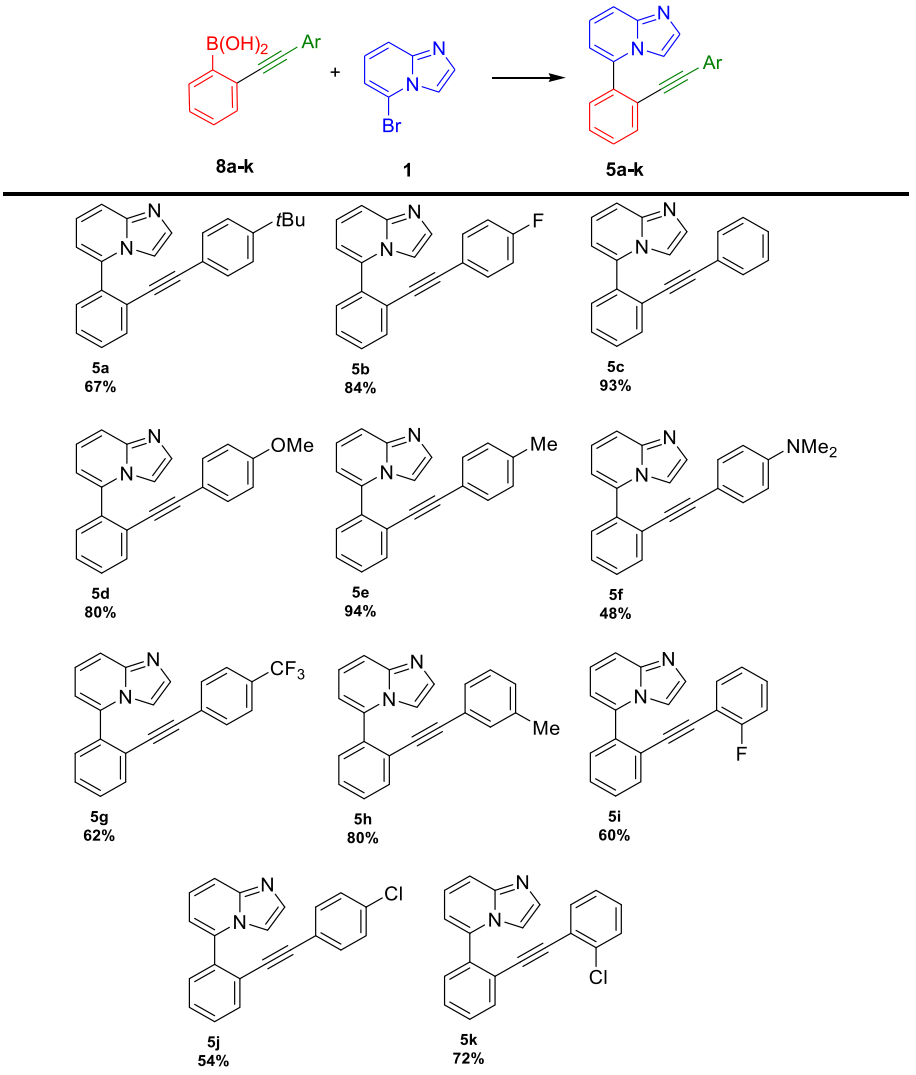

[a]Reaction conditions: **1** (1.0 equiv), $Pd(PPh_3)_4$ (3 mol %), **8a–k** (1.5 equiv), K_2CO_3 (2.4 equiv), *n*-butanol/H_2O, 110 °C, 24 h.

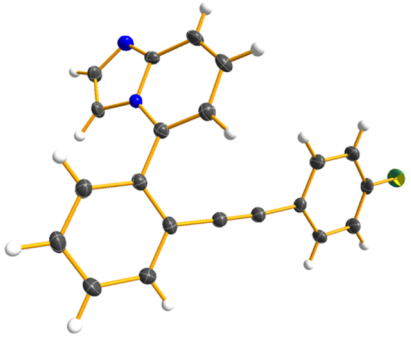

Figure 1. Crystal structure of **5b** (probability of ellipsoids is 50%).

toluenesulfonic acid (*p*TsOH) in toluene or xylene gave exclusively the respective diazaazulene **10a** (entries 2–5). The best yield (37%) was obtained when toluene was used as the solvent (100 °C, 12 h, entry 3). In contrast, imidazoquinoline **9a** instead of **10a** was isolated, albeit in low yields, when *p*TsOH was used in combination with hexafluoroisopropanol (HFIP) or without solvent (entries 6 and 7). The use of methanesulfonic

Scheme 4. Synthesis of 9a and 10a (for Conditions, See Table 2)

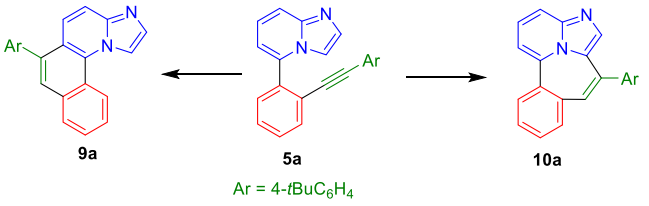

acid (MsOH), trifluoracetic acid, and triflic acid (TfOH) again exclusively afforded **9a** (entries 8, 9, 11–14). Eventually, the best yield of **9a** (69%) was obtained when TfOH (5 equiv) was employed in combination with dichloromethane (0 to 20 °C, 4 h). Interestingly, when water was added to the MsOH solution in toluene, a mixture of products 9 and 10 was isolated, highlighting the impact of water on the regioselectivity. No product at all could be isolated when the Lewis acid $PtCl_2$ was used (the starting material was recovered, entry 15).

As a next step, we studied the scope of the synthesis of benzoimidazoquinolines **9** using our optimized conditions

https://doi.org/10.1021/acs.joc.2c02738
J. Org. Chem. 2023, 88, 7929–7939

Table 2. Optimization of the Synthesis of 9a and 10a

					yield (%)	
entry	acid [equiv]	solvent	temp °C	time h	**9**	**10**
1	pTsOH [10]	toluene	20	2	0	0
2	pTsOH [10]	toluene	100	12	0	19
3	pTsOH [30]	toluene	100	12	0	37
4	pTsOH [30]	xylene	130	12	0	36
5	pTsOH [60]	toluene	100	12	0	36
6	pTsOH [30]		120	12	25	0
7	pTsOH [30]	HFIP	60	24	16	0
8	MsOH [30]	HFIP	60	24	46	0
9	MsOH [30]	toluene	100	12	42	0
10	MsOH [30]	toluene/H_2O	100	12	31	12
11	TFA [35]	toluene	70	12	0	0
12	TFA [35]	toluene	100	12	10	0
13	TfOH [1]	DCM	0–20	4	traces	0
14	TfOH [5]	DCM	0–20	4	69	0
15	$PtCl_2$ [0.1]	toluene	100	12	0	0

(triflic acid, DCM, 0 °C, 4 h). The cycloisomerization of **5a–e** and **5hk** afforded the corresponding benzoimidazoquinolines **9a–e** and **9h–k** in good to excellent yields (Table 3). However, the employment of dimethylamino- and CF_3-substituted derivatives **5f** and **5g** proved to be unsuccessful. This can be explained by the electron withdrawing effect of the CF_3 and dimethylammonium groups. The latter is formed by the protonation of the dimethylamino group during the reaction. In all experiments, exclusively products **9** were formed. Not even trace amounts of product **10** could be detected. The structure of **9c** was independently confirmed by the crystal structure analysis (Figure 2). The benzoimidazoquinoline scaffold forms a

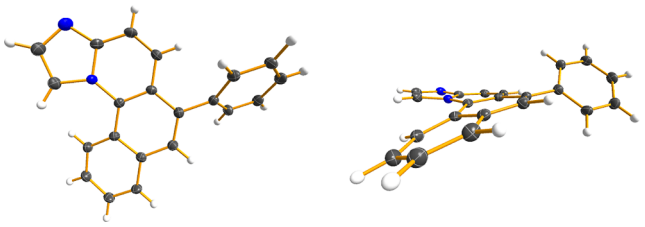

Figure 2. Crystal structure of **9c** (the probability of the ellipsoids is 50%).

Table 3. Synthesis of Benzoimidazoquinolines 9a–k[a]

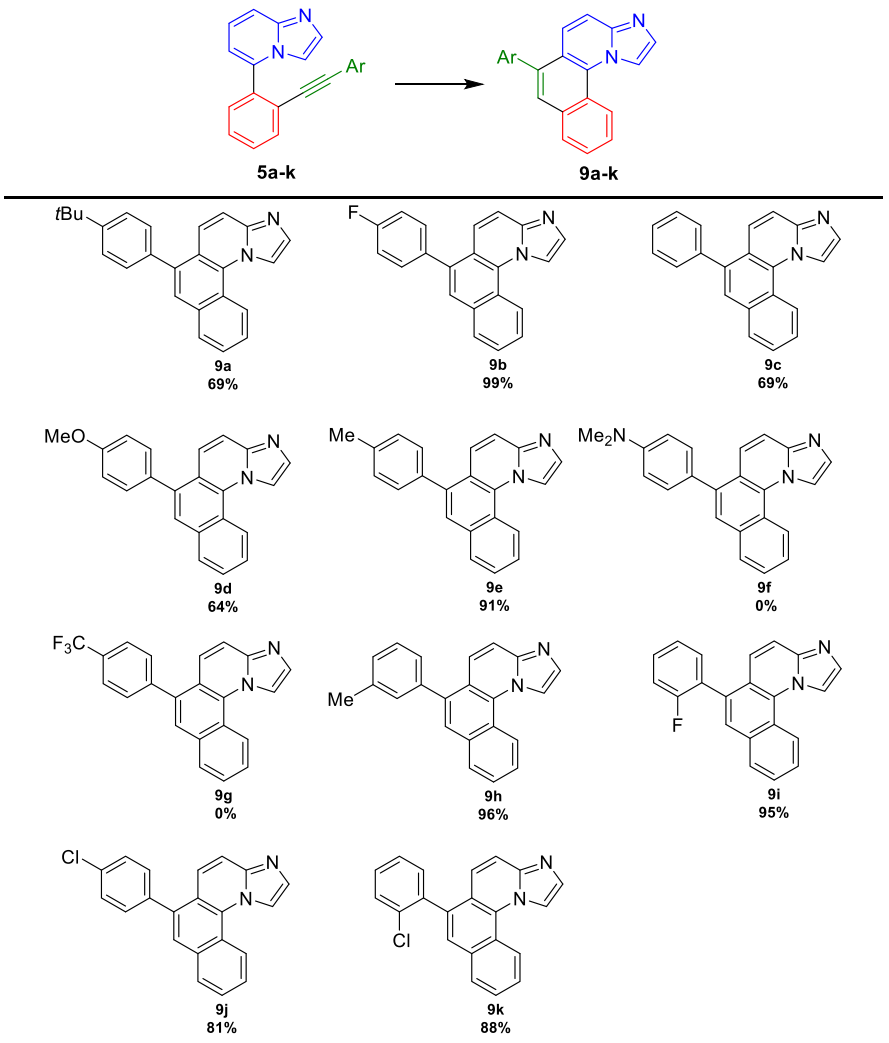

[a]Reaction conditions: **5a–k** (1.0 equiv), TfOH (5.0 equiv), CH_2Cl_2, 0–20, 4 h.

https://doi.org/10.1021/acs.joc.2c02738
J. Org. Chem. 2023, 88, 7929–7939

Table 4. Synthesis of Diazadibenzoazulenes 10a–k[a]

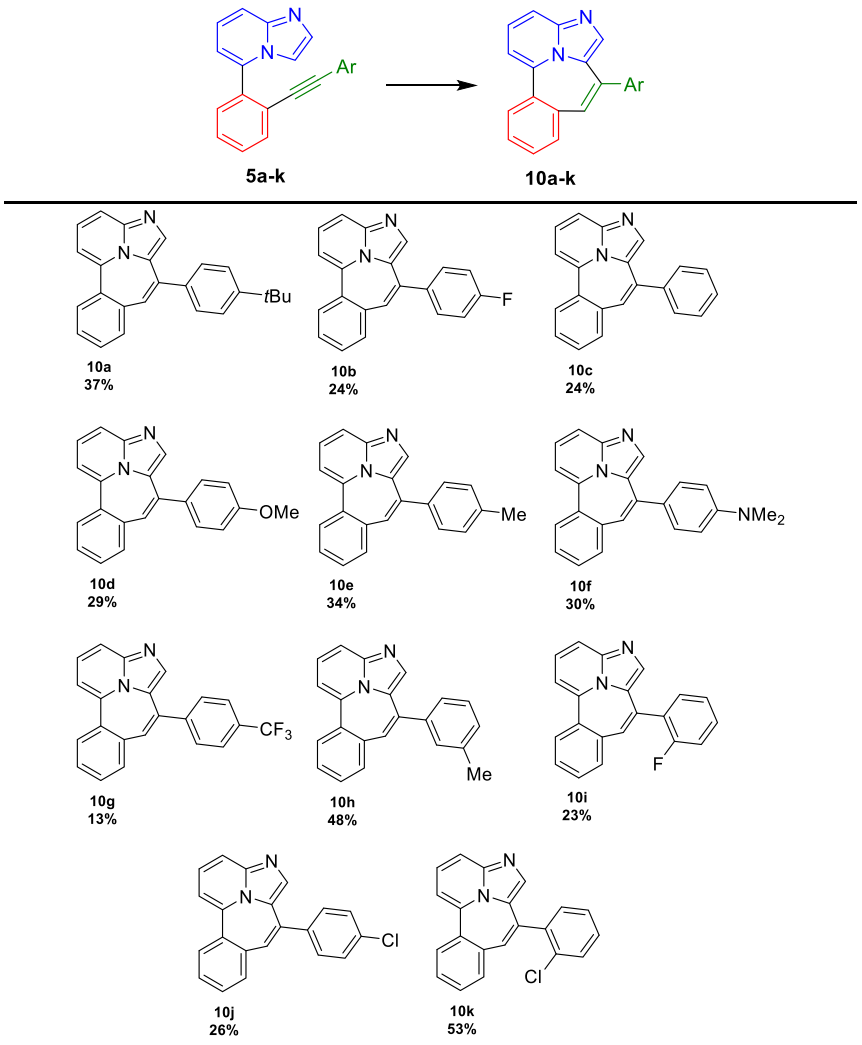

[a]Reaction conditions: **5a–k** (150 mg, 1.0 equiv), *p*TsOH (30 equiv), toluene, 100 °C, 12 h.

[4]helicene structure with a torsion angle of $\theta = 32°$ due to the *ortho*-annulation of the fused aryl rings. The attached phenyl ring is twisted out of plane by 52°. The structure of **9b** was also confirmed by X-ray crystal structure analysis (see Supporting Information).

The cycloisomerization of **5a-k**, carried out using *p*TsOH in toluene (100 °C, 12 h), afforded the corresponding diazadibenzoazulenes **10a–k** in mostly moderate yields (Table 4). The reaction was successful also for derivatives **5f** and **5g** containing a CF_3 and NMe_2 group. The formation of regioisomers **9** as side products was not observed. The synthesis of products **10** from alkynes **5** represents what is, to the best of our knowledge, the first example of a Brønsted acid-mediated cycloisomerization leading to a seven-membered ring. The structure of **10i** was independently confirmed by crystal structure analysis (Figure 3). The obtained crystals showed only a weak diffraction pattern, and molecules in the asymmetric unit are strongly disordered. Although the structure was proven, it could not be deposited at the CCDC, and a detailed discussion of the bond lengths and angles is not possible. However, it can be seen that the fused heterocyclic system shows a deviation from planarity induced by the incorporation of the seven-membered ring. The 2-fluorobenzene ring attached to the double bond is orthogonally twisted from the scaffold by sterical repulsion.

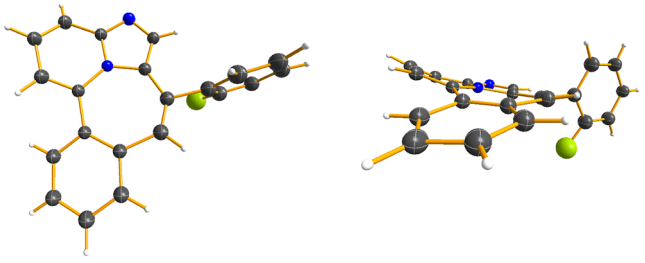

Figure 3. Single crystal structure of **10i** (due to strong crystal disorder, only weak crystal data was obtained, which precludes detailed discussion and deposition at the CCDC).

These results suggest that the choice of acid, solvent, and the temperature play an important role in the selectivity. The cycloisomerization presumably proceeds by protonation of the alkyne, subsequent cyclization via the pyridine or the imidazole moiety and deprotonation. The cyclization via the benzene ring might be faster than the cyclization via the imidazole because of the protonation of the nitrogen atom to the latter. At elevated

https://doi.org/10.1021/acs.joc.2c02738
J. Org. Chem. 2023, 88, 7929–7939

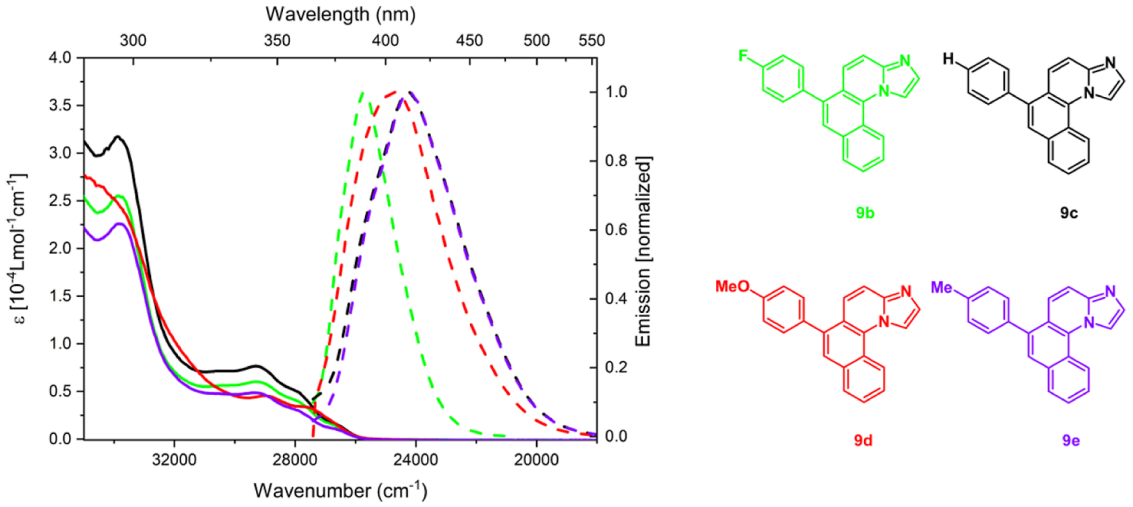

Figure 4. UV−vis and emission spectra (excited @360 nm) of benzo[h]imidazo[1,2-a]quinoline−derivatives **9b−e** in CH_2Cl_2 ($c = 10^{-4}$ M) at 20 °C.

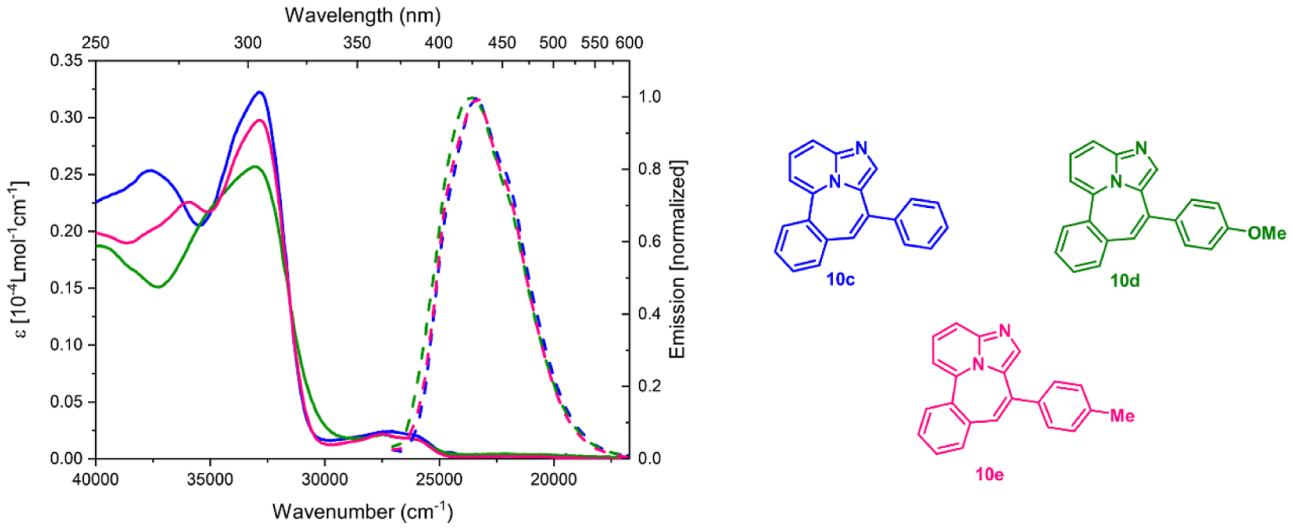

Figure 5. UV−vis (left) and emission spectra (excited @360 nm) of 1,2a[1]-diazadibenzo[cd,f]azulene−derivatives **10c−e** in CH_2Cl_2 ($c = 10^{-5}$ M) at 20 °C.

temperatures, an attack via the imidazole might become viable. It should be noted that *p*TsOH contains one equivalent of water (in contrast to the other acids), which also might play a role in the reaction. In conclusion, the origin of the regioselectivity remains unclear at present.

Physical Properties. As mentioned above, both benzo[h]-imidazo[1,2-a]quinolines **9** and 1,2a-diazadibenzo[cd,f]-azulenes **10** represent, to the best of our knowledge, new heterocyclic entities. Therefore, it was interesting to study the optical and electronic properties. The steady-state absorption and emission properties of selected compounds (**9b−e** and **10c−e**) were studied (Figures 4 and 5). The optical properties of imidazoquinolines **9b−e** show only marginal deviation by variation of the aryl ring in position 6. This can be explained by the fact that the aryl group is twisted out of plane. All compounds show strong absorptions at ∼300 nm and a weaker broad band with a certain fine structure between 320 and 380 nm. Fluorescence quantum yields range between 23 and 28% (Supporting Information, Table S3).[18] Diazadibenzoazulenes **10** show an absorption behavior similar to that of imidazoquinolines **9**. However, the lower energy band is slightly red-shifted with the loss of its fine structure, again indicating the low impact of the aryl rings attached to the heterocyclic scaffold on the optical properties.

Density functional theory (DFT) calculations on the B3LYP 6-311G(d,p) level within IEFPCM for acetonitrile have been performed to gain an improved understanding of the electronic characteristics of both isomers.[19] The calculations reflect the experimental results very well. Visualization of the highest occupied molecular orbital (HOMO) and lowest unoccupied molecular orbital (LUMO) of **9c** and **10c**, accompanied with their associated orbital energies, is depicted in Figure 6. Imidazoquinoline **9c** consists of a more stabilized HOMO as compared to **10c**, while the LUMO is higher in energy. Hence, the resulting energy gap of **10c** is 1.08 eV smaller as compared to **9c**. The contribution of the attached aryl rings to the FMOs is negligible for both isomers, which corresponds with the fact that different derivatives show similar absorption and emission spectra (Figures 4−6). TD-DFT calculations were performed to get further insight into the nature of the excited states of both compounds. For this reason, range-separated CAM-B3LYP hybrid functionals have been examined, which give a well

https://doi.org/10.1021/acs.joc.2c02738
J. Org. Chem. 2023, 88, 7929−7939

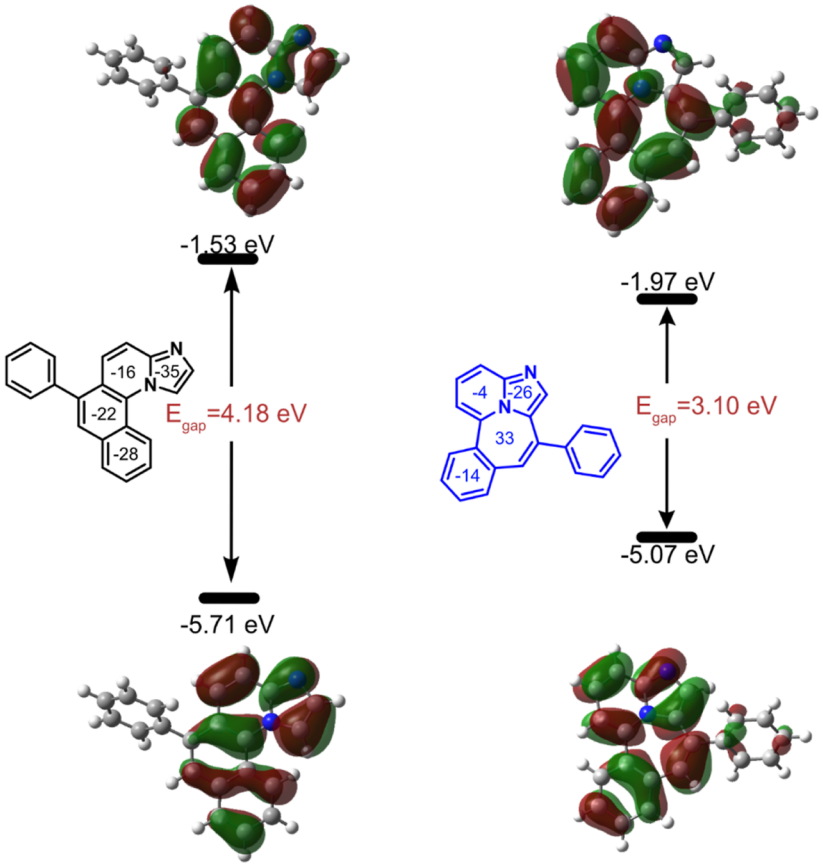

Figure 6. Visualization of HOMO and LUMO with associated energies and calculated NICS values drawn within the molecular structures.

correlated picture with regard to the experimental results. For compound **9c,** the first two transitions S1 ← S0 and S2 ← S0 with low oscillator strength originate mainly from HOMO → LUMO transitions (contribution of ∼50 and 40%, respectively) with admixture of HOMO − 1 → LUMO, HOMO − 1 → LUMO + 1, and HOMO → LUMO + 1 (cf. Supporting Information Table S7). In contrast, for compound **10c**, the S1 ← S0 with low oscillator strength derives only from the HOMO → LUMO transition, while weakly oscillating S2 ← S0 consists mainly of HOMO → LUMO + 1 with admixture of HOMO − 1 → LUMO (cf. Supporting Information Table S8).

Additional NICS(1.7) calculations have been performed to receive further insights into the aromaticity of the obtained polycyclic heterocycle **9c** and **10c,** and the results for each ring are depicted within molecular structures of Figure 6.[20] As expected for **9c,** all rings of the scaffold show distinct aromaticity, while the pyridine entity shows the lowest and the imidazole ring the highest magnetically induced current densities. However, the presence of a seven-membered azepine ring within the polycyclic scaffold of **10c** leads to strong deviations (Figure 6). While the imidazole ring and the benzol ring are still aromatic, NICS calculations reveal weak to non-aromaticity for the pyridine moiety and anti-aromaticity for the central azepine ring, which is in accordance with the strong shielding of the vinylic proton detected in the NMR-spectra of compounds **10** (cf. Supporting Information).

CONCLUSIONS

We developed a site-selective synthesis of benzo[h]imidazo[1,2-a]quinolines and isomeric 1,2a-diazadibenzo[cd,f]azulenes, which constitute, to the best of our knowledge, hitherto unknown heterocyclic core structures. The synthesis is based on the combination of Pd-catalyzed cross-coupling reactions with Brønsted acid-mediated cycloisomerizations. The regioselectivity of the cycloisomerization can be controlled by the choice of acid. The optical and electrochemical properties of the compounds were studied by UV/vis and fluorescence spectroscopy and by cyclovoltammetry. The 1,2a-diazadibenzo[cd,f]-azulenes exhibit bathochromically shifted absorptions and emissions accompanied with a lower oxidation potential as compared to the isomeric benzo[h]imidazo[1,2-a]quinolines. DFT calculations support the experimental results and confirm a negligible contribution of the attached aryl ring to the FMOs.

EXPERIMENTAL SECTION

General Information. If not otherwise stated, all employed have commercially purchased and used without further purification. The nuclear magnetic resonance spectra (^{1}H/^{13}C/^{19}F/^{11}B NMR) were recorded on a Bruker AVANCE 300 III, 250 II, or 500. The analyzed chemical shifts δ are referenced to residual solvent signals of the deuterated solvents $CDCl_3$ (δ = 7.26 ppm/77.16 ppm) or DMSO-d_6 (δ = 2.50 ppm/39.52 ppm). Multiplicities due to spin−spin correlation are reported as follows: s = singlet, d = doublet, dd = double doublet, t = triplet, pt = pseudo triplet, m = multiplet, and further described through their coupling constants *J*. Infrared spectra (IR) were measured as attenuated total reflection (ATR) experiments with a Nicolet 380 FT-IR spectrometer. The signals have been characterized through their wave numbers and their corresponding absorption as very strong (vs), strong (s), medium (m), weak (w), or very weak (vw). UV/vis spectra were recorded on a Cary 60 UV−vis spectrophotometer and emission spectra with an Agilent Cary Eclipse fluorescence spectrophotometer. Cyclovoltammetry (CV) was measured in CH_3CN with 0.1 M nBu$_4$NPF$_6$ as a supporting electrolyte, a glassy carbon working

https://doi.org/10.1021/acs.joc.2c02738
J. Org. Chem. 2023, 88, 7929−7939

electrode, ANE2 ($Ag/AgNO_3$ 0.01 M in CH_3CN) as a reference electrode, and a Pt counter electrode with ferrocene as an external standard (1 mM in CH_3CN). The potential is given versus Fc^+/Fc. The potentiostat used was a PalmSense EmStat3 blue. Basic and high-resolution mass spectra (MS/HRMS) were measured on instruments which were paired with preceding gas chromatography (GC) or liquid chromatography (LC). The samples have been ionized through electron impact ionization (EI) on an Agilent 6890/5973 or Agilent 7890/5977 GC−MS equipped with a HP-5 capillary column using helium carrier gas or by applying electron spray ionization (ESI) on an Agilent 1200/6210 time-of-flight (TOF) LC−MS. X-ray single-crystal structure analysis was performed on a Bruker Apex Kappa-II CCD diffractometer.

Materials. The applied solvents, *n*-butanol, THF, toluene, xylene, HFIP, and DCM, were obtained as dry solvents through commercial sources and employed without further purification. Solvents for extraction and column chromatography were available after previous distillation. If not otherwise stated, all reagents such as alkynes 4, catalysts, ligands, acids, and bases were purchased and used without further purification. Column chromatography was performed using a Merck Silica gel 60 (particle size 63−200 μm).

General Procedure for the Synthesis of Benzo[h]imidazo-[1,2-a]quinolones 9a−k. In a pressure tube under an inert atmosphere, **5a−k** (100 mg, 1 equiv) was dissolved in DCM (2 mL). The mixture was cooled to 0 °C. Then TfOH (5 equiv) was dropwise added. The reaction was stirred at 0 °C for 2 h and then at room temperature for further 2 h. The solution was diluted with ethyl acetate and extracted three times with a saturated solution of sodium bicarbonate. The organic layer was dried with sodium sulfate, filtered, and concentrated in vacuo. The residue was purified by column chromatography (Heptane/EtOAc = 3:1).

General Procedure for the Synthesis of 1,2a-Diazadibenzo-[cd,f]azulenes 10a−k. In a pressure tube under an inert atmosphere were added substances **5a−k** (150 mg, 1 equiv), *p*TsOH (30 equiv) and toluene (5 mL). The mixture was stirred at 100 °C for 12 h in a stainless-steel heating block. Then, the solution was cooled to 20 °C, diluted with ethyl acetate, and extracted three times with a saturated solution of sodium bicarbonate. The organic layer was dried with sodium sulfate, filtered, and concentrated in vacuo. The residue was purified by column chromatography (toluene/EtOAc = 3:1).

*6-(4-(tert-Butyl)phenyl)benzo[h]imidazo[1,2-a]quinoline (**9a**).* Starting from **5a** (100 mg, 0.29 mmol), the compound was isolated as a yellow solid (69 mg, 69%); mp: 185−187 °C. R_f: 0.34 (heptane/ethyl acetate, 3:1). ^{1}H NMR (500 MHz, chloroform-*d*) δ: 9.07 (d, J = 8.5 Hz, 1H), 8.97 (s, 1H), 8.03 (d, J = 6.5 Hz, 1H), 7.94−7.66 (m, 6H), 7.56 (d, J = 8.1 Hz, 2H), 7.45 (d, J = 8.1 Hz, 2H), 1.43 (s, 9H). ^{13}C{1H} NMR (126 MHz, chloroform-*d*) δ: 150.9, 138.7, 136.7, 133.3, 129.8, 129.1, 127.3, 126.7, 126.5, 125.4, 124.9, 123.5, 122.4, 121.3, 116.8, 34.7, 31.4. MS (GC): m/z (%) = 325 (4), 351 (28), 350 (M^+, $C_{25}H_{22}N_2$, 100), 337 (3), 336 (24), 335 (89), 333 (6), 332 (1). HRMS (ESI-TOF) m/z: $[M + H]^+$ calcd for $C_{25}H_{23}N_2$ 351.1861; found, 351.1871. IR (ATR): $\tilde{\nu}$ 2957 (s), 1698 (m), 1597 (m), 1290 (vs), 1267 (s), 1137 (s), 826 (vs), 705 (vs).

*6-(4-Fluorophenyl)benzo[h]imidazo[1,2-a]quinolone (**9b**).* Starting from **5b** (100 mg, 0.32 mmol), the compound was isolated as a yellow solid (99 mg, 99%); mp: 155−157 °C. R_f: 0.28 (heptane/ethyl acetate, 3:1). ^{1}H NMR (126 MHz, chloroform-*d*) δ: 9.15 (s, 1H), 9.08 (d, J = 8.6 Hz, 1H), 8.14 (d, J = 8.0 Hz, 1H), 7.89−7.70 (m, 5H), 7.56−7.47 (m, 3H), 7.37 (t, J = 8.8 Hz, 2H). ^{13}C{1H} NMR (126 MHz, DMSO-d_6) δ: 162.7 (d, J = 248.0 Hz), 137.7, 135.8, 133.4, 133.3, 131.9 (d, J = 8.2 Hz), 130.5, 129.3, 127.7, 127.1, 126.9, 124.7, 123.8, 122.6, 121.3, 117.1, 116.4 (d, J = 21.5 Hz), 115.8 (d, J = 3.6 Hz), 115.6. ^{19}F NMR (471 MHz, chloroform-*d*) δ: −114.1. MS (GC): m/z (%) = 314 (2), 313 (23), 312 (M^+, $C_{21}H_{13}FN_2$, 100), 311 (42), 310 (9), 309 (2), 308 (1). HRMS (EI): calcd for $C_{21}H_{13}N_2F$ (M^+), 312.1057; found, 312.1054. IR (ATR): $\tilde{\nu}$ 1694 (m), 1595 (s), 1506 (s), 1292 (s), 1218 (s), 1156 (s), 828 (s), 721 (vs).

*6-Phenylbenzo[h]imidazo[1,2-a]quinoline (**9c**).* Starting from **5c** (100 mg, 0.34 mmol), the compound was isolated as a colorless solid (69 mg, 69%); mp: 201−203 °C. R_f: 0.28 (heptane/ethyl acetate, 3:1). ^{1}H NMR (250 MHz, DMSO-d_6) δ: 9.31−9.10 (m, 1H), 8.34−8.18 (m, 1H), 7.97 (s, 1H), 7.93−7.72 (m, 4H), 7.69−7.43 (m, 7H). ^{13}C{1H} NMR (75 MHz, chloroform-*d*) δ: 139.9, 138.8, 133.4, 130.2, 129.3, 128.6, 127.9, 127.4, 126.9, 126.6, 124.6, 123.8, 122.6, 121.3, 117.1. MS (GC): m/z (%) = 296 (2), 295 (22), 294 (M^+, $C_{21}H_{13}N_2$, 100), 293 (49), 292 (9), 291 (3), 290 (2). HRMS (EI): calcd for $C_{21}H_{13}N_2$ (M^+), 294.1151; found, 294.1146. IR (ATR): $\tilde{\nu}$ 1669 (m), 1595 (m), 1492 (m), 1393 (m), 1290 (m), 1137 (m), 810 (m), 758 (s).

*6-(4-Methoxyphenyl)benzo[h]imidazo[1,2-a]quinoline (**9d**).* Starting from **5d** (100 mg, 0.31 mmol), the compound was isolated as a yellow solid (64 mg, 64%); mp: 150−152 °C. R_f: 0.21 (heptane/ethyl acetate, 3:1). ^{1}H NMR (500 MHz, DMSO-d_6) δ: 9.79 (d, J = 9.7 Hz, 1H), 9.27−9.06 (m, 1H), 8.24−8.17 (m, 1H), 8.05−7.92 (m, 1H), 7.86−7.62 (m, 3H), 7.48 (d, J = 8.8 Hz, 3H), 7.23−7.09 (m, 3H), 3.85 (s, 3H). ^{13}C{1H} NMR (126 MHz, DMSO-d_6) δ: 159.0, 137.6, 133.6, 132.8, 131.5, 131.1, 130.9, 129.6, 129.1, 127.5, 127.2, 126.3, 123.6, 122.7, 122.6, 120.5, 117.0, 116.3, 114.05, 114.09, 113.9, 55.2. MS (GC): m/z (%) = 327 (1), 326 (3), 325 (25), 324 ($C_{22}H_{16}N_2O$, 100), 323 (6), 310 (3), 309 (12), 308 (3). HRMS (ESI-TOF) m/z: $[M + H]^+$ calcd for $C_{22}H_{17}N_2O$, 325.1341; found, 325.1341. IR (ATR): $\tilde{\nu}$ 2924 (m), 1698 (s), 1597 (s), 1506 (s), 1393 (m), 1238 (vs), 1177 (s), 1030 (s).

*6-(p-Tolyl)benzo[h]imidazo[1,2-a]quinoline (**9e**).* Starting from **5e** (100 mg, 0.32 mmol), the compound was isolated as a dark-yellow solid (91 mg, 91%); mp: 131−133 °C. R_f: 0.30 (heptane/ethyl acetate, 3:1). ^{1}H NMR (250 MHz, chloroform-*d*) δ: 9.06 (d, J = 7.5 Hz, 1H), 8.95 (s, 1H), 8.09−7.98 (m, 1H), 7.87 (s, 1H), 7.82−7.66 (m, 5H), 7.37 (q, J = 8.2 Hz, 4H), 2.49 (s, 3H). ^{13}C{1H} NMR (63 MHz, chloroform-*d*) δ: 138.8, 137.8, 136.9, 133.4, 133.0, 130.1, 129.4, 129.3, 127.5, 126.8, 126.7, 125.1, 123.6, 122.6, 121.5, 116.8, 21.4. MS (GC): m/z (%) = 310 (5), 309 (24), 308 (M^+, $C_{22}H_{16}N_2$, 100), 307 (26), 306 (5), 305 (4), 304 (1), 295 (1), 294 (3), 293 (21), 292 (7), 291 (2), 290 (2). HRMS (ESI-TOF) m/z: $[M + H]^+$ calcd for $C_{22}H_{17}N_2$, 309.1392; found, 309.1402. IR (ATR): $\tilde{\nu}$ 2920 (m), 1694 (m), 1595 (s), 1510 (m), 1391 (m), 1290 (s), 1135 (s), 816 (vs).

*6-(m-Tolyl)benzo[h]imidazo[1,2-a]quinoline (**9h**).* Starting from **5h** (100 mg, 0.32 mmol), the compound was isolated as a yellow solid (96 mg, 96%); mp: 75−77 °C. R_f: 0.30 (heptane/ethyl acetate, 3:1). ^{1}H NMR (300 MHz, chloroform-*d*) δ: 8.94 (d, J = 9.1 Hz, 1H), 8.83 (s, 1H), 7.91 (dd, J = 8.0, 1.6 Hz, 1H), 7.86−7.70 (m, 2H), 7.70−7.62 (m, 1H), 7.61−7.56 (m, 4H), 7.35−7.10 (m, 3H), 2.35 (s, 3H). ^{13}C{1H} NMR (75 MHz, chloroform-*d*) δ: 139.8, 138.9, 138.3, 133.4, 133.4, 132.4, 130.9, 130.1, 129.2, 128.7, 128.5, 127.8, 127.4, 127.3, 126.8, 126.5, 124.8, 122.6, 121.2, 117.3, 117.0, 21.6. MS (GC): m/z (%) = 310 (3), 309 (25), 308 (M^+, $C_{22}H_{16}N_2$, 100), 307 (25), 306 (5), 305 (4), 303 (2), 294 (5), 293 (21), 292 (8), 291 (3), 290 (1). HRMS (ESI-TOF) m/z: $[M + H]^+$ calcd for $C_{22}H_{17}N_2$, 309.1392; found, 309.1389. IR (ATR): $\tilde{\nu}$ 2920 (w), 1696 (w), 1601 (m), 1486 (m), 1292 (s), 1148 (m), 886 (m), 787 (s).

*6-(2-Fluorophenyl)benzo[h]imidazo[1,2-a]quinoline (**9i**).* Starting from **5a** (100 mg, 0.32 mmol), the compound was isolated as a yellow solid (95 mg, 95%); mp: 180−182 °C. R_f: 0.26 (heptane/ethyl acetate, 3:1). ^{1}H NMR (300 MHz, DMSO-d_6) δ: 9.28−9.20 (m, 1H), 9.20−9.14 (m, 1H), 8.24 (dd, J = 7.8, 1.7 Hz, 1H), 8.03 (s, 1H), 7.94−7.74 (m, 4H), 7.69−7.52 (m, 2H), 7.51−7.38 (m, 2H), 7.38−7.31 (m, 1H). ^{13}C{1H} NMR (75 MHz, chloroform-*d*) δ: 160.2 (d, J = 247.1 Hz), 145.8, 133.4, 132.6, 132.4 (d, J = 3.2 Hz), 130.4 (d, J = 8.2 Hz), 130.2, 129.4, 127.6, 127.5, 127.4, 127.3, 127.2, 124.6 (d, J = 3.7 Hz), 124.1, 122.7, 121.5, 117.4, 116.0 (d, J = 22.0 Hz), 115.7. ^{19}F NMR (282 MHz, DMSO-d_6) δ −114.1. MS (GC): m/z (%) = 314 (3), 313 (23), 312 (M^+, $C_{21}H_{13}FN_2$, 100), 311 (32), 310 (6), 309 (1). HRMS (ESI-TOF) m/z: $[M + H]^+$ calcd for $C_{21}H_{14}FN_2$, 313.1141; found, 313.1140. IR (ATR): $\tilde{\nu}$ 2920 (w), 1696 (w), 1601 (m), 1486 (m), 1292 (s), 1148 (m), 886 (m), 707 (vs).

*6-(4-Chlorophenyl)benzo[h]imidazo[1,2-a]quinoline (**9j**).* Starting from **5j** (100 mg, 0.30 mmol), the compound was isolated as a yellow solid (81 mg, 81%); mp: 145−147 °C. R_f: 0.30 (heptane/ethyl acetate, 3:1). ^{1}H NMR (500 MHz) δ: 9.19 (d, J = 33.6 Hz, 1H), 8.79 (d, J = 53.8 Hz, 1H), 8.47−6.59 (m, 11H). ^{13}C{1H} NMR (63 MHz, chloroform-*d*) δ: 138.3, 137.5, 134.2, 133.7, 133.2, 131.5, 129.3, 128.8, 127.6, 127.1,

https://doi.org/10.1021/acs.joc.2c02738
J. Org. Chem. 2023, 88, 7929−7939

126.6, 124.2, 123.8, 122.6, 121.0, 117.4, 115.7. MS (GC): m/z (%) = 332 (1), 331 (7), 330 (34), 329 (28), 328 (M^+, $C_{21}H_{13}ClN_2$, 100), 327 (13), 326 (2), 294 (4), 293 (19), 292 (13), 291 (4), 290 (3), 289 (1). HRMS (ESI-TOF) m/z: $[M + H]^+$ calcd for $C_{21}H_{14}ClN_2$, 329.0845; found, 329.0844. IR (ATR): $\tilde{\nu}$ 1695 (w), 1592 (w), 1487 (s), 1425 (m), 1289 (s), 1133 (m), 1085 (s), 1011 (m).

*6-(2-Chlorophenyl)benzo[h]imidazo[1,2-a]quinoline (**9k**).* Starting from **5k** (100 mg, 0.30 mmol), the compound was isolated as a brown solid (88 mg, 88%); mp: 131−133 °C. R_f: 0.28 (heptane/ethyl acetate, 3:1). ^{1}H NMR (300 MHz, DMSO-d_6) δ: 9.25 (s, 1H), 9.19 (d, J = 9.0 Hz, 1H), 8.23 (dd, J = 7.9, 1.6 Hz, 1H), 7.95 (s, 1H), 7.90−7.75 (m, 4H), 7.72−7.65 (m, 1H), 7.61−7.53 (m, 3H), 7.18 (d, J = 9.5 Hz, 1H). ^{13}C{1H} NMR (75 MHz, DMSO-d_6) δ: 137.9, 135.1, 133.7, 133.0, 132.7, 132.1, 130.2, 129.4, 129.2, 127.8, 127.6, 126.7, 123.2, 123.1, 122.9, 120.4, 117.5, 116.3. MS (GC): m/z (%) = 332 (1), 331 (8), 330 (34), 329 (24), 328 (M^+, $C_{21}H_{13}ClN_2$, 100), 295 (2), 294 (19), 293 (83), 292 (22), 291 (8), 290 (6), 289 (2). HRMS (ESI-TOF) m/z: $[M + H]^+$ calcd for $C_{21}H_{14}ClN_2$, 329.0845; found, 329.0840. IR (ATR): $\tilde{\nu}$ 1632.02 (w), 1475 (m), 1421 (m), 1292 (s), 1137 (m), 1052 (s), 1026 (vs), 813 (s).

*3-(4-(tert-Butyl)phenyl)-1,2a^1-diazadibenzo[cd,f]azulene (**10a**).* Starting from **5a** (150 mg, 0.43 mmol), the compound was isolated as a red solid (56 mg, 37%); mp: 147 °C. R_f: 0.30 (toluene/ethyl acetate, 3:1). ^{1}H NMR (300 MHz, chloroform-d) δ: 7.32−7.26 (m, 2H), 7.20−7.11 (m, 2H), 7.00−6.82 (m, 4H), 6.77−6.66 (m, 2H), 6.57−6.50 (m, 1H), 6.37−6.32 (m, 1H), 5.38 (s, 1H), 1.26 (s, 9H). ^{13}C{1H} NMR (75 MHz, chloroform-d) δ: 151.7, 151.3, 143.1, 140.4, 138.5, 137.3, 136.9, 132.9, 132.7, 131.2, 131.1, 130.5, 129.9, 129.2, 127.8, 127.0, 125.4, 118.5, 113.9, 34.7, 31.4. MS (GC): m/z (%) = 353 (1), 352 (13), 351 (M^+, $C_{25}H_{22}N_2$, 100), 350 (71), 337 (3), 336 (22), 335 (84), 334 (21), 333 (17). HRMS (ESI-TOF) m/z: $[M + H]^+$ calcd for $C_{25}H_{23}N_2$ $[M + H]$, 351.1861; found, 351.1856. IR (ATR): $\tilde{\nu}$ 2959 (m), 1622 (w), 1506 (w), 1473 (m), 1280 (m), 1168 (s), 843 (m), 758 (vs).

*3-(4-Fluorophenyl)-1,2a^1-diazadibenzo[cd,f]azulene (**10b**).* Starting from **5b** (150 mg, 0.48 mmol), the compound was isolated as a red solid (36 mg, 24%); mp: 59 °C. R_f: 0.23 (toluene/ethyl acetate, 3:1). ^{1}H NMR (300 MHz, DMSO-d_6) δ: 7.38−7.32 (m, 2H), 7.25−7.18 (m, 2H), 7.16−7.13 (m, 3H), 6.96−6.91 (m, 2H), 6.83 (dd, J = 6.1, 2.5 Hz, 1H), 6.69 (dd, J = 5.6, 2.7 Hz, 1H), 6.55 (s, 1H), 5.52 (s, 1H). ^{13}C{1H} NMR (75 MHz, DMSO-d_6) δ: 163.3 (d, J = 244.5 Hz), 141.9, 139.1, 137.0, 136.2, 134.7, 133.3, 131.8, 131.3, 131.14 (d, J = 2.0 Hz), 130.08 (d, J = 8.2 Hz), 129.9, 127.1, 118.0, 115.4 (d, J = 21.3 Hz), 114.3. ^{19}F NMR (282 MHz, DMSO-d_6) δ: −113.5. MS (GC): m/z (%) = 314 (3), 313 (23), 312 (M^+, $C_{21}H_{13}FN_2$, 100), 311 (48), 310 (32), 309 (4), 308 (3), 307 (1). HRMS (ESI-TOF) m/z: $[M + H]^+$ calcd for $C_{21}H_{14}N_2F$, 313.1141; found, 313.1139. IR (ATR): $\tilde{\nu}$ 2920 (m), 2852 (m), 1624 (m), 1599 (m), 1504 (s), 1282 (m), 1220 (s), 1156 (s), 839 (s).

*3-Phenyl-1,2a^1-diazadibenzo[cd,f]azulene (**10c**).* Starting from **5c** (150 mg, 0.51 mmol), the compound was isolated as a red solid (36 mg, 24%); mp: 44 °C. Yield: 24%. R_f: 0.22 (toluene/ethyl acetate, 3:1). ^{1}H NMR (500 MHz, DMSO-d_6) δ: 7.44−7.34 (m, 3H), 7.33−7.26 (m, 2H), 7.17−7.11 (m, 3H), 6.97−6.91 (m, 2H), 6.87−6.80 (m, 1H), 6.69 (dd, J = 6.1, 2.3 Hz, 1H), 6.55 (s, 1H), 5.53 (s, 1H). ^{13}C{1H} NMR (126 MHz, DMSO-d_6) δ: 151.0, 142.0, 140.7, 139.2, 136.2, 135.8, 133.3, 131.8, 131.4, 131.1, 131.0, 129.9, 128.8, 128.5, 128.2, 127.8, 126.9, 118.0, 114.3. MS (GC): m/z (%) = 296 (2), 295 (18), 294 (M^+, $C_{21}H_{14}N_2$, 100), 293 (48), 292 (36), 290 (5). HRMS (ESI-TOF) m/z: $[M + H]^+$ calcd for $C_{21}H_{15}N_2$, 295.1235; found, 295.1235. IR (ATR): $\tilde{\nu}$ 2922 (m), 1620 (w), 1607 (w), 1473 (m), 1284 (m), 1164 (s), 754 (vs).

*3-(4-Methoxyphenyl)-1,2a^1-diazadibenzo[cd,f]azulene (**10d**).* Starting from **5d** (150 mg, 0.46 mmol), the compound was isolated as a red oil (44 mg, 29%). R_f: 0.19 (toluene/ethyl acetate, 3:1). ^{1}H NMR (300 MHz, DMSO-d_6) δ: 7.27−7.18 (m, 2H), 7.13 (d, J = 2.9 Hz, 3H), 6.96−6.89 (m, 4H), 6.84−6.75 (m, 1H), 6.67 (dd, J = 5.8, 2.5 Hz, 1H), 6.58 (s, 1H), 5.49 (s, 1H), 3.77 (s, 3H). ^{13}C{1H} NMR (75 MHz, DMSO-d_6) δ: 159.1, 142.0, 139.4, 136.4, 135.4, 133.1, 133.0, 131.8, 131.3, 131.1, 130.8, 129.7, 129.1, 126.5, 118.1, 114.2, 113.8, 55.1. MS (GC): m/z (%) = 326 (3), 325 (24), 324 ($C_{22}H_{16}N_2O$, 100), 323 (8), 310 (5), 309 (23), 308 (83). HRMS (ESI-TOF) m/z: $[M + H]^+$ calcd for $C_{22}H_{17}N_2O$, 325.1341; found, 325.1332. IR (ATR): $\tilde{\nu}$ 2922 (m), 1605 (m), 1504 (s), 1286 (m), 1238 (s), 1164 (s), 1026 (s), 789 (s).

*3-(p-Tolyl)-1,2a^1-diazadibenzo[cd,f]azulene (**10e**).* Starting from **5e** (150 mg, 0.5 mmol), the compound was isolated as a red oil (51 mg, 34%). R_f: 0.23 (toluene/ethyl acetate, 3:1). ^{1}H NMR (500 MHz, DMSO-d_6) δ: 7.19 (s, 4H), 7.14 (d, J = 2.7 Hz, 3H), 6.96−6.92 (m, 2H), 6.84−6.78 (m, 1H), 6.69 (dd, J = 5.8, 2.6 Hz, 1H), 6.58 (s, 1H), 5.51 (s, 1H), 2.32 (s, 3H). ^{13}C{1H} NMR (126 MHz, DMSO-d_6) δ: 142.0, 139.2, 137.9, 137.5, 136.1, 135.7, 133.2, 131.7, 131.3, 131.1, 130.9, 129.9, 129.0, 128.9, 127.7, 126.7, 117.9, 114.3, 20.8. MS (GC): m/z (%) = 310 (3), 309 (24), 308 ($C_{22}H_{16}N_2$, 100), 307 (24), 306 (8), 305 (8), 304 (2) 303 (4), 294 (2), 293 (14), 292 (28), 291 (3), 290 (3). HRMS (ESI-TOF) m/z: $[M + H]^+$ calcd for $C_{22}H_{17}N_2$, 309.1392; found, 309.1396. IR (ATR): $\tilde{\nu}$ 2920 (m), 1622 (m), 1506 (m), 1475 (m), 1280 (m), 1168 (s), 1022 (m), 752 (vs).

*4-(1,2a^1-Diazadibenzo[cd,f]azulen-3-yl)-N,N-dimethylaniline (**10f**).* Starting from **5f** (150 mg, 0.4 mmol), the compound was isolated as a dark brown solid (45 mg, 30%); mp: 152−154 °C. R_f: 0.19 (toluene/ethyl acetate, 3:1). ^{1}H NMR (500 MHz, DMSO-d_6) δ: 7.13−7.07 (m, 5H), 6.96−6.88 (m, 2H), 6.79 (ddd, J = 6.0, 3.9, 2.0 Hz, 1H), 6.72−6.63 (m, 4H), 5.48 (s, 1H), 2.91 (s, 6H). ^{13}C{1H} NMR (126 MHz, DMSO-d_6) δ: 151.0, 150.4, 142.3, 139.9, 136.6, 136.2, 133.0, 131.9, 131.4, 131.3, 130.7, 129.8, 129.3, 128.7, 128.4, 125.9, 118.2, 114.2, 111.9, 39.6. MS (GC): m/z (%) = 339 (4), 338 (27), 337 (M^+, $C_{23}H_{19}N_3$, 100), 336 (23), 323 (4), 322 (12), 321 (13), 320 (8), 319 (2). HRMS (ESI-TOF) m/z: $[M + H]^+$ calcd for $C_{23}H_{20}N_3$, 338.1657; found, 338.1649. IR (ATR): $\tilde{\nu}$ 2800 (w), 1729 (w), 1609 (s), 1521 (s), 1473 (m), 1445 (m), 1346 (s), 1286 (m), 1228 (m), 1168 (s), 750 (vs).

*3-(4-(Trifluoromethyl)phenyl)-1,2a^1-diazadibenzo[cd,f]azulene (**10g**).* Starting from **5g** (150 mg, 0.4 mmol), the compound was isolated as a brown oil (20 mg, 13%). R_f: 0.35 (toluene/ethyl acetate, 3:1). ^{1}H NMR (500 MHz, DMSO-d_6) δ: 8.32 (dd, J = 7.9, 1.5 Hz, 1H), 8.23 (dd, J = 8.2, 1.4 Hz, 1H), 7.85−7.79 (m, 3H), 7.68 (d, J = 8.0 Hz, 2H), 7.63−7.50 (m, 3H), 7.39 (dd, J = 8.9, 7.3 Hz, 1H), 7.31 (s, 1H), 6.98 (s, 1H). ^{13}C{1H} NMR (126 MHz, DMSO-d_6) δ: 143.7, 143.4, 132.6, 132.3, 131.2, 129.3, 129.0, 128.9, 127.9 (q, J = 32.0 Hz), 126.5, 126.3 (q, J = 3.7 Hz), 125.0, 124.9, 124.7, 124.5, 124.4 (q, J = 270.1 Hz), 119.7, 117.3, 116.4, 107.7. ^{19}F NMR (282 MHz, DMSO-d_6) δ: −60.8. MS (GC): m/z (%) = 364 (3), 363 (22), 362 ($C_{22}H_{13}F_3N_2$, 100), 361 (86), 360 (33), 359 (2), 294 (2), 293 (14), 292 (48), 291 (7), 290 (9), 289 (2), 288 (1). HRMS (ESI-TOF) m/z: $[M + H]^+$ calcd for $C_{22}H_{14}F_3N_2$, 363.1109; found, 363.1116. IR (ATR): $\tilde{\nu}$ 2924 (w), 1698 (w), 1603 (m), 1508 (m), 1319 (s), 1156 (s), 1063 (s), 1016 (s).

*3-(m-Tolyl)-1,2a^1-diazadibenzo[cd,f]azulene (**10h**).* Starting from **5h** (150 mg, 0.5 mmol), the compound was isolated as a red solid (72 mg, 48%); mp: 106−108 °C. R_f: 0.26 (toluene/ethyl acetate, 3:1). ^{1}H NMR (300 MHz, chloroform-d) δ: 7.28−7.20 (m, 1H), 7.19−7.09 (m, 1H), 7.09−6.93 (m, 6H), 6.84 (dd, J = 8.9, 7.2 Hz, 1H), 6.72 (s, 1H), 6.66−6.60 (m, 1H), 6.46 (d, J = 6.2 Hz, 1H), 5.46 (s, 1H), 2.35 (s, 2H). ^{13}C{1H} NMR (63 MHz, chloroform-d) δ: 143.1, 141.3, 140.2, 138.2, 137.0, 136.9, 133.0, 131.2, 131.1, 130.7, 129.4, 129.0, 128.8, 128.4, 127.2, 125.3, 118.3, 114.0, 21.5. MS (GC): m/z (%) = 310 (3), 309 (23), 308 (M^+, $C_{22}H_{16}N_2$, 100), 307 (26), 306 (8), 305 (7), 304 (2), 303 (4), 294 (2), 293 (11), 292 (25), 291 (3), 290 (3). HRMS (ESI-TOF) m/z: $[M + H]^+$ calcd for $C_{22}H_{17}N_2$, 309.1392; found, 309.1388. IR (ATR): $\tilde{\nu}$ 2920 (w), 1622 (m), 1517 (m), 1475 (s), 1344 (m), 1282 (m), 1168 (s), 907 (m).

*3-(2-Fluorophenyl)-1,2a^1-diazadibenzo[cd,f]azulene (**10i**).* Starting from **5i** (150 mg, 0.5 mmol), the compound was isolated as a red oil (35 mg, 23%). R_f: 0.23 (toluene/ethyl acetate, 3:1). ^{1}H NMR (500 MHz, DMSO-d_6) δ: 7.43 (t, J = 7.7 Hz, 1H), 7.36 (t, J = 8.6 Hz, 1H), 7.25 (q, J = 8.4, 7.4 Hz, 2H), 7.16 (dt, J = 17.8, 8.6 Hz, 2H), 6.96−6.90 (m, 3H), 6.80 (dd, J = 7.3, 1.7 Hz, 1H), 6.68 (dd, J = 6.1, 2.2 Hz, 1H), 6.36 (s, 1H), 5.53 (s, 1H). ^{13}C{1H} NMR (126 MHz, DMSO-d_6) δ: 159.1 (d, J = 245.0 Hz), 158.1, 151.1, 141.7, 138.6, 135.9, 133.4, 131.5, 131.4, 131.1, 130.7 (d, J = 3.1 Hz), 130.3 (d, J = 8.2 Hz), 129.8, 129.4, 128.1, 127.9, 124.9 (d, J = 3.5 Hz), 118.1, 115.9 (d, J = 22.0 Hz), 114.3. ^{19}F NMR (282 MHz, DMSO-d_6) δ: −114.8. MS (GC): m/z (%) = 314 (3), 313 (22), 312 (M^+, $C_{21}H_{13}FN_2$, 100), 311 (30), 310 (22), 309 (2),

https://doi.org/10.1021/acs.joc.2c02738
J. Org. Chem. 2023, 88, 7929−7939

308 (3). HRMS (ESI-TOF) m/z: $[M + H]^+$ calcd for $C_{21}H_{14}FN_2$, 313.1141; found, 313.1145. IR (ATR): $\tilde{\nu}$ 2922 (m), 2852 (w), 1622 (w), 1453 (m), 1177 (m), 1024 (vs), 995 (vs), 746 (vs).

*3-(4-Chlorophenyl)-1,2a¹-diazadibenzo[cd,f]azulene (**10j**).* Starting from **5j** (150 mg, 0.5 mmol), the compound was isolated as a red oil (39 mg, 26%). R_f: 0.28 (toluene/ethyl acetate, 3:1). ^{1}H NMR (300 MHz, DMSO-d_6) δ: 7.46−7.40 (m, 2H), 7.36−7.30 (m, 2H), 7.14 (q, J = 2.7 Hz, 3H), 6.95−6.91 (m, 2H), 6.81 (td, J = 4.2, 2.0 Hz, 1H), 6.67 (dd, J = 5.9, 2.4 Hz, 1H), 6.56 (s, 1H), 5.51 (s, 1H). ^{13}C{1H} NMR (75 MHz, DMSO-d_6) δ: 141.9, 139.5, 139.0, 136.3, 134.5, 133.3, 132.6, 131.8, 131.3, 131.19, 131.15, 129.8, 128.5, 127.1, 118.1, 114.3. MS (GC): m/z (%) = 332 (1), 331 (7), 330 (34), 329 (28), 328 (M^+, $C_{21}H_{13}ClN_2$, 100), 327 (16), 326 (6), 294 (2), 293 (16), 292 (43), 291 (10), 289 (2). HRMS (ESI-TOF) m/z: $[M + H]^+$ calcd for $C_{21}H_{14}ClN_2$, 329.0845; found, 329.0849. IR (ATR): $\tilde{\nu}$ 2919 (m), 2849 (w), 1636 (w), 1463 (w), 1259 (m), 1022 (vs), 1003 (vs), 758 (s).

*3-(2-Chlorophenyl)-1,2a¹-diazadibenzo[cd,f]azulene (**10k**).* Starting from **5k** (150 mg, 0.5 mmol), the compound was isolated as a red solid (80 mg, 53%); mp: 85−87 °C. R_f: 0.58 (toluene/ethyl acetate, 3:1). ^{1}H NMR (500 MHz, DMSO-d_6) δ: 9.26 (s, 1H), 9.19 (d, J = 8.6 Hz, 1H), 8.24 (d, J = 8.0 Hz, 1H), 7.96 (s, 1H), 7.91−7.86 (m, 2H), 7.85−7.75 (m, 2H), 7.70 (dd, J = 7.5, 1.2 Hz, 1H), 7.61−7.54 (m, 3H), 7.18 (dd, J = 9.6, 1.0 Hz, 1H). ^{13}C{1H} NMR (126 MHz, DMSO-d_6) δ: 144.8, 137.9, 135.1, 133.7, 133.0, 132.7, 132.1, 129.5, 129.3, 127.8, 127.6, 126.6, 123.2, 123.1, 122.9, 120.4, 117.5, 116.3. MS (GC): m/z (%) = 332 (2), 331 (8), 330 (35), 329 (25), 328 (M^+, $C_{21}H_{13}ClN_2$, 100), 327 (3), 326 (1), 295 (2), 294 (20), 293 (92), 292 (25), 291 (9), 290 (6), 289 (2). HRMS (EI): calcd for $C_{21}H_{13}ClN_2$ (M^+), 328.0761; found, 328.0761. IR (ATR): $\tilde{\nu}$ 2921 (m), 1636 (w), 1477 (m), 1419 (m), 1289 (s), 1139 (m), 1026 (s), 1003 (s).

■ ASSOCIATED CONTENT

Data Availability Statement

The data underlying this study are available in the published article and its Supporting Information.

Supporting Information

The Supporting Information is available free of charge at https://pubs.acs.org/doi/10.1021/acs.joc.2c02738.

Single crystal X-ray data; optical data; CV data; computational details; experimental procedures and data; and ^{1}H-, ^{19}F-, and ^{13}C-NMR spectra of isolated compounds (PDF)

Accession Codes

CCDC 2217186 (**7g**), 2217187 (**9b**), 2217188 (**9c**), 2217189 (**5b**), and 2217190 (**8e**) contain the supplementary crystallographic data for this paper. These data can be obtained free of charge via www.ccdc.cam.ac.uk/data_request/cif, or by emailing data_request@ccdc.cam.ac.uk, or by contacting The Cambridge Crystallographic Data Centre, 12 Union Road, Cambridge CB2 1EZ, UK; fax: +44 1223 336033.

■ AUTHOR INFORMATION

Corresponding Author

Peter Langer − *Institut für Chemie, Universität Rostock, Rostock 18059, Germany; Leibniz Institut für Katalyse an der Universität Rostock, Rostock 18059, Germany;* orcid.org/0000-0002-7665-8912; Phone: +49 381 498 6410; Email: peter.langer@uni-rostock.de; Fax: +49 381 498 6412

Authors

Aleksandra Khomutetckaia − *Institut für Chemie, Universität Rostock, Rostock 18059, Germany*

Peter Ehlers − *Institut für Chemie, Universität Rostock, Rostock 18059, Germany;* orcid.org/0000-0001-6444-7563

Alexander Villinger − *Institut für Chemie, Universität Rostock, Rostock 18059, Germany;* orcid.org/0000-0002-0868-9987

Complete contact information is available at: https://pubs.acs.org/10.1021/acs.joc.2c02738

Notes

The authors declare no competing financial interest.

■ ACKNOWLEDGMENTS

Financial support by the State of Mecklenburg-Vorpommern (stipend for A.K.) is gratefully acknowledged.

■ REFERENCES

(1) Gupta, A.; Sasan, S.; Kour, A.; Nelofar, N.; Manikrao Mondhe, D.; Kapoor, K. K. Triarylimidazo[1,2-*a*]pyridine-8-carbonitriles: solvent-free synthesis and their anti-cancer evaluation. *Synth. Commun.* **2019**, *49*, 1813−1822.

(2) Liu, J.; Zuo, D.; Jing, T.; Guo, M.; Xing, L.; Zhang, W.; Zhao, J.; Shen, J.; Gong, P.; Zhang, D.; Zhai, X. Synthesis, biological evaluation and molecular modeling of imidazo[1,2-a]pyridine derivatives as potent antitubulin agents. *Bioorg. Med. Chem.* **2017**, *25*, 4088−4099.

(3) Teng, Q.-H.; Peng, X.-J.; Mo, Z.-Y.; Xu, Y.-L.; Tang, H.-T.; Wang, H.-S.; Sun, H.-B.; Pan, Y.-M. Transition-metal-free C-N and C-C formation: synthesis of benzo[4,5] imidazo [1,2-a] pyridines and 2-pyridones from ynones. *Green Chem.* **2018**, *20*, 2007−2012.

(4) Boldt, S.; Parpart, S.; Villinger, A.; Ehlers, P.; Langer, P. Synthesis and Properties of Aza-ullazines. *Angew. Chem., Int. Ed.* **2017**, *56*, 4575−4578.

(5) Tucker, S. A.; Acree, W. E.; Tanga, M. J.; Tokita, S.; Hiruta, K.; Langhals, H. Spectroscopic Properties of Polycyclic Aromatic Compounds: Examination of Nitromethane as a Selective Fluorescence Quenching Agent for Alternant Polycyclic Aromatic Nitrogen Hetero-Atom Derivatives. *Appl. Spectrosc.* **1992**, *46*, 229−235.

(6) Xu, D.; Zheng, W.-H. Synthesis and Chiroptical Properties of Planar Chiral Azahelicenes Based on [2.2]Paracyclophane. *Org. Lett.* **2021**, *23*, 8612−8616.

(7) Young, D. C.; Tasior, M.; Laurent, A. D.; Dobrzycki, Ł.; Cyrański, M. K.; Tkachenko, N.; Jacquemin, D.; Gryko, D. T. *Photostable orange-red fluorescent unsymmetrical diketopyrrolopyrrole−BF_2 hybrids*. *J. Mater. Chem. C* **2020**, *8*, 7708−7717.

(8) (a) Sobhani, M.; Frey, A.; Rettmann, A.; Thom, R.; Villinger, A.; Ehlers, P.; Langer, P. Synthesis of Dibenzotropones by Alkyne-Carbonyl Metathesis. *J. Org. Chem.* **2021**, *86*, 14420−14432. (b) Chen, D. Y.-K.; Kang, Q.; Wu, T. R. Modular Synthesis of Polyphenolic Benzofurans, and Application in the Total Synthesis of Malibatol A and Shoreaphenol. *Molecules* **2010**, *15*, 5909−5927. (c) Konishi, A.; Morinaga, A.; Yasuda, M. Construction of Polycyclic π-Conjugated Systems Incorporating an Azulene Unit Following the Oxidation of 1,8-Diphenyl-9,10-bis(phenylethynyl)phenanthrene. *Chem.—Eur. J.* **2018**, *24*, 8548−8552.

(9) (a) Goldfinger, M. B.; Crawford, K. B.; Swager, T. M. Directed Electrophilic Cyclizations: Efficient Methodology for the Synthesis of Fused Polycyclic Aromatics. *J. Am. Chem. Soc.* **1997**, *119*, 4578−4593. (b) Yang, W.; Lucotti, A.; Tommasini, M.; Chalifoux, W. A. Bottom-Up Synthesis of Soluble and Narrow Graphene Nanoribbons Using Alkyne Benzannulations. *J. Am. Chem. Soc.* **2016**, *138*, 9137−9144. (c) Takahashi, I.; Fujita, T.; Shoji, N.; Ichikawa, J. Brønsted acid-catalysed hydroarylation of unactivated alkynes in a fluoroalcohol−hydrocarbon biphasic system: construction of phenanthrene frameworks. *Chem. Commun.* **2019**, *55*, 9267−9270. (d) Zhang, J.; Li, S.; Qiao, Y.; Peng, C.; Wang, X.-N.; Chang, J. Metal-free cycloisomerizations of o-alkynylbiaryls. *Chem. Commun.* **2018**, *54*, 12455−12458.

(10) (a) Xu, L.-W.; Li, l.; Lai, G.-G. Recent Examples of Divergent Catalysis in Organic Reactions: Unexpected Findings or Rational Design. *Mini-Rev. Org. Chem.* **2007**, *4*, 217−230. (b) Chintawar, C. C.;

Yadav, A. K.; Kumar, A.; Sancheti, S. P.; Patil, N. T. Divergent Gold Catalysis: Unlocking Molecular Diversity through Catalyst Control. *Chem. Rev.* **2021**, *121*, 8478−8558. (c) Beletskaya, I. P.; Nájera, C.; Yus, M. Stereodivergent Catalysis. *Chem. Rev.* **2018**, *118*, 5080−5200. (d) Li, L.; Chen, Z.; Zhang, X.; Jia, Y. Divergent Strategy in Natural Product Total Synthesis. *Chem. Rev.* **2018**, *118*, 3752−3832.

(11) Boger, D. L.; Zhou, J. CDPI3-enediyne and CDPI3-EDTA conjugates: a new class of DNA cleaving agents. *J. Org. Chem.* **1993**, *58*, 3018−3024.

(12) Bentley, K. W.; Santos, Z. A.; Weiss, M. J.; Wolf, C. Chirality Sensing with Stereodynamic Biphenolate Zinc Complexes. *Chirality* **2015**, *27*, 700−707.

(13) (a) Hsieh, Y.-C.; Wu, C.-F.; Chen, Y.-T.; Fang, C.-T.; Wang, C.-S.; Li, C.-H.; Chen, L.-Y.; Cheng, M.-J.; Chueh, C.-C.; Chou, P.-T.; Wu, Y.-T. 5,14-Diaryldiindeno[2,1-f:1′,2′-j]picene: A New Stable [7]-Helicene with a Partial Biradical Character. *J. Am. Chem. Soc.* **2018**, *140*, 14357−14366. (b) Mule, R. D.; Shaikh, A. C.; Gade, A. B.; Patil, N. T. A new class of N-doped ionic PAHs via intramolecular [4+2]-cycloaddition between arylpyridines and alkynes. *Chem. Commun.* **2018**, *54*, 11909−11912.

(14) Schlepphorst, C.; Wiesenfeldt, M. P.; Glorius, F. Enantioselective Hydrogenation of Imidazo[1,2-a]pyridines. *Chem.—Eur. J.* **2018**, *24*, 356−359.

(15) Janke, S.; Boldt, S.; Ghazargan, K.; Ehlers, P.; Villinger, A.; Langer, P. Synthesis of Benzoacridines and Benzophenanthridines by Regioselective Pd-Catalyzed Cross-Coupling Reactions Followed by Acid-Mediated Cycloisomerizations. *Eur. J. Org. Chem.* **2019**, *2019*, 6177−6197.

(16) Ponce, M. B.; Rodríguez, E. T.; Flader, A.; Ehlers, P.; Langer, P. Synthesis of thieno[2,3-h]-/[3,2-h]quinolines and thieno[2,3-f] quinolines by Brønsted acid mediated cycloisomerisation. *Org. Biomol. Chem.* **2020**, *18*, 6531−6536.

(17) Gicquiaud, J.; Hacıhasanoğlu, A.; Hermange, P.; Sotiropoulos, J.-M.; Toullec, P. Y. Brønsted Acid-Catalyzed Carbocyclization of 2-Alkynyl Biaryls. *Adv. Synth. Catal.* **2019**, *361*, 2025−2030.

(18) Brouwer, A. M. Standards for photoluminescence quantum yield measurements in solution (IUPAC technical report). *Pure Appl. Chem.* **2011**, *83*, 2213−2228.

(19) Frisch, M. J.; Trucks, G. W.; Schlegel, H. B.; Scuseria, G. E.; Robb, M. A.; Cheeseman, J. R.; Scalmani, G.; Barone, V.; Mennucci, B.; Petersson, G. A.; Nakatsuji, H.; Caricato, M.; Li, X.; Hratchian, H. P.; Izmaylov, A. F.; Bloino, J.; Zheng, G.; Sonnenberg, J. L.; Hada, M.; Ehara, M.; Toyota, K.; Fukuda, R.; Hasegawa, J.; Ishida, M.; Nakajima, T.; Honda, Y.; Kitao, O.; Nakai, H.; Vreven, T.; Montgomery, J. A., Jr.; Peralta, J. E.; Ogliaro, F.; Bearpark, M.; Heyd, J. J.; Brothers, E.; Kudin, K. N.; Staroverov, V. N.; Kobayashi, R.; Normand, J.; Raghavachari, K.; Rendell, A.; Burant, J. C.; Iyengar, S. S.; Tomasi, J.; Cossi, M.; Rega, N.; Millam, J. M.; Klene, M.; Knox, J. E.; Cross, J. B.; Bakken, V.; Adamo, C.; Jaramillo, J.; Gomperts, R.; Stratmann, R. E.; Yazyev, O.; Austin, A. J.; Cammi, R.; Pomelli, C.; Ochterski, J. W.; Martin, R. L.; Morokuma, K.; Zakrzewski, V. G.; Voth, G. A.; Salvador, P.; Dannenberg, J. J.; Dapprich, S.; Daniels, A. D.; Farkas, O.; Foresman, J. B.; Ortiz, J. V.; Cioslowski, J.; Fox, D. J. *Gaussian 09*, Revision E.01; Gaussian, Inc.: Wallingford, CT, 2013.

(20) (a) von Ragué Schleyer, P.; Maerker, C.; Dransfeld, A.; Jiao, H.; van Eikema Hommes, N. J. R. Nucleus-Independent Chemical Shifts: A Simple and Efficient Aromaticity Probe. *J. Am. Chem. Soc.* **1996**, *118*, 6317−6318. (b) Stanger, A. Obtaining Relative Induced Ring Currents Quantitatively from NICS. *J. Org. Chem.* **2010**, *75*, 2281−2288.

https://doi.org/10.1021/acs.joc.2c02738
J. Org. Chem. 2023, 88, 7929−7939

II Serendipitous discovery of Pd-catalyzed intramolecular cyclization of ortho-bromo(hetero)aryl-substituted (hetero)aryl-1,2-diketones: Applications in the synthesis of carba- and heterocyclic benzoin derivatives

Erich Ammon, Aleksandra Khomutetckaia, Alexander Villinger, Peter Ehlers, Peter Langer

Tetrahedron. **2023***, 135,* 133335.

DOI: 10.1016/j.tet.2023.133335

Tetrahedron 135 (2023) 133335

Contents lists available at ScienceDirect

Tetrahedron

journal homepage: www.elsevier.com/locate/tet

Serendipitous discovery of Pd-catalyzed intramolecular cyclization of *ortho*-bromo(hetero)aryl-substituted (hetero)aryl-1,2-diketones: Applications in the synthesis of carba- and heterocyclic benzoin derivatives

Erich Ammon [a], Aleksandra Khomutetckaia [a], Alexander Villinger [a], Peter Ehlers [a, b], Peter Langer [a, b, *]

[a] Universität Rostock, Institut für Chemie, A.-Einstein-Str. 3a, 18059, Rostock, Germany
[b] Leibniz Institut für Katalyse an der Universität Rostock, A.-Einstein-Str. 29a, 18059, Rostock, Germany

ARTICLE INFO

Article history:
Received 15 December 2022
Received in revised form
23 February 2023
Accepted 23 February 2023
Available online 3 March 2023

Keywords:
Cyclizations
Cross-coupling
Heterocycles
Palladium
Regioselectivity

ABSTRACT

Carba: and heterocyclic benzoin derivatives were prepared by Sonogashira coupling of alkynes with 1,2-dihaloalkenes and subsequent oxidation of the alkyne to a 1,2-diketone. The Pd-catalyzed reaction of the product with (2-bromophenyl)boronic acid in the presence of phenylacetylene resulted in formation of cyclic benzoin derivatives by Suzuki-Miyaura reaction and subsequent Pd catalyzed nucleophilic addition to the carbonyl group. Hitherto unprecedented 5-hydroxy-5-phenylbenzo[*b*]naphtho[1,2-*d*]thiophene-6(5H)-ones and their regioisomers were prepared from 2,3-dibromobenzothiophene. Phenanthrene benzoin derivatives were prepared from 2-bromo-1-iodobenzene.

1. Introduction

Tertiary α-hydroxyketones are present in a variety of natural products and clinically used drugs, such as the antibiotic doxycyclin and daunorubicin or the analgetic (+)-paeonilacton B isolated from the plant *Paeonia albiflora Pallas* [1]. They are traditionally prepared by oxidation of 1,2-diols [2]. Tertiary α-hydroxyketones are also available by acid mediated α-hydroxylation [3]. In 2013, Liang and Jiao reported a metal free Cs_2CO_3-catalyzed synthesis using oxygen [4]. α-Hydroxyketones also represent important starting materials in organic synthesis [5]. Yamamoto and coworkers reported a Grignard-type Pd-catalyzed cyclization by nucleophilic attack of aryl bromides to ketones to give cyclic alcohols [6]. Kündig et al. reported a Pd-catalyzed synthesis of 3-hydroxyindoles from *N*-(2-halophenyl)-2-oxopropanoic amides [7]. Yang et al. developed a scandium(III) triflate catalyzed intramolecular Friedel-Crafts alkylation of *N*-(2-halophenyl)-2-oxopropanoic amide [8a]. Ritter et al. reported a dinuclear palladium catalyst for the α-hydroxylation of carbonyl compounds with oxygen [8b]. Herein, we report the synthesis of carba- and heterocyclic benzoin derivatives by combination of Pd catalyzed cross-coupling, oxidation and nucleophilic addition reactions. Hitherto unprecedented 5-hydroxy-5-phenylbenzo[*b*]naphtho[1,2-*d*]thiophene-6(5H)-ones and their regioisomers were prepared from 2,3-dibromobenzothiophene. Likewise, phenanthrene benzoin derivatives were prepared from 2-bromo-1-iodobenzene [8].

For clarity, the synthetic strategy is summarized in Scheme 1 for one derivative. The Sonogashira reaction of 2,3-dibromobenzothiophene (**1a**) with phenylacetylene (**2a**) afforded 2-alkynyl-3-bromobenzothiophene **3a** and subsequent oxidation of the alkyne gave 1,2-dione **4a**. The Suzuki-Miyaura reaction of **4a** with 2-bromophenylboronic acid (**5a**) gave product **6a**. The latter was transformed to α-hydroxyketone **7a** which was accompanied by its isomer **8a**. This key reaction was discovered basically by serendipity. Originally we planned to carry out a Sonogashira reaction at the bromide of **6a** with phenylacetylene. However, instead of the expected cross-coupling, a Grignard-type cyclization was

* Corresponding author. Universität Rostock, Institut für Chemie, A.-Einstein-Str. 3a, 18059, Rostock, Germany.
E-mail address: peter.langer@uni-rostock.de (P. Langer).

https://doi.org/10.1016/j.tet.2023.133335
0040-4020/

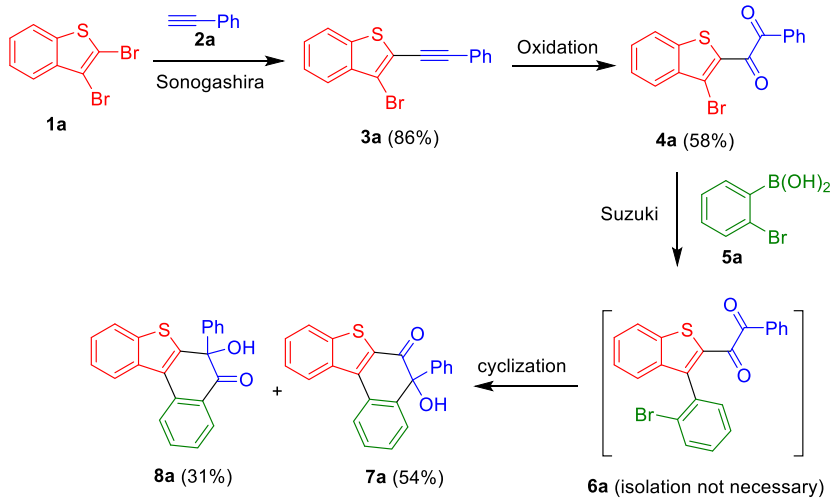

Scheme 1. Synthetic strategy.

observed in which phenylacetylene served as a reducing agent (Glaser coupling). Although (unstable) **6a** could be isolated and characterized, it later turned out that the transformation of **5a** to **7a** and **8a** could be carried out as a one-pot reaction.

2. Results and discussion

The Sonogashira reaction of commercially available 2,3-dibromobenzothiophene (**1**) with alkynes **2a-e**, following conditions reported by Lyaskovskyy et al. [9], afforded 2-alkynyl-3-bromobenzothiophenes **3a-e** in 57–86% yields (Scheme 2). The best yield was observed for product **3a** derived from phenylacetylene. The reaction of commercially available 2,3-dibromothiophene (**1b**) with phenylacetylene, following conditions reported by Kivrak et al., [10] gave product **3f** in 75%. Products **3e** and **3f** contained a small amount of impurities which, however, could be separated after the next step.

The oxidation of alkynes **3a-f**, following conditions reported by Wu and coworkers for the oxidation of diarylalkynes [11], afforded 1,2-diones **4a-f** in 26–60% yields (Scheme 3). The yields were significantly lower as compared to the yields reported for diarylalkynes. The yields of **4e** and **4f** are based on **1a** and **1b**, respectively (two steps), because products **3e** and **3f** could not be isolated in entirely pure form and were employed without purification in the oxidation. The Structure of **4a** was independently confirmed by Xray crystallography (Fig. 1).

The Suzuki-Miyaura reaction of **4a** with 2-bromophenylboronic acid (**5a**), following conditions reported by Kiyosei et al. for the reaction of 2-bromobenzo[*b*]thiophene with **5a** [12], afforded the desired product **6a** in 75% yield (Scheme 4). However, **6a** turned out to be unstable and had to be rapidly used for the following transformation. In the following step, we attempted to carry out a Sonogashira cross-coupling reaction of **6a** with phenylacetylene (**2a**). In order to improve the solubility of the starting materials in neat diisopropylamine, it proved to be important to add DMF to reaction mixture and to carry out the reaction at 140 °C. Much to our surprise, the Pd catalyzed reaction of **6a** with **2a** afforded the cyclic α-hydroxyketones **7a** and **8a**, albeit, in only 23% combined yield rather than the expected coupling product **9**. The structures of **7a, 8a** and **8c** were independently confirmed by X-ray crystal structure analyses (Figs. 2–4).

The optimization of the combined yield of products **7a** and **8a**, which could not be efficiently separated at this stage, was studied next (SI, Table S1). As a catalyst was used $Pd(PPh_3)_2Cl_2$ (5–20 mol%). Employment of diisopropylamine (DIPA) as the solvent gave the desired products in only 5% yield, due to low solubility of the starting materials. The use of 1,4-dioxane, DMSO and DMF proved to be rather unsuccessful as well. The best solvent turned out to be acetonitrile. The yield could not be improved by change of the catalyst. Only trace amounts of product were obtained when $Pd(CH_3CN)_2Cl_2$ (5 mol%) in the presence of SPhos (10 mol%) were used as catalyst and ligand, respectively. In contrast, employment of acetonitrile and $HP(^tBu)_3BF_4$ in the presence of a high amount of **2a** (1.8 equiv.) allowed to improve the yield to 75%. The yield decreased to 51% when only half amount of solvent was used. This might be explained by solubility problems. Further variation of the solvent

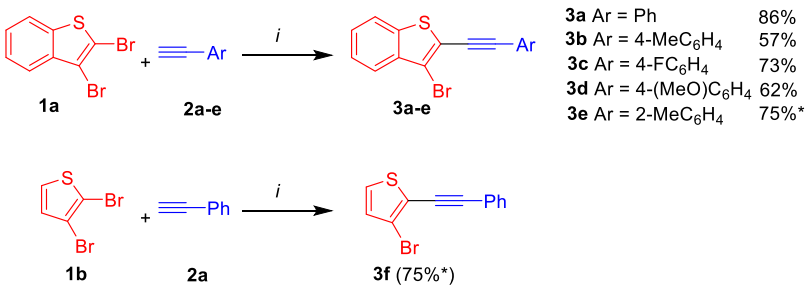

Scheme 2. Synthesis of 3-bromo-2-(arylethynyl)benzothiophenes **3a-e**. Isolated yields; conditions: For **3a-e**: *i*, **1a** (1 equiv.), **2a-e** (1.05 equiv.), $Pd(PPh_3)_2Cl_2$ (2 mol%), CuI (1 mol%), NEt_3, 20 °C, 20 h. For **3f**: *i*, **1b** (1 equiv.), **2a** (1.05 equiv.), $Pd(PPh_3)_2Cl_2$ (4 mol%), CuI (2 mol%), NEt_3, 60 °C, 3 h *The products contained a small amount of impurities.

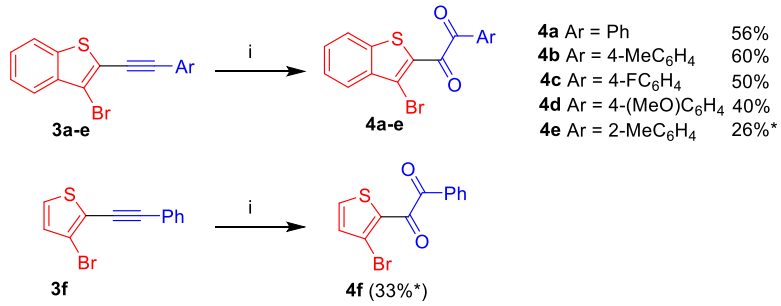

Scheme 3. Synthesis of 1,2-diones **4a-f**. Isolated yields. *The yields of **4e** and **4f** are based on **1a** and **1b**, respectively (two steps). Conditions: i, $Pd(OAc)_2$ (0.1 equiv.), $CuBr_2$ (0.1 equiv.), DMSO, 120 °C, 16 h.

Fig. 1. ORTEP of **4a**.

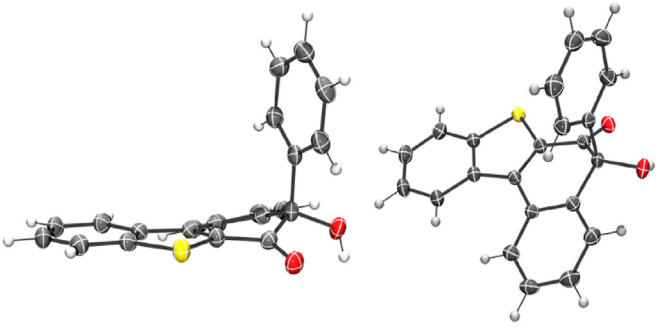

Fig. 2. ORTEP of **7a**.

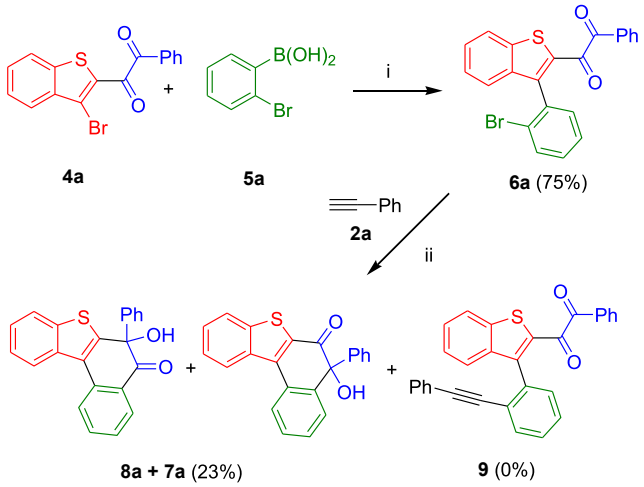

Scheme 4. Transformation of **4a** to **6a** and **7a**. *Conditions*: *i*: $Pd(PPh_3)_4$ (5 mol%), **5a** (1.2 equiv.), Na_2CO_3 (3 equiv.), DME/H_20 (4:1), 2 h, 85 °C; *ii*, $Pd(PPh_3)_2Cl_2$ (10 mol%), CuI (10 mol%), **2a** (1.2 equiv.), diisopropylamine, 20 h, 20 -> 50 °C, then DMF, 140 °C, 8 h.

was not studied. The presence of alkyne **2a** proved to be mandatory and can be explained by its function as reducing agent (*vide infra*). In fact, in the absence of **2a**, using acetonitrile as the solvent, no product was formed at all (entry 5). In case of DMSO, trace amounts of product were formed which can be explained by the fact that DMSO, in contrast to acetonitrile, may also act as a reducing agent.

We observed that products **7a** and **8a** were formed in small amounts already during the Suzuki-Miyaura reaction of **4a**. Therefore, we studied the possibility to develop a one-pot synthesis of **7a** and **8a** from **4a** (Scheme 5). At the beginning, we studied reaction conditions which rely on work-up of the reaction mixture after the first coupling reaction based on extraction, filtration, removal of solvent and employment of the crude product mixture in the following step. Later, we observed that much better yields were obtained when no aqueous work-up was carried out. After much experimentation, we found that best results were obtained using $Pd(PPh_3)_2Cl_2$ (5 mol%) and $HP(^tBu)_3BF_4$ (10 mol%) for both steps and acetonitrile/water as the solvent. The presence of an excess of alkyne **2a** proved to be important, but the presence of a copper co-catalyst was not necessary. In fact, no conversion was observed under otherwise identical conditions when **2a** was not added. In the crude product mixture (before chromatography), the ratio of **7a** and **8a** was 2.8:1. At this stage, we also extensively studied the separation of the two isomers. Eventually, an efficient separation was possible by chromatography (silica gel) using toluene as the eluent containing a few drops of diethyl ether. Isomers **7a** and **8a** were isolated in pure form in 54% and 31% yields, respectively.

The formation of products **7a** and **8a** might be explained by the mechanism depicted in Scheme 6. Oxidative addition of the Pd(0) catalyst to **4a** gave intermediate **A1** which is in equilibrium with **A2**. Grignard-type cyclization of **A1** afforded intermediate **B1** which subsequently reacted with water to afford product **7a** and a Pd(II) species. The latter is reduced by phenylacetylene (**2a**) by means of a Glaser reaction to give diyne **C** which could be detected by TLC. As mentioned above, Kündig et al. reported [7] a related Grignard-type cyclization using *n*-butanol (2.0 equiv.) as an additive. The latter served as a reducing agent and butyric aldehyde was detected in the reaction mixture. The mechanism discussed above is related to the one previously suggested by Yamamoto for a related transformation [6]. The formation of isomer **8a** might be explained as follows: Intermediate **A2** underwent a cyclization to give

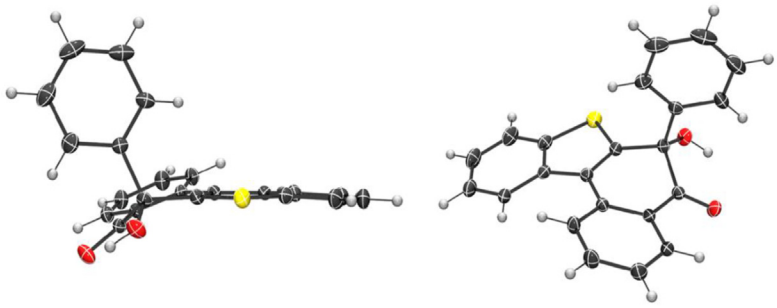

Fig. 3. ORTEP of **8a**.

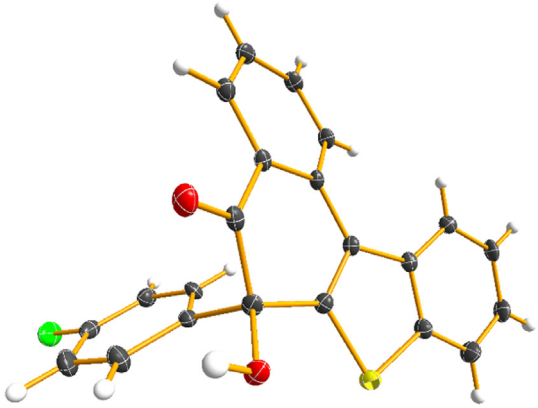

Fig. 4. ORTEP of **8c**.

intermediate **B2** which subsequently underwent a rearrangement to give **B3**. Reaction of the latter with water gave product **8a**. Alternatively, intermediate **B1** might undergo a rearrangement to **B3** by extrusion of $[PdBrL_2]^+$, which acts as a Lewis acid, to give intermediate **B4** and subsequent 1,2-shift of the phenyl group (Scheme 7).

To shed light on the rearrangement, we studied the transformation of **7a** to its isomer **8a**. While all attempts to induce a rearrangement by Brønsted acid failed, a rearrangement could be successfully induced by employment of two equivalents of silver triflate to give **8a**, albeit, in only 33% yield (Scheme 8). The Lewis acids $Cu(OTf)_2$ and $Tl(OTf)_3$ in fluorinated solvents, such as benzotrifluoride and tetrafluorobenzene also promoted the rearrangement. However, the yields were very low. The formation of **8a** can be explained by interaction of the carbonyl group with the Lewis acid to give intermediate **A**, 1,2-shift of the phenyl group to give intermediate **B**, protonation and extrusion of the Lewis acid. Although this process should, in principle, be a catalytic reaction, employment of catalytic amounts of Lewis acid did not promote the reaction. This result shows that a Lewis acid mediated rearrangement of **B1** to **B3** via **B4** might be possible and might explain the formation of isomer **8a**.

The preparative scope was studied next (Scheme 9). The reaction of **4a-e** with **5a** afforded the desired products **7a-e** and **8a-e** in good yields. The ratio of the two isomers was usually in the range of 1.7:1 to 2.3:1 which was also reflected by the yields of isolated products. However, in case of *p*-methoxy derivatives **7d** and **8d**, the ratio was nearly 1:1 which was again reflected by the isolated yields. In case of thiophene derivatives **7f** and **8f**, derived from **4f** and **5a**, the ratio of the isomers in the crude product mixture (4.3:1) was significantly shifted in favour of the main isomer. After chromatography, **7f** and **8f** were isolated in 73 and 17% yields, respectively. The reaction of **4a** with (4-bromothien-3-yl)boronic acid (**5b**) afforded products **7g** (76%) and **8g** (16%). The ratio of the isomers in the crude product mixture was 4.8:1. The influence of the substituents might be explained as follows. The rearrangement of **B1** to **B3** via cationic intermediate **B4** is expected to be accelerated by the presence of an electron donating methoxy group which stabilizes the cationic intermediate. This might explain the relatively high amount of **8d** in case of the formation of **7d** and **8d**. Unfortunately, strongly electron-withdrawing substituents (nitro) or pyridine instead of benzothiophene could not be successfully employed.

The application of the methodology to benzene derivatives was next studied. The Sonogashira-reaction of commercially available 2-bromo-1-iodobenzene (**10a**) with phenylacetylene (**2a**), following conditions reported by Kikuchi et al. [13], afforded diarylacetylene **11a** in 93% yield (Scheme 10). Likewise, **11b** and **11c** were prepared from **10a** and acetylenes **2f** and **2g**, respectively. The application of the conditions used for the oxidation of benzothiophene **3a** to give 1,2-dione **4a** to substrate **11a** afforded 1,2-dione **12a**, albeit, in only 29% yield. Increasement of the amount of $CuBr_2$ from 0.1 to 0.2 equiv. allowed to improve the yield to 41%. Increasement of the temperature from 120 to 130 °C resulted in a further increase of the yield to 55%. However, the reaction proceeded less cleanly and the chromatographic purification turned out to be more difficult. Thus, derivatives **12b** and **12c** were eventually prepared using 0.2 equiv. of $CuBr_2$ at 120 rather than 130 °C.

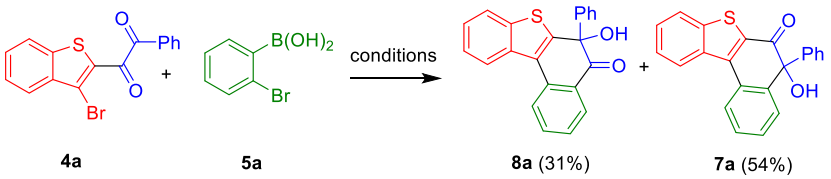

Scheme 5. One-pot synthesis of **7a** and **8a** from **4a**. *Conditions*: *i*, $Pd(PPh_3)_2Cl_2$ (5 mol%), $HP(^tBu)_3BF_4$ (10 mol%), **5a** (1.5 equiv.), K_3PO_4 (3 equiv.), acetonitrile/H_2O, 80 °C, 20 h; no work-up; *ii*, $Pd(PPh_3)_2Cl_2$ (10 mol%), $HP(^tBu)_3BF_4$ (20 mol%), DIPA, **2a** (1.8 equiv.), 80 °C, 5 h.

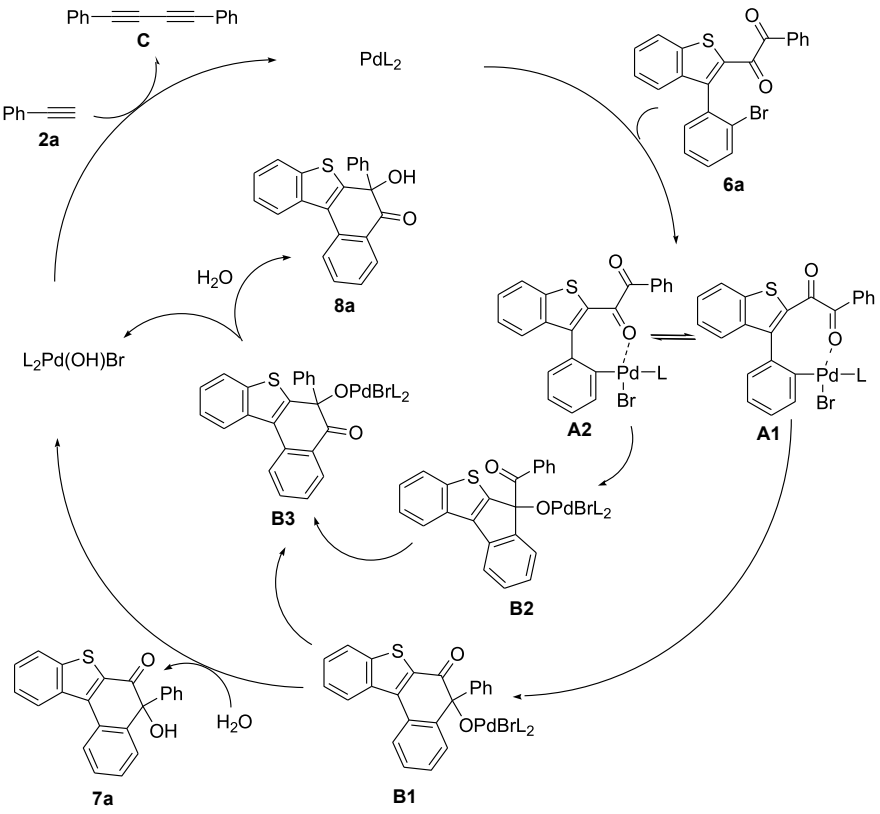

Scheme 6. Possible mechanism of the formation of **7a** and **8a**.

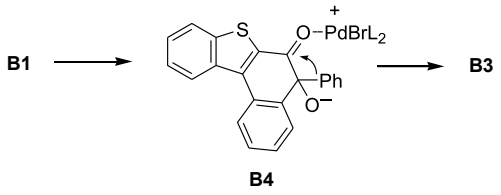

Scheme 7. Possible mechanism of the transformation of **B1** to **B3**.

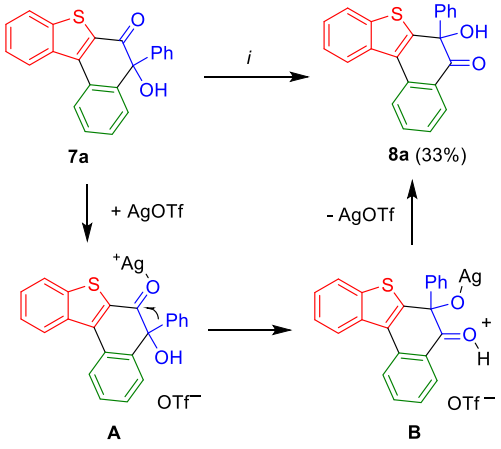

Scheme 8. Transformation of **7a** to **8a**. Conditions: AgOTf (2 equiv.), $C_6H_5CF_3$, 100 °C, 5 h.

The one-pot reaction of **12a** with (2-bromophenyl)boronic acid (**5a**) to give α-hydroxyketone **13a**, which can be regarded as a phenanthrene derivative, was studied next. Due to the symmetrical character of the starting material, only one isomer can be formed in this reaction (in contrast to the corresponding reactions of **4a**). The application of the conditions developed for the one-pot reaction of **4a** to **7a/8a** resulted in formation of only trace amounts of product, due to low conversion. Therefore, in the following experiments the catalyst was changed. The yield of **13a** was optimized to 55% using Pd_2dba_3. An amount of 2.5 mol% of catalyst was added in the first step and additional 5 mol% was added in the second step of the one-pot reaction. Employment of the ligand SPhos gave the best results (addition of 10 mol% in the first step and 20 mol% in the second step). The use of $Pd(OAc)_2$/XPhos resulted in formation of the product in a bit lower yield (45%). Similar to the synthesis of **7a/8a**, it was important to use 1.8 equiv. of phenylacetylene (**2a**). In fact, employment of only 0.2 equiv. of **2a** resulted in a decrease of the yield to 17%. This result suggests that **2a** again acts as a reducing agent. Decrease of the amount of SPhos to 7.5 mol% in the first step resulted in a decrease of the yield to 40%. Employment of sodium hydroxide instead of potassium phosphate as the base resulted in formation of a complex mixture from which the desired product could not be isolated. As a result, Pd_2dba_3/SPhos was further employed as the best catalytic system and derivatives **13b** and **13c** could be prepared, albeit, in only moderate yields (Table 1). Starting with 2-bromo-4,5-difluoro-1-iodobenzene (**10b**), a separable mixture of **13d** (38%) and **14d** (9%) was prepared via intermediates **11d** and **12d**. The reaction of **12a** with 3-bromothiophene-4-boronic acid (**5b**) afforded **13e** in 76% yield (Scheme 11). The structure of **13a** was independently confirmed by X-ray crystal structure analysis (Fig. 5). The structure shows that the biaryl unit is slightly twisted out of plane.

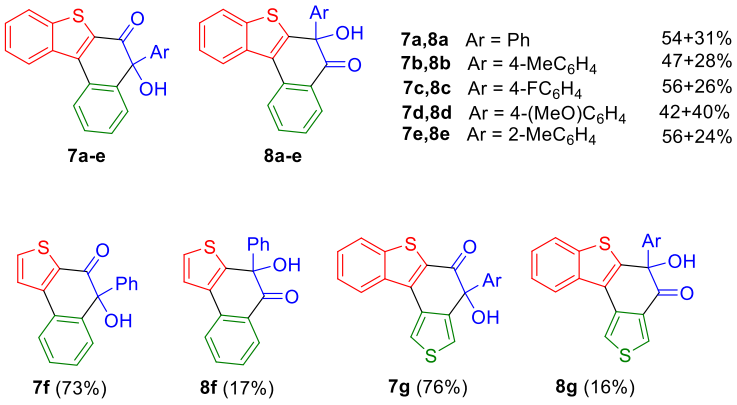

Scheme 9. Synthesis of **7a-g** and **8a-g**.

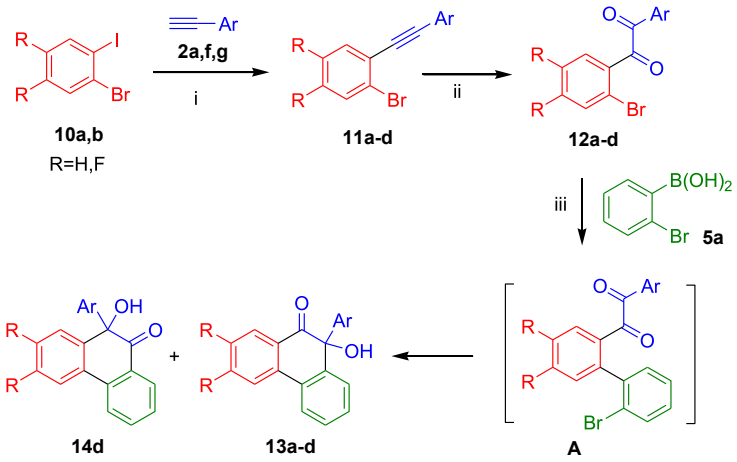

Scheme 10. Synthesis of **13a-d** and **14d**. *Conditions*: *i*, $Pd(PPh_3)_2Cl_2$ (2.5 mol%), CuI (5 mol%), **2a,f,g** (1.1 equiv.), NEt_3, 20 °C, 5 h; *ii*, $Pd(OAc)_2$ (10 mol%), $CuBr_2$ (0.2 equiv.), DMSO, 16 h; *iii*, 1) Pd_2dba_3 (2.5 mol%), SPhos (10 mol%), **5a** (1.5 equiv.), K_3PO_4 (3 equiv.), acetonitrile/H_2O (4:1), 80 °C, 20 h; 2) Pd_2dba_3 (5 mol%), SPhos (20 mol%), DIPA (10 equiv.), **2a** (1.8 equiv.), 80 °C, 5 h.

Table 1
Synthesis of **13a-d** and **14d**.

	R	Ar	**11** (%)[a]	**12** (%)[a]	**13** (%)[a]	**14** (%)[a]
a	H	Ph	97	41	55	/
b	H	4-*t*BuC_6H_4	99	54	36	/
c	H	4-(F_3C)C_6H_4	93	32	38	/
d	F	Ph	43	63	26	9

[a] Isolated yields.

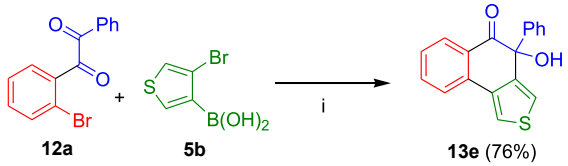

Scheme 11. Synthesis of **13e**. *Conditions*: *i*, 1) Pd_2dba_3 (2.5 mol%), SPhos (10 mol%), **5b** (1.5 equiv.), K_3PO_4 (3 equiv.), acetonitrile/H_2O (4:1), 80 °C, 20 h; 2) Pd_2dba_3 (5 mol%), SPhos (20 mol%), DIPA (10 equiv.), **2a** (1.8 equiv.), 80 °C, 5 h.

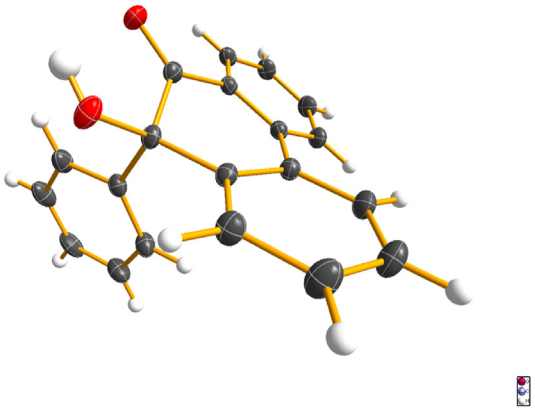

Fig. 5. ORTEP of **13a**.

3. Conclusions

In conclusion, we have reported a synthesis of benzoin derivatives by Sonogashira coupling of alkynes with 1,2-

dihaloalkenes, oxidation of the alkyne to a 1,2-diketone and Pd-catalyzed reaction of the product with (2-bromophenyl)- and (3-bromothien-4-yl)boronic acid in the presence of phenylacetylene. The final reaction was discovered by serendipity and optimized in detail. The reaction was successfully applied to carba- and heterocyclic substrates.

4. Experimental section

General. The nuclear magnetic resonance spectra ($^{1}H/^{13}C/^{19}F$ NMR) were recorded on a Bruker AVANCE 300 III, 250 II or 500. The analyzed chemical shifts δ are referenced to residual solvents signals of the deuterated solvents $CDCl_3$ (δ = 7.26 ppm/77.0 ppm), or TFA-d (δ = 11.50 ppm/164.2 ppm). Multiplicities due to spin-spin correlation are reported as follows: s = singlet, d = doublet, dd = double doublet, t = triplet, pt = pseudo triplet, m = multiplet and further described through their coupling constants J. Infrared spectra (IR) were measured as attenuated total reflection (ATR) experiments with a Nicolet 380 FT-IR spectrometer. The signals have been characterized through their wave numbers $\tilde{\nu}$ and their corresponding absorption as very strong (vs), strong (s), medium (m), weak (w) or very weak (vw). Mass- and high resolution mass spectra (MS/HRMS) were measured on instruments which are paired with a preceding gas chromatograph (GC) or liquid chromatograph (LC). The samples have been ionized through electron impact ionization (EI) on an Agilent 6890/5973 or Agilent 7890/5977 GC-MS equipped with a HP-5 capillary column using helium carrier gas or by applying electron spray ionization (ESI) on an Agilent 1200/6210 Time-of-Flight (TOF) LC-MS. Melting points (mp) were determined by a Micro-Hot-Stage GalenTM III Cambridge Instruments and are not corrected. Crystal structures are deposited at the CCDC [14].

Synthesis of 3a-f. To a mixture of **1a** (1.37 mmol), $Pd(PPh_3)_2Cl_2$ (2 mol%) and CuI (1 mol%) was added 6 mL of trimethylamine under Argon atmosphere. Subsequently, the arylacetylene (1.44 mmol) was dropwise added and the solution was purged with Argon for 1 min. The solution was stirred at 20 °C for 20 h. To the mixture was added water and the mixture was extracted with dichloromethane (3x). The combined organic layers were dried ($MgSO_4$), filtered and concentrated in vacuo. The residue was purified by chromatography (silica gel, heptane).

3-Bromo-2-(phenylethynyl)benzo[*b*]thiophene (3a). Starting with **1a** (1200 mg) and **2a** (474.0 µl), **3a** was isolated as a colourless solid (1107 mg, 86%); mp.: 72–75 °C. ^{1}H NMR (250 MHz, $CDCl_3$): δ = 7.84–7.73 (m, 2H, H_{Ar}), 7.65–7.60 (m, 2H, H_{Ar}), 7.49–7.43 (m, 2H, H_{Ar}), 7.42–7.37 (m, 3H, H_{Ph}) ppm. ^{13}C NMR (63 MHz, $CDCl_3$): δ = 138.4, 137.6 (C_{Ar}), 131.9, 129.3, 128.6, 126.7, 125.6, 123.8 (CH_{Ar}), 122.4 (C_{Ar}), 122.4 (CH_{Ar}), 120.5, 113.9 (C_{Ar}), 99.3, 81.8 (C_{Alkin}) ppm. IR (ATR): $\tilde{\nu}$ = 3056 (w), 2207 (w), 1595 (w), 1521 (w), 1480 (w), 1430 (w), 1243 (w), 818 (w), 748 (m), 721 (m), 705 (m), 666 (m), 528 (w), 511 (w), 435 (m) cm^{-1}. MS (EI, 70 eV): *m/z* (%) = 315 (17), 314 ([M]$^+$, $C_{16}H_9^{81}BrS$, 100), 313 (19), 312 ([M]$^+$, $C_{16}H_9^{79}BrS$, 98), 233 (8), 232 (35), 189 (48), 187 (22), 163 (13), 150 (8), 116 (9), 69 (11). HRMS (EI): calcd for $C_{16}H_9^{79}BrS$ ([M]$^+$) 311.96029, found 311.96087; calcd for $C_{16}H_9^{81}BrS$ ([M]$^+$) 313.95824, found 313.95872.

3-Bromo-2-(*p*-tolylethynyl)benzo[*b*]thiophene (3b). Starting with **1a** (1200 mg) and **2b** (547.2 µl), **3b** was isolated as a beige solid (755 mg, 57%); mp.: 119–120 °C. ^{1}H NMR (300 MHz, $CDCl_3$): δ = 7.82–7.78 (m, 1H, H_{Ar}), 7.77–7.73 (m, 1H, H_{Ar}), 7.51 (d, ^{3}J = 8.1 Hz, 2H, H_{Ar}), 7.47–7.40 (m, 2H, H_{Ar}), 7.19 (d, ^{3}J = 7.8 Hz, 2H, H_{Ar}), 2.39 (s, 3H, CH_3) ppm. ^{13}C NMR (75 MHz, $CDCl_3$): δ = 139.6, 138.4, 137.7 (C_{Ar}), 131.8, 129.4, 126.6, 125.6, 123.8, 122.4 (CH_{Ar}), 119.4, 113.5, 99.6 (C_{Ar}), 81.2 (C_{Alkin}), 21.8 (CH_3) ppm. IR (ATR): $\tilde{\nu}$ = 2918 (w), 2201 (w), 1529 (w), 1494 (w), 1430 (w), 1306 (w), 1245 (w), 1016 (w), 925 (w), 814 (m), 744 (w), 719 (w), 528 (w), 515 (w), 416 (m) cm^{-1}. MS (EI, 70 eV): *m/z* (%) = 329 (19), 328 ([M]$^+$, $C_{17}H_{11}^{81}BrS$, 100), 327 (29), 326 ([M]$^+$, $C_{17}H_{11}^{79}BrS$, 96), 247 (6), 246 (9), 245 (29), 215 (6), 202 (13), 123 (11). HRMS (EI): calcd for $C_{17}H_{11}^{79}BrS$ ([M]$^+$) 325.97594, found 325.97577; calcd for $C_{17}H_{11}^{81}BrS$ ([M]$^+$) 327.97389, found 327.97395.

3-Bromo-2-((4-fluorophenyl)ethynyl)benzo[*b*]thiophene (3c). Starting with **1a** (1200 mg) and **2c** (509.7 µl), **3c** was isolated as a beige solid (987 mg, 73%); mp.: 88–89 °C. ^{1}H NMR (300 MHz, $CDCl_3$): δ = 7.82–7.78 (m, 1H, H_{Ar}), 7.78–7.73 (m, 1H, H_{Ar}), 7.61 (d, ^{3}J = 8.9 Hz, 2H, H_{Ar}), 7.48–7.43 (m, 2H), 7.09 (pt, ^{3}J = 8.8 Hz, 2H, H_{Ar}) ppm. ^{13}C NMR (75 MHz, $CDCl_3$): δ = 163.15 (d, $^{1}J_{C\text{-}F}$ = 251.1 Hz, C_{Ar}) 138.4, 137.6, 134.7, 134.6 (C_{Ar}), 133.90 (d, $^{3}J_{C\text{-}F}$ = 8.5 Hz, CH_{Ar}), 126.7, 125.7, 123.8, 122.4 (CH_{Ar}), 120.3 (C_{Ar}), 118.6 (d, $^{4}J_{C\text{-}F}$ = 3.5 Hz, C_{Ar}), 116.00 (d, $^{2}J_{C\text{-}F}$ = 22.2 Hz, CH_{Ar}), 113.9 (C_{Ar}), 98.1 (C_{Alkin}), 81.6 (d, $^{5}J_{C\text{-}F}$ = 1.5 Hz, C_{Alkin}) ppm.^{19}F NMR (282 MHz, $CDCl_3$): δ = −109.26 ppm. IR (ATR): $\tilde{\nu}$ = 1597 (m), 1523 (m), 1490 (m), 1154 (m), 1090 (w), 1012 (w), 927 (w), 803 (m), 744 (m), 719 (m), 699 (m), 528 (m), 517 (m), 424 (m) cm^{-1}. MS (EI, 70 eV): *m/z* (%) = 333 (19), 332 ([M]$^+$, $C_{16}H_8^{81}BrFS$, 100), 331 (19), 330 ([M]$^+$, $C_{16}H_8^{79}BrFS$, 98), 250 (26), 207 (34), 205 (11), 166 (8), 165 (7), 125 (10). HRMS (EI): calcd for $C_{16}H_8^{79}BrFS$ ([M]$^+$) 329.95086, found 329.95081; calcd for $C_{16}H_8^{81}BrFS$ ([M]$^+$) 331.94981, found 331.94981.

3-Bromo-2-((4-methoxyphenyl)ethynyl)benzo[*b*]thiophene (3d). Starting with **1a** (1200 mg) and **2d** (559.8 µl), **3d** was isolated as a beige solid (893 mg, 64%); mp.: 94–98 °C. ^{1}H NMR (300 MHz, $CDCl_3$): δ = 7.84–7.70 (m, 2H. H_{Ar}), 7.56 (d, ^{3}J = 8.9 Hz, 2H, H_{Ar}), 7.50–7.39 (m, 2H, H_{Ar}), 6.91 (d, ^{3}J = 9.0 Hz, 2H, H_{Ar}), 3.85 (s, 3H, OCH_3) ppm. ^{13}C NMR (75 MHz, $CDCl_3$): δ = 160.5, 138.3, 137.7 (C_{Ar}), 133.5, 126.5, 125.6, 123.67, 122.4 (CH_{Ar}), 120.9, 114.5 (C_{Ar}), 114.3 (CH_{Ar}), 113.2 (C_{Ar}), 99.6, 80.7 (C_{Alkin}) 55.5 (OCH_3) ppm. IR (ATR): $\tilde{\nu}$ = 2926 (m), 2835 (w), 2205 (w), 1599 (m), 1494 (m), 1434 (m), 1294 (m), 1245 (m), 1170 (m), 1028 (m), 835 (m), 816 (m), 738 (m), 534 (m), 429 (m) cm^{-1}. MS (EI, 70 eV): *m/z* (%) = 346 (7), 345 (19), 344 ([M]$^+$, $C_{17}H_{11}^{81}BrOS$, 100), 343 (20), 342 ([M]$^+$, $C_{17}H_{11}^{79}BrOS$, 100), 329 (40), 301 (13), 299 (14), 220 (10), 219 (26), 176 (17), 172 (8), 171 (8). HRMS (EI): calcd for $C_{17}H_{11}^{79}BrOS$ ([M]$^+$)341.97085, found 341.97072; calcd for $C_{17}H_{11}^{81}BrOS$ ([M]$^+$) 343.96880, found 343.96911.

3-Brom-2-(*o*-tolylethinyl)benzo[*b*]thiophene (3e). Starting with **1a** (1200 mg) and **2e** (543.6 µl), **3e** was isolated as a beige solid (968 mg, 75%); a small amount of impurity could not be removed. The compound was used as is for the synthesis of **4f**; mp.: 73–77 °C. MS (EI, 70 eV): *m/z* (%) = 329 (19), 328 ([M]$^+$, $C_{17}H_{11}^{81}BrS$, 100), 326 ([M]$^+$, $C_{17}H_{11}^{79}BrS$, 97), 248 (13), 246 (32), 245 (79), 215 (26), 213 (11), 203 (13), 202 (30), 200 (11), 123 (16), 101 (10). HRMS (EI): calcd for $C_{17}H_{11}^{79}BrS$ ([M]$^+$) 325.97594, found 325.97678; calcd for $C_{17}H_{11}^{81}BrS$ ([M]$^+$) 327.97389, found 327.97516.

Synthesis of 11a-c. To a mixture of **10a** (1.77 mmol), $Pd(PPh_3)_2Cl_2$ (2.5 mol%) and CuI (5 mol%) was added 6 mL of trimethylamine under Argon atmosphere. Subsequently, the arylacetylene (1.95 mmol) was dropwise added and the solution was purged with Argon for 1 min. The solution was stirred at 20 °C for 5 h. To the mixture was added water and the mixture was extracted with dichloromethane (3x). The combined organic layers were dried ($MgSO_4$), filtered and concentrated in vacuo. The residue was purified by chromatography (silica gel, heptane).

1-Bromo-2-(phenylethynyl)benzene (11a). Starting with **10a** (500 mg) and phenylacetylene (214 µl), **11a** was isolated as a colourless solid (441 mg, 97%); R_f: 0.49 (Heptane). ^{1}H NMR (250 MHz, $CDCl_3$): δ = 7.62–7.57 (m, 4H, H_{Ar}), 7.39–7.36 (m, 5H, H_{Ph}) ppm.^{13}C NMR (63 MHz, $CDCl_3$): δ = 133.4, 132.6, 131.8, 129.5, 128.8, 128.5, 127.2 (CH_{Ar}), 125.8, 125.6, 123.1 (C_{Ar}), 94.1, 88.2 (C_{Alkin}) ppm. IR (ATR): $\tilde{\nu}$ = 3056 (w), 2219 (w), 1597 (w), 1490 (m), 1463 (m), 1432 (w), 1041 (m), 1024 (m), 748 (vs), 686 (vs), 653 (m), 546 (m), 517 (m), 441(m) cm^{-1}. MS (EI, 70 eV): *m/z* (%) = 259 (16), 258 ([M]$^+$,

$C_{14}H_9^{81}Br$, 99), 257 (18), 256 ([M]$^+$, $C_{14}H_9^{79}Br$, 100), 177 (19), 176 (92), 151 (35), 150 (36), 126 (14), 98 (18), 88 (15), 75 (14), 74 (17), 63 (14), 51 (18), 50 (20), 39 (22). HRMS (EI): calcd for $C_{14}H_9^{79}Br$ ([M]$^+$) 255.98821, found 255.98826; calcd for $C_{14}H_9^{81}Br$ ([M]$^+$) 257.98617, found 257.98660.

1-Bromo-2-((4-(*tert*-butyl)phenyl)ethynyl)benzene (11b). Starting with **10a** (500 mg) and 4-*tert*-butylphenylacetylene (351.3 μL), **11b** was isolated as a colourless solid (548 mg, 99%); mp.: 62–67 °C. ^{1}H NMR (250 MHz, $CDCl_3$): δ = 7.66–7.54 (m, 2H, H_{Ar}), 7.55 (d, ^3J = 8.5 Hz, 2H, H_{Ar}), 7.41 (d, ^3J = 8.5 Hz, 2H, H_{Ar}), 7.34–7.25 (m, 1H, H_{Ar}), 7.21–7.14 (m, 1H, H_{Ar}), 1.35 (s, 9H, $C(CH_3)_3$) ppm. ^{13}C NMR (63 MHz, $CDCl_3$): δ = 152.1 (C_{Ar}), 133.3, 132.5, 131.6, 129.3, 127.1 (CH_{Ar}), 125.8, 125.8 (C_{Ar}), 125.5 (CH_{Ar}), 120.0 (C_{Ar}), 94.3, 87.6 (C_{Alkin}), 35.0 ($C(CH_3)_3$), 31.3 (CH_3) ppm. IR (ATR): $\tilde{\nu}$ = 2955 (w), 2221 (w), 1501 (w), 1465 (w), 1433 (w), 1359 (w), 1266 (w), 1100 (w), 1027 (w), 829 (m), 750 (m), 559 (m), 442 (m) cm^{-1}. MS (EI, 70 eV): *m/z* (%) = 314 ([M]$^+$, $C_{18}H_{17}^{81}Br$, 43), 312 ([M]$^+$, $C_{18}H_{17}^{79}Br$, 43), 300 (20), 299 (99), 298 (20), 297 (100), 218 (21), 203 (27), 202 (48), 189 (23), 176 (29), 41 (21), 39 (21).

1-Bromo-2-((4-(trifluormethyl)phenyl)ethynyl)benzene (11c). Starting with **10a** (500 mg) and 4-(trifluormethyl)phenylacetylene (345.5 μl), **11c** was isolated as a colourless solid (557.4 mg, 97%); mp.: 68–74 °C. ^{1}H NMR (300 MHz, $CDCl_3$): δ = 7.70–7.60 (m, 5H, H_{Ar}), 7.57 (dd, ^3J = 7.7 Hz, ^3J = 1.8 Hz, 1H, H_{Ar}), 7.34–7.29 (m, 1H, H_{Ar}), 7.25–7.19 (m, 1H, H_{Ar}). ppm.^{13}C NMR (75 MHz, $CDCl_3$): δ = 133.5, 132.1 (CH_{Ar}), 130.4 (q, $^2J_{C\text{-}F}$ = 32.7 Hz, C_{Ar}), 130.1, 127.3 (CH_{Ar}), 126.9 (q, $^5J_{C\text{-}F}$ = 1.6 Hz, C_{Ar}), 126.0, 125.9, 125.6 (CH_{Ar}), 125.5 (q, $^4J_{C\text{-}F}$ = 3.8 Hz, CH_{Ar}), 124.06 (q, $^1J_{C\text{-}F}$ = 272.1 Hz, CF_3) 92.5, 90.4 (C_{Alkin}) ppm. ^{19}F NMR (282 MHz, $CDCl_3$): δ = −62.83 ppm. IR (ATR): $\tilde{\nu}$ = 2924 (w), 1611 (w), 1319 (m), 1170 (m), 1154 (m), 1104 (m), 1063 (m), 839 (m), 752 (m), 709 (m), 655 (w), 596 (m), 517 (w), 455 (w), 439 (w) cm^{-1}. MS (EI, 70 eV): *m/z* (%) = 327 (16), 326 ([M]$^+$, $C_{15}H_8^{81}BrF_3$, 95), 325 (16), 324 ([M]$^+$, $C_{15}H_8^{79}BrF_3$, 100), 245 (12), 225 (40), 199 (12), 176 (49), 175 (18), 150 (13), 98 (13), 69 (16). HRMS (EI): calcd for $C_{15}H_8^{79}BrF_3$ ([M]$^+$) 323.97560, found 323.97499; calcd for $C_{15}H_8^{81}BrF_3$ ([M]$^+$) 325.97355, found 325.97269.

1-Bromo-4,5-difluoro-2-(phenylethynyl)benzene (11d). Starting with **10b** (1600 mg, 5.88 mmol) and phenylacetylene (646 μl, 600 mg, 5.88 mmol), **11d** was isolated as a colourless solid (746 mg, 43%). ^{1}H NMR (300 MHz, Chloroform-*d*) δ 7.56–7.52 (m, 3H, H_{Ar}), 7.40–7.31 (m, 4H, H_{Ar}). ^{13}C NMR (75 MHz, Chloroform-*d*) δ 132.65 (CH_{Ar}), 129.35 (CH_{Ar}), 128.59 (CH_{Ar}), 121.95 (C_{Ar}), 81.70 (C≡C), 74.06 (C≡C). ^{19}F NMR ^{19}F NMR (282 MHz, Chloroform-*d*) δ −133.08 (d, J = 21.0 Hz, 1 F, CF_{Ar}), −138.07 (d, J = 21.0 Hz, 1 F, CF_{Ar}). IR (ATR): $\tilde{\nu}$ = 1588 (w), 1483 (m), 1438 (m), 1392 (w), 1324 (w), 1184 (w), 1067 (w), 1024 (w), 912 (m), 750 (vs).

Synthesis of 4a-g and 12a-c. Compound **3a-f** (1 equiv.), $Pd(OAc)_2$ (0.1 equiv.) and $CuBr_2$ (0.1 equiv.) were dissolved in 20 mL of DMSO. In case of **11a-c**, 0.2 equiv. of $CuBr_2$ were employed. The solution was stirred at 120 °C for 14 h. To the mixture was added water and the mixture was extracted with ethyl acetate (3x). The combined organic layers were dried ($MgSO_4$), filtered and concentrated in vacuo. The residue was purified by chromatography (silica gel, heptane/EtOAc).

1-(3-Bromobenzo[*b*]thien-2-yl)-2-phenylethane-1,2-dione (4a). Starting with **3a** (878 mg, 2.8 mmol), **4a** was isolated as a beige solid (561 mg, 58%); mp.: 122–129 °C. ^{1}H NMR (300 MHz, $CDCl_3$): δ = 8.03 (dd, ^3J = 8.4 Hz, ^4J = 1.3 Hz, 2H, $H_{Ar/Ph}$), 7.97 (ddd, ^3J = 8.0 Hz, ^4J = 1.4 Hz, ^5J = 0.7 Hz, 1H, H_{Ar}), 7.91–7.87 (m, 1H, $H_{Ar/Ph}$), 7.72–7.66 (m, 1H, $H_{Ar/Ph}$), 7.62–7.49 (m, 4H, $H_{Ar/Ph}$) ppm. ^{13}C NMR (75 MHz, $CDCl_3$): δ = 192.2, 188.5 (C═O), 141.1, 138.7 ($C_{Ar/Ph}$), 135.1 ($CH_{Ar/Ph}$), 134.7, 132.9 ($C_{Ar/Ph}$), 130.3, 129.5, 129.2, 126.3, 126.0, 123.2 ($CH_{Ar/Ph}$), 117.0 ($C_{Ar/Ph}$) ppm. IR (ATR): $\tilde{\nu}$ = 3058 (w), 2922 (w), 1671 (m), 1636 (m), 1591 (m), 1492 (m), 1449 (w), 1426 (w), 1309 (w), 1247 (m), 1203 (m), 1107 (m), 999 (w), 909 (w), 846 (m), 781 (m), 754 (m), 707 (m), 649 (m), 612 (m) cm^{-1}. MS (EI, 70 eV): *m/z* (%) = 346 ([M]$^+$, $C_{16}H_9^{81}BrO_2S$, 2), 344 ([M]$^+$, $C_{16}H_9^{81}BrO_2S$, 3), 265 (22), 241 (43), 239 (42), 213 (19), 211 (19), 132 (67), 105 (83), 93 (17), 77 (100), 51 (42), 50 (17). HRMS (EI): calcd for $C_{16}H_9O_2^{79}BrS$ ([M]$^+$) 343.95011, found 343.95031; calcd for $C_{16}H_9O_2^{81}BrS$ ([M]$^+$) 345.94807, found 345.94805.

1-(3-Bromobenzo[*b*]thien-2-yl)-2-(*p*-tolyl)ethane-1,2-dione (4b). Starting with **3b** (735 mg, 2.25 mmol), **4b** was isolated as a beige solid (514 mg, 60%); mp.: 150–154 °C. ^{1}H NMR (300 MHz, $CDCl_3$): δ = 7.99–7.87 (m, 2H), 7.92 (d, ^3J = 8.3 Hz, 2H, H_{Ar}), 7.61–7.48 (m, 2H, H_{Ar}), 7.34 (d, ^3J = 8.0 Hz, 2H, H_{Ar}), 2.46 (s, 3H, CH_3) ppm. ^{13}C NMR (75 MHz, $CDCl_3$): δ = 191.9, 188.6 (C═O), 146.4, 141.0, 138.8, 134.8, 130.5 (C_{Ar}), 130.4, 130.4, 130.0, 130.0, 129.5, 126.2, 126.0, 123.2 (CH_{Ar}), 116.9 (C_{Ar}), 22.1 (CH_3) ppm. IR (ATR): $\tilde{\nu}$ = 2918 (m), 1663 (w), 1636 (w), 1494 (w), 1244 (w), 1200 (w), 1171 (m), 909 (w), 814 (w), 755 (m), 716 (m), 684 (m), 606 (m), 584 (m), 479 (m) cm^{-1}. MS (EI, 70 eV): *m/z* (%) = 360 ([M]$^+$, $C_{17}H_{11}^{81}BrO_2S$, 1), 358 ([M]$^+$, $C_{17}H_{11}^{79}BrO_2S$, 1), 279 (12), 241 (15), 239 (15), 132 (16), 119 (100), 91 (22). HRMS (EI): calcd for $C_{17}H_{11}^{79}BrO_2S$ ([M]$^+$) 357.96576, found 357.96513; calcd for $C_{17}H_{11}^{81}BrO_2S$ ([M]$^+$) 359.96372, found 359.96440.

1-(3-Bromobenzo[*b*]thien-2-yl)-2-(4-fluorophenyl)ethane-1,2-dione (4c). Starting with **3c** (914 mg, 2.76 mmol), **4c** was isolated as a red solid (502 mg, 50%); mp.: 122–126 °C. ^{1}H NMR (300 MHz, $CDCl_3$): δ = 8.08 (d, ^3J = 9.0 Hz, 2H, H_{Ar}), 7.97 (ddd, ^3J = 7.9 Hz, ^4J = 1.4 Hz, ^5J = 0.7 Hz, 1H, H_{Ar}), 7.91–7.87 (m, 1H, H_{Ar}), 7.59 (ddd, ^3J = 8.1 Hz, ^3J = 7.1 Hz, ^4J = 1.4 Hz, 1H, H_{Ar}), 7.52 (ddd, ^3J = 8.1 Hz, ^3J = 7.1 Hz, ^4J = 1.2 Hz, 1H, H_{Ar}), 7.22 (d, ^3J = 8.8 Hz, 2H, H_{Ar}) ppm. ^{13}C NMR (75 MHz, $CDCl_3$): δ = 190.5, 188.0 (C═O), 167.0 (d, $^1J_{C\text{-}F}$ = 258.4 Hz, C_{Ar}) 141.1, 138.7, 134.4 (C_{Ar}), 133.1 (d, $^3J_{C\text{-}F}$ = 9.8 Hz, CH_{Ar}), 129.6 (CH_{Ar}), 129.37 (d, $^4J_{C\text{-}F}$ = 3.0 Hz, C_{Ar}), 126.3, 126.0, 123.2 (CH_{Ar}), 117.1 (C_{Ar}), 116.7 (d, $^2J_{C\text{-}F}$ = 22.3 Hz, CH_{Ar}) ppm. ^{19}F NMR (282 MHz, $CDCl_3$): δ = −101.02 (s, 1 F, CF_{Ar}) ppm. IR (ATR): $\tilde{\nu}$ = 3075 (w), 2962 (w), 1670 (w), 1641 (w), 1592 (w), 1496 (w), 1237 (w), 1196 (w), 1151 (w), 821 (m), 753 (m), 721 (m), 606 (m), 581 (m), 503 (w), 425 (w) cm^{-1}. MS (EI, 70 eV): *m/z* (%) = 364 ([M]$^+$, $C_{14}H_9^{81}BrO_2S$, 5), 362 ([M]$^+$, $C_{14}H_9^{79}BrO_2S$, 4), 283 (15), 242 (10), 241 (100), 240 (11), 239 (98), 213 (14), 211 (13), 132 (39), 123 (73), 95 (33), 75 (10). HRMS (EI): calcd for $C_{14}H_9^{79}BrO_2S$ ([M]$^+$) 361.94069, found 361.94082; calcd for $C_{14}H_9^{81}BrO_2S$ ([M]$^+$) 363.93865, found 363.93849.

1-(3-Bromobenzo[*b*]thien-2-yl)-2-(4-methoxyphenyl) ethane-1,2-dione (4d). Starting with **3d** (871 mg, 2.54 mmol), **4d** was isolated as a beige solid (374 mg, 40%); mp.: 140–143 °C. ^{1}H NMR (300 MHz, $CDCl_3$): δ = 8.00 (d, ^3J = 9.1 Hz, 2H, H_{Ar}), 7.96 (ddd, ^3J = 7.9 Hz, ^4J = 1.4 Hz, ^5J = 0.7 Hz, 1H, H_{Ar}), 7.88 (ddd, ^3J = 8.1 Hz, ^4J = 1.2 Hz, ^5J = 0.7 Hz, 1H, H_{Ar}), 7.57 (ddd, ^3J = 8.1 Hz, ^3J = 7.1 Hz, ^4J = 1.4 Hz, 1H, H_{Ar}), 7.50 (ddd, ^3J =8.0 Hz, ^3J = 7.1 Hz, ^4J = 1.3 Hz, 1H, H_{Ar}), 7.01 (d, ^3J = 9.1 Hz, 2H, H_{Ar}), 3.90 (s, 3H, OCH_3) ppm. ^{13}C NMR (75 MHz, $CDCl_3$): δ = 190.8, 188.6 (C═O), 165.2, 141.0, 138.8, 134.7 (C_{Ar}), 132.7, 132.7, 129.4, 126.2, 126.0 (CH_{Ar}), 125.9 (C_{Ar}), 123.2 (CH_{Ar}), 116.8 (C_{Ar}), 114.6, 114.6 (CH_{Ar}), 55.8 (OCH_3) ppm. IR (ATR): $\tilde{\nu}$ = 3058 (w), 2847 (w), 1651 (w), 1594 (m), 1565 (m), 1474 (m), 1423 (m), 1262 (m), 1149 (m), 1015 (m), 912 (m), 887 (m), 838 (m), 787 (m), 753 (m), 723 (m), 567 (m), 508 (m) cm^{-1}. MS (EI, 70 eV): *m/z* (%) = 376 ([M]$^+$, $C_{17}H_{11}^{81}BrO_3S$, 0.2), 374 ([M]$^+$, $C_{17}H_{11}^{79}BrO_3S$, 0.2), 241 (4), 136 (9), 135 (100), 132 (8), 107 (4), 92 (7), 77 (8). HRMS (EI): calcd for $C_{17}H_{11}^{79}BrO_3S$ ([M]$^+$) 373.96068, found 373.96124; calcd for $C_{17}H_{11}^{81}BrO_3S$ ([M]$^+$) 375.95863, found 375.95875.

1-(3-Brombenzo[*b*]thiophene-2-yl)-2-(*o*-tolyl)ethan-1,2-dion (4e). Starting with **3e** (969 mg, 2.96 mmol), **4e** was isolated as a beige solid (274 mg, 26% over two steps based on **1a**); mp.: 102–105 °C. ^{1}H NMR (250 MHz, $CDCl_3$): δ =8.00–7.94 (m, 1H, H_{Ar}), 7.92–7.87 (m, 1H, H_{Ar}), 7.74 (dd, ^3J = 7.8 Hz, ^4J = 1.3 Hz, 1H, H_{Ar}), 7.62–7.48 (m, 3H, H_{Ar}), 7.39–7.28 (m, 2H, H_{Ar}), 2.74 (s, 3H, CH_3)

ppm. ^{13}C NMR (63 MHz, $CDCl_3$): δ = 193.9, 188.6 (C═O), 142.0, 141.0, 138.8, 135.0 (C_{Ar}), 134.1, 133.2, 132.8 (CH_{Ar}), 131.4 (C_{Ar}), 129.4, 126.2, 126.2, 125.9, 123.2 (CH_{Ar}), 116.6 (C_{Ar}), 22.2 (CH_3) ppm. IR (ATR): $\tilde{\nu}$ = 3060 (w), 2923 (w), 1668 (m), 1636 (m), 1489 (m), 1306 (w), 1249 (w), 1196 (m), 912 (w), 848 (w), 755 (m), 716 (m), 643 (m), 616 (m) cm^{-1}. MS (EI, 70 eV): ([M]$^+$, $C_{17}H_{11}^{81}BrO_2S$, 1), 358 ([M]$^+$, $C_{17}H_{11}^{79}BrO_2S$, 1), 279 (15), 241 (16), 239 (15), 132 (19), 119 (100), 91 (29). HRMS (EI): calcd for $C_{17}H_{11}^{79}BrO_2S$ ([M]$^+$) 357.96576, found 375.96494; calcd for $C_{17}H_{11}^{81}BrO_2S$ ([M]$^+$) 359.96372, found 389.96393.

1-(3-Bromothien-2-yl)-2-phenylethane-1,2-dione (4f). Starting with **3f** (885 mg, 3.36 mmol), **4f** was isolated as a beige solid (470 mg, 34% over two steps based on **1b**); mp.: 54–56 °C. ^{1}H NMR (300 MHz, $CDCl_3$): δ = 8.02–7.99 (m, 2H, H_{Ph}), 7.74 (d, ^3J = 5.1 Hz, 1H, $H_{Thiophene}$), 7.70–7.64 (m, 1H, H_{Ph}), 7.56–7.50 (m, 2H, H_{Ph}), 7.17 (d, ^3J = 5.1 Hz, 1H, $H_{Thiophene}$) ppm. ^{13}C NMR (75 MHz, $CDCl_3$): δ = 192.0, 186.1 (C═O), 136.0, 135.0 ($CH_{Ar/Thio}$), 134.3 ($C_{Ar/Thio}$), 133.7 ($CH_{Ar/Thio}$), 132.8 ($C_{Ar/Thio}$), 130.3, 129.2 ($CH_{Ar/Thio}$), 118.9 ($C_{Ar/Thio}$) ppm. IR (ATR): $\tilde{\nu}$ = 3097 (w), 3984 (w), 2923 (w), 1675 (m), 1626 (m), 1489 (w), 1399 (m), 1205 (m), 1005 (w), 885 (m), 745 (m), 716 (m), 684 (m), 682 (m), 638 (m), 484 (m) cm^{-1}. MS (EI, 70 eV): 296 ([M]$^+$, $C_{12}H_7^{81}BrO_2S$, 2), 294 ([M]$^+$, $C_{12}H_7^{79}BrO_2S$, 2), 215 (4), 191 (24), 189 (24), 106 (8), 105 (100), 82 (11), 77 (34), 51 (10), 50 (4). HRMS (EI): calcd for $C_{12}H_7^{79}BrO_2S$ ([M]$^+$) 293.93446, found 293.93440; calcd for $C_{12}H_7^{81}BrO_2S$ ([M]$^+$) 295.93242, found 295.93246.

1-(2-Bromophenyl)-2-phenylethane-1,2-dione (12a). Starting with **11a** (911 mg, 3.54 mmol), **12a** was isolated as a beige oil (430 mg, 41%); R_f: 0.25 (Heptane/EtOAc 20:1). ^{1}H NMR (300 MHz, $CDCl_3$): δ = 8.10–8.06 (m, 2H, H_{Ar}), 7.84–7.80 (m, 1H, H_{Ar}), 7.70–7.62 (m, 2H, H_{Ar}), 7.58–7.51 (m, 2H, H_{Ar}), 7.50–7.42 (m, 2H, H_{Ar}). ^{13}C NMR (75 MHz, $CDCl_3$): δ = 194.3, 191.6 (C═O), 136.2 (C_{Ar}), 134.6, 134.5, 133.9 (CH_{Ar}), 132.9 (C_{Ar}), 132.7, 130.5, 129.0, 128.0 (CH_{Ar}), 122.0 (C_{Ar}) ppm. IR (ATR): $\tilde{\nu}$ = 3026 (w), 1672 (s), 1585 (m), 1449 (m), 1432 (m), 1253 (m), 1203 (s), 1965 (w), 1026 (m), 876 (m), 857 (m), 742 (m), 723 (s), 684 (m), 633 (s), 451 (m) cm^{-1}. MS (EI, 70 eV): *m/z* (%) = 290 ([M]$^+$, $C_{14}H_9^{81}BrO_2$, 1), 288 ([M]$^+$, $C_{14}H_9^{79}BrO_2$, 1), 185 (40), 183 (42), 157 (12), 155 (13), 106 (7), 105 (100), 77 (33), 76 (10), 75 (8), 51 (9), 50 (7). HRMS (EI): calcd for $C_{14}H_9^{79}BrO_2$ ([M]$^+$) 287.97804, found 287.97772; calcd for $C_{14}H_9^{81}BrO_2$ ([M]$^+$) 289.97600, found 289.97590.

1-(2-Bromophenyl)-2-(4-(*tert*-butyl)phenyl)ethane-1,2-dione (12b). Starting with **11b** (1321 mg, 4.22 mmol), **12b** was isolated as a beige solid (670 mg, 46%); mp.: 64–70 °C. ^{1}H NMR (250 MHz, $CDCl_3$): δ = 8.00 (d, ^3J = 8.5 Hz, 2H, H_{Ar}), 7.83–7.78 (m, 1H, H_{Ar}), 7.66–7.61 (m, 1H, H_{Ar}), 7.55 (d, ^3J = 8.5 Hz, 2H, H_{Ar}), 7.48–7.42 (m, 2H, H_{Ar}), 1.37 (s, 9H, $C(CH_3)_3$) ppm. ^{13}C NMR (63 MHz, $CDCl_3$): δ = 194.5, 191.4 (C═O), 158.7, 136.3 (C_{Ar}), 134.3, 133.9, 132.7, 130.5 (CH_{Ar}), 130.3 (C_{Ar}), 127.90, 126.1 (CH_{Ar}), 121.9 (C_{Ar}), 35.5 ($C(CH_3)_3$), 31.2 ($C(CH_3)$) ppm. IR (ATR): $\tilde{\nu}$ = 3062 (w), 2960 (w), 1668 (m), 1599 (m), 1587 (m), 1565 (m), 1460 (m), 1408 (m), 1364 (m), 1257 (m), 1213 (m), 1186 (m), 1110 (m), 1066 (w), 877 (m), 740 (m), 665 (m), 640 (m), 547 (m), 496 (m) cm^{-1}. MS (EI, 70 eV): *m/z* (%) = 346 ([M]$^+$, $C_{18}H_{17}^{81}BrO_2$, 0.09), 344 ([M]$^+$, $C_{18}H_{17}^{79}BrO_2$, 0.11), 185 (6), 183 (6), 162 (12), 161 (100), 155 (4), 146 (7), 118 (9), 115 (4), 91 (5). HRMS (ESI-TOF): calcd for $C_{18}H_{18}^{79}BrO_2$ ([M+Na]$^+$ 367.0309, found 367.0310.

1-(2-Bromophenyl)-2-(4-(trifluoromethyl)phenyl)ethane-1,2-dione (12c). Starting with **11c** (1678 mg, 5.16 mmol), **12c** was isolated as a beige solid (608 mg, 33%); mp.: 110–115 °C. ^{1}H NMR (300 MHz, $CDCl_3$): δ = 8.20 (d, ^3J = 8.0 Hz, 2H, H_{Ar}), 7.84–7.79 (m, 3H, H_{Ar}), 7.66–7.62 (m, 1H, H_{Ar}), 7.50 (ddd, ^3J = 6.6 Hz, ^3J = 4.1 Hz, ^4J = 1.9 Hz, 2H, H_{Ar}) ppm. ^{13}C NMR (75 MHz, $CDCl_3$): δ = 193.8, 190.1 (C═O), 136.1 (C_{Ar}), 135.6 (q, $^2J_{C\text{-}F}$ = 32.8 Hz, C_{Ar}) 135.5 (C_{Ar}) 134.8, 133.7, 132.6, 130.8, 128.2 (CH_{Ar}), 126.0 (q, $^3J_{C\text{-}F}$ = 3.7 Hz, CH_{Ar}), 123.58 (q, $^1J_{C\text{-}F}$ = 273.0 Hz, CF_3). 121.90 (C_{Ar}) ppm. IR (ATR): $\tilde{\nu}$ = 1681(w), 1667 (w), 1585 (w), 1510 (w), 1438 (w), 1409 (w), 1323 (m), 1285 (w), 1206 (w), 1173 (m), 1059 (m), 873 (w), 840 (w), 765 (w), 744 (m), 666 (w) cm^{-1}. HRMS (ESI): calcd for $C_{18}H_{17}^{79}Br$ ([M+H]$^+$) 312.05081, found 312.05067; calcd for $C_{18}H_{17}^{81}Br$ ([M+H]$^+$) 314.04877, found 314.04916.

1-(2-Bromo-4,5-difluorophenyl)-2-phenylethane-1,2-dione (12d). Starting with **11d** (746 mg, 2.55 mmol), **12d** was isolated as a colourless solid (521 mg, 63%). ^{1}H NMR (300 MHz, Chloroform-d) δ 8.08–8.00 (m, 2H, HAr), 7.77–7.64 (m, 2H, HAr), 7.59–7.41 (m, 3H, HAr). ^{13}C NMR (75 MHz, Chloroform-d) δ 191.89 (C═O), 190.85 (C═O), 155.35–151.70 (m, CAr), 151.67–148.22 (m, CAr), 134.96 (CHAr), 132.99 (CAr), 132.54(CAr), 130.51(CHAr), 129.14 (CHAr), 123.05 (d, J = 20.5 Hz, CHAr), 121.47 (dd, J = 19.5, 2.0 Hz, CHAr), 116.72 (d, J = 3.9 Hz, CAr). ^{19}F NMR (282 MHz, Chloroform-d) δ −126.06 (d, J = 21.0 Hz, 1 F, CFAr), −136.00 (d, J = 20.9 Hz, 1 F, CFAr).

Synthesis of 7a-g and 8a-g. To a mixture of **4a-f** (0.88 mmol, 1 equiv.), $Pd(PPh_3)_2Cl_2$ (5 mol%), $HP(^tBu)_3BF_4$ (10 mol%), **5a,b** (1.5 equiv.) and K_3PO_4 (3 equiv.) was added acetonitrile/water (8:2) and the mixture was purged with Argon. The solution was stirred at 80 °C for 20 h. The solution was cooled to 20 °C and $Pd(PPh_3)_2Cl_2$ (10 mol%), $HP(^tBu)_3BF_4$ (20 mol%), diisopropylamine (409 µl) and phenylacetylene (1.8 equiv) were added and the mixture was purged with Argon. The solution was stirred at 80 °C for 5 h. To the mixture was added water and the mixture was extracted with ethyl acetate (3x). The combined organic layers were dried ($MgSO_4$), filtered and concentrated in vacuo. The residue was purified by chromatography (silica gel, toluene with a few drops of diethyl ether).

(*R*/*S*)-5-Hydroxy-5-phenylbenzo[*b*]naphtho[1,2-*d*]thiophene-6(5*H*)-one (7a). Starting with **4a** (300 mg, 0.88 mmol), **7a** was isolated as a yellow solid (161 mg, 54%); mp.: 187–189 °C. ^{1}H NMR (250 MHz, DMSO-d_6): δ = 8.83–8.78 (m, 1H, H_{Ar}), 8.53 = 8.48 (m, 1H, H_{Ar}), 8.20–8.14 (m, 1H, H_{Ar}), 7.74–7.69 (m, 1H, H_{Ar}), 7.67–7.63 (m, 2H, H_{Ar}), 7.58–7.48 (m, 2H, H_{Ar}), 7.31–7.27 (m, 2H, H_{Ar}), 7.22–7.18 (m, 3H, H_{Ar}), 6.81 (s, 1H, OH) ppm. ^{13}C NMR (63 MHz, DMSO-d_6): δ = 195.4 (C═O), 144.4, 143.0, 142.0, 139.9, 135.5, 133.5 (C_{Ar}), 129.1 (CH_{Ar}), 128.8 (C_{Ar}), 128.7, 128.5, 128.4, 128.3, 127.8, 126.4, 125.7, 125.7, 124.9, 124.5 (CH_{Ar}), 80.3 (C_{OH}) ppm. IR (ATR): $\tilde{\nu}$ = 3439 (w), 2920 (w), 2852 (w), 1727 (w), 1657 (m), 1500 (w), 1356 (w), 1251 (w), 1148 (m), 978 (m), 783(m), 767 (m), 721 (m), 694 (m), 604 (m) cm^{-1}. MS (EI, 70 eV): *m/z* (%) = 343 (10), 342 ([M]$^+$, $C_{22}H_{14}O_2S$, 44), 238 (14), 237 (82), 222 (17), 221 (100), 220 (13), 219 (15), 208 (19), 189 (14), 176 (22), 165 (32), 164 (11), 163 (15), 105 (99), 77 (80), 51 (35), 50 (12). HRMS (EI): calcd for $C_{22}H_{14}O_2S$ ([M]$^+$) 342.07090, found 342.07073.

(*R*/*S*)-5-Hydroxy-5-(*p*-tolyl)benzo[*b*]naphtho[1,2-*d*]thiophene-6(5*H*)-one (7b). Starting with **4b** (316 mg, 0.88 mmol), **7b** was isolated as a yellow solid (147 mg, 47%); mp.: 142–152 °C. ^{1}H NMR (250 MHz, $CDCl_3$): δ = 8.67–8.56 (m, 1H, H_{Ar}), 8.33 (dd, ^3J = 7.6 Hz, ^4J = 1.7 Hz, 1H, H_{Ar}), 7.96–7.89 (m, 1H, H_{Ar}), 7.86–7.81 (m, 1H, H_{Ar}), 7.61–7.43 (m, 4H, H_{Ar}), 7.18 (d, ^3J = 8.4 Hz, 2H, H_{Ar}), 6.98 (d, ^3J = 7.9 Hz, 2H, H_{Ar}), 4.56 (s, 1H, OH), 2.21 (s, 3H, CH_3) ppm. ^{13}C NMR (63 MHz, $CDCl_3$): δ = 196.8 (C═O), 152.3, 144.5, 142.0, 141.8, 138.9, 138.4, 136.0 (C_{Ar}), 129.5, 129.3 (CH_{Ar}), 129.2 (C_{Ar}), 128.5, 128.4, 128.1, 126.2, 125.9, 125.0, 124.3 (CH_{Ar}), 81.3 (C_{OH}), 21.1 (CH_3). ppm. IR (ATR): $\tilde{\nu}$ = 3456 (w), 2920 (w), 1660 (w), 1504 (w), 1359 (w), 1191 (w), 975 (w), 814 (w), 775 (w), 731 (m), 584 (w), 508 (w), 420 (w) cm^{-1}. MS (EI, 70 eV): *m/z* (%) = 356 ([M]$^+$, $C_{23}H_{16}O_2S$, 53), 340 (58), 328 (23), 327 (47), 311 (28), 295 (23), 237 (86), 236 (22), 208 (19), 165 (26), 148 (22), 119 (100), 91 (18). HRMS (EI): calcd for $C_{23}H_{16}O_2S$ ([M]$^+$) 356.08655, found 356.08549.

(*R*/*S*)-5-(4-Fluorophenyl)-5-hydroxybenzo[*b*]naphtho[1,2-*d*]thiophene-6(5*H*)-one (7c). Starting with **4b** (320 mg, 0.88 mmol), **7c** was isolated as a yellow solid (178 mg, 56%); mp.: 128–138 °C.

^{1}H NMR (300 MHz, $CDCl_3$): δ = 8.64–8.60 (m, 1H, H_{Ar}), 8.34 (dd, ^3J = 7.6 Hz, ^4J = 1.6 Hz, 1H, H_{Ar}), 7.97–7.92 (m, 1H, H_{Ar}), 7.84–7.80 (m, 1H, H_{Ar}), 7.59–7.55 (m, 2H, H_{Ar}), 7.52 (dd, ^3J = 7.6 Hz, ^4J = 1.8 Hz, 1H, H_{Ar}), 7.48 (td, ^3J = 7.5 Hz, ^4J = 1.5 Hz, 1H, H_{Ar}), 7.29 (d, ^3J = 9.1 Hz, 2H), 6.87 (d, ^3J = 8.5 Hz, 2H, H_{Ar}), 4.57 (s, 1H, OH) ppm. ^{13}C NMR (75 MHz, $CDCl_3$): δ = 196.5 (C=O), 162.7 (d, $^1J_{C\text{-}F}$ = 247.8 Hz, C_{Ar}), 144.6, 141.9, 141.7, 139.1 (d, $^5J_{C\text{-}F}$ = 1.4 Hz, C_{Ar}), 137.6 (d, $^4J_{C\text{-}F}$ = 3.1 Hz, C_{Ar}), 135.9, 132.1 (C_{Ar}), 129.4, 128.7, 128.4, 128.3 (CH_{Ar}), 128.0 (d, $^3J_{C\text{-}F}$ = 8.4 Hz, CH_{Ar}), 126.2, 126.1, 125.2, 124.4 (CH_{Ar}), 115.6 (d, $^3J_{C\text{-}F}$ = 21.7 Hz, CH_{Ar}), 80.8 (C_{OH}) ppm. ^{19}F NMR (282 MHz, $CDCl_3$): δ = −113.77 (s, 1 F, CF_{Ar}) ppm. IR (ATR): $\tilde{\nu}$ = 3059 (w), 2920 (w), 1663 (m), 1599 (w), 1358 (w), 1236 (m), 1148 (m), 981 (w), 942 (w), 911 (w), 833 (m), 777 (m), 738 (m), 616 (w), 581 (w), 558 (m), 511 (m) cm^{-1}. MS (EI, 70 eV): *m/z* (%) = 361 (13), 360 ([M]$^+$, $C_{22}H_{13}F_2O_2S$, 66), 332 (36), 331 (58), 316 (12), 315 (35), 238 (28), 237 (100), 236 (14), 165 (18), 165 (18), 132 (13), 123 (30), 104 (13), 95 (12). HRMS (EI): calcd for $C_{22}H_{13}F_2O_2S$ ([M]$^+$) 360.06148, found 360.06109.

(*R*/*S*)-5-Hydroxy-5-(4-methoxyphenyl)benzo[*b*]naphtho[1,2-*d*]thiophene-6(5*H*)-one (7d). Starting with **4d** (330 mg, 0.88 mmol), **7d** was isolated as a yellow solid (138 mg, 42%); mp.: 148–158 °C. ^{1}H NMR (250 MHz, $CDCl_3$): δ = 8.66–8.54 (m, 1H, H_{Ar}), 8.38–8.27 (m, 1H, H_{Ar}), 7.98–7.87 (m, 2H, H_{Ar}), 7.90–7.79 (m, 1H, H_{Ar}), 7.61–7.43 (m, 4H, H_{Ar}), 7.21 (d, ^3J = 9.0 Hz, 2H, H_{Ar}), 6.70 (d, ^3J = 8.9 Hz, 2H, H_{Ar}), 4.56 (s, 1H, OH), 3.68 (s, 3H, OCH_3) ppm. ^{13}C NMR (63 MHz, $CDCl_3$): δ = 196.7 (C=O), 159.7, 144.4, 142.0, 141.6, 135.9, 133.7, 132.3, 129.5 (C_{Ar}), 129.2, 128.5, 128.4, 128., 1127.5, 126.1, 125.9, 125.0, 124.3, 114.1 (CH_{Ar}), 81.1 (C_{OH}), 55.3 (OCH_3) ppm. IR (ATR): $\tilde{\nu}$ = 3419 (w), 2920 (m), 2852 (m), 1663 (m), 1601 (w), 1504 (m), 1459 (m), 1356 (m), 1245 (m), 1028 (m), 981 (m), 833 (m), 777 (m), 734 (m), 587 (m) cm^{-1}. MS (EI, 70 eV): *m/z* (%) = 360 ([M]$^+$, $C_{22}H_{13}F_2O_2S$, 23), 357 (10), 356 (33), 327 (11), 284 (12), 237 (21), 236 (18), 208 (10), 165 (11), 135 (100). HRMS (EI): calcd for $C_{22}H_{13}F_2O_2S$ ([M]$^+$) 372.08147, found 372.08139.

(*R*/*S*)-5-Hydroxy-5-(*o*-tolyl)benzo[*b*]naphtho[1,2-*d*]thiophene-6(5*H*)-one (7e). Starting with **4e** (316 mg, 0.88 mmol), **7e** was isolated as a yellow solid (176 mg, 56%); mp.: 218–225 °C. ^{1}H NMR (300 MHz, $CDCl_3$): δ = 8.68–8.63 (m, 1H, H_{Ar}), 8.44–8.40 (m, 1H, H_{Ar}), 7.99–7.95 (m, 1H, H_{Ar}), 7.75–7.70 (m, 1H, H_{Ar}), 7.59–7.55 (m, 2H, H_{Ar}), 7.51 (ddd, ^3J = 7.9 Hz, ^3J = 6.9 Hz, ^4J = 1.9 Hz, 1H, H_{Ar}), 7.40 (ddd, ^3J = 7.8 Hz, ^4J = 1.9 Hz, ^5J = 0.4 Hz, 1H, H_{Ar}), 7.38–7.32 (m, 1H, H_{Ar}), 7.23–7.20 (m, 2H, H_{Ar}) 7.09–7.05 (m, 1H, H_{Ar}), 3.53 (s, 1H, OH), 1.99 (s, 3H, CH_3) ppm. ^{13}C NMR (75 MHz, $CDCl_3$): δ = 194.8 (C=O), 144.5, 141.8, 140.6, 140.2, 136.3, 136.1, 134.0 (C_{Ar}), 132.1, 130.2 (CH_{Ar}), 130.1 (C_{Ar}), 129.3, 128.9, 128.4, 128.1, 126.8, 126.3, 126.0, 126.0, 124.9, 124.3 (CH_{Ar}), 79.6 (C_{OH}) 20.6 (CH_3) ppm. IR (ATR): $\tilde{\nu}$ = 3064 (w), 3058 (w), 2923 (w), 2852 (w), 1729 (w), 1621 (w), 1501 (w), 1455 (w), 1340 (w), 1249 (w), 1029 (w), 985 (w), 767 (w), 743 (w), 716 (w), 640 (w), 628 (w), 569 (w), 510 (w), 447 (w), 415 (w) cm^{-1}. MS (EI, 70 eV): *m/z* (%) = 357 (74), 356 ([M]$^+$, $C_{23}H_{16}O_2S_2$, 100), 340 (54), 338 (65), 328 (82), 327 (94), 311 (50), 310 (44), 309 (55), 238 (38), 237 (90), 236 (68), 208 (38), 165 (66), 132 (91), 119 (75), 104 (58), 91 (63). HRMS (EI): calcd for $C_{23}H_{16}O_2S$ ([M]$^+$) 356.08655, found 356.08594.

(*R*/*S*)-5-Hydroxy-5-phenylnaphtho[2,1-*b*]thiophene-4(5*H*)-one (7f). Starting with **4f** (260 mg, 0.88 mmol), **7f** was isolated as a brownish solid (188 mg, 73%); mp.: 149–151 °C. ^{1}H NMR (300 MHz, $CDCl_3$): δ = 7.84 (d, ^3J = 5.1 Hz, 1H, $H_{Thiophene}$), 7.78–7.75 (m, 1H, $H_{Ar/Ph}$), 7.66–7.63 (m, 1H, $H_{Ar/Ph}$), 7.60 (d, ^3J = 5.1 Hz, 1H, $H_{Ar/Ph}$), 7.45–7.35 (m, 2H, $H_{Ar/Ph}$), 7.31–7.27 (m, 2H, $H_{Ar/Ph}$), 7.23–7.19 (m, 3H, $H_{Ar/Ph}$), 4.55 (s, 1H, OH) ppm. ^{13}C NMR (75 MHz, $CDCl_3$): δ = 194.3 (C=O), 148.7, 142.7, 142.4 (C_{Ar}), 137.4 (CH_{Ar}), 131.5, (C_{Ar}), 128.7, 128.6, 128.5, 128.2 (CH_{Ar}), 128.0 (C_{Ar}), 125.5, 124.7, 124.2 (CH_{Ar}), 81.2 (C_{OH}) ppm. IR (ATR): $\tilde{\nu}$ = 3447 (w), 3106 (w), 1634 (w), 1445 (w), 1413 (w), 1362), 1266 (w), 1193 (W), 978 (w), 904 (w), 821 (w), 770 (w), 738 (w), 721 (w), 692 (w), 613 (w), 422 (w) cm^{-1}. MS (EI, 70 eV): *m/z* (%) = 293 (21), ([M]$^+$, $C_{18}H_{12}O_2S$, 100), 264 (13), 263 (38), 247 (25), 235 (15), 231 (15), 202 (14), 187 (58), 115 (20), 105 (17), 77 (14). HRMS (EI): calcd for $C_{18}H_{12}O_2S$ ([M]$^+$) 292.05525, found 292.05493.

(*R*/*S*)-4-Hydroxy-4-phenyl-[2]benzothiole[5,4-*b*]benzothiophene-5-one (7g). Starting with **4g** (300 mg, 0.88 mmol), **7g** was isolated as a brownish solid (230 mg, 76%); mp.: 200–204 °C. ^{1}H NMR (300 MHz, $CDCl_3$): δ = 8.43–8.38 (m, 1H, $H_{Ar/Ph}$), 8.06 (d, ^4J = 2.8 Hz, 1H, $H_{Thiophene}$), 7.94–7.90 (m, 1H, $H_{Ar/Ph}$), 7.58 (d, ^4J = 2.9 Hz, 1H, $H_{Thiophene}$), 7.59–7.54 (m, 3H, $H_{Ar/Ph}$), 7.32–7.28 (m, 2H, $H_{Ar/Ph}$), 7.24–7.20 (m, 3H, $H_{Ar/Ph}$) ppm. ^{13}C NMR (75 MHz, $CDCl_3$): δ = 195.6 (C=O), 144.2, 143.2, 142.3, 139.0, 135.7, 131.8, 130.7 (C_{Ar}), 128.8, 128.5, 128.5, 126.1, 125.8, 125.4, 124.4, 124.1, 121.8 (CH_{Ar}), 80.6 (C_{OH}) ppm. IR (ATR): $\tilde{\nu}$ = 3469 (w), 3097 (w), 2920 (w), 2852 (w), 1729 (w), 1643 (w), 1472 (w), 1448 (w). 1279 (w), 1249 (w), 1134 (w), 980 (w), 829 (w), 802 (w), 723 (m), 699 (m), 650 (m), 603 (m), 444 (w), 422 (m) cm^{-1}. MS (EI, 70 eV): *m/z* (%) = 349 (24), 348 ([M]$^+$, $C_{20}H_{12}O_2S_2$, 100), 332 (16), 321 (21), 320 (56), 319 (51), 303 (27), 291 (24), 258 (21), 245 (15), 243 (82), 171 (25), 105 (15), 77 (21). HRMS (EI): calcd for $C_{20}H_{12}O_2S_2$ ([M]$^+$) 348.02732, found 348.02664.

(*R*/*S*)-6-Hydroxy-6-phenylbenzo[*b*]naphtho[1,2-*d*]thiophene-5(6*H*)-one (8a). Starting with **4a** (300 mg, 0.88 mmol), **8a** was isolated as a brownish solid (92 mg, 31%); mp.: 219–222 °C. ^{1}H NMR (250 MHz, $CDCl_3$): δ = 8.43–8.39 (m, 1H, H_{Ar}), 8.28–8.24 (m, 1H, H_{Ar}), 7.93 (ddd, ^3J = 7.9 Hz, ^4J = 1.3 Hz, ^5J = 0.7 Hz, 1H, H_{Ar}), 7.85 (ddd, ^3J = 7.6 Hz, ^4J = 1.5 Hz, ^5J = 0.4 Hz, 1H, H_{Ar}), 7.72 (ddd, ^3J = 7.9 Hz, ^3J = 7.5 Hz, ^4J = 1.5 Hz, 1H, H_{Ar}), 7.53 (ddd, ^3J = 8.3 Hz, ^3J = 7.1, ^4J = 1.4 Hz, 1H, H_{Ar}), 7.47–7.40 (m, 1H, CH_{Ar}), 7.37–7.29 (m, 3H, H_{Ar}), 7.24–7.18 (m, 3H, H_{Ar}), 4.84 (s, 1H, OH) ppm. ^{13}C NMR (63 MHz, $CDCl_3$): δ = 201.0 (C=O), 145.5, 141.0, 139.4, 136.2, 136.2 (C_{Ar}), 135.4, 129.2, 128.9, 128.8 (CH_{Ar}), 128.3 (C_{Ar}), 127.6 (CH_{Ar}), 126.8 (C_{Ar}), 125.9, 125.5, 125.0, 124.1, 123.7, 123.2 (CH_{Ar}), 80.8 (C_{OH}) ppm. IR (ATR): $\tilde{\nu}$ = 3462 (w), 2920 (w), 1686 (w), 1697 (w), 1480 (w), 1362 (w), 1271 (w), 1189 (w), 1148 (w), 987 (w), 863 (w), 767 (m), 723 (m), 694 (m), 420 (w) cm^{-1}. MS (EI, 70 eV): *m/z* (%) = 342 ([M]$^+$, $C_{22}H_{14}O_2S$, 25), 314 (18), 313 (28), 297 (17), 284 (10), 252 (10), 238 (17), 237 (100), 236 (12), 208 (25), 165 (49), 164 (15), 163 (24), 105 (32), 78 (12), 77 (54), 51 (21). HRMS (EI): calcd for $C_{22}H_{14}O_2S$ ([M]$^+$) 342.07090, found 342.07070.

(*R*/*S*)-6-Hydroxy-6-(*p*-tolyl)benzo[*b*]naphtho[1,2-*d*]thiophene-5(6*H*)-one (8b). Starting with **4b** (316 mg, 0.88 mmol), **8b** was isolated as a brownish solid (88 mg, 28%); mp.: 170–179 °C. ^{1}H NMR (250 MHz, DMSO-d_6): δ = 8.55 (d, ^3J = 8.2 Hz, 1H, H_{Ar}), 8.39 (d, ^3J = 7.8 Hz, 1H, H_{Ar}), 8.14–8.03 (m, 1H, H_{Ar}), 7.84–7.75 (m, 2H, H_{Ar}), 7.61–7.52 (m, 1H, H_{Ar}), 7.51–7.35 (m, 2H, H_{Ar}), 7.27 (s, 1H, OH), 7.17 (d, ^3J = 8.3 Hz, 2H, H_{Ar}), 7.02 (d, ^3J = 8.3 Hz, 2H, H_{Ar}), 2.16 (s, 3H, CH_3) ppm. ^{13}C NMR (63 MHz, DMSO-d_6): δ = 199.3 (C=O), 148.7, 139.9, 137.8, 136.8, 135.8 (C_{Ar}), 135.3 (CH_{Ar}), 134.7 (C_{Ar}), 129.1 (CH_{Ar}), 128.7 (C_{Ar}), 128.4, 127.7 (CH_{Ar}), 126.0 (C_{Ar}), 125.7, 125.6, 124.9, 124.1, 123.6, 123.3 (CH_{Ar}), 79.9 (C_{OH}), 20.5 (CH_3) ppm. IR (ATR): $\tilde{\nu}$ = 3468 (w), 2992 (w), 2852 (w), 1677 (m), 1597 (w), 1482 (w), 1269 (w), 1191 (w), 1148 (m), 985 (w), 795 (m), 769 (m), 727 (m), 670 (m), 618 (w), 497 (m) cm^{-1}. MS (EI, 70 eV): *m/z* (%) = 357 (22), 356 ([M]$^+$, $C_{23}H_{16}O_2S$, 52), 340 (83), 328 (28), 327 (48), 311 (41), 295 (21), 237 (88), 236 (37), 147 (26), 142 (32), 119 (100). HRMS (EI): calcd for $C_{23}H_{16}O_2S$ ([M]$^+$) 356.08655, found 356.08574.

(*R*/*S*)-6-(4-Fluorophenyl)-6-hydroxybenzo[*b*]naphtho[1,2-*d*]thiophene-5(6*H*)-one (8c). Starting with **4c** (320 mg, 0.87 mmol), **8c** was isolated as a brownish solid (83 mg, 26%); mp.: 184–187 °C. ^{1}H NMR (300 MHz, $CDCl_3$): δ = 8.43–8.39 (m, 1H, H_{Ar}), 8.27–8.24 (m, 2H, H_{Ar}), 7.94 (ddd, ^3J = 8.0 Hz, ^4J = 1.3 Hz, ^5J = 0.7 Hz, 1H, H_{Ar}), 7.85 (ddd, ^3J = 7.6 Hz, ^4J = 1.5 Hz, ^5J = 0.4 Hz, 1H, H_{Ar}), 7.74 (ddd, ^3J = 7.9 Hz, ^3J = 7.5 Hz, ^4J = 1.5 Hz, 1H, H_{Ar}), 7.54 (ddd, ^3J = 8.3 Hz,

^3J = 7.2 Hz, ^4J = 1.3 Hz, 1H, H_{Ar}), 7.48–7.42 (m, 1H, H_{Ar}), 7.34 (td, ^3J = 7.6 Hz, ^4J = 1.1 Hz, 1H, H_{Ar}), 7.28 (d, ^3J = 9.1 Hz, 1H, H_{Ar}), 6.90 (d, ^3J = 8.5 Hz, 2H, H_{Ar}), 4.82 (s, 1H, OH) ppm. ^{13}C NMR (75 MHz, $CDCl_3$): δ = 209.4, 163.1 (d, $^1J_{C\text{-}F}$ = 240.6 Hz, C_{Ar}), 145.9, 141.0, 136.1, 136.0 (C_{Ar}), 135.5 (CH_{Ar}), 135.2 (d, $^4J_{C\text{-}F}$ = 3.0 Hz, C_{Ar}), 129.2 (CH_{Ar}), 128.2 (C_{Ar}), 128.0 (d, $^3J_{C\text{-}F}$ = 8.5 Hz, CH_{Ar}), 127.7 (CH_{Ar}), 126.9 (C_{Ar}), 125.6, 125.2, 124.1, 123.7, 123.3 (CH_{Ar}), 115.79 (d, $^2J_{C\text{-}F}$ = 21.7 Hz, CH_{Ar}), 80.3 (C_{OH}) ppm. ^{19}F NMR (282 MHz, $CDCl_3$): δ = −113.21 (s, 1 F, CF_{Ar}) ppm. IR (ATR): $\tilde{\nu}$ = 3456 (w), 2920 (w), 1680 (w), 1597 (w), 1232 (w), 1144 (w), 826 (w), 804 (w), 773 (w), 729 (w), 672 (w), 420 (w) cm^{-1}. MS (EI, 70 eV): *m/z* (%) = 360 ([M]$^+$, $C_{22}H_{13}F_2O_2S$, 30), 344 (9), 332 (16), 331 (28), 315 (18), 238 (17), 237 (100), 165 (11), 123 (19), 104 (8). HRMS (EI): calcd for $C_{22}H_{13}F_2O_2S$ ([M]$^+$) 360.06148, found 360.06149.

(*R*/*S*)-6-Hydroxy-6-(4-methoxyphenyl)benzo[*b*]naphtho[1,2-*d*]thiophene-5(6*H*)-one (8d). Starting with **4d** (330 mg, 0.88 mmol), **8d** was isolated as a brownish solid (131 mg, 40%); mp.: 204–209 °C. ^{1}H NMR (250 MHz, DMSO-d_6): δ = 8.54 (d, ^3J = 8.2 Hz, 1H, H_{Ar}), 8.39 (d, ^3J = 8.0 Hz, 1H, H_{Ar}), 8.10 (d, ^3J = 7.7 Hz, 1H, H_{Ar}), 7.85–7.73 (m, 2H, H_{Ar}), 7.57 (ddd, ^3J = 8.4 Hz, ^3J = 7.2 Hz, ^4J = 1.4 Hz, 1H, H_{Ar}), 7.54–7.33 (m, 2H, H_{Ar}), 7.24 (s, 1H, OH), 7.20 (d, ^3J = 8.9 Hz, 2H, H_{Ar}), 6.79 (d, ^3J = 8.9 Hz, 2H, H_{Ar}), 3.63 (s, 3H, OCH_3) ppm. ^{13}C NMR (63 MHz, DMSO-d_6): δ = 199.2 (C=O), 159.3, 148.8, 139.9, 135.8 (C_{Ar}), 135.2 (CH_{Ar}), 134.7, 131.5, 128.7 (C_{Ar}), 128.4, 127.6, 127.2 (CH_{Ar}), 126.0 (C_{Ar}), 125.6, 124.90, 124.0, 123.6, 123.3, 113.9 (CH_{Ar}), 79.6 (C_{OH}), 55.1 (OCH_3) ppm. IR (ATR): $\tilde{\nu}$ = 3466 (w), 2920 (w), 2859 (w), 1682 (w), 1599 (w), 1504 (w), 1252 (w), 10149 (w), 1019 (w), 985 (w), 826 (w), 777 (m), 728 (m), 674 (m), 650 (w), 579 (w), 417 (w) cm^{-1}. MS (EI, 70 eV): *m/z* (%) = 372 ([M]$^+$, $C_{23}H_{16}O_3S$, 28), 356 (26), 344 (14), 343 (21), 327 (15), 284(12), 237 (27), 236 (21), 208 (11), 165 (13), 136 (11), 135 (100). HRMS (EI): calcd for $C_{23}H_{16}O_3S$ ([M]$^+$) 372.08147, found 372.08116.

(*R*/*S*)-6-Hydroxy-6-(*o*-tolyl)benzo[*b*]naphtho[1,2-*d*]thiophene-5(6*H*)-one (8e). Starting with **4e** (316 mg, 0.88 mmol), **8e** was isolated as a brownish solid (75 mg, 24%); mp.: 145–148 °C. ^{1}H NMR (300 MHz, $CDCl_3$): δ = 8.42–8.38 (m, 1H, H_{Ar}), 8.22–8.17 (m, 1H, H_{Ar}), 7.91 (ddd,^3J = 7.9 Hz, ^4J = 1.3 Hz, ^5J = 0.7 Hz, 1H, H_{Ar}), 7.85 (ddd, ^3J = 7.6 Hz, ^4J = 1.5 Hz, ^5J = 0.6 Hz, 1H, H_{Ar}), 7.68 (ddd, ^3J = 8.0 Hz, ^3J = 7.5 Hz, ^4J = 1.5 Hz, 1H, H_{Ar}), 7.53 (ddd, ^3J = 8.4 Hz, ^3J = 7.2 Hz, ^4J = 1.3 Hz, 1H, H_{Ar}), 7.47–7.41 (m, 1H, H_{Ar}), 7.33 (td, ^3J = 7.6 Hz, ^4J = 1.1 Hz, 1H, H_{Ar}), 7.24–7.08 (m, 4H, H_{Ar}), 7.05–6.99 (s, 1H, OH), 2.32 (s, 3H, CH_3) ppm.^{13}C NMR (75 MHz, $CDCl_3$): δ = 200.2 (C=O), 145.7, 141.2, 138.0, 136.9, 136.2, 135.3 (C_{Ar}), 134.8, 132.7 (CH_{Ar}), 129.3 (C_{Ar}), 129.0, 128.7 (CH_{Ar}), 127.9 (C_{Ar}), 127.7, 127.0, 126.3, 125.5, 125.1, 123.9, 123.7, 123.3 (CH_{Ar}), 81.1 (C_{OH}) 32.3 (CH_3) ppm. IR (ATR): $\tilde{\nu}$ = 3405 (w), 2920 (w), 2852 (w), 1687 (w), 1597 (w), 1457 (w), 1264 (w), 1024 (w), 980 (w), 802 (w), 772 (w), 753 (w), 728 (w), 420 (w) cm^{-1}. MS (EI, 70 eV): *m/z* (%) = 356 ([M]$^+$, $C_{23}H_{16}O_2S_2$, 21), 340 (31), 327 (10), 295 (16), 238 (10), 237 (67), 208 (10), 132 (11), 119 (100), 118 (11), 104 (14), 91 (21), 57 (13). HRMS (EI): calcd for $C_{23}H_{16}O_2S$ ([M]$^+$) 356.08655, found 356.08575.

(*R*/*S*)-4-Hydroxy-4-phenylnaphtho[2,1-*b*]thiophene-5(4*H*)-one (8f). Starting with **4f** (260 mg, 0.88 mmol), **8f** was isolated as a brownish solid (41 mg, 16%); mp.: 161–163 °C. ^{1}H NMR (300 MHz, $CDCl_3$): δ = 7.84 (ddd, ^3J = 7.7 Hz, ^4J = 1.3 Hz, ^5J = 0.6 Hz, 1H, $H_{Ar/Ph}$), 7.68 (ddd, ^3J = 7.8 Hz, ^4J = 1.6 Hz, ^5J = 0.6 Hz, 1H, $H_{Ar/Ph}$), 7.66–7.61 (m, 1H, $H_{Ar/Ph}$), 7.47 (d, ^3J = 5.2 Hz, 1H, $H_{Thiophene}$), 7.44 (d, ^3J = 5.2 Hz, 1H, $H_{Thiophene}$), 7.32–7.28 (m, 1H, $H_{Ar/Ph}$), 7.27–7.24 (m, 2H, $H_{Ar/Ph}$), 7.24–7.20 (m, 3H, $H_{Ar/Ph}$), 4.72 (s, 1H, OH) ppm. ^{13}C NMR (75 MHz, $CDCl_3$): δ = 201.4 (C=O), 142.9, 140.7, 135.8 (C_{Ar}), 135.7 (CH_{Ar}), 133.3 (C_{Ar}), 129.1, 128.8, 128.6, 127.8, 127.5 (CH_{Ar}), 127.3 (C_{Ar}), 125.6, 123.9, 122.6 (CH_{Ar}), 80.2 (C_{OH}) ppm. IR (ATR): $\tilde{\nu}$ = 3471 (w), 2920 (w), 2852 (w), 1675 (w), 1602 (w), 1284 (w), 1264 (w), 1181 (w), 1134 (W), 985 (w), 865 (w), 770 (w), 745 (w), 714 (m), 699 (w), 665 (w), 611 (w), 491 (w), 430 (w) cm^{-1}. MS (EI, 70 eV): *m/z* (%) = 293 (18), 292 ([M]$^+$, $C_{18}H_{12}O_2S$, 93), 264 (17), 263 (88), 247 (25), 188 (17), 187 (100), 115 (22), 107 (17), 105 (50), 77 (16). HRMS (EI): calcd for $C_{18}H_{12}O_2S$ ([M]$^+$) 292.05525, found 292.05485.

(*R*/*S*)-5-Hydroxy-5-phenyl-[2]benzothiole[5,4-*b*]benzothiophene-4-one (8g). Starting with **4g** (300 mg, 0.88 mmol), **8g** was isolated as a brownish solid (52 mg, 17%); mp.: 174–184 °C. ^{1}H NMR (300 MHz, $CDCl_3$): δ = 8.24–8.20 (m, 1H, $H_{Ar/Ph}$), 8.21 (d, ^4J = 2.8 Hz, 1H, $H_{Thiophene}$), 7.89 (ddd, ^3J = 8.0 Hz, ^4J = 1.2 Hz, ^5J = 0.7 Hz, 1H, $H_{Ar/Ph}$), 7.83 (d, ^4J = 2.8 Hz, 1H, $H_{Thiophene}$), 7.57–7.51 (m, 1H, $H_{Ar/Ph}$), 7.46–7.41 (m, 1H, $H_{Ar/Ph}$), 7.34–7.30 (m, 2H, $H_{Ar/Ph}$), 7.25–7.22 (m, 3H, $H_{Ar/Ph}$), 4.67 (s, 1H, OH) ppm. ^{13}C NMR (75 MHz, $CDCl_3$): δ = 194.2 (C=O), 145.3, 140.9, 140.6, 135.7, 135.4 (C_{Ar}), 134.0 (CH_{Ar}), 133.5 (C_{Ar}), 128.9, 128.7, 125.5, 125.4, 125.2 (CH_{Ar}), 125.2 (C_{Ar}), 123.5, 122.8, 118.6 (CH_{Ar}), 81.0 (C_{OH}) ppm. IR (ATR): $\tilde{\nu}$ = 3471 (w), 3104 (w), 2920 (w), 2850 (w), 1731 (w), 1682 (w), 1448 (w), 1132 (m), 1000 (w), 802 (m), 765 (m), 723 (m), 692 (m), 660 (m), 589 (m), 567 (m), 457 (m) cm^{-1}. MS (EI, 70 eV): *m/z* (%) = 349 (24), 348 ([M]$^+$, $C_{20}H_{12}O_2S_2$,100), 332 (18), 321 (16), 320 (57), 319 (52), 303 (29), 291 (24), 258 (20), 245 (15), 244 (15), 243 (83), 171 (25), 105 (16), 77 (20). HRMS (EI): calcd for $C_{20}H_{12}O_2S_2$ ([M]$^+$) 348.02732, found 348.02689.

Synthesis of 13a-c. To a mixture of **12a** (0.427 mmol, 1 equiv.), Pd_2dba_3 (2.5 mol%), SPhos (10 mol%), **5a** (1.5 equiv.), K_3PO_4 (3 equiv.) was added acetonitrile/water (8:2) and the mixture was purged with Argon. The solution was stirred at 80 °C for 20 h. The solution was cooled to 20 °C and Pd_2dba_3 (5 mol%), SPhos (20 mol %), diisopropylamine (603 μl) and phenylacetylene (1.8 equiv) were added and the mixture was purged with Argon. The solution was stirred at 80 °C for 5 h. To the mixture was added water and the mixture was extracted with ethyl acetate (3x). The combined organic layers were dried ($MgSO_4$), filtered and concentrated in vacuo. The residue was purified by chromatography (silica gel, heptane/EtOAc).

10-Hydroxy-10-phenylphenanthren-9(10*H*)-one (13a). Starting with **12a** (371 mg, 1.28 mmol), **13a** was isolated as a beige solid (202 mg, 55%); mp.: 100–104 °C. ^{1}H NMR (300 MHz, $CDCl_3$): δ = 7.95 (ddd, ^3J = 7.3 Hz, ^4J = 1.8 Hz, ^5J = 0.9 Hz, 2H, $H_{Ar/Ph}$), 7.82 (ddd, ^3J = 7.7 Hz, ^4J = 1.5 Hz, ^5J = 0.5 Hz, 1H, $H_{Ar/Ph}$), 7.79–7.76 (m, 1H, $H_{Ar/Ph}$), 7.65 (ddd, ^3J = 8.0 Hz, ^3J = 7.4, ^4J = 1.5 Hz, 1H, $H_{Ar/Ph}$), 7.52–7.42 (m, 2H, $H_{Ar/Ph}$), 7.34 (ddd, ^3J = 8.6 Hz, ^3J = 5.7 Hz, ^4J = 1.1 Hz, 1H, $H_{Ar/Ph}$), 7.17–7.15 (m, 5H, H_{Ar}), 4.88 (s, 1H, OH) ppm. ^{13}C NMR (75 MHz, $CDCl_3$): δ = 201.5 (C=O), 141.6, 139.7, 137.9 ($C_{Ar/Ph}$), 135.3 ($CH_{Ar/Ph}$), 130.5 ($C_{Ar/Ph}$), 129.8, 128.9, 128.6, 128.6 ($CH_{Ar/Ph}$), 128.5 ($C_{Ar/Ph}$), 128.3, 128.2, 128.0, 126.3, 123.9, 123.3 ($CH_{Ar/Ph}$), 80.5 (C_{OH}) ppm. IR (ATR): $\tilde{\nu}$ = 3476 (w), 2920 (w), 1684 (m), 1597 (w), 1267 (w), 1199 (m), 1160 (m), 997 (m), 754 (m), 727 (m), 696 (m), 664 (m), 620 (m), 476 (m) cm^{-1}. MS (EI, 70 eV): *m/z* (%) = 286 ([M]$^+$, $C_{20}H_{14}O_2$, 16), 257 (27), 241 (14), 239 (14), 182 (14), 181 (100), 153 (25), 152 (74), 151 (30), 126 (10), 105 (30), 78 (12), 77 (70), 76 (14), 51 (32), 50 (14). HRMS (EI): calcd for $C_{20}H_{14}O_2$ ([M]$^+$) 286.09883, found 286.09915.

10-(4-(*tert*-Butyl)phenyl)-10-hydroxyphenanthren-9(10*H*)-one (13b). Starting with **12b** (442 mg, 1.28 mmol), **13b** was isolated as a beige solid (158 mg, 36%); mp.: 48–50 °C. ^{1}H NMR (500 MHz, $CDCl_3$): δ = 7.98–7.95 (m, 1H, H_{Ar}), 7.94–7.92 (m, 1H, H_{Ar}), 7.87–7.84 (m, 1H, H_{Ar}), 7.79–7.76 (m, 1H, H_{Ar}), 7.67–7.64 (m, 1H, H_{Ar}), 7.48–7.44 (m, 3H, H_{Ar}), 7.36–7.33 (m, 1H, H_{Ar}), 7.17 (d, ^3J = 8.8 Hz, 2H, H_{Ar}), 7.08 (d, ^3J = 8.8 Hz, 2H, H_{Ar}), 4.84 (s, 1H, OH), 1.19 (s, 9H, CH_3) ppm. ^{13}C NMR (126 MHz, $CDCl_3$) δ = 201.5 (C=O), 151.1, 139.9, 138.5, 138.0 (C_{Ar}), 135.3 (CH_{Ar}), 130.2 (C_{Ar}), 129.8, 128.8 (CH_{Ar}), 128.6 (C_{Ar}), 128.6, 128.2, 128.0, 125.9, 125.7, 123.9, 123.3 (CH_{Ar}), 80.3 (C–OH), 34.5 ($C(CH_3)_3$, 31.3 (CH_3). ppm. IR (ATR): $\tilde{\nu}$ = 2955 (w), 2862 (W), 2221 (w), 1504 (w), 1463 (m), 1432 (w), 1360 (w), 1265 (w), 1102 (w), 1026 (m), 828 (m), 750 (m), 661 (m), 560 (m), 441 (w) cm^{-1}. MS (EI, 70 eV): *m/z* (%) = 342 ([M]$^+$,

$C_{24}H_{22}O_2$, 15), 257 (33), 181 (75), 180 (33), 161 (91), 153 (36), 152 (100), 151 (34), 118 (36), 117 (24), 115 (23), 91 (39), 77 (24), 57 (25), 41 (24). HRMS (ESI-TOF): calcd for $C_{24}H_{23}O_2$ ($[M+Na]^+$) 365.1517, found 365.1514.

10-Hydroxy-10-(4-(trifluoromethyl)phenyl)phenanthren-9(10*H*)-one (13c). Starting with **12c** (457 mg, 1.28 mmol), **13c** was isolated as a beige solid (150 mg, 33%); mp.: 48–50 °C. ^{1}H NMR (300 MHz, $CDCl_3$): δ = 8.01–7.97 (m, 1H, H_{Ar}), 7.97–7.93 (m, 1H, H_{Ar}), 7.85–7.81 (m, 1H, H_{Ar}), 7.76–7.73 (m, 1H, H_{Ar}), 7.72–7.66 (m, 1H, H_{Ar}), 7.53–7.45 (m, 2H, H_{Ar}), 7.42–7.39 (m, 2H, H_{Ar}), 7.37–7.31 (m, 3H, H_{Ar}), 4.95 (s, 1H, OH) ppm.^{13}C NMR (75 MHz, CDCl3): δ = 200.9 (C=O), 145.5 (C_{Ar}), 143.5 (CH_{Ar}), 139.1, 137.9 (C_{Ar}), 135.8 (CH_{Ar}), 135.0 (C_{Ar}), 130.6 (CH_{Ar}), 130.4 (q, $^2J_{C\text{-}F}$ = 32.5 Hz, C_{Ar}), 130.1 (C_{Ar}), 130.0 (CH_{Ar}), 129.3, 129.1, 128.9, 128.5, 128.3 (CH_{Ar}), 128.1 (C_{Ar}), 127.9, 126.7 (CH_{Ar}), 125.60 (q, $^3J_{C\text{-}F}$ = 3.8 Hz, CH_{Ar}), 124.1, 123.5 (CH_{Ar}), 123.99 (q, $^1J_{C\text{-}F}$ = 272.2 Hz, C–F), 80.15 (C–OH) ppm. ^{19}F NMR (282 MHz, $CDCl_3$): δ = −62.75 (s, 3 F, CF_3) ppm. MS (EI, 70 eV): *m/z* (%) = 354 ($[M]^+$, $C_{21}H_{13}O_2F_3$, 51), 326 (16), 325 (59), 309 (16), 209 (11),182 (35), 181 (100), 173 (12), 153 (20), 152 (28), 145 (13), 104 (12), 76 (10). HRMS (EI): calcd for $C_{21}H_{13}O_2F_3$ ($[M]^+$] 354.08622, found 354.08635.

6,7-Difluoro-10-hydroxy-10-phenylphenanthren-9(10*H*)-one (13d). Starting with **12d** (863 mg, 2.65 mmol), **13d** was isolated as a yellow solid (222 mg, 26%). ^{1}H NMR (300 MHz, Chloroform-d) δ 7.86–7.77 (m, 2H, HAr), 7.75–7.66 (m, 2H, HAr), 7.66–7.54 (m, 1H, HAr), 7.37 (td, *J* = 7.5, 1.1 Hz, 1H, HAr), 7.21–7.12 (m, 5H, HAr), 4.85 (s, 1H, OH). ^{13}C NMR (75 MHz, Chloroform-d) δ 200.36 (C=O), 135.62 (CHAr), 129.17 (CHAr), 128.81(CHAr), 128.57 (CHAr), 128.45 (CHAr), 126.06 (CHAr), 123.39 (CHAr), 117.40 (CHAr), 113.04 (CHAr), 79.97 (C–OH). ^{19}F NMR (282 MHz, Chloroform-d) δ −135.09 (d, *J* = 21.9 Hz, 1 F, CFAr), −137.29 (d, *J* = 21.5 Hz, 1 F, CFAr). MS (GC): *m/z* (%) = 322 (C20H12F2O2, 20), 293 (23), 217 (60), 105 (100). HRMS (EI): calcd for C20H12F2O2, 322.0799, found 322.0802. IR (ATR): = 3486 (m), 1683 (s), 1596 (m), 1510 (s), 1487 (m), 1448 (s), 1417 (m), 1306 (m), 1267 (s), 1137 (s), 1013 (s).

4-Hydroxy-4-phenylnaphtho[1,2-*c*]thiophene-5(4H)-one (13e). Starting with **12a** (747 mg, 2.58 mmol), **13e** was isolated as a yellow solid (576 mg, 76%). ^{1}H NMR (250 MHz, Chloroform-d) δ 8.05 (d, *J* = 2.9 Hz, 1H, HAr), 7.77–7.61 (m, 2H, HAr), 7.61–7.53 (m, 1H, HAr), 7.48 (d, *J* = 3.0 Hz, 1H, HAr), 7.35–7.17 (m, 1H, HAr), 7.10 (d, *J* = 0.7 Hz, 5H, HAr), 4.69 (s, 1H, OH). ^{13}C NMR (63 MHz, Chloroform-d) 200.42 (C=O), 135.03 (CHAr), 133.13 (CAr), 129.22 (CAr), 128.80 (CAr), 128.67 (CHAr), 128.34 (CHAr), 128.24 (CHAr), 128.12 (CHAr), 126.10 (CHAr), 126.02 (CHAr), 124.40 (CHAr), 123.85 (CAr), 123.75 (CHAr), 121.11 (CHAr), 119.38 (CHAr), 80.40 (C–OH). MS (GC): *m/z* (%) = 292 ($C_{18}H_{12}O_2S$, 84), 264 (24), 263 (48), 247 (30), 187 (100). HRMS (ESI): calcd for $C_{18}H_{12}O_2S$, 292.0553, found 292.0553. IR (ATR): = 1671 (vs), 1582 (s), 1448 (m), 1432 (m), 1252 (m), 1203 (vs), 1178 (s), 1065 (m), 1026 (m), 857 (s).

Declaration of competing interest

The authors declare that they have no known competing financial interests or personal relationships that could have appeared to influence the work reported in this paper.

Data availability

Data will be made available on request.

Acknowledgements

Financial support by the State of Mecklenburg-Vorpommern (stipend for A. K.) is gratefully acknowledged.

Appendix A. Supplementary data

Supplementary data to this article can be found online at https://doi.org/10.1016/j.tet.2023.133335.

References

[1] M.G. Edwards, Angew. Chem. Int. Ed. (2008) 1935–1937.
[2] E.J. Corey, Tetrahedron Lett. 1973 (1974) 287–290.
[3] G. Shevchenko, S. Dehn, B. List, Synlett 29 (2018) 2298–2300.
[4] Y.-F. Liang, N. Jiao, Angew. Chem. Int. Ed. 53 (2014) 548–552.
[5] a) H. Brunner, H. Kagan, G. Kreutzer, Tetrahedron Asymmetry 12 (2001) 497–499;
b) K. Jia, Y. Pan, Y. Chen, Angew. Chem. Int. Ed. 56 (2017) 2478–2481;
c) C. Palomo, M. Oiarbide, J.M. García, Chem. Soc. Rev. 41 (2012) 4150–4164;
d) Y. Shingai, J. Chem. Soc. Perkin Trans. I (1991) 957–959;
e) F.A. Davis, M.C. Weismiller, J. Org. Chem. (1990) 3715–3717.
[6] L.G. Quan, M. Lamrani, Y. Yamamoto, J. Am. Chem. Soc. 122 (2000) 4827–4828.
[7] Y.-X. Jia, D. Katayev, E.P. Kündig, Chem. Comm 46 (2010) 130–132.
[8] a) H.-L. Wang, Y.-M. Li, G.-W. Wang, H. Zhang, S.-D. Yang, Asian J. Org. Chem. 2 (2013) 486–490;
b) G.J. Chuang, W. Wang, E. Lee, T. Ritter, J. Am. Chem. Soc. 133 (2011) 1760–1762 (and references cited therein).
[9] V. Lyaskovskyy, R. Fröhlich, E.-U. Würthwein, Chemistry (Weinheim an der Bergstrasse, Germany) 13 (2007) 3113–3119.
[10] E. Kavak, M.A.S. Algso, M. Konus, C. Yılmaz, A. Lazoğlu, S.U. Karaağaç, A. Kivrak, Russ. J. Org. Chem. 57 (2021) 91–99.
[11] A. Gao, F. Yang, Y. Wu, Tetrahedron 68 (2012) 4950–4954.
[12] Y. Nagamoto, Y. Yamaoka, S. Fujimura, Y. Takemoto, K. Takasu, Org. Lett. 16 (2014) 1008–1011.
[13] T. Ishida, S. Kikuchi, T. Tsubo, T. Yamada, Org. Lett. 15 (2013) 848–851.
[14] CCDC 2218362-2218366 contain the supplementary crystallographic data for this paper. These data can be obtained free of charge from The Cambridge Crystallographic Data Centre via, www.ccdc.cam.ac.uk/structures/.

III Synthesis and Properties of Diindeno[1,2,3-*cd*:1′,2′,3′-*mn*]pyrene and Two of Its Aza-Analogs

Aleksandra Khomutetckaia, Niels Hildebrandt, Peter Ehlers, Alexander Villinger, Peter Langer. *Eur. J. Org. Chem.* **2023***, e202301101*

DOI: 10.1002/ejoc.202301101

EurJOC
European Journal of Organic Chemistry

Research Article
doi.org/10.1002/ejoc.202301101

Chemistry Europe
European Chemical Societies Publishing

www.eurjoc.org

Synthesis and Properties of Diindeno[1,2,3-*cd*:1′,2′,3′-*mn*]pyrene and Two of Its Aza-Analogs

Aleksandra Khomutetckaia,[a] Niels Hildebrandt,[a] Peter Ehlers,[a] Alexander Villinger,[a] and Peter Langer*[a, b]

The incorporation of heteroatoms into polycyclic aromatic hydrocarbons (PAHs) has been recognized as valuable tool to alter their inherent optical and electrochemical properties and are thought as promising next-generation semiconductor materials. We herein report the synthesis of diindenopyrene, a fragment of C_{70} and two of its nitrogen-doped aza-analogs. The developed synthetic procedure is based on Brønsted-acid-mediated cycloisomerization followed by Pd-catalyzed C–H-activation as key-steps. The impact of N-doping on the optical and electrochemical properties has been studied and the experimental results are supported by DFT calculations.

Introduction

Polycyclic aromatic hydrocarbons (PAHs) are of considerable current interest in materials science. This interest is amplified not only by the unique electronic and optical properties for application in electronic devices, but also by the opportunity to fine-tune these properties by the substitution pattern, structural alternation, or incorporation of heteroatoms.[1–5]

In this context, pyrene is one of the most studied compounds with regard to their photophysical properties and there is an increased interest in the employment of pyrene-based compounds for organic electronics.[6–8] Indeno[1,2,3-*cd*]pyrenes can be regarded as a pyrene annulated to an indene moiety and represent a substructure of fullerene C_{70}. Compared to Buckminster fullerene C_{60}, C_{70} shows higher extinction coefficients and lower lying HOMO and LUMO levels.[9] However, most research is devoted to the synthesis of C_{60} fragments. The incorporation of heteroatoms to these substructures, in order to alter their inherent physical properties, is still elusive which is most likely due to the lack of expedient synthetic methodologies.[10–16]

Indenopyrenes can be prepared by electrophilic aromatic substitution or Pd-catalyzed cross-coupling reaction and C–H activation (Figure 1).[17–19] For example, Scott and co-workers synthesized several indenopyrenes by Pd-catalyzed C–H activation using aryl triflates and their optical properties were thoroughly investigated.[20] Later, the group of Mastalerz revisited the synthesis of tetraindopyrene and diindenopyrenes and demonstrated their application as p-channel charge carriers.[21] Recently, the group of Amsharov developed a synthetic strategy to non-alternant PAHs using activated γ-alumina.[22]

Despite these recent advancements, there is still a lack of synthetic methodologies towards those C_{70} substructures. In addition, the implementation of heteroatoms to alter the optical and electrochemical properties has, to the best of our knowledge, not been reported to date. Hence, we herein report the synthesis and properties of diindenopyrene **3a** which has been once mentioned in a patent for application as an organic thin film solar cell material, but lacking details related to synthesis, characterization and structural, optical and electrochemical features.[23] In addition, we report the synthesis and properties of hitherto unknown azadiindenopyrenes **3b** and **3c**.

Results and Discussion

The synthesis of **3a–c** is connected to our previous work related to the synthesis of azapyrene derivatives (Scheme 1). Starting materials **1** were synthesized by site- and chemoselective cross-coupling reactions, adapting previously reported procedures (see SI).[24,25] The synthesis of diaryl(aza)pyrenes **2a–c** was accomplished by acid-mediated cycloisomerization. While for **2b** and **2c** Brønsted acids were used, they led to decomposition of the starting material in case of **2a**. Thus, $PtCl_2$ was employed following conditions reported by Schreiner and co-workers.[26] Final products **3a–c** were obtained by Pd catalyzed C–H activation. Orange-red diindenopyrene **3a** was isolated in 40% yield, accompanied by one-side cyclized indenopyrene **3a'** (shown in SI) in 22%. Yellow azadiindenopyrenes **3b** and **3c** were obtained in 24% and 26% yields under the same conditions. The reactions were carried out using $PdCl_2(PhCN)_2$ as catalyst, PCy_3 as ligand, pivalic acid and cesium carbonate. *N,N*-Dimethylacetamide was employed as the solvent (150 °C, 14 h). Variation of catalyst, base, catalyst loading, or prolongation of the reaction time did not improve the yield of **3a–c** (Table S5, SI).

[a] *A. Khomutetckaia, N. Hildebrandt, Dr. P. Ehlers, Dr. A. Villinger, Prof. Dr. P. Langer*
Institute of Chemistry
University of Rostock
Albert-Einstein-Str. 3a
18059 Rostock (Germany)
E-mail: peter.langer@uni-rostock.de
Homepage: www.langer.chemie.uni-rostock.de

[b] *Prof. Dr. P. Langer*
Leibniz Institute for Catalysis
at the University of Rostock e.V.
Albert-Einstein-Str. 29a
18059 Rostock (Germany)

Supporting information for this article is available on the WWW under https://doi.org/10.1002/ejoc.202301101

Research Article
doi.org/10.1002/ejoc.202301101

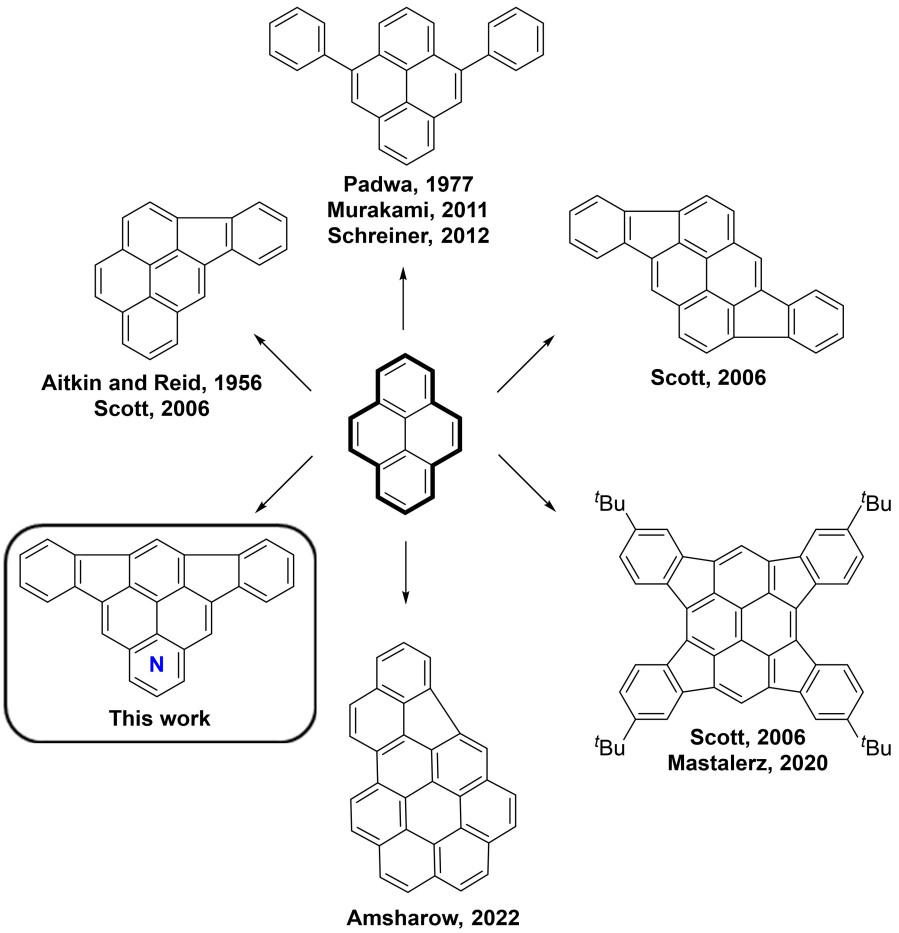

Figure 1. Known di-, tri and tetraindenopyrenes in comparison with this work.

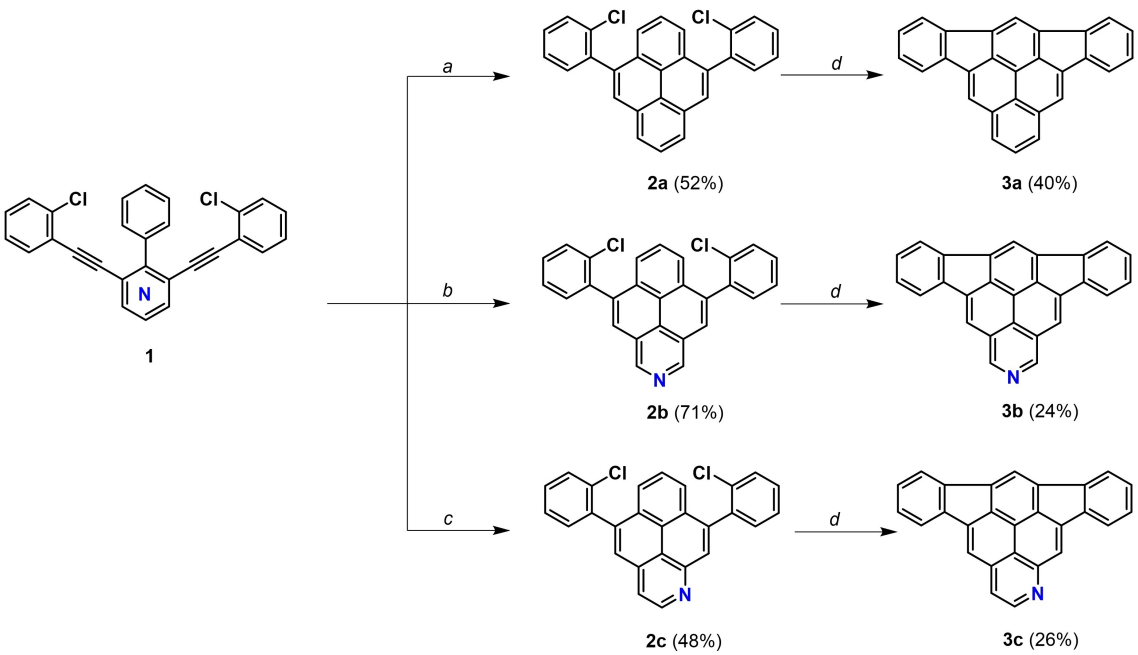

Scheme 1. Synthesis of (aza)diindenopyrenes. Conditions: a) MsOH, 120 °C, 16 h; b) *p*TsOH, xylene, 130 °C, 24 h; c) $PtCl_2$, toluene, 110 °C, 20 h; d) $PdCl_2(PhCN)_2$ (10 mol %), PCy_3 (20 mol %), Cs_2CO_3 (2.0 eq.) PivOH (40 mol %), DMA, 16 h.

Research Article
doi.org/10.1002/ejoc.202301101

The structure of **3a** was independently confirmed by X-ray crystal structure analysis (Figure 2).[27] Compound **3a** crystallized in the orthorhombic space group P21 21 21 and displays a planar structure with herringbone-like packing. Parallel molecules occupy a slipped face-to-face orientation with a distance of 3.423 Å which is about the sum of van der Waals radii. Short π-CH contacts of 2.787 Å are found between two adjacent molecules which occupy an orthogonal orientation (89.76°) to each other.

Steady-state UV-Vis and photoluminescence spectra (PL) of synthesized diindenopyrenes were recorded in dichloromethane. The corresponding spectra are shown in Figure 3 and the respective optical data are reported in Table 1.

Diindenopyrene **3a** shows strong absorption in the ultraviolet region accompanied with a weak and broad low energy band up to ~520 nm, incorporating certain vibrionic progression, which is in accordance with other indenopyrenes. In general, the obtained absorption spectra display close similarity to already described tri- and tetraindenopyrenes, but with blue shifted absorption maxima, due to its reduced conjugation length.[20,21] Doping of the diindenopyrene core structure by nitrogen results in minor modification of the spectral shape, leading to a hypsochromically shifted low-energy absorption band. This effect is more pronounced for symmetric aza-diindenopyrene **3b** compared to non-symmetric **3c**. Typical absorption features of pyrene and azapyrene are still maintained and typical B_b, L_a and L_b bands are observed between 300–400 nm.[24] Hence, broad, but weak low-energy bands from 400–500 nm of all three compounds result from the π-expanded scaffold. TD-DFT on a B3LYP/6-311+G(d,p) level of theory revealed that S0→S1 transition is mainly derived from HOMO→LUMO transition with

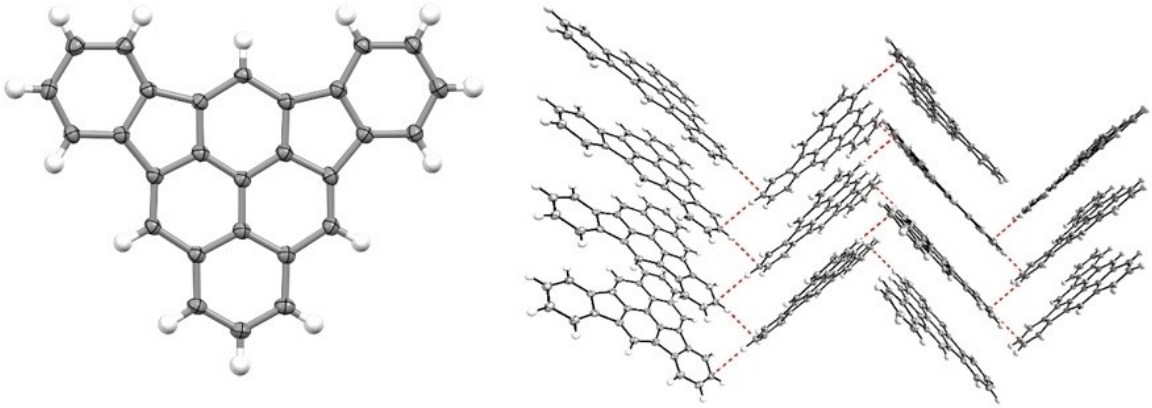

Figure 2. ORTEP of **3a**. The thermal ellipsoids are drawn at the 50% probability level.

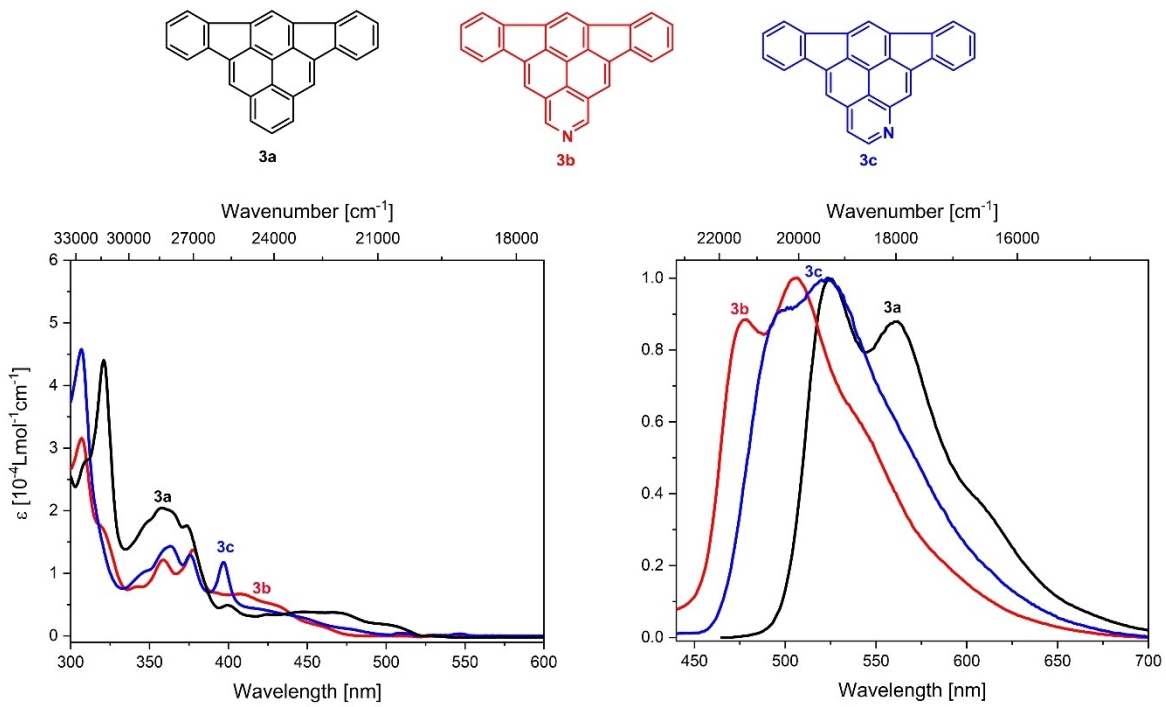

Figure 3. UV-vis (left) and emission spectra (excitated @450 nm) of **3a** and (excitated @408 nm) of **3b**, **3c** in CH_2Cl_2 ($c = 10^{-5}$ M) at 20 °C.

Research Article
doi.org/10.1002/ejoc.202301101

Table 1. Optical spectroscopic data of **3a–c** in dichloromethane ($c = 10^{-5}$ M).

	$\lambda_{1,abs}$ [nm]	ε_1[a]	$\lambda_{2,abs}$ [nm]	ε_1	$\lambda_{3,abs}$ [nm]	ε_1[a]	$\lambda_{1,em}$ [nm]	$\lambda_{2,em}$ [nm]	φ
3a	497^{sh}	0.19	468	0.37	448	0.38	524	561	0.05
3b	454^{sh}	0.18	427^{sh}	0.51	408	0.67	478	506	0.03
3c	474^{sh}	0.12	439^{sh}	0.33	416	0.44	500	523	0.07

[a] [10^{-4} L mol^{-1} cm^{-1}]; [b] Fluorescence standard: coumarine 153 in EtOH ($\phi = 0.38$, $\lambda_{exc} = 430$ nm for **3a** and $\lambda_{exc} = 408$ nm for **3b**, **3c**, respectively)[28] and measured in dichloromethane.

low oscillator strength for all three compounds which correlates to their small extinction coefficients.

Photoluminescence (PL) spectra reveal two distinct emission maxima accompanied by a weak shoulder at higher wavelength. Similar to the absorption spectra, the emission band of hydrocarbon **3a** is bathochromically shifted as compared to its aza-analogs **3b** and **3c**, while **3b** shows emission at higher energies than **3c**. Relative quantum yields were determined using Coumarin 153 as fluorescence standard and range between 3–7%. Interestingly, the quantum yield of diindenopyrene **3a** is still 7.5 times higher compared to tetraindenopyrene.[20,21]

In addition, CV measurements were performed to further elucidate the electronic properties of diindenopyrenes **3a–c** (Figure 4). Compound **3a** shows two quasi-reversible oxidation events. In contrast, **3b** and **3c** show only one broad irreversible oxidation at higher potential. Hence, the electron withdrawing effect of the imine-type nitrogen might reduce the electron density of the scaffold and hence oxidation is hampered for **3b** and **3c**. The onset potentials of the first oxidations were used to determine the HOMO energies which range between −5.66 eV for **3a** and −5.88 eV for **3c**.

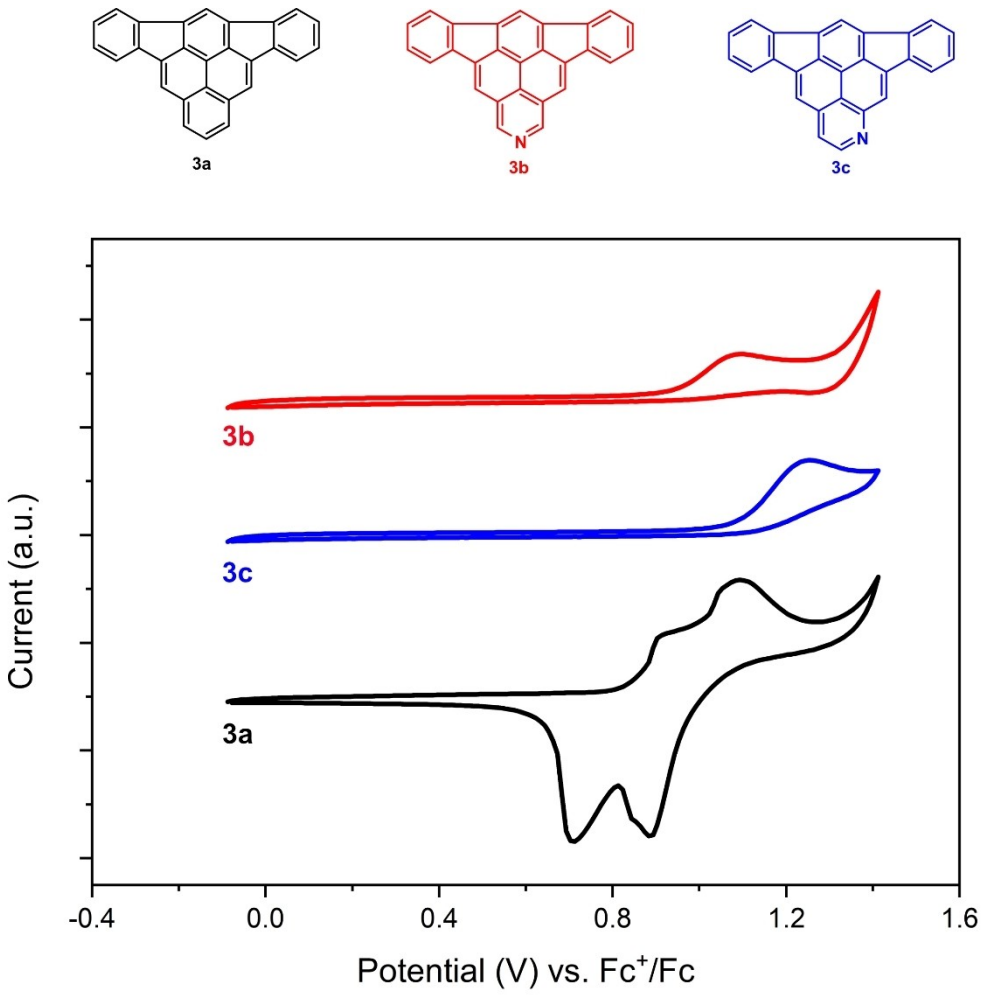

Figure 4. Cyclic voltammetry of compounds **3a–c** measured in DCM, 0.1 M nBu$_4$NPF$_6$, glassy carbon working electrode, ANE2 as the reference electrode, and Pt counter-electrode with ferrocene as standard.

Research Article
doi.org/10.1002/ejoc.202301101

Chemistry Europe
European Chemical Societies Publishing

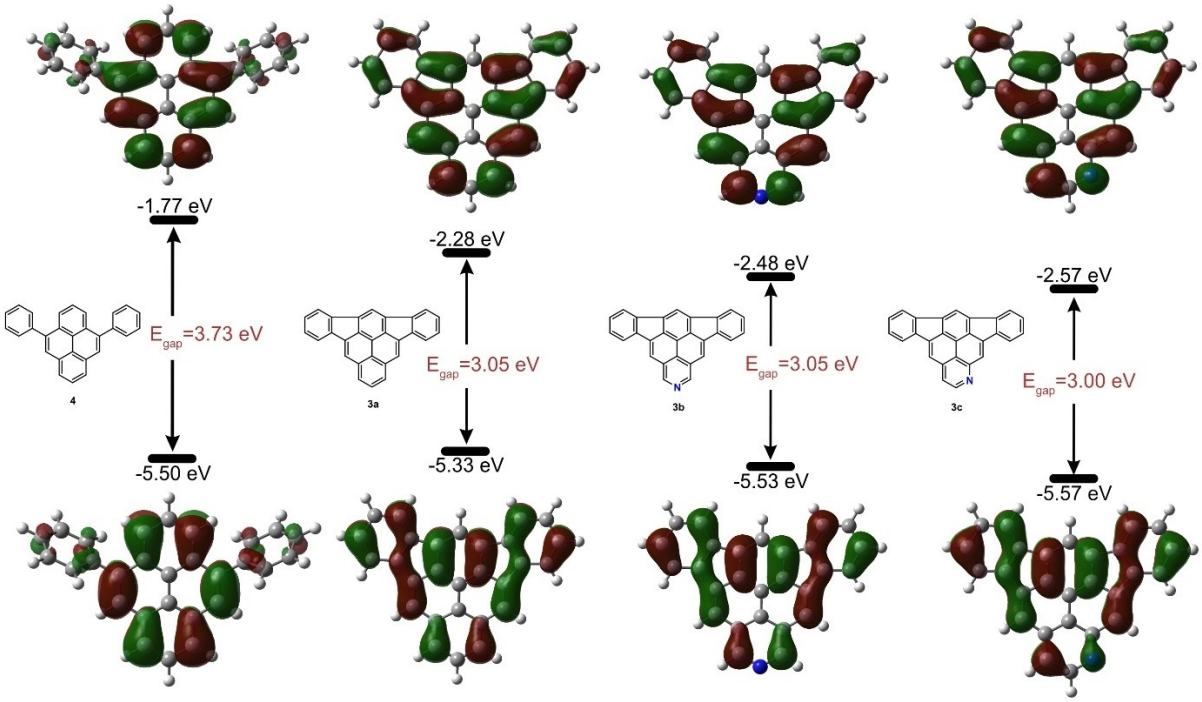

Figure 5. Calculated frontier molecular orbitals and energy levels at the B3LYP/6-311G(d,p) level of theory (isovalue = 0.02 a.u.).[32]

Finally, DFT calculations for **3a–c** and uncyclized 4,10-diphenylpyrene **4** were carried out to verify the experimental results.[29] The HOMO-LUMO band gaps have been determined to ~3.0 eV for **3a–c** and are in very good agreement with the experimental results. The calculated HOMO energies correlate very well with experimentally determined values from CV measurements. Visualization of the frontier molecular orbitals (Figure 5) further explains the differences of oxidation potentials of **3b** and **3c**. While the nitrogen atom of **3b** is located at a nodal plane, the nitrogen atom of **3c** contributes to the HOMO what explains the lowered oxidation potential and HOMO energy vice versa. In contrast, uncyclized compound **4** has an increased bandgap of 3.7 eV (Figure 5; Table 2). The reduction of the band gap by annulation of the phenyl rings is mainly based on stabilization of the LUMO energies, while HOMO levels are only slightly affected.[30,31] Stabilization of HOMO and LUMO energies of **3a–c** might be due to the improved contribution of the annulated phenyl rings to both frontier molecular orbitals (FMOs). Introduction of nitrogen in **3b** and **3c** leads to further reduction of both HOMO- und LUMO energy levels. This effect is less pronounced for **3b** than for **3c** as the nitrogen atom of **3b** is localized in the nodal plane of the symmetric diindenopyrene scaffold.

Table 2. Optical, electrochemical, and theoretical data for **3a–c**.

	$E_g^{opt.}$ (eV)[a]	E^{ox} (V)[b]	$HOMO^{cv}$ (eV)[c]	$HOMO^{DFT}$ (eV)[c]	$LUMO^{DFT}$ (eV)[c]	ΔE_g^{DFT} (eV)
3a	2.51	1.04	−5.66	−5.58	−2.53	3.05
3b	2.81	1.24	−5.74	−5.77	−2.71	3.05
3c	2.69	1.41	−5.88	−5.81	−2.82	3.00

[a] Determined from the intersection of normalized absorption and emission spectra; [b] versus Fc^+/Fc; [c] calculated using the equation: $E(HOMO)^{cv} = -e[(E_{Ox}$ vs $Fc^+/Fc) + 4.80]$; [d] Calculated DFT energy levels at the B3LYP/6-311G(d,p) level of theory.

To gain further insights into the impact of nitrogen doping on the aromaticity, nuclear independent chemical shift (NICS) calculations have been performed for **3a–c** and **4** and the corresponding ring-currents have been determined and visualized using the NICS2BC Wizard program developed by Paenurk and Gershoni-Poranne.[33] NICS calculations have been performed on the GIAO-B3LYP/6-311+G(d,p) level of theory[34] with the optimized gas-phase structures at the B3LYP/6-311G(d,p) level a height of 1.7 Å.[35] The results are presented in Figure 6 and in agreement with previous studies on azapyrenes.[24]

For all compounds, rings A, B, C and E show aromatic behavior, while NICS values for rings D suggest only weak to non-aromatic behavior. Annulation of the E ring to the pyrene scaffold leads to reduced aromaticity of the C-ring, while A and B rings are largely unaffected. An impact of the presence of nitrogen on the aromaticity of the fused rings A, B and E is not observed (cf. Figure 6). Despite the fusion of their E-rings, compounds **3a–c** manifest a strong semi-global ring current of its inherent pyrene moiety and a local ring-current for ring E. Only a weak global ring current can be observed for **3a** and **3b** which completely vanished for **3c**. Hence, annulation of the E rings and planarization does not affect the aromaticity of the system and diindenopyrenes **3** behave largely like isolated (aza−)pyrenes with two attached phenyl rings.

Research Article
doi.org/10.1002/ejoc.202301101

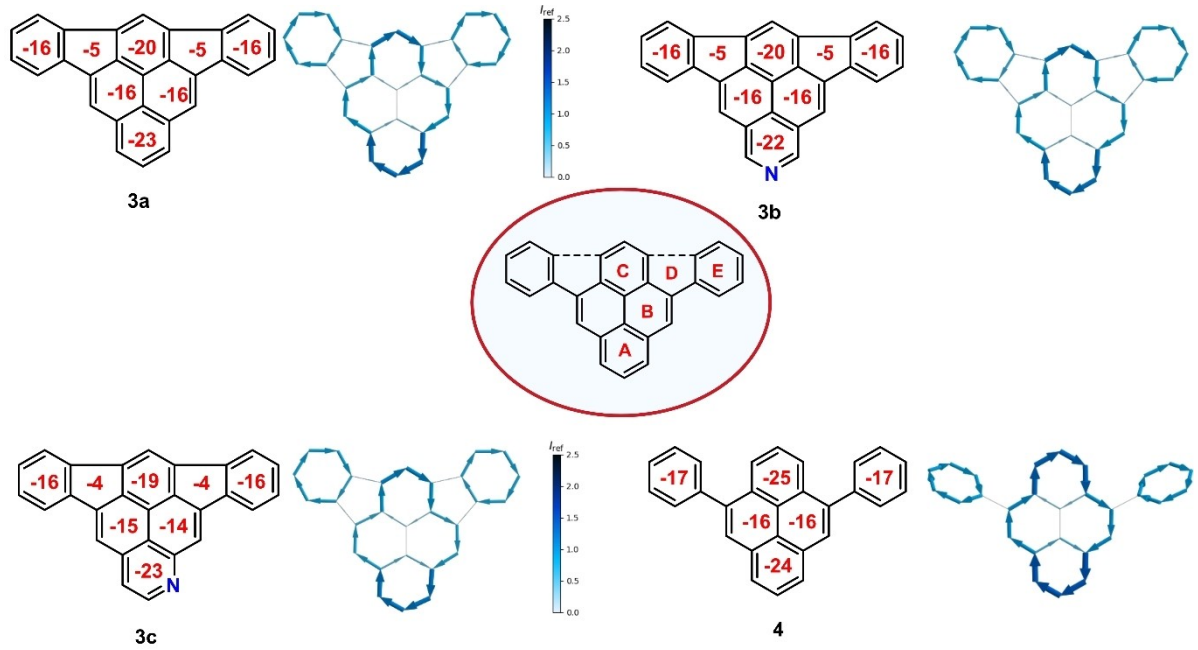

Figure 6. Calculated nucleus-independent chemical shifts (NICS) for (aza)-diindenopyrenes **3a–c** and 4,10-diphenylpyrene **4**. Left: structure of molecule with respective NICS(1.7) values in the geometric center of each ring. Right: NICS2BC graphs (current was calculated from NICS(1.25); strength relative to I_{ref} = 11.5 nA T^{-1} (ring current of benzene).

Conclusions

In summary, we have developed a novel synthetic method for diindenopyrene **3a** and its aza-analogs **3b** and **3c**. The impact of nitrogen doping on the optical and electrochemical properties have been studied experimentally and by DFT calculations. The presence and position of nitrogen in the scaffold has a drastic impact on the electronic properties. Hence, non-symmetric **3c** shows more pronounced changes of the absorption and emission properties as well as oxidation potentials than **3b** with respect to **3a**. Incorporation of nitrogen into the scaffold leads to stabilized HOMO and LUMO levels, while their band-gap remains largely unaffected. Hence, incorporation of nitrogen to indenopyrenes is a good handle to fine-tune the inherent electronic properties. Future studies will be devoted toward the synthesis of extended heteroatom-doped indenopyrenes.

Experimental Section

General Information: The nuclear magnetic resonance spectra (^{1}H/^{13}C/^{19}F NMR) were recorded on a Bruker AVANCE 300 III, 250 II, or 500. The analyzed chemical shifts δ are referenced to residual solvents signals of the deuterated solvents $CDCl_3$ (δ = 7.26 ppm/77.16 ppm), or DMSO-d_6 (δ = 2.50 ppm/39.52 ppm). Multiplicities due to spin–spin correlation are reported as follows, s = singlet, d = doublet, dd = double doublet, t = triplet, pt = pseudo triplet, m = multiplet, and further described through their coupling constants *J*. Infrared spectra (IR) were measured as attenuated total reflection (ATR) experiments with a Nicolet 380 FT-IR spectrometer. The signals have been characterized through their wave numbers and their corresponding absorption as very strong (vs), strong (s), medium (m), weak (w), or very weak (vw). UV/vis spectra were recorded on a Cary 60 UV–vis spectrophotometer and emission spectra with an Agilent Cary Eclipse fluorescence spectrophotometer. Cyclovoltammetry (CV) was measured in DCM with 0.1 M *n*-Bu_4NPF_6 as supporting electrolyte, glassy carbon working electrode, ANE2 ($Ag/AgNO_3$ 0.01 M in CH_3CN) as reference electrode, and Pt counter electrode with ferrocene as external standard (1 mM in CH_3CN). The potential is given vs FcH/FcH^+. The potentiostat used was an AMETEK PARSTAT 4000. Basic and high-resolution mass spectra (MS/HRMS) were measured on instruments which are paired with a preceding gas chromatograph (GC) or liquid chromatograph (LC). The samples have been ionized through electron impact ionization (EI) on an Agilent 6890/5973 or Agilent 7890/5977 GC-MS equipped with a HP-5 capillary column using helium carrier gas or by applying electron spray ionization (ESI) on an Agilent 1200/6210 Time-of-Flight (TOF) LC–MS. X-ray single-crystal structure analysis was performed on a Bruker Apex Kappa-II CCD diffractometer.

Materials: The applied solvents, DMSO, MeCN, Toluene, 1,4-Dioxane, DMA were obtained as dry solvents through commercial sources and employed without further purification. Solvents for extraction and column chromatography were available after previous distillation. Other reagents, catalysts, ligands, acids, and bases were utilized in purchased purity. Column chromatography was performed using a Merck Silica gel 60 (particle size 35–70 μm). The starting materials 1,3-dibromo-2-iodobenzene,[36] 3,5-dibromo-4-chloropyridine[24] and 3-chloropyridine-2,4-diyl bis(trifluoromethane-sulfonate)[25] were synthesized according to known procedures.

General procedure for synthesis of diindeno[1′,2′,3′:3,4;1″,2″,3″:6,7]phenaleno[1,9-*cd*]pyridine (3a-c): In a pressure tube with inert atmosphere were added **2a–c** (100 mg, 1.0 equiv.), $PdCl_2(PhCN)_2$ (10 mol%), PCy_3 (20 mol%), Cs_2CO_3 (2.0 equiv.), PivOH (40 mol%) and DMA (4 ml) as a solvent. The reaction was heated in an alumina metal block at 150 °C for 18 h. Then the cooled solution was diluted with dichloromethane and washed with water 3 times, dried with sodium sulfate and purified by column chromatography (Heptane:EtOAc = 5 : 1). Compounds **3a–c** purified by column chromatography Heptane:DCM = 20 : 1.

Supporting Information

The authors have cited additional references within the Supporting Information (Ref. [37–42]).

Acknowledgements

Financial Support by the state of Mecklenburg-Western Pomerania (stipend for A. K.) is gratefully acknowledged.

Conflict of Interests

The authors declare no conflict of interest.

Data Availability Statement

The data that support the findings of this study are available in the supplementary material of this article.

Keywords: C–H activation · catalysis · cyclization · diindenopyrene · polycyclic aromatic hydrocarbons

[1] M. Stępień, E. Gońka, M. Żyła, N. Sprutta, *Chem. Rev.* **2017**, *117*, 3479–3716.
[2] C. Wang, H. Dong, W. Hu, Y. Liu, D. Zhu, *Chem. Rev.* **2012**, *112*, 2208–2267.
[3] X. Y. Wang, X. Yao, A. Narita, K. Müllen, *Acc. Chem. Res.* **2019**, *52*, 2491–2505.
[4] P. Samorí, X. Feng, D. Bonifazi, *ChemPlusChem* **2019**, *84*, 1177–1178.
[5] A. Narita, X. Y. Wang, X. Feng, K. Müllen, *Chem. Soc. Rev.* **2015**, *44*, 6616–6643.
[6] T. M. Figueira-Duarte, K. Müllen, *Chem. Rev.* **2011**, *111*, 7260–7314.
[7] M. E. Østergaard, P. J. Hrdlicka, *Chem. Soc. Rev.* **2011**, *40*, 5771–5788.
[8] A. Mateo-Alonso, *Chem. Soc. Rev.* **2014**, *43*, 6311–6324.
[9] J. Liu, S. Osella, J. Ma, R. berger, D. Beljonne, D. Schollmeyer, X. Feng, K. Müllen, *J. Am. Chem. Soc.* **2016**, *138*, 8364–8367.
[10] J. M. Quimby, L. T. Scott, *Adv. Synth. Catal.* **2009**, *351*, 1009–1013.
[11] D. Lungerich, H. Hoelzel, K. Harano, N. Jux, K. Y. Amsharov, E. Nakamura, *ACS Nano.* **2021**, *15*, 12804–12814.
[12] H. Nakazawa, Y. Uetake, Y. Yakiyama, H. Sakurai, *Synlett* **2023**, *34*, 374–378.
[13] S. Hishikawa, Y. Okabe, R. Tsuruoka, S. Higashibayashi, H. Ohtsu, M. Kawano, Y. Yakiyama, H. Sakurai, *Chem. Lett.* **2017**, *46*, 1556–1559.
[14] Y. Yakiyama, S. Hishikawa, H. Sakurai, *Beilstein J. Org. Chem.* **2020**, *16*, 681–690.
[15] A. De Meijere, B. Stulgies, K. Albrecht, K. Rauch, H. A. Wegner, H. Hopf, L. T. Scott, L. Eshdat, I. Aprahamian, M. Rabinovitz, *Pure Appl. Chem.* **2006**, pp. 813–830.
[16] Y. Wei, J. Zheng, S. Cui, X. Song, Y. Su, W. Deng, Z. Wu, X. Wang, W. Wang, M. Rao, Y. Lin, C. Wang, K. Amine, F. Pan, *J. Am. Chem. Soc.* **2015**, *137*, 8364–8367.
[17] C. Lütke Eversloh, Y. Avlasevich, C. Li, K. Müllen, *Chem. Eur. J.* **2011**, *17*, 12756–12762.
[18] B. P. Cho, R. G. Harvey, *J. Org. Chem.* **1987**, *52*, 5668–5678.
[19] Y. Choi, T. Chatterjee, J. Kim, J. S. Kim, E. J. Cho, *Org. Biomol. Chem.* **2016**, *14*, 6804–6810.
[20] S. M. Elbert, A. Haidisch, T. Kirschbaum, F. Rominger, U. Zschieschang, H. Klauk, M. Mastalerz, *Chem. Eur. J.* **2020**, *26*, 10585–10590.
[21] H. A. Wegner, H. Reisch, K. Rauch, A. Demeter, K. A. Zachariasse, A. De Meijere, L. T. Scott, *J. Org. Chem.* **2006**, *71*, 9080–9087.
[22] V. Akhmetov, M. Feofanov, C. Ruppenstein, J. Lange, D. Sharapa, M. Krstić, F. Hampel, E. A. Kataev, K. Amsharov, *Chem. Eur. J.* **2022**, *28*, e202200584.
[23] H. S. C. Ikeda, R. S. C. Maeda, M. S. C. Matsuura, *WO 2010/013520*, **2011**.
[24] R. Molenda, S. Boldt, A. Villinger, P. Ehlers, P. Langer, *J. Org. Chem.* **2020**, *85*, 12823–12842.
[25] A. Vardanyan, S. Boldt, A. Villinger, P. Ehlers, P. Langer, *J. Org. Chem.* **2022**, *87*, 11296–11308.
[26] M. M. MacHuy, C. Würtele, P. R. Schreiner, *Synthesis.* **2012**, *44*, 1405–1409.
[27] Deposition Number a) 2293598 (for **1 a**) and 2293599 (for **3 a**) contain(s) the supplementary crystallographic data for this paper. These data are provided free of charge by the joint Cambridge Crystallographic Data Centre and Fachinformationszentrum Karlsruhe Access Structures service.
[28] A. M. Brouwer, *Pure Appl. Chem.* **2011**, *83*, 2213–2228.
[29] M. J., Frisch, G. W. Trucks, H. B. Schlegel, G. E. Scuseria, M. A. Robb, J. R. Cheeseman, G. Scalmani, V. Barone, B. Mennucci, G. A. Petersson, H. Nakatsuji, M. Caricato, X. Li, X.; Hratchian, A. F. Izmaylov, J. Bloino, G. Zheng, J. L. Sonnenberg, M. Hada, M. Ehara, K. Toyota, R. Fukuda, J. Hasegawa, M. Ishida, T. Nakajima, Y. Honda, O. Kitao, H. Nakai, T. Vreven, J. A. Montgomery, J. E. Peralta, F. Ogliaro, M. Bearpark, J. J. Heyd, E. Brothers, K. N. Kudin, V. N. Staroverov, R. Kobayashi, J. Normand, K. Raghavachari, A. Rendell, J. C. Burant, S. Iyengar, J. Tomasi, M. Cossi, N. Rega, J. M. Millam, M. Klene, J. E. Knox, J. B. Cross, V. Bakken, C. Adamo, J. Jaramillo, R. Gomperts, R. E. Stratmann, O. Yazyev, A. J. Austin, R. Cammi, C. Pomelli, J. W. Ochterski, R. L. Martin, K. Morokuma, V. G. Zakrzewski, G. A. Voth, P. Salvador, J. J. Dannenberg, S. Dapprich, A. D. Daniels, O. Farkas, J. B. Foresman, J. V. Ortiz, J. Cioslowski, D. J. Fox, *Gaussian 09*, revision E.01; Gaussian, Inc.: Wallingford, CT, **2013**.
[30] H. Zhang, P. Zhou, A. Daaoub, S. Sangtarash, S. Zhao, Z. Yang, Y. Zhou, Y.-L. Zou, S. Decurtins, R. Häner, Y. Yang, H. Sadeghi, S.-X. Liu, W. Hong, *Chem. Sci.* **2023**, *14*, 6079–6086.
[31] C. Si, Y.-N. Hu, D. Sun, K. Wang, X.-H. Zhang, E. Zysman-Colman, *J. Mater. Chem. C* **2023**, *11*, 12174–12184.
[32] A. D. Becke, *J. Chem. Phys.* **1993**, *98*, 5648–5652.
[33] E. Paenurk, R. Gershoni-Poranne, *Phys. Chem. Chem. Phys.* **2022**, *24*, 8631–8644.
[34] K. Wolinski, J. F. Hinton, P. Pulay, *J. Am. Chem. Soc.* **1990**, *112*, 8251–8260.
[35] R. Gershoni-Poranne, A. Stanger, *Chem. Eur. J.* **2014**, *20*, 5673–5688.
[36] T. Dumslaff, B. Yang, A. Maghsoumi, G. Velpula, K. S. Mali, C. Castiglioni, S. De Feyter, M. Tommasini, A. Narita, X. Feng, K. Müllen, *J. Am. Chem. Soc.* **2016**, *138*, 4726–4729.
[37] E. Anklam, *Magn. Reson. Chem.* **1989**, *27*, 503–506.
[38] N. H. Chang, X. C. Chen, H. Nonobe, Y. Okuda, H. Mori, K. Nakajima, Y. Nishihara, *Org. Lett.* **2013**, *15*, 3558–3561.
[39] A. C. Whalley, K. N. Plunkett, A. A. Gorodetsky, C. L. Schenck, C. Y. Chiu, M. L. Steigerwald, C. Nuckolls, *Chem. Sci.* **2011**, *2*, 132–135.
[40] T. C. Wu, H. J. Hsin, M. Y. Kuo, C. H. Li, Y. T. Wu, *J. Am. Chem. Soc.* **2011**, *133*, 16319–16321.
[41] P. Li, Q. Li, H. Weng, J. Diao, H. Yao, A. Lin, *Org. Lett.* **2019**, *21*, 6765–6769.
[42] W. Hagui, H. Doucet, J.-F. O. Soulé, *Chem.* **2019**, *5*, 2277.

Manuscript received: October 27, 2023
Revised manuscript received: November 6, 2023
Accepted manuscript online: November 27, 2023
Version of record online: ■■, ■■

RESEARCH ARTICLE

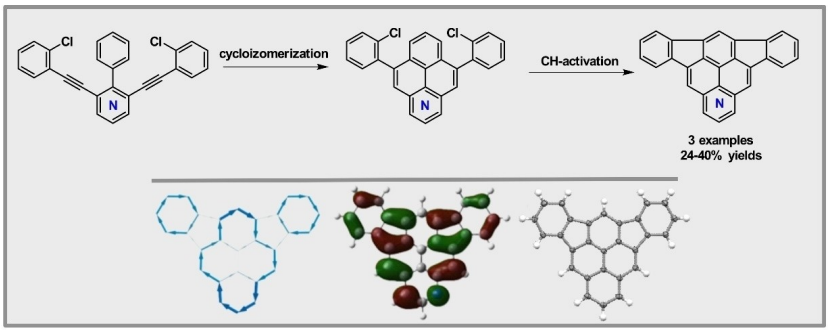

*A. Khomutetckaia, N. Hildebrandt, Dr. P. Ehlers, Dr. A. Villinger, Prof. Dr. P. Langer**

1 – 8

Synthesis and Properties of Diindeno[1,2,3-*cd*:1′,2′,3′-*mn*]pyrene and Two of Its Aza-Analogs

Diindeno[1,2,3-*cd*:1′,2′,3′-*mn*]pyrene, a substructure of fullerene C_{70}, and two of its aza-analogs were prepared by Pd-catalyzed cross-coupling reactions and acid-mediated cycloisomerization and final Pd-catalyzed C–H-activation. The optical and electrochemical properties and the impact of *N*-doping on the physical properties have been studied.

IV Synthesis and Properties of Azadibenzo[*a*,*e*]pyrenes

Aleksandra Khomutetckaia, Peter Ehlers, Alexander Villinger, Peter Langer.

Eur. J. Org. Chem. **2024**, e202301299.

DOI: 10.1002/ejoc.202301299

EurJOC
European Journal of Organic Chemistry

Research Article
doi.org/10.1002/ejoc.202301299

Chemistry Europe
European Chemical Societies Publishing

www.eurjoc.org

Synthesis and Properties of Azadibenzo[*a,e*]pyrenes

Aleksandra Khomutetckaia,[a] Peter Ehlers,[a] Alexander Villinger,[a] and Peter Langer*[a, b]

Four different isomeric azadibenzo[*a,e*]pyrenes (benzo[4,10]anthra[9,1-*gh*]isoquinolines and benzo[4,10]anthra[1,9-*fg*]isoquinolines) were prepared by combination of Pd-catalyzed Sonogashira and Suzuki cross-coupling, Brønsted acid mediated cycloisomerization and Pd-catalysed CH-activation reactions. The optical properties have been studied by steady-state absorption and emission spectroscopy in different solvents and during acid titration. Trifluoroacetic acid protonation strongly affects absorption and emission properties, with variations depending on the position of the nitrogen atom of the specific compound. Electrochemical analysis showed distinct oxidation and reduction potentials. DFT calculations provided further insights into electronic properties.

Introduction

Significant amounts of polycyclic heteroaromatic compounds (PHAs) and their derivatives, containing nitrogen, sulfur and oxygen, are found in the environment. They are released from various sourcess such as natural oil seepage, oil spills, bilge discharges and inland sources. Many of these substances are toxic and cause adverse effects. At the same time, these substances can be used in a variety of applications, including the synthesis and development of pharmaceuticals, dyes, plastics, pesticides and even in the field of circularly polarized luminescence (CPL) lasers,[1] organic photovoltaic cells (OPVs),[2] organic light-emitting diodes (OLEDs)[3] and organic field-effect transistors (OFETs).[4,5] In this context, *peri*-fused arenes, such as pyrene, are of special interest, due to their photophysical and electronic properties. In fact, pyrene derivatives have become prominent building blocks in organic electronics[4,6] and biomedical applications.[7]

The presence of a nitrogen atom in the PHA framework usually leads to a change of the optical and electrochemical properties and allows to adjust photoluminescence, redox behaviour, optical absorption, stabilisation of HOMO-LUMO energy levels, reduction of electron bandgaps and electron acceptance. Aza-analogues of pyrene (azapyrenes) are important materials for applications in organic semiconductor devices, such as OLEDs, OFETs OPVs.[8] In addition, they show self-assembling properties, have been used as main units of molecular machines and act as DNA intercalators.[9]

While phenanthridines (azaphenanthrenes) constitute a well-known class of compounds showing a variety of biological activities, such as antimalarial, cytotoxic, antimycobacterial and antitumour activity,[10] aza-pyrenes have only scarcely been reported in the literature so far. In 1968, Kirchlechner reported the synthesis of unsubstituted (parent) 2-azapyrene (**A**).[11] In recent years, we have synthesized substituted azapyrenes and observed that incorporation of nitrogen to the pyrene system stabilizes both the HOMO and LUMO levels, whereby functional groups at the K-region allow modulation of the photophysical and electrochemical properties.[12] In 2015, Han and co-workers obtained quinolinopyrene **B**.[13] In continuation of this work, during the last three years, the groups of List, Ito and our group reported the synthesis of N-doped benzo- and napththopyrenes **C**, **D** and **E**, which underlines the importance of this substance class (Scheme 1).[14]

Herein, we wish to report the synthesis and properties of what are, to the best of our knowledge, hitherto unknown azadibenzo[*a,e*]pyrenes **5a,b** and **9a,b**. These compounds, formally named benzo[*4,10*]anthra[*9,1-gh*]isoquinolines and benzo[*4,10*]anthra[*1,9-fg*]isoquinolines, can be regarded as aza-analogues of parent dibenzo[*a,e*]pyrene (**F**) containing a phenanthridine substructure which was first mentioned in the literature by Bruno Schiedt in 1938, working at the University of Rostock at that time.[15]

Results and Discussion

Synthesis

Our strategy for the synthesis of azadibenzo[*a,e*]pyrene is based on the functionalization of dibromopyridines by Sonogashira reaction with 1-chloro-2-ethynylbenzene, Suzuki-Miyaura reaction with 2-naphthylboronic acid, acid mediated cyclization of the alkyne with the naphthalene moiety and subsequent cyclization by CH-activation *via* the chloride (Scheme 2). The four regioisomeric products are obtained by variation of the dibromopyridine and by the order of Sonogashira and Suzuki-Miyaura reactions.

Sonogashira reaction of 2,3-dibromopyridine (**1a**) with 1-chloro-2-ethynylbenzene regioselectively afforded 2-alkynyl-3-bromopyridine **2a**. Suzuki-Miyaura reaction of **2a** with 2-

[a] *A. Khomutetckaia, P. Ehlers, A. Villinger, P. Langer*
Universität Rostock, Institut für Chemie,
A.-Einstein-Str. 3a, 18059 Rostock, Germany

[b] *P. Langer*
Leibniz Institut für Katalyse an der Universität Rostock,
A.-Einstein-Str.29a, 18059 Rostock, Germany
Tel.: +49 381 498 6410
Fax: +49 381 498 6412
E-mail: peter.langer@uni-rostock.de

Supporting information for this article is available on the WWW under https://doi.org/10.1002/ejoc.202301299

Research Article
doi.org/10.1002/ejoc.202301299

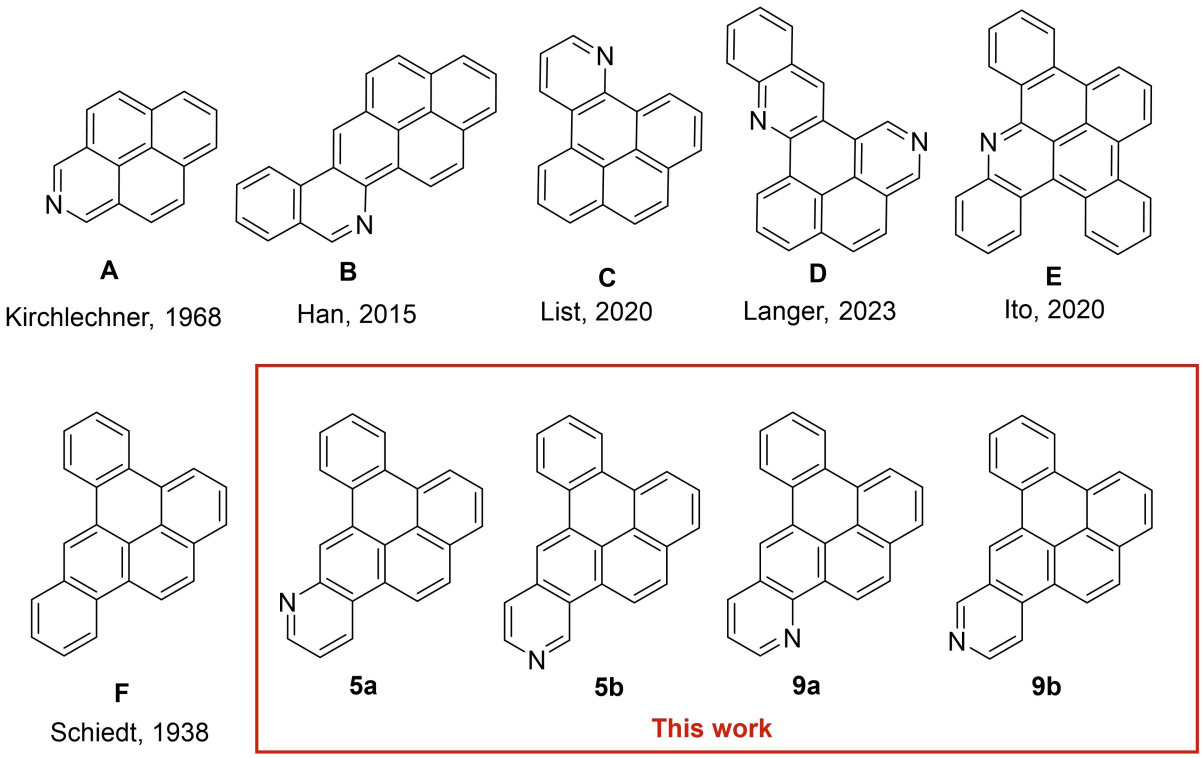

Scheme 1. Target molecules of this work in the context of related compounds

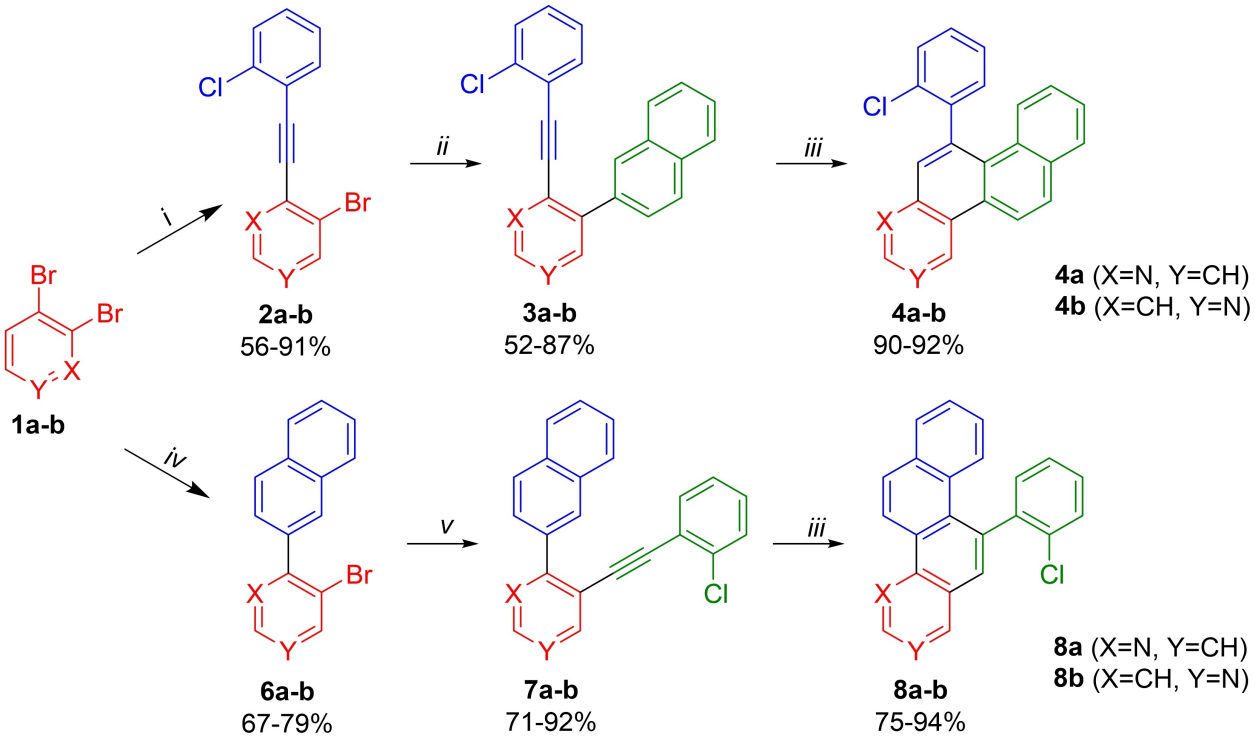

Scheme 2. Synthesis of **4a,b** and **8a,b**. Conditions: *i* For **2a**: **1a** (1.0 equiv.), 1-chloro-2-ethynylbenzene (1.2 equiv.), $Pd(PPh_3)_4$ (5 mol%), CuI (2 mol%), HN^iPr_2, 40 °C, 1 h. For **2b**: **1b** (1.0 equiv.), 1-chloro-2-ethynylbenzene (1.2 equiv.), $Pd(PPh_3)_4$ (10 mol%), CuI (10 mol%), HN^iPr_2, 40 °C, 3 h; *ii*, **2a,b** (1.0 equiv.), 2-naphthaleneboronic acid (1.1 equiv.), $Pd(PPh_3)_4$ (5 mol%), K_3PO_4 (2.0 equiv.), 1,4-dioxane/H_2O (6 : 1), 100 °C, 3 h; *iii*, **3a,b**, **7a,b** (1.0 equiv.), MsOH (30 equiv.), 120 °C, 18 h. For **6a**: *iv*, **1a** (1.0 equiv.), 2-naphthaleneboronic acid (1.1 equiv.), $Pd(OAc)_2$ (5 mol%), PPh_3 (10 mol%), K_2CO_3 (2.0 equiv.), CH_3CN/CH_3OH (2 : 1), 50 °C, 21 h. For **6b**: *iv*, **1b** (1.0 equiv.), 2-naphthaleneboronic acid (1.1 equiv.), $Pd(PPh_3)_4$ (5 mol%), K_3PO_4 (2.0 equiv.), 1,4-dioxane, 90 °C, 3 h; *v*, **6a,b** (1.0 equiv.), 1-chloro-2-ethynylbenzene (1.1 equiv.), $PdCl_2(PPh_3)_2$ (5 mol%), CuI (5 mol%), NEt_3, DMA, 90 °C, 6 h.

Research Article
doi.org/10.1002/ejoc.202301299

naphthylboronic acid gave 2-alkynyl-3-naphthylpyridine **3a**. Subsequent cycloisomerization[16] in the presence of methanesulfonic acid (MsOH) afforded naphtho[2,1-*f*]quinoline (1-azachrysene) **4a**. Likewise, 3-azachrysene **4b** was prepared from 3,4-dibromopyridine (**1b**). 4-Azachrysene **8a** and 2-azachrysene **8b** were prepared from **1a** and **1b**, respectively, by changing the order of Sonogashira and Suzuki-Miyaura reactions. The structure of **4b** was independently confirmed by crystal structure analysis (Figure 1). The tetracyclic ring system deviates slightly from planarity due to distortion at both cove-regions with dihedral angles of ~8 ° and 16 ° (Figure 1) and the attached 2-chlorophenyl ring is twisted by ~60 °. Molecules are stacked in a slipped head-tail orientation comprising close π-π- and CH-π-contacts. Additionally, two molecules of neighbouring stacks undergo hydrogen bonding incorporating the pyridine nitrogen atoms.

The cyclization of azachrysenes to azadibenzo[*a*,*e*]pyrenes by Pd-catalyzed CH-activation reactions was studied next (Scheme 3). Treatment of **4a** with $PdCl_2$ as the catalyst, tricyclohexylphosphine (PCy_3) as the ligand, and 1,8-Diazabicyclo[5.4.0]undec-7-ene (DBU) as the base and *N*-methyl-2-pyrrolidone (NMP) as the solvent afforded benzo[*4,10*]anthra[*1,9-fg*]quinoline **5a** in 78% yield.[17] In contrast, employment of $PdCl_2(PhCN)_2$ and pivalic acid (PivOH), conditions reported by Nishihara and coworkers,[18] proved to be unsuccessful. While products **5a,b** and **9a** were obtained in good to very good yields, only a moderate yield of **9b** was obtained. In addition, for the synthesis of **9b** a higher amount of catalyst was required.

The structure of **9a** was independently confirmed by crystal structure analysis (Figure 2). The planar compound **9a** crystallizes triclinic with -P1 space group. The molecules are aligned in

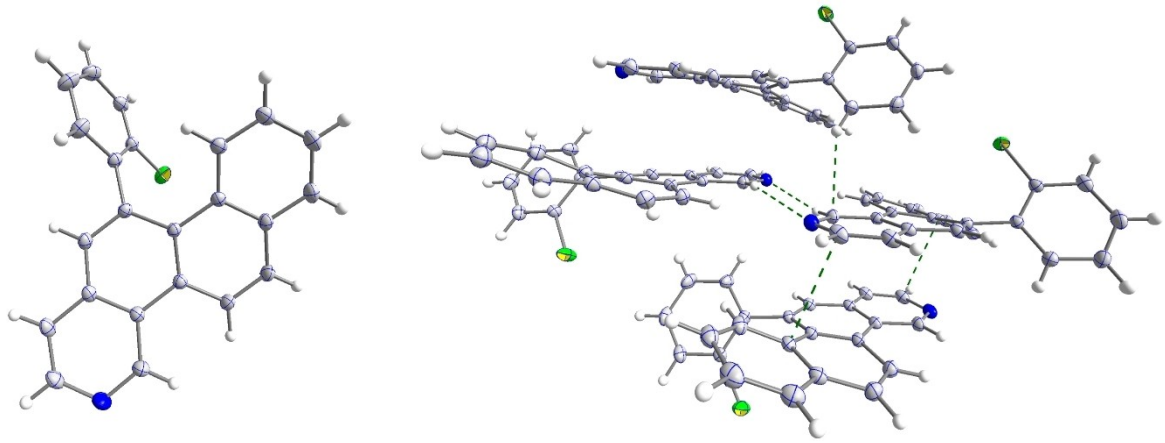

Figure 1. Crystal structure of **4b** (probability of ellipsoids is 50%; CCDC: 2295828).

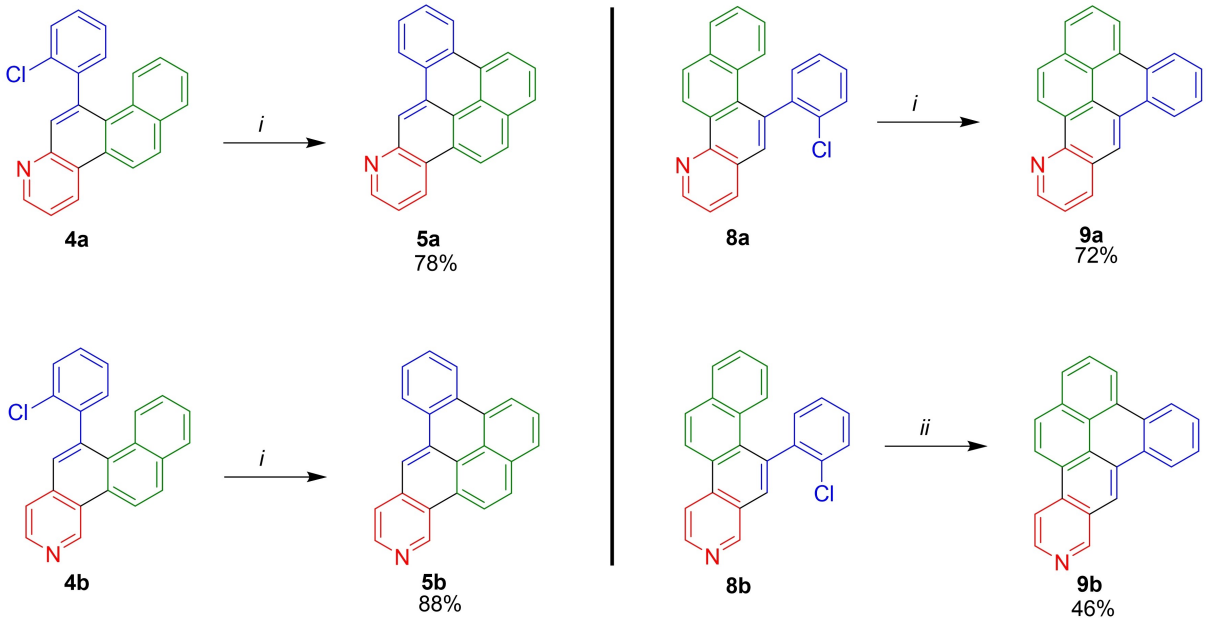

Scheme 3. Synthesis of **5a,b** and **9a,b**. Conditions: *i*, **4a,b, 8a**, $PdCl_2$ (0.2 equiv.), PCy_3 (0.4 equiv.), DBU (3.0 equiv.), NMP, 150 °C, 18 h; *ii*, **8b**, $PdCl_2$ (0.4 equiv.), PCy_3 (0.8 equiv.), DBU (6.0 equiv.), NMP, 150 °C, 18 h.

Research Article
doi.org/10.1002/ejoc.202301299

Chemistry Europe
European Chemical Societies Publishing

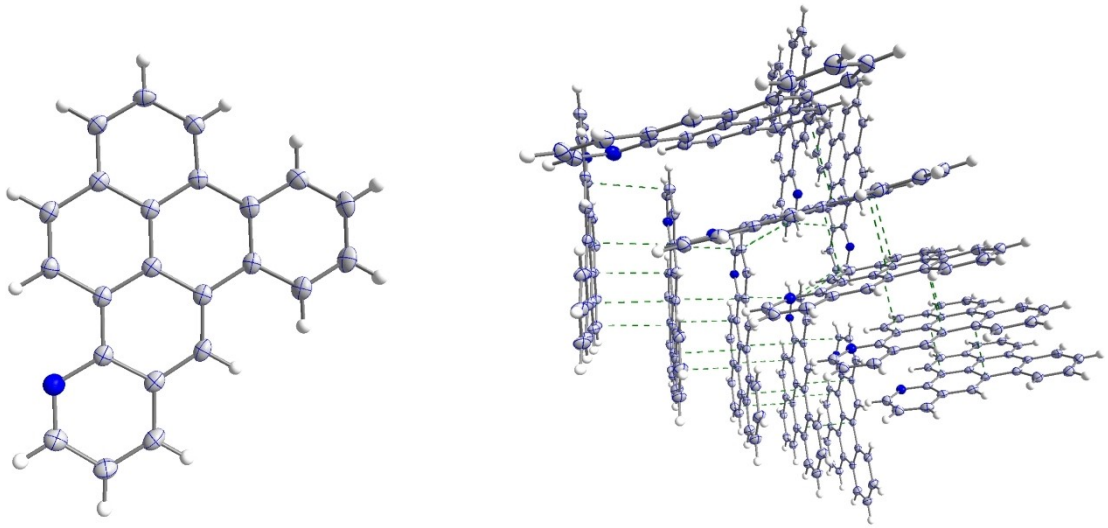

Figure 2. Crystal structure of **9a** (probability of ellipsoids is 50%; CCDC: 2295829).

a slipped head – head orientation in the crystal lattice with close π-π-contacts of 3.4 Å.

Physical Properties

We performed steady-state absorption and photoluminescence (PL) measurements for azadibenzo[*a,e*]pyrenes **5a,b** and **9a,b** which all represent yellow solids. All measurements were carried out in dichloromethane. For quantum yield determination, quinine hemisulfate monohydrate in 0.05 M H_2SO_4 was used as standard. The main optical data are given in Table 1 and Figure 3. All compounds exhibit broad low energy absorption bands between 330 nm and 400 nm with a certain fine-structure. Analysing the lowest energy absorption ($S_0 \leftarrow S_1$) at approx. 400 nm by TD-DFT calculations[19] on the B3LYP-311G(d,p) level of theory reveals that this transition is mainly derived from a HOMO-LUMO transition with high oscillator strength for all synthesized compounds and with minor admixture from HOMO→LUMO+1 for **5a,b**, **9b** and HOMO-2→LUMO+1 for **9a**. Comparison with all-carbon analogue **F** shows that incorporation of nitrogen into the scaffold results in no obvious shift of the absorption bands. However, extinction values differ. Extinction values for $\lambda_{abs.1}$ are strongly increased for nitrogen containing compounds compared to **F**, while extinction values of **F** for $\lambda_{abs,2}$ – $\lambda_{abs,3}$ are twice as high compared to its nitrogen doped analogues.

Emission spectra comprises of three emission bands at ~400 nm, ~425 nm and ~450 nm, while the lowest energy band of **5a,b** and **9a** appears as a shoulder. The determined fluorescence quantum yields range from 23 to 34%. Hence, isomeric azadibenzopyrenes **5a,b** and **9a,b** show only marginally altered absorption and emission properties.

Further studies of the excited and ground states were carried out by solvatochromic experiments for compound **9a**, using cyclohexane, toluene, dichloromethane and acetonitrile (Table 2, Figure 4). Based on empirical parameters, cyclohexane is the least polar solvent in this series, while acetonitrile is the

Table 1. Optical data of **5** and **9**.

	5a	5b	9a	9b	F[20]
λ_{abs1}[nm]	397	396	398	402	399
(ε_1[a])	0.89	1.05	0.97	0.59	0.17
λ_{abs2}[nm]	377	384	377	379	380
(ε_2[a])	1.25	1.19	1.29	1.13	2.29
λ_{abs3}[nm]	362	376	363	372	360
(ε_3[a])	1.07	1.34	1.23	1.34	2.09
λ_{em1}[nm]	426	451[sh]	426	456	/
λ_{em2}[nm]	408	424	406	429	/
λ_{em3}[nm]		402		406	/
φ [%][b]	33	34	29	23	/

[a] [10^{-4} L mol^{-1} cm^{-1}]; measured in dichloromethane; [b] Fluorescence standard: quinine hemisulfate monohydrate in 0.05 M H_2SO_4 ($\phi = 0.51$)[21]; sh = shoulder.

Research Article
doi.org/10.1002/ejoc.202301299

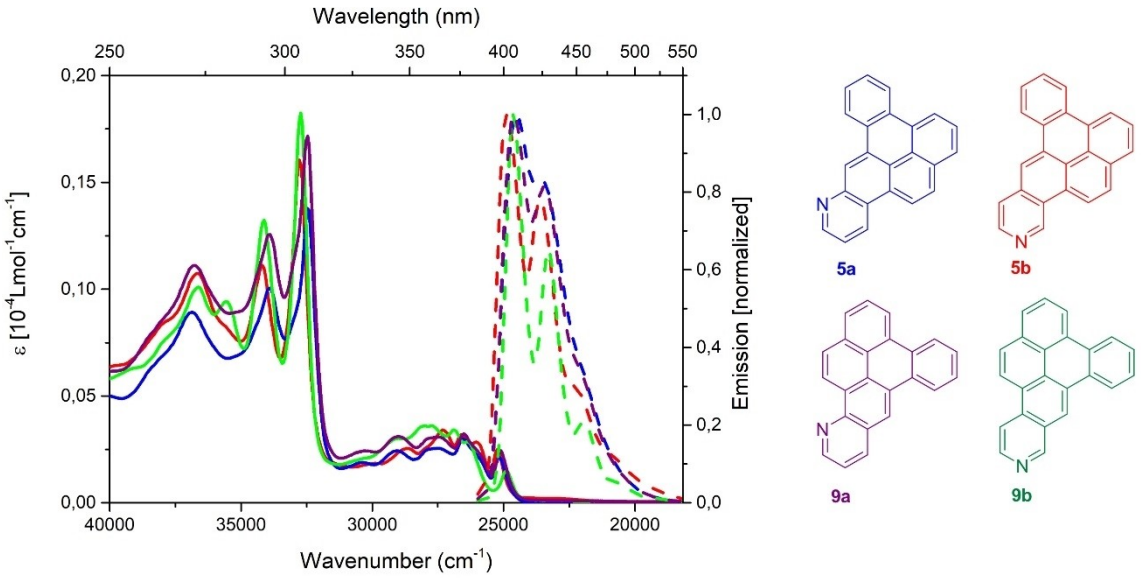

Figure 3. UV – Vis and emission spectra (excited @370 nm) of **5a**, **5b**, **9a**, **9b** in CH_2Cl_2 ($c = 10^{-5}$ M) at 20 °C.

Table 2. Quantum yields of **9a** in different solvents.

	Acetonitrile	Cyclohexane	Toluene	Dichloromethane
φ [%]	31	35	40	29

Fluorescence standard: quinine hemisulfate monohydrate in 0.05 M H_2SO_4 ($\phi = 0.51$)[20]

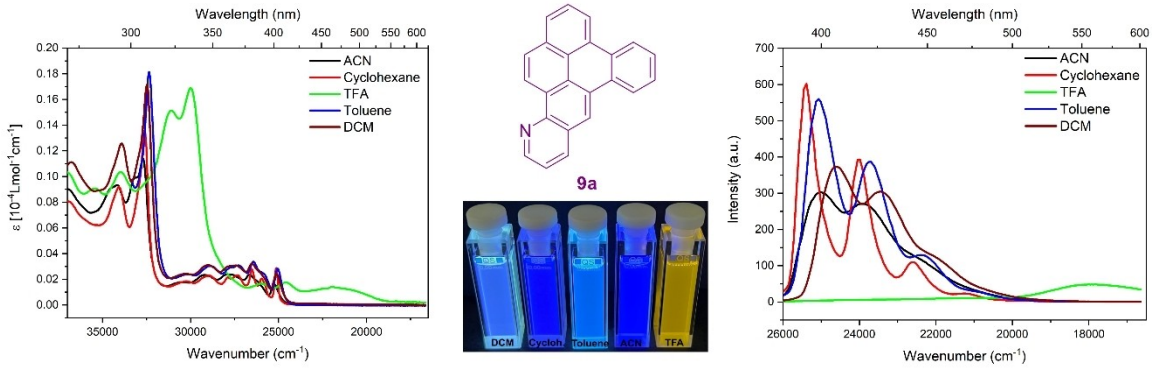

Figure 4. UV/Vis (left) and emission spectra (excited @370 nm) in different solvents (acetonitrile – black, cyclohexane – red, TFA – green, toluene – blue, DCM – yellow) of **9a** with $c = 10^{-5}$ M at 20 °C.

most polar one.[22] The absorption spectrum shows insignificant changes, while the emission maxima display broadening in more polar solvents and quantum yield differ only slightly (table 2).

However, the most pronounced effect was observed for trifluoroacetic acid (TFA) as solvent. Protonation of the pyridine nitrogen leads to strong bathochromic shifts and loss of the fine structure of the absorption and emission spectra. Hence, protonation experiments were performed for all four synthesized compounds **5** and **9** (Figure 5 and Figures S2-S4).

The absorption and emission properties are strongly influenced by TFA. Even addition of only 0.6 equiv. of TFA, changes the absorption properties of **5a** and **9b** and a new band is observed at higher wavelength, whose intensity increases with higher acid concentration for both compounds. For **5b** and **9a** comparable effects are observed but at higher acid concentration. Similar effects are observed in the emission spectra. The emission spectra of **5a** and **9b** show a decrease of intensity of the original bands and occurrence of a new emission band at higher wavelength already with 0.6 eq of TFA which remains approximately constant until 1.0 eq. Higher concentration of acids intensifies this effect until the original emission bands are vanished and the new band at higher wavelength is maximized. **5b** behaves slightly different compared to **5a** and **9b**. Analogous spectral changes are only observed at a TFA concentration of 0.8 eq and then constantly

Research Article
doi.org/10.1002/ejoc.202301299

Chemistry Europe
European Chemical Societies Publishing

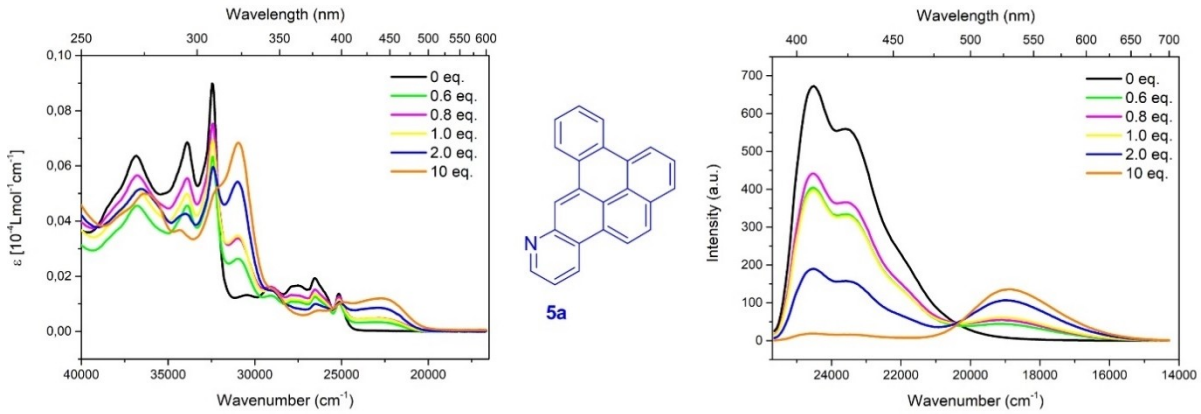

Figure 5. UV-Vis and emission spectra (excited @380 nm) of **5a** in CH_2Cl_2 ($c = 10^{-5}$ M) at 20 °C in dependence of the TFA concentration.

enhance with increasing acid equivalents. In particular, novel bands are observed at higher wavelength, while original band decrease in both absorption and emission bands. For **9a** similar effects are detected with high access of TFA. Hence, **9a** seem to have reduced basicity as compared to the other derivatives and the location of the pyridinic nitrogen within the cove region of **9a** might be a potential explanation.

The electrochemical properties of **5** and **9** were examined by performing cyclic voltammetry (CV) and differential pulse voltammetry (DPV) in dichloromethane which is exemplarily shown for compound **5a** (Figure 6 and SI). CV-and DPV experiments revealed that compounds **5** and **9** exhibit one oxidation peak within the studied potential range. The oxidation onsets are found in the range from 0.76 – 0.85 V vs. Fc^+/Fc redox couple. These oxidation potentials are slightly increased compared to their carbon analogue **F** with E_{ox} of 0.74 V vs. Fc^+/Fc what might be explained the presence of the electron deficient pyridine ring.[23] This observation is an indication that electrochemical properties can be fine-tuned by orientated instalment of nitrogen. Finally, energies of the highest occupied molecular orbitals (HOMOs) were determined for compounds **5** and **9** with very similar values in the range of −5.56 eV to −5.65 eV (Table 3).

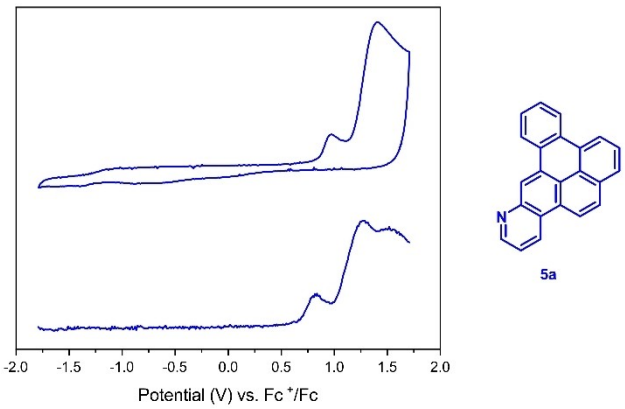

Figure 6. Cyclic voltammetry and differential pulse voltammetry of **5a** measured in DCM (c = 1 mM), with 0.1 M nBu$_4$NPF$_6$, glassy carbon working electrode, ANE2 as the reference electrode, and Pt counter-electrode with ferrocene as standard.

Density Functional Theory (DFT) calculations were carried out to gain a more complete understanding of the electronic structures.[19] The calculations were performed using the B3LYP functionals together with the 6–311 + G(d,p) basis set. Visualisation of the HOMO and LUMO (Figure 7) displays the electron density distribution on the entire azadibenzo[*a,e*]pyrene scaffold for compounds **5a,b** and **9a,b**. A comparison of the HOMO and LUMO levels shows little variations between compounds **5** and **9**, ranging from −5.71 eV to −5.80 eV, while the LUMO levels are range from −2.20 eV to −2.28 eV. The calculated HOMO and LUMO energy levels of **5** and **9** are in very good agreement with the CV data confirming the experimental results (Table 3). The energy gap between the HOMO and

Table 3. Optical, electrochemical, and theoretical data of **5a,b** and **9a,b**.

	$E_g^{opt.}$ (eV)[a]	E_{ox}^{CV} (V)[b]	$HOMO^{CV}$ (eV)[c]	$HOMO^{DFT}$ (eV)[d]	$LUMO^{DFT}$ (eV)[d]	ΔE_g^{DFT} (eV)	ΔE_g^{TD-DFT} (eV)
5a	3.16	0.85	−5.65	−5.75	−2.24	3.51	3.49
5b	3.17	0.79	−5.59	−5.80	−2.28	3.52	3.50
9a	3.16	0.76	−5.56	−5.71	−2.20	3.51	3.49
9b	3.15	0.79	−5.59	−5.73	−2.20	3.53	3.51

[a] Estimated from the intersection of normalized absorption and emission spectra. [b] determined from the onset oxidation potential of the CV-spectrum [c] Calculated using the equation: $E(HOMO)^{DPV} = -e[(E_{Ox}$ vs $Fc/Fc^+) + 4.80]$. [c] Calculated DFT and TD-DFT energy levels at the B3LYP/6-311G(d,p) level of theory.

Research Article
doi.org/10.1002/ejoc.202301299

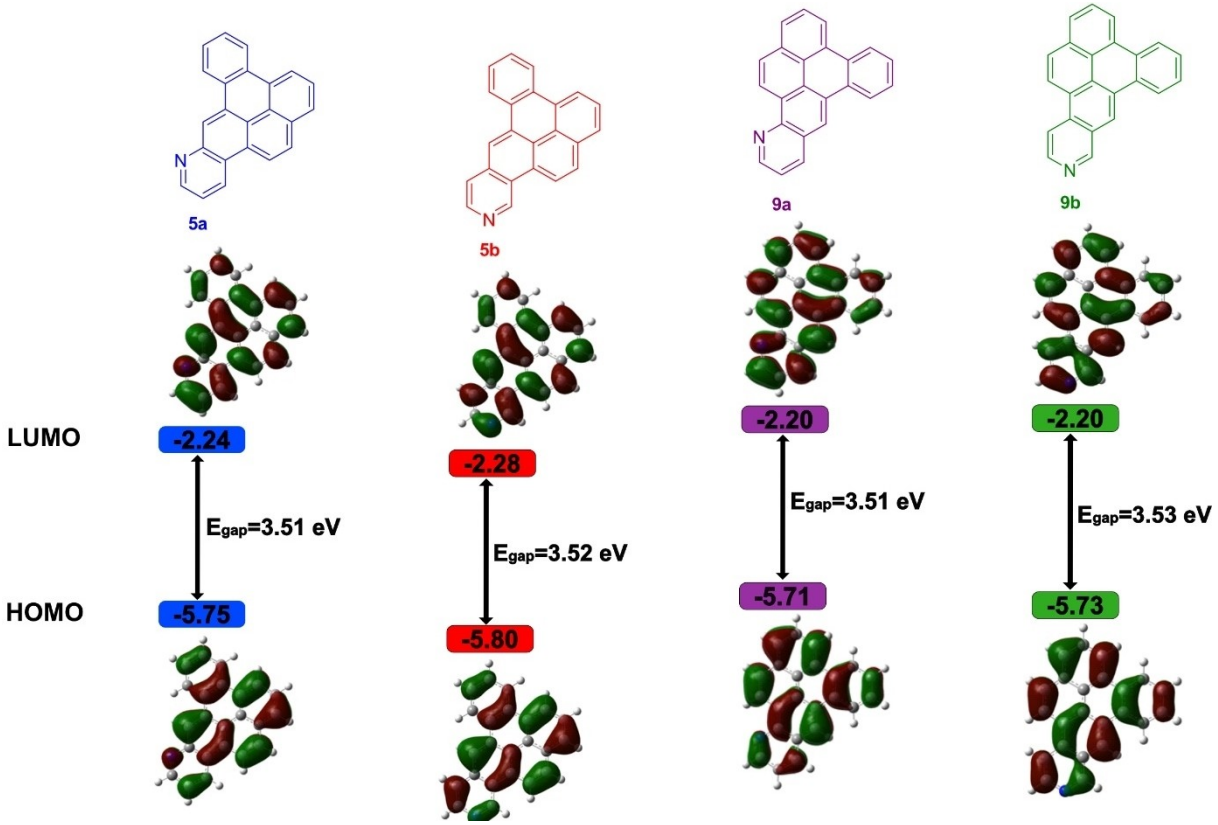

Figure 7. Visualization of HOMO and LUMO with associated energies.

LUMO levels remain relatively consistent across the compounds, with values ranging from 3.51 eV to 3.53 eV. These slight variations can be attributed to the introduction of the nitrogen atom into the scaffold.

NICS calculation and respective ring currents as criteria of aromaticity were obtained to gain further information on the electronic properties on the as-prepared azadibenzopyrene derivates (representatively shown for compound **5 a**; Figure 8 and SI, Figures S5-S7).[24] All rings A–E show aromatic properties in all studied compounds. Only ring C shows slightly reduced aromaticity. Ring currents are visualized by the NICS2BC wizard software developed by Gershoni-Poranne *et al.*.[25] The calculations reflect the result from NICS calculation revealing a strong diatropic global ring current on the entire molecule. Whereas some minor paratropic ring currents can be observed on rings C what explains the lower NICS values of this ring. Hence, an impact on the aromaticity from the different position of Nitrogen-doping cannot be deduced.

Conclusions

In conclusion, we have reported the synthesis of four different isomeric azadibenzo[*a*,*e*]pyrenes (benzo[4,10]anthra[9,1-

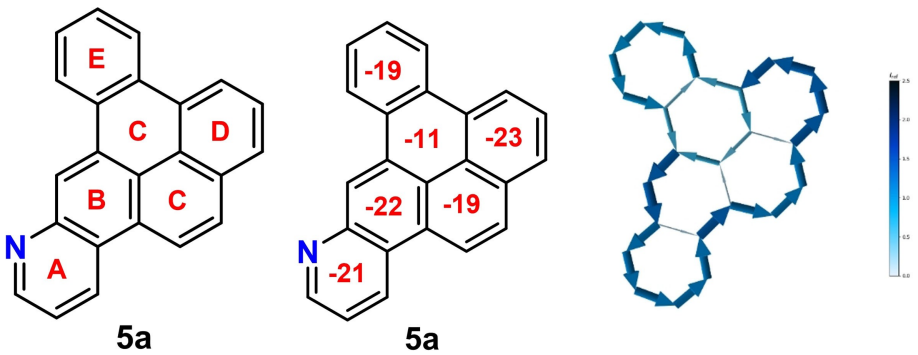

Figure 8. NICS $(1.7)_{zz}$ values and Ring Current of compound **5 a**; left structure of **5 a**, center: **5 a** with NICS$(1.7)_{zz}$ values; right: NICS2BC graph of **5 a** (current was calculated form NICS$(1.25)_{zz}$ strength relative to I_{ref} (ring current of benzene, 11.5 nA T^{-1})).

Research Article
doi.org/10.1002/ejoc.202301299

gh]isoquinolines and benzo[*4,10*]anthra[*1,9-fg*]isoquinolines) by combination of Pd-catalyzed Sonogashira and Suzuki cross-coupling, Brønsted acid mediated cycloisomerization and Pd-catalysed CH-activation reactions. Absorption and emission features of the studied compounds are very similar which were also validated by TD-DFT calculations. Protonation by trifluoroacetic acid strongly affected the absorption and emission properties of the studied compounds, with variations depending on the position of the nitrogen atom within the azadibenzo[*a,e*]pyrene scaffold.

Experimental Section

General Information. The nuclear magnetic resonance spectra ($^1H/^{13}C$ NMR) were recorded on a Bruker AVANCE 300 III, 250 II, or 500. The analyzed chemical shifts δ are referenced to residual solvents signals of the deuterated solvents $CDCl_3$ (δ = 7.26 ppm/77.16 ppm), or DMSO-d_6 (δ = 2.50 ppm/39.52 ppm). Multiplicities due to spin–spin correlation are reported as follows, s = singlet, d = doublet, dd = double doublet, t = triplet, pt = pseudo triplet, m = multiplet, and further described through their coupling constants *J*. Infrared spectra (IR) were measured as attenuated total reflection (ATR) experiments with a Nicolet 380 FT-IR spectrometer. The signals have been characterized through their wave numbers and their corresponding absorption as very strong (vs), strong (s), medium (m), weak (w), or very weak (vw). UV/Vis spectra were recorded on a Cary 60 UV–vis spectrophotometer and emission spectra with an Agilent Cary Eclipse fluorescence spectrophotometer. Cyclovoltammetry (CV) was measured in CH_3CN with 0.1 M nBu_4NPF_6 as supporting electrolyte, glassy carbon working electrode, ANE2 ($Ag/AgNO_3$ 0.01 M in CH_3CN) as reference electrode, and Pt counter electrode with ferrocene as external standard (1 mM in CH_3CN). The potential is given vs Fc^+/Fc. The potentiostat used was a PARSTAT 4000 Potentiostat/Galvanostat/EIS Analyzer. Basic and high-resolution mass spectra (MS/HRMS) were measured on instruments which are paired with a preceding gas chromatograph (GC) or liquid chromatograph (LC). The samples have been ionized through electron impact ionization (EI) on an Agilent 6890/5973 or Agilent 7890/5977 GC-MS equipped with a HP-5 capillary column using helium carrier gas or by applying electron spray ionization (ESI) on an Agilent 1200/6210 Time-of-Flight (TOF) LC–MS. X-ray single-crystal structure analysis was performed on a Bruker Apex Kappa-II CCD diffractometer.

Materials. The applied solvents, 1,4-Dioxane, N-Methyl-2-pyrrolidone, DMA, DCM were obtained as dry solvents through commercial sources and employed without further purification. Solvents for extraction and column chromatography were available after previous distillation. If not otherwise stated all reagents such as 1-chloro-2-ethynylbenzene, 2-naphthaleneboronic acid, methanesulfonic acid, catalysts, ligands and bases were purchased and used without further purification. Column chromatography was performed using a Merck Silica gel 60 (particle size 63–200 μm).

General procedure for the synthesis of benzo[4,10]anthra[9,1-*gh*]isoquinoline 5a-b, 9a. In a pressure tube under an inert atmosphere were added **4a**, **4b** or **8a** (109-390 mg, 1.0 equiv.), $PdCl_2$ (0.2 equiv.), PCy_3 (0.4 equiv.), DBU (3.0 equiv.) and NMP. The reaction was carried out in a pressure tube and heated in a metal block at 150°C for 18 h. The solution was diluted with distilled water and extracted three times with a dichloromethane, then extracted five to six times with distilled water to remove NMP. The organic layer was dried with sodium sulfate, filtered, and concentrated *in vacuo*. The residue was purified by column chromatography (Heptane/EtOAc = 3 : 1).

Benzo[4,10]anthra[1,9-*fg*]quinoline (5a). Starting with **4a** (120 mg, 0.35 mmol), **5a** was isolated as a yellow solid (83 mg, 78%); mp.: 215–218 °C. ^1H NMR (300 MHz, DMSO-d_6/TFA) δ 9.06 (dd, *J* = 42.6, 6.9 Hz, 2H), 8.31 – 7.03 (m, 11H). $^{13}C\{1H\}$ NMR (75 MHz, DMSO-d_6/TFA) δ 143.9, 140.4, 129.9, 129.7, 127.4, 120.6. MS (GC): m/z (%) = 305 (3), 304 (24), 303 (M+, $C_{23}H_{13}N$, 100), 302 (11), 301 (14), 300 (2). HRMS (ESI-TOF) m/z: $[M+H]^+$ calcd for $C_{23}H_{14}N$ 304.1126, found 304.1129. IR (ATR): ν̃ = 2922 (m), 2852 (m), 1595 (m), 1513 (m), 1480 (w), 1455 (m), 1426 (m), 1405 (m), 1381 (m), 1313 (m), 1257 (m), 1150 (m), 1071 (m).

Benzo[4,10]anthra[9,1-*gh*]isoquinoline (5b). Starting with **4b** (109 mg, 0.32 mmol), **5b** was isolated as a yellow solid (76 mg, 88%); mp.: 148–150 °C. ^1H NMR (300 MHz, DMSO-d_6) δ 10.51 (s, 1H), 9.44 (s, 1H), 9.35 (d, *J* = 9.1 Hz, 1H), 9.04 (t, *J* = 7.4 Hz, 2H), 8.97 – 8.77 (m, 2H), 8.44 (dd, *J* = 24.4, 8.4 Hz, 2H), 8.24 (d, *J* = 5.6 Hz, 1H), 8.10 (t, *J* = 7.8 Hz, 1H), 7.85 – 7.79 (m, 2H), 5.75 (s, 1H).$^{13}C\{1H\}$ NMR (75 MHz, DMSO-d6) δ 148.1, 143.4, 133.5, 131.3, 130.9, 130.3, 129.2, 129.1, 128.6, 128.3, 127.3, 126.9, 124.7, 124.0, 123.5, 122.7, 121.5, 121.2, 120.9, 118.8. MS (GC): m/z (%) = 305 (2), 304 (28), 303 (M+, $C_{23}H_{13}N$, 100), 302 (10), 301 (18), 300 (3). HRMS (ESI-TOF) m/z: [M+H]+ calcd for $C_{23}H_{14}N$ 304.1126, found 304.1127. IR (ATR): ν̃ = 2924 (m), 2850 (m), 1601 (m), 1422 (w), 1344 (w), 1257 (m), 1148 (w), 1018 (m), 948 (w).

Benzo[4,10]anthra[9,1-*gh*]quinoline (9a). Starting with **8a** (390 mg, 1.15 mmol), **9a** was isolated as a yellow solid (212 mg, 61%); mp.: 206–208 °C. ^1H NMR (300 MHz, DMSO-d_6) δ 9.60 (d, *J* = 9.0 Hz, 1H), 9.40 (s, 1H), 9.23 (dd, *J* = 4.2, 1.8 Hz, 1H), 9.04 – 8.77 (m, 4H), 8.39 (dd, *J* = 16.7, 8.4 Hz, 2H), 8.10 (t, *J* = 7.8 Hz, 1H), 7.86 – 7.76 (m, 3H). $^{13}C\{1H\}$ NMR (75 MHz, DMSO-d_6) δ 149.2, 142.4, 136.0, 131.7, 129.7, 129.2, 128.7, 128.0, 127.9, 127.7, 127.3, 127.2, 126.49, 126.48, 125.1, 123.9, 123.8, 123.5, 123.3, 122.2, 121.5, 120.4, 119.2. MS (GC): m/z (%) = 305 (4), 304 (30), 303 (M+, $C_{23}H_{13}N$, 100), 302 (12), 301 (16), 300 (3), 299 (3). HRMS (ESI-TOF) m/z: [M+H]+ calcd for $C_{23}H_{14}N$ 304.1126, found 304.1132. IR (ATR): ν̃ = 3039 (m), 1593 (m), 1572 (m), 1508 (m), 1477 (m), 1428 (m), 1318 (m), 1300 (m), 1201 (m), 1158 (m), 1028 (w).

Synthesis of benzo[4,10]anthra[1,9-*fg*]isoquinoline (9b). In a pressure tube under an inert atmosphere were added **8b** (120 mg, 1.0 equiv.), $PdCl_2$ (0.4 equiv.), PCy_3 (0.8 equiv.), DBU (6.0 equiv.) and NMP. The reaction was carried out in a pressure tube and heated in a metal block at 150 °C for 18 h. The solution was diluted with distilled water and extracted three times with dichloromethane, then extracted five to six times with distilled water to remove NMP. The organic layer was dried with sodium sulfate, filtered, and concentrated *in vacuo*. The residue was purified by column chromatography (Heptane/EtOAc = 2 : 1). Starting with **8b** (120 mg, 0.35 mmol), **9b** was isolated as a yellow solid (46 mg, 46%); mp.: 199–201 °C. ^1H NMR (300 MHz, DMSO-d6) δ 9.68 (s, 1H), 9.37 (s, 1H), 8.99 – 8.80 (m, 3H), 8.76 (dt, *J* = 9.8, 5.9 Hz, 3H), 8.34 – 8.22 (m, 2H), 8.03 (t, *J* = 7.8 Hz, 1H), 7.78 – 7.69 (m, 2H).$^{13}C\{1H\}$ NMR (75 MHz, DMSO-d_6) δ 152.5, 142.9, 131.7, 130.4, 129.4, 129.1, 128.8, 128.0, 127.8, 127.6, 126.7, 126.4, 125.5, 125.3, 124.0, 123.7, 123.3, 123.2, 121.2, 120.4, 118.8, 115.2. MS (GC): m/z (%) = 305 (3), 304 (24), 303 (M+, $C_{23}H_{13}N$, 100), 302 (11), 301 (14), 300 (2). MS (GC): m/z (%) = 308 (9), 307 (8), 306 (13), 305 (28), 304 (71), 303 (M+, C23H13 N, 86), 302 (33), 301 (52), 300 (9). HRMS (ESI-TOF) m/z: $[M+H]^+$ calcd for $C_{23}H_{14}N$ 304.1126, found 304.1122. IR (ATR): ν̃ = 2961 (w), 2922 (m), 2852 (w), 1578 (m), 1463 (m), 1436 (w), 1401 (w), 1259 (s), 1086 (s), 1014 (s).

Supporting Information Statement

Single crystal X-ray data, optical, cv-data, computational details, experimental procedures and data, ^{1}H-, ^{19}F- and ^{13}C-NMR spectra of isolated compounds

Accession Codes

Deposition Numbers 2295828 (for **4a**) and 2295829 (for **9a**), contain the supplementary crystallographic data for this paper. These data can be obtained free of charge by the joint Cambridge Crystallographic Data Ventre and Fachinformationszentrum Karlsruhe Access Structures Service http://www.ccdc.cam.ac.uk/structures.

Acknowledgements

Financial support by the State of Mecklenburg-Vorpommern (stipend for A. K.) is gratefully acknowledged.

Conflict of Interests

The authors declare no conflict of interest.

Data Availability Statement

The data that support the findings of this study are available in the supplementary material of this article.

Keywords: catalysis · heterocycles · palladium · regioselectivity

[1] a) G. Ouyang, J. Rühe, Y. Zhang, M.-J. Lin, M. Liu, F. Würthner, *Angew. Chem. Int. Ed.* **2022**, *134*, e202206706; b) Z.-P. Yan, L. Yuan, Y. Zhang, M.-X. Mao, X.-J. Liao, H.-X. Ni, Z.-H. Wang, Z. An, Y.-X. Zheng, J.-L. Zuo, *Adv. Mater.* **2022**, *34*, e2204253; c) H. Zhang, J. Han, X. Jin, P. Duan, *Angew. Chem. Int. Ed.* **2021**, *133*, 4625–4630.

[2] a) C. Cebrián, *J. Mater. Chem. C* **2018**, *6*, 11943–11950; b) C. L. Chochos, A. Avgeropoulos, E. Lidorikis, *J. Chem. Phys.* **2013**, *138*, 064901–1-064901-6; c) J. Huang, Y. Li, *Front. Chem.* **2018**, *6*, 341; d) L. Ma, Y. Han, Q. Shi, H. Huang, *J. Mater. Chem. C* **2023**, *11*, 16429–16438; e) K. Zhang, J. Guo, H. Liu, X. Wang, Y. Yao, K. Yang, Z. Zeng, *Chem. Commun.* **2023**, *59*, 4947–4950.

[3] a) X.-F. Luo, H.-X. Ni, A.-Q. Lv, X.-K. Yao, H.-L. Ma, Y.-X. Zheng, *Adv. Opt. Mater.* **2022**, *10*; b) S. M. Elbert, M. Reinschmidt, K. Baumgärtner, F. Rominger, M. Mastalerz, *Eur. J. Org. Chem.* **2018**, *2018*, 532–536; c) U. H. F. Bunz, *Acc. Chem. Res.* **2015**, *48*, 1676–1686; d) P. Qiang, Z. Sun, M. Wan, X. Wang, P. Thiruvengadam, C. Bingi, W. Wei, W. Zhu, D. Wu, F. Zhang, *Org. Lett.* **2019**, *21*, 4575–4579.

[4] C. Wang, H. Dong, W. Hu, Y. Liu, D. Zhu, *Chem. Rev.* **2012**, *112*, 2208–2267.

[5] a) A. Borissov, Y. K. Maurya, L. Moshniaha, W.-S. Wong, M. Żyła-Karwowska, M. Stępień, *Chem. Rev.* **2022**, *122*, 565–788; b) M. Schaffroth, B. D. Lindner, V. Vasilenko, F. Rominger, U. H. F. Bunz, *J. Org. Chem.* **2013**, *78*, 3142–3150; c) W. Jiang, Y. Li, Z. Wang, *Chem. Soc. Rev.* **2013**, *42*, 6113–6127; d) S. Kilaru, R. Gade, Y. bhongiri, A. Tripathi, P. Chetti, S. Pola, *Mater. Sci. Semicond. Process.* **2022**, *147*, 106730; e) Y. Yuan, J.-X. Chen, F. Lu, Q.-X. Tong, Q.-D. Yang, H.-W. Mo, T.-W. Ng, F.-L. Wong, Z.-Q. Guo, J. Ye et al., *Chem. Mater.* **2013**, *25*, 4957–4965.

[6] a) Y. Shirota, H. Kageyama, *Chem. Rev.* **2007**, *107*, 953–1010; b) J. E. Anthony, *Angew. Chem. Int. Ed.* **2008**, *47*, 452–483; c) T. M. Figueira-Duarte, K. Müllen, *Chem. Rev.* **2011**, *111*, 7260–7314; d) S. Karuppannan, J.-C. Chambron, *Chem. Asian J.* **2011**, *6*, 964–984; e) X. Feng, J.-Y. Hu, H. Tomiyasu, N. Seto, C. Redshaw, M. R. J. Elsegood, T. Yamato, *Org. Biomol. Chem.* **2013**, *11*, 8366–8374; f) Y. Zhang, T.-W. Ng, F. Lu, Q.-X. Tong, S.-L. Lai, M.-Y. Chan, H.-L. Kwong, C.-S. Lee, *Dyes Pigm.* **2013**, *98*, 190–194; g) A. O. El-Ballouli, R. S. Khnayzer, J. C. Khalife, A. Fonari, K. M. Hallal, T. V. Timofeeva, D. Patra, F. N. Castellano, B. Wex, B. R. Kaafarani, *J. Photochem. Photobiol. A* **2013**, *272*, 49–57; h) J. M. Casas-Solvas, J. D. Howgego, A. P. Davis, *Org. Biomol. Chem.* **2014**, *12*, 212–232; i) Y. Niko, H. Moritomo, H. Sugihara, Y. Suzuki, J. Kawamata, G.-I. Konishi, *J. Mater. Chem. B* **2015**, *3*, 184–190; j) X. Feng, J.-Y. Hu, C. Redshaw, T. Yamato, *Chem. Eur. J.* **2016**, *22*, 11898–11916.

[7] a) M. Inouye, K. Fujimoto, M. Furusyo, H. Nakazumi, *J. Am. Chem. Soc.* **1999**, *121*, 1452–1458; b) P. Somerharju, *Chem. Phys. Lipids* **2002**, *116*, 57–74; c) H. Abe, Y. Mawatari, H. Teraoka, K. Fujimoto, M. Inouye, *J. Org. Chem.* **2004**, *69*, 495–504; d) I. V. Astakhova, V. A. Korshun, J. Wengel, *Chem. Eur. J.* **2008**, *14*, 11010–11026; e) M. Endo, H. Sugiyama, *ChemBioChem* **2009**, *10*, 2420–2443; f) M. Printz, C. Richert, *Chem. Eur. J.* **2009**, *15*, 3390–3402; g) M. E. Østergaard, P. J. Hrdlicka, *Chem. Soc. Rev.* **2011**, *40*, 5771–5788; h) J. Wu, Y. Zou, C. Li, W. Sicking, I. Piantanida, T. Yi, C. Schmuck, *J. Am. Chem. Soc.* **2012**, *134*, 1958–1961.

[8] a) S. Geib, S. C. Martens, U. Zschieschang, F. Lombeck, H. Wadepohl, H. Klauk, L. H. Gade, *J. Org. Chem.* **2012**, *77*, 6107–6116; b) W.-C. Chen, I. Chao, *J. Phys. Chem. C* **2014**, *118*, 20176–20183; c) B. Feng, D. Wan, L. Yan, V. D. Kadam, J. You, G. Gao, *RSC Adv.* **2016**, *6*, 66407–66411; d) T. Nakazato, T. Kamatsuka, J. Inoue, T. Sakurai, S. Seki, H. Shinokubo, Y. Miyake, *Chem. Commun.* **2018**, *54*, 5177–5180; e) Y. Han, Z. Hu, M. Liu, M. Li, T. Wang, Y. Chen, *J. Org. Chem.* **2019**, *84*, 3953–3959.

[9] a) P. H. Dinolfo, M. E. Williams, C. L. Stern, J. T. Hupp, *J. Am. Chem. Soc.* **2004**, *126*, 12989–13001; b) M. Vybornyi, A. V. Rudnev, S. M. Langenegger, T. Wandlowski, G. Calzaferri, R. Häner, *Angew. Chem. Int. Ed.* **2013**, *52*, 11488–11493; c) V. Balzani, A. Credi, S. J. Langford, F. M. Raymo, J. F. Stoddart, M. Venturi, *J. Am. Chem. Soc.* **2000**, *122*, 3542–3543; d) J. Sun, Z. Liu, W.-G. Liu, Y. Wu, Y. Wang, J. C. Barnes, K. R. Hermann, W. A. Goddard, M. R. Wasielewski, J. F. Stoddart, *J. Am. Chem. Soc.* **2017**, *139*, 12704–12709; e) H.-C. Becker, B. Nordén, *J. Am. Chem. Soc.* **1997**, *119*, 5798–5803; f) S. Marczi, L. Glavas-Obrovac, I. Karner, *Chemotherapy* **2005**, *51*, 217–222; g) I. Piantanida, M. Žinić, S. Marczi, L. Glavaš-Obrovac, *J. Phys. Org. Chem.* **2007**, *20*, 285–295.

[10] a) R. H. F. Manske, A. Brossi, *The Alkaloids: Chemistry and Pharmacology V25. Chemistry and Pharmacology V25*, Elsevier textbooks, s.l., **1985**; b) I. Azad, R. Ahmad, T. Khan, M. Saquib, F. Hassan, Y. Akhter, A. R. Khan, M. Nasibullah, *Future Med. Chem.* **2020**, *12*, 709–739; c) T. Ishikawa, *Med. Res. Rev.* **2001**, *21*, 61–72; d) R. Shi, H. Niu, L. Lu, A. Lei, *Chem. Commun.* **2017**, *53*, 1908–1911; e) V. Talukdar, A. Vijayan, N. Kumar Katari, K. V. Radhakrishnan, P. Das, *Adv. Synth. Catal.* **2021**, *363*, 1202–1245; f) F. Stuck, M. C. Dietl, M. Meißner, F. Sebastian, M. Rudolph, F. Rominger, P. Krämer, A. S. K. Hashmi, *Angew. Chem. Int. Ed.* **2022**, *61*, e202114277.

[11] R. Kirchlechner, C. Jutz, *Angew. Chem. Int. Ed.* **1968**, *7*, 376–377.

[12] a) R. Molenda, S. Boldt, A. Villinger, P. Ehlers, P. Langer, *J. Org. Chem.* **2020**, *85*, 12823–12842; b) A. Vardanyan, S. Boldt, A. Villinger, P. Ehlers, P. Langer, *J. Org. Chem.* **2022**, *87*, 11296–11308; c) R. Molenda, J. Polkaehn, M. A. Argüello Cordero, A. Villinger, P. Ehlers, S. Lochbrunner, P. Langer, *J. Org. Chem.* **2023**, *88*, 8802–8824.

[13] W. Han, X. Zhou, S. Yang, G. Xiang, B. Cui, Y. Chen, *J. Org. Chem.* **2015**, *80*, 11580–11587.

[14] a) G. G. Gerosa, S. A. Schwengers, R. Maji, C. K. De, B. List, *Angew. Chem. Int. Ed.* **2020**, *59*, 20485–20488; b) F. Spruner von Mertz, R. Molenda, S. Boldt, A. Villinger, P. Ehlers, P. Langer, *Chem. Eur. J.* **2023**, *29*, e202204011; c) K. P. Kawahara, W. Matsuoka, H. Ito, K. Itami, *Angew. Chem. Int. Ed.* **2020**, *132*, 6445–6450; d) K. Fujishiro, Y. Morinaka, Y. Ono, T. Tanaka, L. T. Scott, H. Ito, K. Itami, *J. Am. Chem. Soc.* **2023**, *145*, 8163–8175.

[15] a) B. Schiedt, *Chem. Ber.* **1938**, *71*, 1248–1253; b) A. Zinke, W. Zimmer, *Monatsh. Chem.* **1950**, *81*, 783–785.

[16] a) A. N. Shestakov, A. S. Pankova, M. A. Kuznetsov, *Chem. Heterocycl. Compd.* **2017**, *53*, 1103–1113; b) P. Langer, *Synlett* **2022**, *33*, 1707–1715.

[17] H.-I. Chang, H.-T. Huang, C.-H. Huang, M.-Y. Kuo, Y.-T. Wu, *Chem. Commun.* **2010**, *46*, 7241–7243.

[18] X.-C. Chen, S. Nishinaga, Y. Okuda, J.-J. Zhao, J. Xu, H. Mori, Y. Nishihara, *Org. Chem. Front.* **2015**, *2*, 536–541.

[19] M. J. Frisch, G. W. Trucks, H. B. Schlegel, G. E. Scuseria, M. A. Robb, J. R. Cheeseman, G. Scalmani, V. Barone, B. Mennucci, G. A. Petersson, H.

Nakatsuji, M. Caricato, X. Li, X. Hratchian, A. F. Izmaylov, J. Bloino, G. Zheng, J. L. Sonnenberg, M. Hada, M. Ehara, K. Toyota, R. Fukuda, J. Hasegawa, M. Ishida, T. Nakajima, Y. Honda, O. Kitao, H. Nakai, T. Vreven, J. A. Montgomery, J. E. Peralta, F. Ogliaro, M. Bearpark, J. J. Heyd, E. Brothers, K. N. Kudin, V. N. Staroverov, R. Kobayashi, J. Normand, K. Raghavachari, A. Rendell, J. C. Burant, S. Iyengar, J. Tomasi, M. Cossi, N. Rega, J. M. Millam, M. Klene, J. E. Knox, J. B. Cross, V. Bakken, C. Adamo, J. Jaramillo, R. Gomperts, R. E. Stratmann, O. Yazyev, A. J. Austin, R. Cammi, C. Pomelli, J. W. Ochterski, R. L. Martin, K. Morokuma, V. G. Zakrzewski, G. A. Voth, P. Salvador, J. J. Dannenberg, S. Dapprich, A. D. Daniels, O. Farkas, J. B. Foresman, J. V. Ortiz, J. Cioslowski, D. J. Fox, *Gaussian 09*, Gaussian, Inc.:, Wallingford, CT, **2013**.

[20] K. F. Lang, M. Zander, *Chem. Ber.* **1965**, *98*, 597–600.

[21] Albert M. Brouwer, *Pure Appl. Chem.* **1351**, *83*, 2213–2228.

[22] a) C. Reichardt, *Angew. Chem. Int. Ed.* **1965**, *4*, 29–40; b) C. Reichardt, *Chem. Rev.* **1994**, *94*, 2319–2358.

[23] E. S. Pysh, N. C. Yang, *J. Am. Chem. Soc.* **1963**, *85*, 2124–2130.

[24] a) R. Gershoni-Poranne, A. Stanger, *Chem. Eur. J.* **2014**, *20*, 5673–5688; b) P. v. R. Schleyer, C. Maerker, A. Dransfeld, H. Jiao, N. J. R. van Eikema Hommes, *J. Am. Chem. Soc.* **1996**, *118*, 6317–6318.

[25] E. Paenurk, R. Gershoni-Poranne, *Phys. Chem. Chem. Phys.* **2022**, *24*, 8631–8644.

Manuscript received: December 20, 2023
Revised manuscript received: March 1, 2024
Accepted manuscript online: March 4, 2024
Version of record online: ■■, ■■

RESEARCH ARTICLE

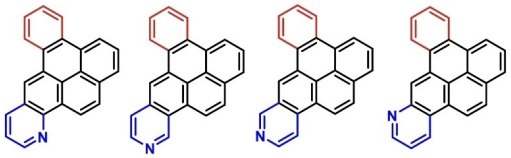

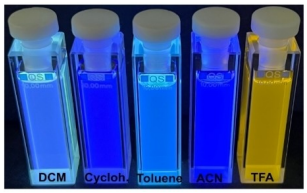

*A. Khomutetckaia, P. Ehlers, A. Villinger, P. Langer**

1 – 11

Synthesis and Properties of Azadibenzo[*a,e*]pyrenes

Four different isomeric azadibenzo-[*a,e*]pyrenes are prepared by combination of Pd-catalyzed Sonogashira and Suzuki cross-coupling, Brønsted acid mediated cycloisomerization and Pd-catalysed CH-activation reactions. The optical and electrochemical properties are studied by experimental and theoretical methods.

Appendix

Additional Analytical Data of Unpublished Compounds

Applications in the synthesis of benzo[4',5']thieno[2',3':3,4]-naphthobenzofurans

The paragraph presented here is work in collaboration with my colleague Dr. Erich Ammon as a continuing project on the Pd-catalyzed intramolecular cyclization of ortho-bromo(hetero)aryl-substituted (hetero)aryl-1,2-diketones and its application to the synthesis of carba- and heterocyclic benzoin derivatives (manuscript II).

Since some of the compounds have not yet been published, the synthesis scheme and the analytical data for each of them can be found in the following section.

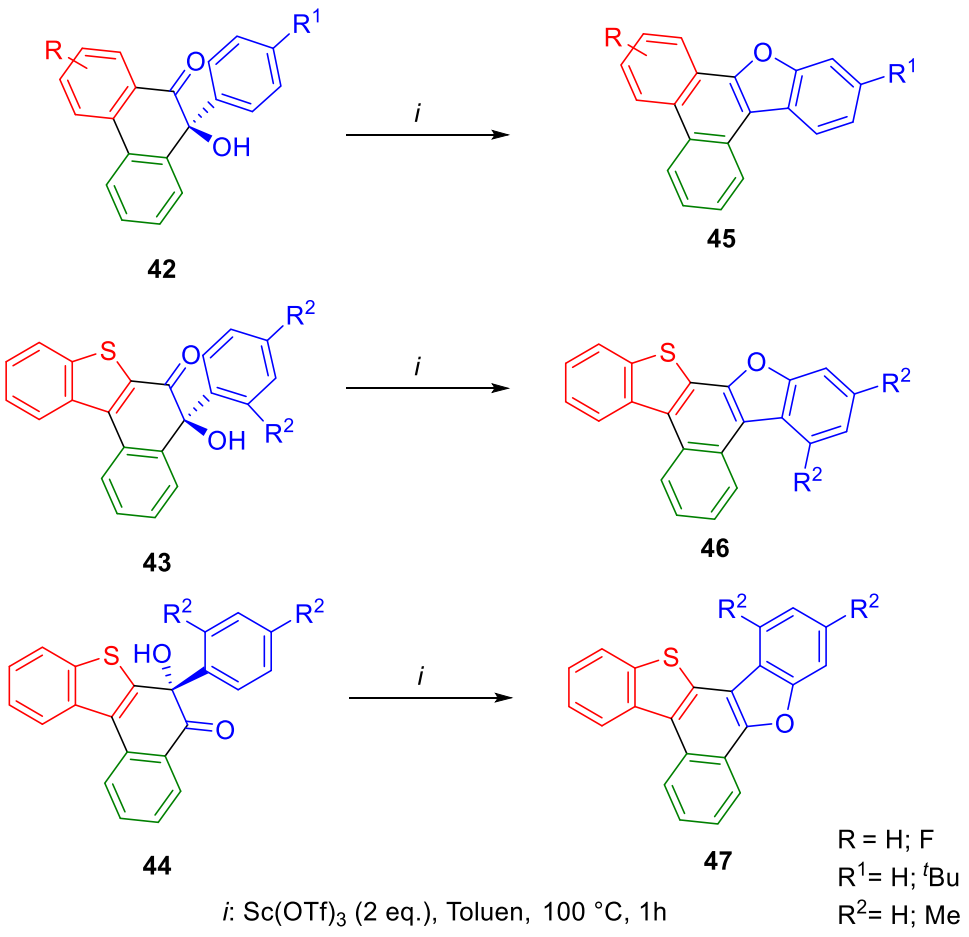

Scheme 19. Synthesis of benzo[4',5']thieno[2',3':3,4]naphtho[2,1-*b*]benzofurans and benzo[4',5']-thieno[2',3':3,4]naphtho[1,2-*b*]benzofurans.

(*S*)-10-hydroxy-10-phenylphenanthren-9(10*H*)-one **42**, (*S*)-5-hydroxy-5-phenylbenzo[*b*]naphtho[1,2-*d*]thiophen-6(5*H*)-one **43** and its regioisomer **44** were prepared as previously reported (manuscript II) by Sonogashira reaction of 1,2-dibromobenzothiophene with phenylacetylene, oxidation of the alkyne to 1,2-diketone and subsequent cyclization with (2-bromophenyl)boronic acid. Treatment of substances **42-44** with $Sc(OTf)_3$ afforded products **45-47** in yields ranging from 11-73%.

6,7-difluorophenanthro[9,10-*b*]benzofuran (45a)

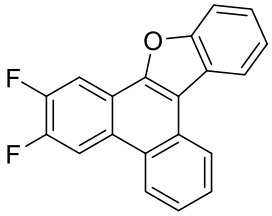

Starting with **42a** (100 mg, 0.31 mmol) and $Sc(OTf)_3$ (153 mg, 0.31mmol), **45a** was isolated as a colourless solid (65 mg, 69%); mp: 169-171 °C. ^{1}H NMR (500 MHz, DMSO-d6) δ 9.00 (s, 1H, H_{Ar}), 8.88 (d, J = 8.1 Hz, 1H, H_{Ar}), 8.72 (d, J = 7.8 Hz, 1H, H_{Ar}), 8.59 (d, J = 18.0 Hz, 1H, H_{Ar}), 8.40 (d, J = 7.3 Hz, 1H, H_{Ar}), 8.29 (s, 1H, H_{Ar}), 7.93 – 7.68 (m, 2H, H_{Ar}), 7.62 – 7.49 (m, 1H, H_{Ar}). ^{13}C NMR (126 MHz, DMSO-d_6) δ 154.6 (C_{Ar}), 154.5 (C_{Ar}), 150.4 (C_{Ar}), 128.0 (CH_{Ar}), 127.7 (CH_{Ar}), 127.4 (CH_{Ar}), 126.0 (d, J = 10.8 Hz, CH_{Ar}), 125.4 (C_{Ar}), 124.2 (d, J = 19.5 Hz, CH_{Ar}), 123.9 – 123.4 (m, CH_{Ar}), 121.6 (d, J = 34.0 Hz, CH_{Ar}), 120.67 (C_{Ar}), 114.0 (C_{Ar}), 112.2 (d, J = 23.3 Hz, CH_{Ar}), 111.5 (d, J = 8.7 Hz, CH_{Ar}), 111.0 (d, J = 18.7 Hz, CH_{Ar}). ^{19}F NMR (471 MHz, DMSO-d_6) δ -136.3 (d, J = 116.1 Hz, CF), -139.0 (d, J = 22.9 Hz, CF). MS (GC): m/z (%) = 304 ($C_{20}H_{10}F_2O$, 100), 275 (24). HRMS (ESI): calcd for $C_{20}H_{10}F_2O$, 304.0694, found 304.0694. IR (ATR): $\tilde{\nu}$ = 2919 (m), 2851 (m), 1528 (m), 1454 (m), 1364 (m), 1267 (m), 1201 (m), 1149 (s), 1024 (s), 997 (s).

11-(tert-butyl)phenanthro[9,10-*b*]benzofuran (45b)

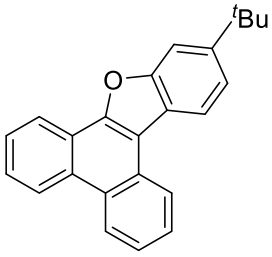

Starting with **42b** (100 mg, 0.29 mmol) and $Sc(OTf)_3$ (287 mg, 0.58 mmol), **45b** was isolated as a colourless solid (30 mg, 32%); mp: 139-141 °C. ^{1}H NMR (300 MHz, DMSO-d_6) δ 8.98 – 8.93 (m, 2H, H_{Ar}), 8.71 (dd, J = 8.2, 1.4 Hz, 1H, H_{Ar}), 8.46 – 8.40 (m, 2H, H_{Ar}), 7.89 (d, J = 1.7 Hz, 1H. H_{Ar}), 7.85 (s, 1H, H_{Ar}), 7.83 – 7.70 (m, 3H, H_{Ar}), 7.56 (dd, J = 8.4, 1.7 Hz, 1H, H_{Ar}), 1.41 (s, 9H, ^{t}Bu). ^{13}C NMR (75 MHz, DMSO-d_6) δ 155.6 (C_{Ar}), 150.2 (C_{Ar}), 149.7 (C_{Ar}), 129.8 (C_{Ar}), 128.0 (CH_{Ar}), 127.7 (CH_{Ar}), 127.6 (CH_{Ar}), 127.5 (CH_{Ar}), 125.6 (CH_{Ar}), 124.2 (CH_{Ar}), 124.0 (CH_{Ar}), 122.0 (C_{Ar}), 121.4 (CH_{Ar}), 120.9 (CH_{Ar}), 113.8 (C_{Ar}), 108.7 (CH_{Ar}), 34.9 (C), 31.4 (^{t}Bu). MS (GC): m/z (%) = 324 ($C_{24}H_{20}O$, 69), 309 (100), 281 (23). HRMS (ESI): calcd for $C_{24}H_{20}O$, 324.1508, found 324.1513. IR (ATR): $\tilde{\nu}$ =

2959 (m), 1685 (s), 1650 (m), 1617 (s), 1599 (s), 1493 (m), 1448 (s), 1337 (s), 1267 (s), 1188 (s).

11-methylbenzo[4',5']thieno[2',3':3,4]naphtho[2,1-*b*]benzofuran (46a)

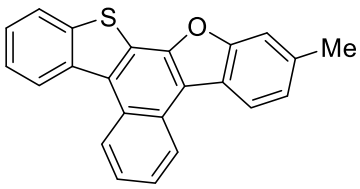

Starting with **43a** (100 mg, 0.28 mmol) and $Sc(OTf)_3$ (276 mg, 0.56 mmol), **46a** was isolated as a colourless solid (54 mg, 57%); mp: 213-215 °C. ^{1}H NMR (250 MHz, DMSO-d_6) δ 9.20 (d, J = 8.4 Hz, 1H, H_{Ar}), 8.98 (d, J = 8.2 Hz, 1H, H_{Ar}), 8.61 – 8.52 (m, 1H, H_{Ar}), 8.24 (d, J = 8.0 Hz, 1H, H_{Ar}), 8.03 (d, J = 7.9 Hz, 1H, H_{Ar}), 7.95 – 7.65 (m, 4H, H_{Ar}), 7.59 (t, J = 7.5 Hz, 1H, H_{Ar}), 7.42 (d, J = 7.9 Hz, 1H, H_{Ar}), 2.59 (s, 3H, CH_3). ^{13}C NMR (63 MHz, DMSO-d_6) δ 155.5 (C_{Ar}), 136.8 (C_{Ar}), 135.3 (C_{Ar}), 127.1 (CH_{Ar}), 125.3 (CH_{Ar}), 124.7 (CH_{Ar}), 124.5 (CH_{Ar}), 123.6 (CH_{Ar}), 123.4 (CH_{Ar}), 121.1 (CH_{Ar}), 119.7 (CH_{Ar}), 111.6 (CH_{Ar}), 20.7 (CH_3). MS (GC): m/z (%) = 338 ($C_{23}H_{14}OS$, 100), 308 (7), 169 (11). HRMS (ESI): calcd for $C_{23}H_{14}OS$, 338.0759, found 338.0759. IR (ATR): $\tilde{\nu}$ = 2917 (m), 1580 (m), 1446 (m), 1362 (m), 1345 (m), 1228 (s), 1193 (m), 1055 (s), 803 (s).

9-methylbenzo[4',5']thieno[2',3':3,4]naphtho[2,1-*b*]benzofuran (46b)

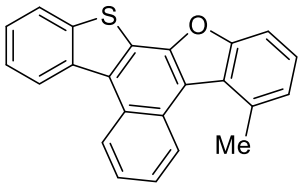

Starting with **43b** (100 mg, 0.28 mmol) and $Sc(OTf)_3$ (276 mg, 0.56 mmol), **46b** was isolated as a colourless solid (61 mg, 64%); mp: 199-201 °C. ^{1}H NMR (250 MHz, DMSO-d6) δ 9.27 – 9.21 (m, 1H, H_{Ar}), 9.02 (d, J = 8.4 Hz, 1H, H_{Ar}), 8.94 – 8.83 (m, 1H, H_{Ar}), 8.42 (d, J = 7.4 Hz, 1H, H_{Ar}), 8.25 (d, J = 7.6 Hz, 1H, H_{Ar}), 7.91 – 7.81 (m, 2H, H_{Ar}), 7.77 – 7.60 (m, 2H, H_{Ar}), 7.52 – 7.40 (m, 2H, H_{Ar}), 2.71 (s, 3H, CH_3).^{13}C NMR (63 MHz, DMSO-d6) δ 154.0 (C_{Ar}), 138.6 (C_{Ar}), 135.7 (C_{Ar}), 129.4 (C_{Ar}), 127.0 (CH_{Ar}), 125.9 (CH_{Ar}), 125.4 (CH_{Ar}), 125.2 (CH_{Ar}), 124.3 (CH_{Ar}), 124.1 (CH_{Ar}), 123.7 (CH_{Ar}), 123.6 (CH_{Ar}), 123.3 (CH_{Ar}), 121.3 (C_{Ar}), 119.1 (CH_{Ar}), 115.4 (C_{Ar}), 14.1 (CH_3). MS (GC): m/z (%) = 324 ($C_{23}H_{14}OS$, 100), 308 (9), 169 (8). HRMS (ESI): calcd for $C_{23}H_{14}OS$, 338.0759, found 338.0757. IR (ATR): $\tilde{\nu}$ = 2919 (m), 2851 (m), 1543 (m), 1528 (m), 1448 (m), 1341 (m), 1259 (m), 1219 (m), 772 (s), 735 (vs).

3-methylbenzo[4',5']thieno[2',3':3,4]naphtho[1,2-*b*]benzofuran (47a)

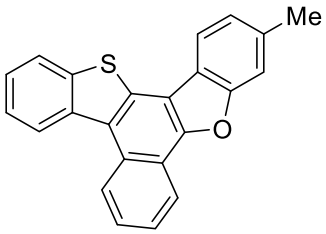

Starting with **44a** (100 mg, 0.28 mmol) and $Sc(OTf)_3$ (276 mg, 0.56 mmol), **47a** was isolated as a colourless solid (69 mg, 73%); mp: 214-216 °C. ^{1}H NMR (250 MHz, DMSO-d6, 100°C) δ 9.18 (d, J = 8.8 Hz, 1H, H_{Ar}), 8.95 (d, J = 8.2 Hz, 2H, H_{Ar}), 8.55 (d, J = 6.8 Hz, 1H, H_{Ar}), 8.21 (d, J = 7.6 Hz, 1H, H_{Ar}), 8.01 (d, J = 7.9 Hz, 1H, H_{Ar}), 7.95 – 7.62 (m, 3H, H_{Ar}), 7.61 – 7.55 (m, 1H, H_{Ar}), 7.40 (d, J = 7.9 Hz, 1H, H_{Ar}), 2.58 (s, 3H, CH_3). ^{13}C NMR (63 MHz, DMSO-d_6, 100°C) δ 155.4 (C_{Ar}), 150.0 (C_{Ar}), 138.0 (C_{Ar}), 136.7 (C_{Ar}), 135.2 (C_{Ar}), 138.5 (C_{Ar}), 127.0 (CH_{Ar}), 125.0 (C_{Ar}), 124.9 (CH_{Ar}), 124.5 (CH_{Ar}), 124.4 (CH_{Ar}), 123,5 (CH_{Ar}), 123.3 (CH_{Ar}), 122.9 (CH_{Ar}), 121.0 (CH_{Ar}), 119.6 (CH_{Ar}), 119.2 (CH_{Ar}), 111.5 (CH_{Ar}), 20.7 (CH_3). MS (GC): m/z (%) = 338 ($C_{23}H_{14}OS$, 100), 337 (22), 169 (10). HRMS (ESI): calcd for $C_{23}H_{14}OS$, 338.0759, found 338.0760. IR (ATR): $\tilde{\nu}$ = 2917 (m), 1580 (m), 1487 (m), 1446 (m), 1362 (m), 1226 (s), 119 (m), 1052 (s), 756 (vs).

1-methylbenzo[4',5']thieno[2',3':3,4]naphtho[1,2-*b*]benzofuran (47b)

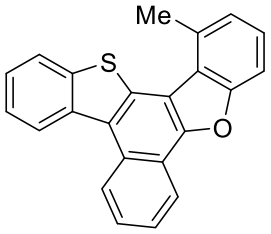

Starting with **44b** (100 mg, 0.28 mmol) and $Sc(OTf)_3$ (276 mg, 0.56 mmol), **47b** was isolated as a colourless solid (10 mg, 11%); mp: 92-94 °C. ^{1}H NMR (250 MHz, DMSO-d_6, 100°C) δ 9.28 – 9.19 (m, 1H, H_{Ar}), 9.02 (d, *J* = 8.2 Hz, 1H, H_{Ar}), 8.70 – 8.63 (m, 1H, H_{Ar}), 8.27 (ddd, *J* = 7.9, 1.3, 0.6 Hz, 1H, H_{Ar}), 8.05 – 7.99 (m, 1H, H_{Ar}), 7.95 – 7.81 (m, 2H, H_{Ar}), 7.76 – 7.68 (m, 1H, H_{Ar}), 7.64 – 7.47 (m, 3H, H_{Ar}), 2.76 (s, 3H, CH_3). ^{13}C NMR (63 MHz, DMSO-d_6, 100°C) δ 127.4 (CH_{Ar}), 125.3 (CH_{Ar}), 125.1 (CH_{Ar}), 124.6 (CH_{Ar}), 123.6 (CH_{Ar}), 123.5 (CH_{Ar}), 123.1 (C_{Ar}), 117.6(C_{Ar}). MS (GC): m/z (%) = 338 ($C_{23}H_{14}OS$, 100), 169 (15). HRMS (ESI): calcd for $C_{23}H_{14}OS$, 338.0759, found 338.0753. IR (ATR): $\tilde{\nu}$ = 2919 (s), 2851 (m), 1578 (m), 1452 (m), 1364 (m), 1347 (m), 1221 (m), 1188 (s), 1085 (m), 1026 (s).

Synthesis and Properties of 1*H*-Pyrrolo[3',2':3,4]fluoreno-[9,1-*gh*]quinolines and 7*H*-Pyrrolo[2',3',4':4,10]anthra[1,9-*fg*]-quinolines

The paragraph presented here focuses on the synthesis and applications of nitrogen-containing heterocyclic compounds using C-H activation reactions. The research highlights the strategic

synthesis of isomers of specific derivatives. Isomeric 1*H*-pyrrolo[3',2':3,4]fluoreno[9,1-*gh*]quinolines and 7*H*-pyrrolo[2',3',4':4,10]anthra[1,9-*fg*]quinolines were prepared in four steps from 2,3- and 3,4-dibromopyridine by Pd-catalyzed Sonogashira and Suzuki-Miyaura reactions, acid mediated cycloisomerization and subsequent Pd-catalyzed C-H activation.

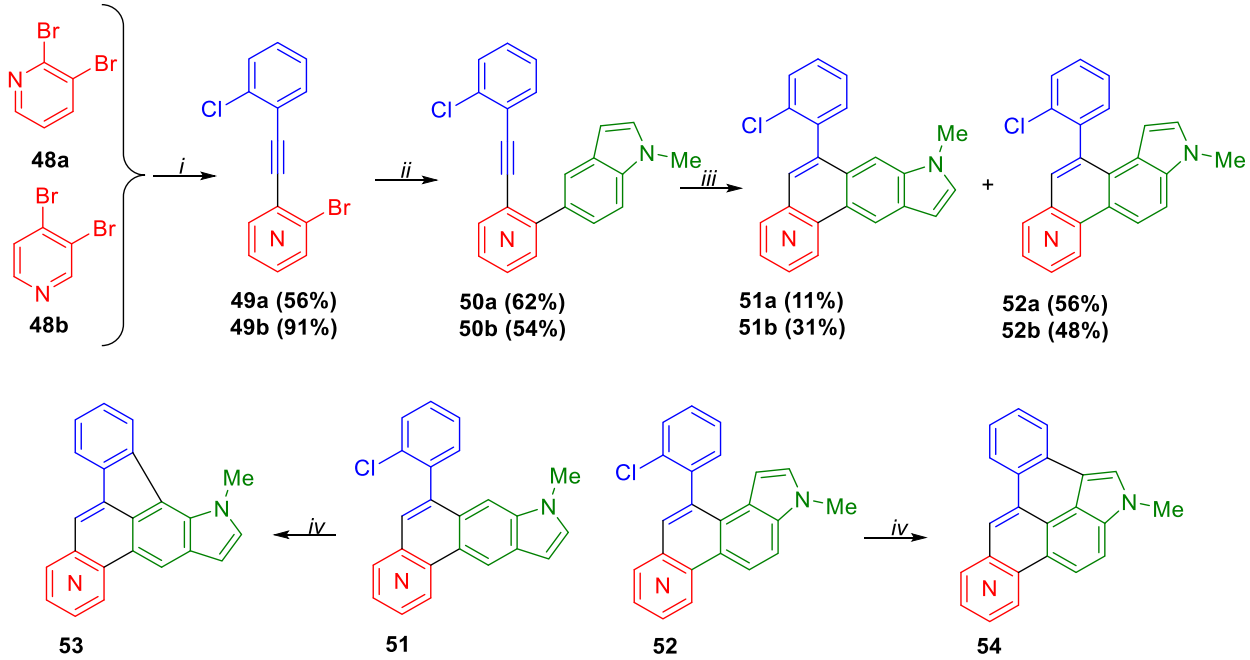

Scheme 20. Synthesis strategy for of 1*H*-pyrrolo[3',2':3,4]fluoreno-[9,1-*gh*]quinolines and 7*H*-pyrrolo[2',3',4':4,10]anthra[1,9-*fg*]-quinolines - derivatives. *Conditions: i (for **49a**),* **48a** (1.0 equiv.), 1-chloro-2-ethynylbenzene (1.2 equiv.), $Pd(PPh_3)_4$ (5 mol%), CuI (2 mol%), HN^iPr_2, 40 °C, 1 h; *(for **49b**),* **48b** (1.0 equiv.), 1-chloro-2-ethynylbenzene (1.2 equiv.), $Pd(PPh_3)_4$ (10 mol%), CuI (10 mol%), HN^iPr_2, 40 °C, 3 h; *ii,* **49** (1.0 equiv.), 2-naphthaleneboronic acid (1.2 equiv.), $Pd(PPh_3)_4$ (5 mol%), K_3PO_4 (2.0 equiv.), 1,4-dioxane/H_2O (6:1), 100 °C, 3 h; *iii,* **50** (1.0 equiv.), MsOH (30 equiv.), 120 °C, 18 h; *iv,* **51** and **52** (53 – 120 mg, 1.0 equiv), $PdCl_2$ (0.2 equiv.), PCy_3 (0.4 equiv.), DBU (3.0 equiv.), NMP, 150 °C, 18 h.

Transition metal-catalysed C-H activation under palladium catalysis was carried out using the synthesised precursors **4** and **5** according to previously published studies (manuscript IV). This stage does not require optimization, reaction works well with Palladium-catalyst $PdCl_2$, PCy_3, DBU in NMP and yield of the final product reaches from 80 to 99%.

5-(2-((2-chlorophenyl)ethynyl)pyridin-3-yl)-1-methyl-1*H*-indole (50a).

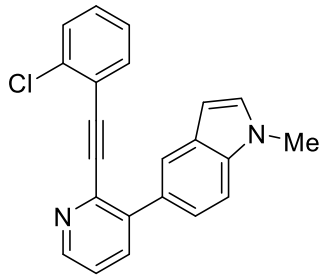

Starting with **49a** (250 mg, 0.86 mmol), **50a** was isolated as a yellow solid (183 mg, 62%); mp.: 112-114°C. ^{1}H NMR (500 MHz, Chloroform-*d*) δ 8.62 (dd, *J* = 4.7, 1.7 Hz, 1H), 7.99 (dd, *J* = 1.8, 0.7 Hz, 1H), 7.81 (dd, *J* = 7.8, 1.7 Hz, 1H), 7.54 (dd, *J* = 8.4, 1.8 Hz, 1H), 7.45 (dd, *J* = 7.7, 1.7 Hz, 1H), 7.40 (d, *J* = 8.4 Hz, 1H), 7.36 – 7.30 (m, 2H), 7.20 (td, *J* = 7.7, 1.8 Hz, 1H), 7.18 – 7.09 (m, 2H), 6.55 (dd, *J* = 3.2, 0.9 Hz, 1H), 3.83 (s, 3H). ^{13}C NMR (126 MHz, Chloroform-*d*) δ 148.2, 141.5, 141.2, 137.6, 136.7, 136.4, 134.1, 129.7, 129.7, 129.3, 129.2, 128.6, 126.4, 123.3, 123.2, 122.9, 122.2, 109.2, 101.7, 94.0, 87.9, 33.1. MS (GC): m/z (%) = 345 (3), 344 (13), 343 (13), 342 (M+, $C_{22}H_{15}ClN_2$, 38), 341 (11), 309 (3), 308 (27), 307 (100), 306 (11), 305 (8), 304 (2). HRMS (ESI-TOF) m/z: [M+H]+ calcd for $C_{22}H_{16}ClN_2$ 343.1002, found 343.0999. IR (ATR): ṽ=1618 (w), 1552 (w), 1475 (m), 1438 (m), 1416 (s), 1339 (m), 1249 (m), 1156 (w), 1076 (m), 1053 (m).

5-(4-((2-chlorophenyl)ethynyl)pyridin-3-yl)-1-methyl-1*H*-indole (50b).

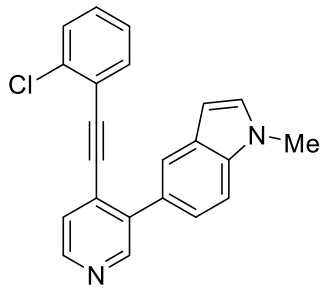

Starting with **49b** (250 mg, 0.86 mmol), **50b** was isolated as a yellow solid (159 mg, 54%); mp.: 84-86°C. ^{1}H NMR (500 MHz, Chloroform-*d*) δ 8.69 (s, 1H), 8.45 (d, *J* = 5.1 Hz, 1H), 7.91 (d, *J* = 1.0 Hz, 1H), 7.47 (dd, *J* = 8.5, 1.7 Hz, 1H), 7.44 (d, *J* = 5.1 Hz, 1H), 7.32 (d, *J* = 8.4 Hz, 1H), 7.28 (dd, *J* = 3.9, 1.5 Hz, 1H), 7.26 (dd, *J* = 4.3, 1.5 Hz, 1H), 7.17 – 7.12 (m, 1H), 7.07 (td, *J* = 7.6, 1.2 Hz, 1H), 7.01 (d, *J* = 3.1 Hz, 1H), 6.46 (dd, *J* = 3.0, 0.9 Hz, 1H), 3.74 (s, 3H). ^{13}C NMR (126 MHz, Chloroform-*d*) δ 150.90, 147.2, 139.3, 136.7, 136.3, 133.8, 130.0, 129.7, 129.4, 129.1, 128.6, 128.0, 126.7, 126.5, 123.3, 122.7, 122.2, 109.3, 101.7, 92.7, 92.2, 33.1. MS (GC): m/z (%) = 345 (6), 344 (27), 343(22), 342 (M+, $C_{22}H_{15}ClN_2$, 76), 341 (10), 340 (3), 309 (2), 308 (26), 307 (100), 306 (26), 305 (15), 304 (4). HRMS (ESI-TOF) m/z: [M+H]+ calcd for $C_{22}H_{16}ClN_2$ 343.1002, found 343.0995. IR (ATR): ṽ=1613 (w), 1578 (m), 1510 (m), 1484 (m), 1442 (m), 1397 (m), 1339 (m), 1245 (m), 1080 (m), 1055 (m).

6-(2-chlorophenyl)-8-methyl-8*H*-indolo[5,6-f]quinoline (51a).

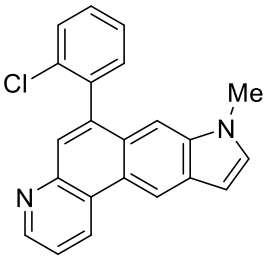

Starting with **50a** (350 mg, 1.02 mmol), **51a** was isolated as a yellow solid (38 mg, 11%); mp.: 198-200°C. ^{1}H NMR (250 MHz, Chloroform-*d*) δ 9.10 – 8.99 (m, 1H), 8.97 (s, 1H), 8.88 (dd, *J* = 4.4, 1.6 Hz, 1H), 7.74 (s, 1H), 7.62 – 7.41 (m, 5H), 7.33 (s, 1H), 7.24 (d, *J* = 3.6 Hz, 1H), 6.71 (dd, *J* = 3.2, 0.9 Hz, 1H), 3.73 (s, 3H). ^{13}C NMR (63 MHz, Chloroform-*d*) δ 148.69, 147.27, 140.80, 139.71, 137.47, 134.23, 132.81, 132.12, 130.25, 129.88, 129.63, 129.34, 127.43, 127.02, 126.77, 126.68, 123.53, 121.36, 114.66, 105.44, 100.93, 33.18. MS (GC): m/z (%) = 345 (8), 344 (34), 343 (26), 342 (M+, $C_{22}H_{15}ClN_2$, 100), 341 (2), 309 (2), 308 (17), 307 (72), 306 (11), 305 (14), 304 (3). HRMS (ESI-TOF) m/z: [M+H]+ calcd for $C_{22}H_{16}ClN_2$ 343.1002, found 343.1000. IR (ATR): ṽ=2920 (m), 1737 (w), 1620 (w), 1510 (m), 1461 (m), 1414 (m), 1374 (m), 1265 (m), 1082 (m), 1053 (m), 1032 (m).

6-(2-chlorophenyl)-8-methyl-8*H*-indolo[*6,5-h*]isoquinoline (51b).

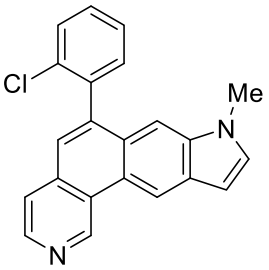

Starting with **50b** (350 mg, 1.02 mmol), **51b** was isolated as a yellow solid (109 mg, 31%); mp.: 103-105°C. ^{1}H NMR (300 MHz, Chloroform-*d*) δ 10.16 (s, 1H), 9.16 (s, 1H), 8.68 (s, 1H), 7.67 (d, *J* = 5.2 Hz, 1H), 7.64 – 7.59 (m, 1H), 7.51 – 7.43 (m, 4H), 7.35 (s, 1H), 7.30 (d, *J* = 3.2 Hz, 1H), 6.77 (dd, *J* = 3.2, 0.9 Hz, 1H), 3.75 (s, 3H). ^{13}C NMR (63 MHz, Chloroform-*d*) δ 146.23, 144.59, 141.60, 139.61, 137.36, 134.64, 134.12, 133.07, 131.95, 130.05, 129.93, 129.49, 127.31, 127.01, 126.18, 124.08, 123.02, 121.32, 113.90, 105.70, 101.16, 33.15. MS (GC): m/z (%) = 345 (8), 344 (33), 343 (24), 342 (M+, $C_{22}H_{15}ClN_2$, 100), 309 (2), 308 (18), 307 (74), 306 (9), 305 (11), 304 (3). HRMS (ESI-TOF) m/z: [M+H]+ calcd for $C_{22}H_{16}ClN_2$ 343.1002, found 343.0997. IR (ATR): ṽ=2922 (m), 1504 (m), 1461 (m), 1424 (s), 1414 (m), 1381 (m), 1337 (m), 1232 (s), 1053 (s), 1030 (m).

4-(2-chlorophenyl)-1-methyl-1*H*-indolo[5,4-f]quinoline (52a).

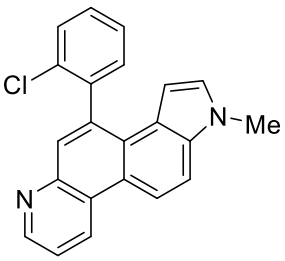

Starting with **50a** (350 mg, 1.02 mmol), **52a** was isolated as a yellow solid (195 mg, 56%); mp.: 176-178°C. ^{1}H NMR (250 MHz, Chloroform-*d*) δ 9.04 (d, *J* = 9.2 Hz, 1H), 8.96 (dd, *J* = 4.3, 1.5 Hz, 1H), 8.56 (d, *J* = 9.1 Hz, 1H), 7.98 (d, *J* = 0.8 Hz, 1H), 7.70 (dd, *J* = 9.0, 0.9 Hz, 1H), 7.64 – 7.58 (m, 1H), 7.58 – 7.53 (m, 1H), 7.52 – 7.41 (m, 3H), 6.91 (d, *J* = 3.2 Hz, 1H), 5.35 (dd, *J* = 3.2, 0.9 Hz, 1H), 3.85 (s, 3H). ^{13}C NMR (63

MHz, Chloroform-*d*) δ 149.04, 146.36, 141.82, 139.48, 135.41, 134.37, 131.53, 130.95, 129.76, 129.46, 129.20, 127.80, 127.23, 126.27, 125.30, 124.36, 123.98, 121.42, 117.15, 111.26, 102.72, 33.24. MS (GC): m/z (%) = 345 (3), 344 (11), 343 (8), 342 (M+, $C_{22}H_{15}ClN_2$, 32), 341 (1), 309 (3), 308 (24), 307 (100), 306 (30), 305 (7), 304 (1). HRMS (ESI-TOF) m/z: [M+H]+ calcd for $C_{22}H_{16}ClN_2$ 343.1002, found 343.1006. IR (ATR): ṽ=2922 (w), 1576 (w), 1504 (w), 1469 (m), 1414 (m), 1346 (m), 1317 (m), 1261 (m), 1053 (m), 1032 (m).

4-(2-chlorophenyl)-1-methyl-1*H*-indolo[*4,5-h*]isoquinoline (52b).

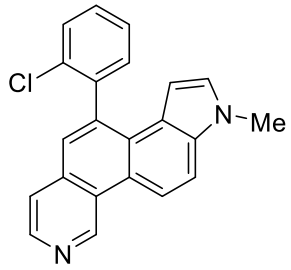

Starting with **50b** (350 mg, 1.02 mmol), **52b** was isolated as a yellow solid (168 mg, 48%); mp.: 180-182°C. ^{1}H NMR (250 MHz, Chloroform-*d*) δ 10.18 (s, 2H), 8.78 (d, *J* = 9.1 Hz, 1H), 8.68 (d, *J* = 5.4 Hz, 1H), 7.80 – 7.70 (m, 1H), 7.67 – 7.59 (m, 2H), 7.56 – 7.42 (m, 3H), 6.92 (d, *J* = 3.2 Hz, 1H), 5.33 (dd, *J* = 3.2, 0.9 Hz, 1H), 3.87 (s, 3H). ^{13}C NMR (63 MHz, Chloroform-*d*) δ 147.25, 143.61, 141.72, 140.35, 135.38, 134.21, 133.73, 131.35, 129.82, 129.62, 127.88, 127.25, 126.06, 125.98, 125.86, 124.25, 124.08, 121.07, 116.39, 111.97, 102.62, 33.27. MS (GC): m/z (%) = 345 (2), 344 (10), 343 (8), 342 (M+, $C_{22}H_{15}ClN_2$, 27), 341 (2), 309 (2), 308 (22), 307 (100), 306 (17), 305 (6), 304 (1). HRMS (ESI-TOF) m/z: [M+H]+ calcd for $C_{22}H_{16}ClN_2$ 343.1002, found 343.1004. IR (ATR): ṽ=1590 (vw), 1504 (w), 1414 (w), 1348 (w), 1304 (m), 1228 (vs), 1181 (s), 1121 (s), 1059 (m), 981 (s).

1-methyl-1*H*-pyrrolo[*3',2':3,4*]fluoreno[*1,9-fg*]quinoline (53a).

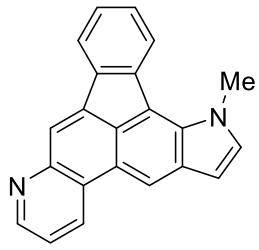

Starting with **51a** (53 mg, 0.15 mmol), **53a** was isolated as a yellow solid (38 mg, 80%); mp.: 230-232°C. ^{1}H NMR (500 MHz, DMSO-d_6) δ 9.28 (d, *J* = 8.2 Hz, 1H), 8.98 (dd, *J* = 15.2, 3.3 Hz, 2H), 8.61 (s, 1H), 8.53 (d, *J* = 7.8 Hz, 1H), 8.34 (d, *J* = 7.4 Hz, 1H), 7.72 (dd, *J* = 8.3, 4.3 Hz, 1H), 7.66 (d, *J* = 2.6 Hz, 1H), 7.51 (t, *J* = 7.5 Hz, 1H), 7.44 (t, *J* = 7.3 Hz, 1H), 6.88 – 6.83 (m, 1H), 4.49 (s, 3H). ^{13}C NMR (126 MHz, DMSO-d_6) δ 148.70, 148.23, 139.02, 137.65, 137.25, 135.15, 134.35, 133.50, 130.91, 128.91, 126.97, 126.01, 123.82, 122.69, 121.58, 120.58, 120.04, 117.49, 115.53, 102.49, 38.63. MS (GC): m/z (%) = 308 (3), 307 (24), 306 (M+, $C_{22}H_{14}N_2$, 100), 305 (25), 304 (4), 303 (3). HRMS (ESI-TOF) m/z: [M+H]+ calcd for $C_{22}H_{15}N_2$ 307.1235, found 307.1232. IR (ATR): ṽ=2920 (w), 1583 (w), 1527 (w), 1426 (m), 1401 (m), 1350 (m), 1315 (m), 1259 (s), 1080 (s), 1016 (s).

1-methyl-1*H*-pyrrolo[*3',2':3,4*]fluoreno[*9,1-gh*]isoquinoline (53b).

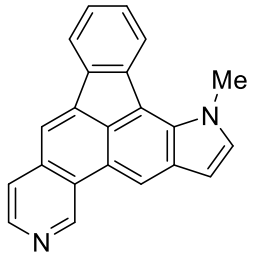

Starting with **51b** (73 mg, 0.21 mmol), **53b** was isolated as a yellow solid (57 mg, 87%); mp.: 207-209°C. ^{1}H NMR (300 MHz, DMSO-d_6) δ 10.15 (s, 1H), 9.03 (s, 1H), 8.70 (d, J = 5.4 Hz, 1H), 8.48 – 8.41 (m, 2H), 8.19 (dd, J = 7.2, 0.9 Hz, 1H), 8.00 (d, J = 4.7 Hz, 1H), 7.64 (d, J = 3.2 Hz, 1H), 7.45 (dtd, J = 22.7, 7.4, 1.2 Hz, 2H), 6.82 (d, J = 3.2 Hz, 1H), 4.43 (s, 3H). ^{13}C NMR (75 MHz, DMSO-d_6) δ 146.49, 144.37, 139.38, 138.11, 136.95, 135.57, 135.32, 134.70, 133.34, 129.13, 127.55, 126.03, 124.79, 123.81, 122.50, 122.34, 119.39, 117.69, 117.40, 114.78, 102.55, 39.24. MS (GC): m/z (%) = 308 (3), 307 (24), 306 (M+, $C_{22}H_{14}N_2$, 100), 305 (27), 304 (6), 303 (2). HRMS (ESI-TOF) m/z: [M+H]+ calcd for $C_{22}H_{15}N_2$ 307.1235, found 307.1231. IR (ATR): ṽ=2922 (m), 1595 (m), 1529 (m), 1447 (m), 1352 (m), 1317 (m), 1259 (m), 1199 (m), 1086 (s), 1016 (s).

7-methyl-7*H*-pyrrolo[2',3',4':4,10]anthra[*1,9-fg*]quinoline (54a).

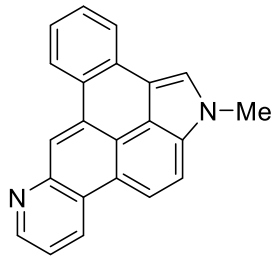

Starting with **52a** (120 mg, 0.35 mmol), **54a** was isolated as a yellow solid (102 mg, 95%); mp.: 198-200°C. ^{1}H NMR (500 MHz, DMSO-d_6) δ 9.29 (d, J = 6.9 Hz, 1H), 9.05 (dd, J = 4.1, 1.6 Hz, 1H), 9.00 (s, 1H), 8.85 (d, J = 7.9 Hz, 1H), 8.71 (d, J = 8.9 Hz, 1H), 8.22 (d, J = 11.9 Hz, 2H), 8.06 (d, J = 8.8 Hz, 1H), 7.71 (dd, J = 8.3, 4.2 Hz, 1H), 7.64 (t, J = 6.8 Hz, 1H), 7.58 – 7.53 (m, 1H), 4.19 (s, 3H). ^{13}C NMR (126 MHz, DMSO-d_6) δ 148.85, 146.57, 131.06, 130.76, 130.48, 129.63, 128.98, 128.71, 125.65, 125.45, 124.36, 123.72, 122.46, 122.15, 121.00, 120.88, 120.72, 119.34, 117.32, 112.30, 112.05, 33.73. MS (GC): m/z (%) = 308 (3), 307 (29), 306 (M+, $C_{22}H_{14}N_2$, 100), 305 (16), 304 (3), 303 (2). HRMS (ESI-TOF) m/z: [M+H]+ calcd for $C_{22}H_{15}N_2$ 307.1235, found 307.1233. IR (ATR): ṽ=1607 (w), 1529 (w), 1475 (w), 1418 (w), 1374 (m), 1350 (m), 1282 (w), 1230 (m), 1170 (w), 1043 (m).

1-methyl-1*H*-pyrrolo[*2',3',4':4,10*]anthra[*9,1-gh*]isoquinoline (54b).

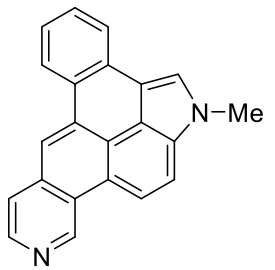

Starting with **52b** (95 mg, 0.28 mmol), **54b** was isolated as a yellow solid (84 mg, 99%); mp.: 232-234°C. ^{1}H NMR (300 MHz, Chloroform-*d*) δ 10.01 (s, 1H), 8.67 (d, J = 5.5 Hz, 1H), 8.50 (dd, J = 8.1, 1.4 Hz, 1H), 8.44 (d, J = 8.9 Hz, 1H), 8.36 (s, 1H), 7.94 (dd, J = 7.8, 1.4 Hz, 1H), 7.83 (dd, J = 5.6, 0.9 Hz, 1H), 7.59 – 7.43 (m, 4H), 3.98 (s, 3H). ^{13}C NMR (75 MHz, Chloroform-*d*) δ 146.63, 142.70, 134.38, 132.29, 130.82, 130.00, 129.42,

128.60, 125.50, 125.15, 124.19, 123.43, 122.55, 122.31, 122.09, 121.52, 120.32, 116.23, 116.19, 113.08, 111.36, 33.87. MS (GC): m/z (%) = 308 (3), 307 (20), 306 (M+, $C_{22}H_{14}N_2$, 100), 305 (15), 304 (3), 303 (2). HRMS (ESI-TOF) m/z: [M+H]+ calcd for $C_{22}H_{15}N_2$ 307.1235, found 307.1237. IR (ATR): $\tilde{\nu}$=1607 (m), 1531 (m), 1453 (m), 1412 (m), 1372 (m), 1350 (m), 1224 (s), 1148 (m), 1039 (m).

Resume

Personal Data

Name: Aleksandra Khomutetckaia

Date/place of birth: 02.01.1997 in Kirghizstan

Citizenship: Russian Federation

Education

Since October 2020 — **PhD: Organic Chemistry,** University of Rostock

- working group Prof. Dr. Peter Langer: Catalytic coupling and cyclization reactions, drug synthesis, heterocycles, carbohydrates, new organic materials
- PhD Thesis: "Synthesis of Polycyclic Heteroaromatic Hydrocarbons by C-H Activation Reactions: Application of Cycloisomerization and Pd-catalyzed Cross-Coupling Reactions"

September 2018 - July 2020 — **M.Sc.: Pharmaceutical Chemistry,** Immanuel Kant Baltic Federal University

- working group Dr. sc. chem. Alexander Bulychev: Asymmetric synthesis and catalysis
- Thesis topic: "Synthesis and Immobilization of Chiral Anionic Complexes of Co(III) Aromatic Aldehydes and β-hydroxy-α-amino Acids on Magnetic Nanoparticles"

September 2014 - July 2018 — **B.Sc.: Chemistry,** Immanuel Kant Baltic Federal University

- working group Dr. sc. chem. Alexander Bulychev: Asymmetric synthesis and catalysis
- Thesis topic: “Synthesis of Co(III) Complexes of Schiff Base of 2-Hydroxyaromatic Aldehydes with (S)-Glutamic Acid”

Publications

A. Khomutetckaia, P. Ehlers, A. Villinger, P. Langer. *Synthesis and Properties of Azadibenzo[a,e]pyrenes. Eur. J. Org. Chem.* **2024***, e202301299*.

A. Khomutetckaia, N. Hildebrandt, P. Ehlers, A. Villinger, P. Langer. *Synthesis and Properties of Diindeno[1,2,3-cd:1',2',3'-mn]pyrene and Two of Its Aza-Analogs. Eur. J. Org. Chem.* **2023**, e20230110.

A. Khomutetckaia, P. Ehlers, A. Villinger, P. Langer. *Synthesis and Properties of Benzo[h]imidazo[1,2-a]quinolines and 1,2a-Diazadibenzo[cd,f]azulenes. J. Org. Chem.* **2023**, *88*, 7929–7939.

E. Ammon, **A. Khomutetckaia**, A. Villinger, P. Ehlers, P. Langer. *Serendipitous discovery of Pd-catalyzed intramolecular cyclization of ortho-bromo(hetero)aryl-substituted (hetero)aryl-1,2-diketones: Applications in the synthesis of carba- and heterocyclic benzoin derivatives*. *Tetrahedron.* **2023**, *135*.